AMERICAN PHYSICAL SOCIETY

OFFICERS OF THE SOCIETY

[illegible] Princeton University, Princeton, N.J.
[illegible] University of Chicago, Chicago, Ill.
[illegible] Columbia University, New York City.
[illegible] Columbia University, New York City.
[illegible] University of Minnesota, Minneapolis, Minn.

[illegible] L. Watson Stanford University, Calif.

THE PHYSICAL REVIEW

Published by the American Physical Society at 450 Ahnaip St., Menasha, Wis. Entered at the Post Office at Minneapolis, Minn. Two volumes annually.

[illegible] Series, Vol. 1, 1893, to January 1, 1913, the Review was conducted by Edward Nichols Merritt and Frederick Bedell, with the financial support of Cornell University. Four volumes were issued annually; subsequent volumes, semi-monthly. Twenty-five volumes in all.

[illegible] January 1, 1913, the Review was transferred to the American Physical Society, as announced on the first page of the new series which was then begun. It is now conducted by a Board of Editors elected by the Society. Semi-monthly issues, on the 15th of January and July.

[illegible] and referred to page 2 of the advertisements for further information.

[illegible] Subscription. Throughout the Postal Union, $5.00 in advance.

[illegible] Rates.

[illegible] Series, Complete, $20.00, in advance.

Volumes, $4.00 per volume; Back Numbers, $1.00 per copy. Postage is free if [illegible] accompanies order; otherwise postage is extra. No bound volumes can be [illegible] The Society offers to purchase a limited number of First Series, Vol. 1, No. 1 (out of print); Second Series, Vol. 7, No. 1, January 1916; Vol. 7, No. 2, February 1916; Vol. 7, No. 3, April 1916; and Vol 7, No. 5, May 1916 (at $1.00 each).

[illegible] Issues will be supplied by the Editor on request. Copy for each number [illegible] Minneapolis before the 1st of the preceding month; old copy is [illegible] if received. Send electrotypes about 4½ in. to printers, George Banta [illegible] Menasha, Wisconsin.

[illegible] one year must be allowed subscription agencies and members of the American [illegible]

[illegible] and Complaints of failure to receive the Review, in the case of [illegible] Physical Society, should be addressed to 450 Ahnaip St., Menasha, Wis., [illegible] Secretary, to the Editor. *Back copies will be sent free if complaint is* [illegible] *three months of date of issue.*

[illegible] should be addressed to the Physics Review, University [illegible] Minn.

[illegible] Minn., [illegible] matter.

[illegible] Act of October 3, [illegible] authorized September 7.

Second Series *September, 1928* *Vol. 32, No. 3*

THE

PHYSICAL REVIEW

FINE STRUCTURE OF THE SCATTERED RADIATION FROM GRAPHITE

By Bergen Davis and Dana P. Mitchell

Abstract

This analysis of the "undisplaced" scattered radiation was made with double x-ray spectrometer previously described. (Davis and Purks, Proc. Nat. Acad. Vol. 13, No. 6, June 1927, Vol. 14, No. 2, Feb. 1928.) A special double target (Mo) x-ray tube was used with a block of graphite between the targets as the scattering element. The crystals were placed for reflection at first order. Four lines were observed: (a) an undisplaced line at position of Mo $K\alpha_1$; (b) a line displaced 80″ (0.0012A) from $K\alpha_1$ position; (c) a line displaced 140″ (0.002A) from $K\alpha_1$; (d) a line displaced 780″ (0.0113A) from $K\alpha_1$. These are all on the long wave-length side of Mo $K\alpha_1$. The undisplaced line (a) is scattered from whole atom. The line displaced (0.0113A) closely agrees with $h\nu' = h\nu - Ve$, where Ve is the energy level (287 volts) of the carbon atom. The line (b) is displaced (0.0012A). This is equivalent to 29 volts which does not agree with the L_{III} level of carbon (11.2 volts). The line (c) is displaced (0.002A). This is equivalent to 50 volts, and does not agree with the L_I level of carbon which is 34 volts. In the case of these two lines the relation $h\nu' = h\nu - Ve$ does not hold. A search was made for scattered radiation on the short wave-length side of the Mo $K\alpha_1$ position, corresponding to the relation $h\nu' = h\nu + Ve$. No positive results were obtained.

THE recent improvement in the resolving power of the ionization x-ray spectrometer suggests its application to the further study of various x-ray phenomena. So far it has been applied to the investigation of fine structure in the K series of molybdenum,[1] copper and nickel,[2] and to the problem of the natural breadth of spectral lines.[1] In addition, some observations have been made on the effect of chemical combination on the structure of the K absorption limit (See article by Davis and Purks in this issue.)

The double x-ray spectrometer has the advantage that its resolving power is independent of the width of the slits. This fact permits sufficient energy to make it possible to observe effects that would be beyond the power of the single crystal instrument with the narrow slits that are necessary for high resolution.

[1] Davis and Purks, Proc. Nat. Acad. **13,** 419 (June, 1927) and **14,** 172 (Feb., 1928).

[2] Purks, Phys. Rev. **31,** 931 (June, 1928).

The spectrometer measurements of the "undisplaced" scattered radiation by Compton[3] and the photographs of this same radiation by Ross[4] show a broadening of the spectral line. The experiments here reported show that this broadening is due to fine structure and a small displacement.

Two separate experiments were made on the "undisplaced" scattered radiation from graphite: (1) with double target x-ray tube with the scattering element between the targets; (2) with two narrow cylindrical tubes placed side by side with the scattering element between them. The double target tube, the slits and the crystals are shown schematically in Fig. 1. The two targets are of molybdenum placed close together. The electron sources are two standard Coolidge cathodes. The scattering element C is a small prism of graphite about one centimeter broad at the base. The distance from the focal spots on the targets to the graphite is about 1.5 cm. The slits are 5 mm wide and 2 cm high. The crystals are of split calcite (Iceland spar) and are set for first order reflection.

The angular displacements ($2d\theta_1$) are the displacements of the analyzing crystal B from the undisplaced Mo $K\alpha_1$ position.

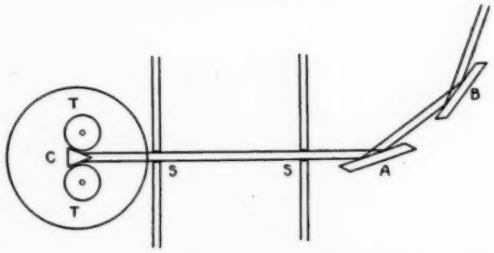

Fig. 1. Diagram of apparatus. T, T, targets of double x-ray tube; C, graphite scattering element; S, S, slits (5 mm wide); A collimating crystal; B, analyzing crystal.

The x-ray tube was carefully exhausted. The graphite element C was completely out-gassed by electron bombardment. The tube operated very steadily with 35 milliamperes on each target and a P.D. of 40000 volts. The total input was 2800 watts. The intensity of the scattered radiation made it possible to measure the fine structure with fair accuracy. Such an intense source is necessary. The undisplaced scattered radiation as ordinarily observed is here divided into four parts. In addition each of these parts is further reduced by two reflections.

In the case of experiment No. 2, the arrangement was similar to that shown in Fig. 1, except that instead of one double x-ray tube, two independent tubes were used. These tubes were each 4 cm in diameter. They were mounted side by side in a vertical position with a wedge of graphite between them.

The distance from the focal spots on the targets to the graphite was about 2.5 cm. The energy input was about the same as in the case of the double

[3] A. H. Compton, Phys. Rev. **22**, 409 (Nov., 1923).
[4] P. A. Ross, Proc. Nat. Acad. **10**, 304 (1924).

target tube. The results obtained in the two experiments are in agreement. The accuracy obtained is probably of the order of $2d\theta_1 = \pm 10''$ arc. This is equivalent to ± 0.15 X-Units.

The experimental curves obtained by experiment No. 1 (double tube) are shown in Fig. 2. Those obtained by experiment No. 2 are similar in character and position.

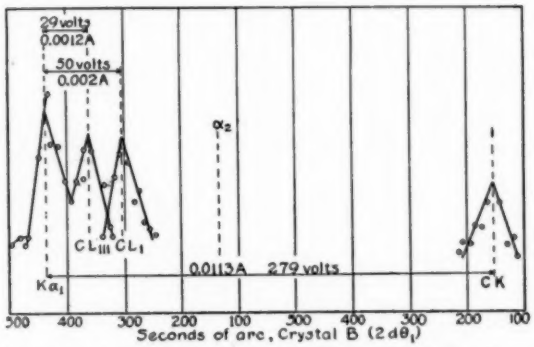

Fig. 2. Analysis of the "undisplaced" scattered radiation from carbon.

The so-called undisplaced scattered radiation from graphite is really composed of four frequencies. A line at position of Mo $K\alpha_1$, one displaced ($2d\theta_1 = 80''$), one displaced ($2d\theta_1 = 140''$) and still another displaced ($2d\theta_1 = 780''$), all on the long wave-length side of the Mo $K\alpha_1$ position. The results are given in Table I.

TABLE I. *Results of the two experiments.*

Observed	$2d\theta_1$	$d\lambda$	Volts	Carbon, energy, levels, volts.
		Experiment No. 1		
$K\alpha_1$	0	0	0	—
CL_{III}	80″	.0012	29	11.2
CL_I	140	.002	50	34
C. K.	780	.0113	279	287
		Experiment No. 2		
$K\alpha_1$	0	0	0	—
CL_{III}	90″	.0013	34	11.2
CL_I	158	.0023	57	34.
CK	780	.0113	279	287

The displaced lines are designated by C L_{III}, C L_I, and C K. They are ascribed to the two electrons in each of the L levels and the K level of the carbon atom.

The displaced lines are designated by C L_{III}, C L_I and C K. They are ascribed to the two electrons in each of the L levels and the K level of the carbon atom.

Since the wave-length at first order is expressed by $\lambda = 2d \sin\theta$, the corresponding $d\lambda$ is given by $d\lambda = d \cos\theta(2d\theta_1)$, where $(2d\theta_1)$ is the angular displacement of crystal B from the original Mo $K\alpha_1$ position.

The energy relations of a quantum $h\nu$ scattered from an atom have been given by Compton as[5]:

$$h\nu - h\nu' = Ve + mc^2[(1-\beta^2)^{-1/2} - 1] + Mv^2/2. \quad (1)$$

The first term on the right represents the energy level of an electron. The second term is the kinetic energy of an electron after ejection. The last term which represents the kinetic energy of the atom imparted by the quantum is very small and may be neglected.

The second term on the right gives the normal Compton scattering from a free electron. The undisplaced $K\alpha_1$ line observed in these experiments arises from scattering from the whole atom. In this case all three terms on the right are practically zero.

The C K line corresponds to an energy loss of 279 volts. This is in good agreement with K energy level of carbon. The values of the K levels of carbon as given by the Report on Critical Potentials (Bulletin of the National Research Council, No. 48, 1924) range from 280 volts to 290 volts. A more recent determination by Dauvillier[6] gives 287 volts. The experimental value of 279 volts indicates that all the terms on the right of Eq. (1) are zero except the first. That is, $h\nu' = h\nu - Ve$. The quantum loses energy of lifting through the K level but does not give the electrons any energy or momentum.

The displacements of the two L_{II} and L_I lines do not agree with the two L energy levels of carbon as determined from the carbon atom in the gaseous state. The relation $h\nu' = h\nu - Ve$ does not hold for these lines. Two views are suggested to account for the greater displacement. The L energy levels of crystal carbon may be much greater in the crystal form than in the gas form. This, however, is not probable as an energy change from 11 to 29 volts and from 34 to 50 volts would give a very large heat of formation of graphite, much larger than is actually observed. The other view is that the quantum lifts the L electrons to the limit of the atom and gives them energy and momentum. A difficulty, however, arises from the fact that the C L lines are just as narrow as the C K line or the α_1 line (see Fig. 2). If these electrons are given much energy and momentum after ejection the lines should be diffuse just as the Compton effect lines are diffuse. We have observed the Compton effect with the double x-ray spectrometer and the angular spread is very great. This is to be expected from the angle law $(1-\cos\theta)$. The x-rays falling on the scattering element (Fig. 1) are quite divergent. If the L electrons are given a kinetic energy after removal a broadening due to the angular divergence should be observed as in the Compton effect. The magnitude would be less. The narrowness of the C L lines indicate that the effect of divergence $(1-\cos\theta)$ is very small.

A search was made for scattered line radiation on the short wave-length side of the Mo $K\alpha_1$ position. Such scattered radiation might occur. If the atom were in an excited state, that is, if an L electron for example were at

[5] A. H. Compton, Phys. Rev. **24**, 168 (1924).
[6] Dauvillier, Jour de Phys. et La Radium, [VI], 7 No. 12 (Dec., 1926).

a higher level or at the limit, and were acted on by a quantum $h\nu$ at the moment of return, the energies might add. The emitted energy would be $h\nu' = h\nu + Ve$. No positive results were obtained, but we hope to return to the question again with a more intense source of energy.

The investigation of the scattered radiation will be continued by one of us (D. P. M.). It is proposed to ascertain if the displacement depends at all on the angle. Also, other scattering elements will be used such as beryllium and aluminium to determine the dependence of this effect on the values of the energy levels. It is possible also that the energy levels in the (CH) compounds, such as paraffin may differ from those of carbon in graphite.

PHYSICS LABORATORY,
COLUMBIA UNIVERSITY,
June, 1928.

NOTE ON THE EFFECT OF CHEMICAL COMBINATION ON THE STRUCTURE OF THE K ABSORPTION LIMIT

By Bergen Davis and Harris Purks

Abstract

The structure of the K absorption limits of some chemical compounds was examined with the double x-ray spectrometer. This instrument has been previously described. The K absorption limits of the elements Ag, Mo and Cu and the compounds Ag_2S, Ag_2O, also MoO_3, MoS_2 and Mo_2O_3 were examined for increase in width or fine structure. The width for the pure element decreases with increasing atomic number. The general effect of the chemical action was to broaden the absorption limit, but there was little displacement. In one case, M_2O_3, there was evidence of fine structure. The silver salts appeared to be considerably reduced by the x-rays.

Effect of temperature on the K absorption limit.—Recent experiments of H. S. Read (Phys. Rev. **27**, p. 373, April 1926, and **28**, p. 898, Nov. 1926) indicate an increase of absorption due to temperature of the absorbing element. Also the results were interpreted as due to a shift in the absorption limit. This matter was examined with double spectrometer. A strip of Mo was heated to incandescence in vacuum. The position and form of the K limit was compared to that for cold strip. They were identical. No effect of temperature was detectable. This method would probably detect one-tenth the displacement estimated by Read.

THIS is a report of some experiments designed to test the possibilities of the double x-ray spectrometer in the investigation of minute effects. The instrument as used for high resolution has been already described and need not be repeated here.[1]

Both structure and shift of position in the K absorption limit of elements of small atomic number due to chemical combination have been observed by Bergengren and Lindh.[2] This indicates that chemical action not only involves the valence electrons but extends throughout the atom affecting even the inner energy levels. This effect has not been heretofore observed in the case of elements of higher atomic number such as silver and molybdenum.

The energy of chemical action is very small compared to the energy of the inner levels of atoms of high atomic number. The disturbance of these levels should be small, the readjustment of mutual energies being largely confined to the outer levels of the atoms. The double spectrometer here used gives the width of the absorption limit if correction is made for crystal inperfections.[1] We have investigated a few compounds of silver and molybdenum. This included of course the absorption limits of the elements themselves.

The metal was used in the form of thin sheets rolled to the proper thickness to give a convenient discontinuity at the K limit. The first crystal (A) was set at proper angle to reflect a wide region each side of the limit. The second crystal was then rocked through a small angle each side of the absorption limit positions. The forms of the discontinuities observed for silver, molybdenum and copper are shown in Fig. 1. These curves are not corrected for crystal imperfection. The break is quite sharp, and the sharpness increases with increasing atomic number. The full width being: for Ag, 0.38 XU; Mo,

[1] Bergen Davis and Harris Purks, Proc. Nat. Acad. **13**, No. 6 (June 1927) and **14**, No. 2 (Feb. 1928.)

[2] Siegbahn, Spectroscopy of X-rays, p. 142.

0.48 XU; and for Cu, 0.70 XU. We expect in the near future to extend these observations to elements of the highest atomic number.

The absorption limits of the compounds MoO_3, Mo_2O_3 and MoS_2 and also the two compounds of silver Ag_2S and Ag_2O were then investigated. These compounds were all used in the powdered form. A thin film of waterglass was painted on a piece of paper. While still wet, the powder was sprinkled on the water-glass to a thickness that would give a convenient absorption. Waterglass was used as a binder rather than organic compounds containing carbon such as sugars or glues. The carbon of such substances would assist in the reduction of the compounds under the action of x-rays.

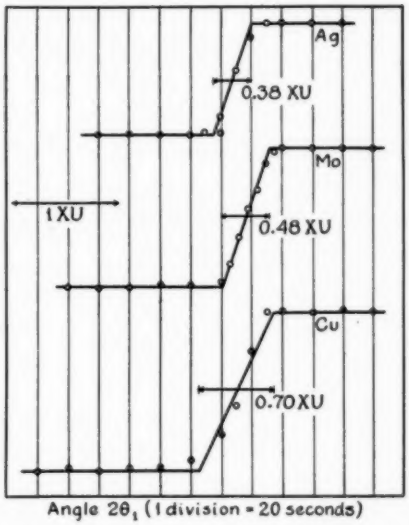

Fig. 1. Forms of the discontinuities for silver, molybdenum and copper.

The curves for the molybdenum compounds are shown in Fig. 2. The limit is much broadened in the case of MoO_3 and MoS_2. The center of gravity of the limit, however, is only slightly displaced.

In the case of Mo_2O_3 there is marked evidence of fine structure. Fine structure may be present to a less degree in the other two compounds. The results obtained for the two compounds of silver are shown in Fig. 3. The

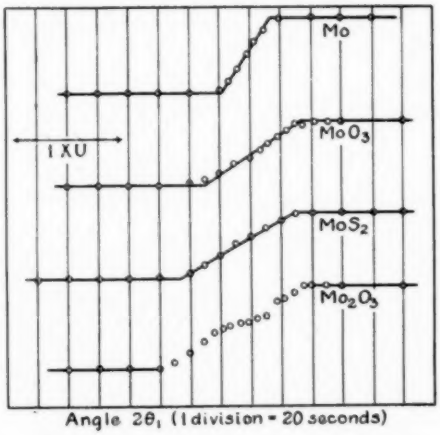

Fig. 2. The discontinuities for molybdenum compounds.

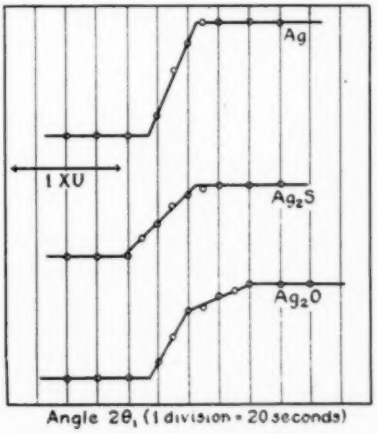

Fig. 3. The discontinuities for silver compounds.

absorption limit is broadened by chemical action. The center of gravity is only slightly displaced. The curve for Ag_2O shows a break that may be due to fine structure. The lower part of the curve is nearly the same as that for pure silver, the upper part is shifted toward the long wave-length. The effect may be due to the partial reduction of the silver salt by the x-rays. The lower part which is identical with the curve for pure silver, arises from the part of the salt that has been reduced. It was observed that the silver salt

turned dark after a few minutes exposure to the radiation. The molybdenum salts did not appreciably change color under the action of the radiation.

These results indicate that in the case of chemical combination, the readjustment of energy is not confined to the outer layers of the atom, but extends throughout the whole atomic system. These results also suggest that there are possible errors in the wave-length measurements of the several series of some of the elements. Many elements cannot be used directly as a target in an x-ray tube. In these cases stable compounds of the elements have been used. The K limit is affected by the chemical combination and the K emission series is probably similarly affected. The spectral lines would at least be broadened. They should also contain fine structure not present in the radiation from the element. The L and M series would be affected to a still greater extent. This suggests an investigation of the fine structure in the emission series of compounds.

Note on the Effect of Temperature on the K Absorption Limit

H. S. Read[3] has reported an effect of temperature on the absorption of x-rays. An increase of absorption with increase of temperature was found in every case investigated. This effect, if confirmed, is of interest and importance, more especially as it is not anticipated by our theories of emission and absorption of radiation. In the second paper Read reports an investigation of the dependence of the effect on wave-length. The absorbing element of silver was given a temperature range from 20°C to 850°C. The results were interpreted as indicating a shift of the K absorption limit. The shift assigned being 0.2 XU, which is equivalent to 11 volts.

We have investigated this temperature effect in molybdenum using the double x-ray spectrometer. A strip of this metal about 6 mm wide and of proper thickness to give a convenient break at the absorption limit was mounted in a Pyrex tube with thin windows. The strip was attached to large tungsten lead-in wires and could be heated to any desired temperature by an electric current. The tube was exhausted and mounted between the two slits of the spectrometer in such way that the beam of x-rays would pass through the strip of molybdenum.

The K discontinuity with cold strip was identical with that shown in Figs. 1 and 2. The Mo strip was then heated to incandescence and the absorption break again measured. No effect whatever was observed. Within the errors of experiment the readings were the same as those with a cold absorber. We certainly could have observed a shift of three seconds of arc on the second crystal. A shift of 0.05 XU could have been observed. This is equivalent to 1.3 volts. The temperature of the strip of molybdenum was much higher than that of the silver used by Read. The temperature, however was not measured as the strip evaporated through at one point just at the close of the experiment. Since the results were negative it was not considered worth while to re-perform the experiment and measure the temperature with an optical pyrometer.

Physics Laboratory,
Columbia University,
June, 1928.

[3] H. S. Read, Phys. Rev. **27**, 373 (1926) and **28**, 898 (1926).

THE SELF CONSISTENT FIELD AND THE STRUCTURE OF ATOMS

By J. C. Slater

Abstract

The method proposed by Hartree for the solution of problems in atomic structure is examined as to its accuracy as a method of solving Schrödinger's equation. A wave function is set up at once from his method, and the matrix of the energy computed with respect to it. The non-diagonal terms are shown to be small, indicating that the function is a good approximation to a real solution. The energy levels are found by perturbation theory from this matrix, and are compared with the term values as found by Hartree. His values should be corrected for three reasons: he has neglected the fact that electron distributions are not really spherical; he has not considered the resonant interactions between electrons; and he has made an approximation which amounts to neglecting the polarization energy. The sizes of these corrections are estimated, and they are found to be of the order of the errors actually present in the numerical cases he has worked out.

HARTREE[1] has recently proposed a method of approximate solution of problems in atomic structure by using central fields defined in a certain way, which he calls "self-consistent" fields. He has justified his method only by qualitative arguments and by the agreement of his calculations with experiment (particularly in the case of Rb, the atom which he has investigated in greatest detail). It is the purpose of the present paper to show to what extent his method is really a solution of the problem by wave mechanics, and to estimate the errors which should be present in it. It appears that Hartree's procedure has in fact a good theoretical foundation, and that the estimated errors are in general of the order of magnitude of the discrepancy between his calculations and experiment.

Hartree's method is the following: he sets up a separate wave function for each electron of the atom; he assumes the individual electrons to have charge density corresponding to their $\psi\psi^*$'s, averaged over different directions to give a spherical distribution of density; he adds these distributions for all the electrons but one, and finds the electric potential of the resulting charge; then he subjects the wave function of the remaining electron to the condition that it be a solution, with proper quantum numbers, of the wave equation connected with the central field so defined. By applying this condition to each electron of the atom, the problem becomes determinate. Finally, he takes the sum of the density distributions of all the electrons to be the real density distribution in the atom; and he assumes the characteristic numbers of his various central field problems to be the energy values of the corresponding terms of the spectrum. The latter agree well with the observed terms, except in the optical case, in which there is a discrepancy

[1] D. R. Hartree, Proc. Camb. Phil. Soc., **24**, 89 (1928).

which he assumes due to the polarization of the core by the valence electron. Hartree considers this agreement to be only empirically justified, since it is not obvious that the method takes into account the rearrangement of the electrons in the ion when one electron is removed.

One can set up a wave function for the problem by taking the product of Hartree's functions for the individual electrons. The resulting function proves to be in fact a good approximation to a solution of Schrödinger's equation, which we verify by computing the non-diagonal terms of the matrix of the energy referred to these wave functions, and by showing that they are remarkably small. To a lower order of accuracy, we can set up a wave function for the ion found by removing an electron, merely by leaving the wave function of that electron out of the product. Then by perturbation theory we can calculate the various ionization potentials. These prove to differ from the term values of the one-electron problem (which Hartree takes as representing them) on three distinct accounts: first, there is a term arising because the process of averaging densities over different directions to produce a central field is not strictly justified; second, there is a term on account of resonance between the electrons. These two corrections are in close relation to each other; they are more important for x-ray electrons, except *s* electrons, than for optical electrons; and they can be estimated, and prove not to be much larger than the divergences between Hartree's calculation and experiment. Finally there is a term which arises because the wave function of the ion is of a lower order of accuracy than that of the atom, and appreciable second-order terms in the energy arise from it. For the x-ray spectra, this is of opposite sign to the errors mentioned above, and may reasonably cancel part of them. For the optical terms, it proves to be a polarization term, of just the sort demanded to bring Hartree's calculations into better agreement with experiment.

2. The first step in discussing Hartree's method is to formulate his process mathematically. Let the separate wave function of the ith electron be u_i, a function of the coordinates x_i of this electron. The density of charge connected with this electron is u_i^2 (neglecting for simplicity the possibility that u_i may be complex). Let this density averaged over all orientations, viz., $(1/4\pi)\int u_i^2(r,\theta,\phi)\sin\theta d\theta d\phi$ be $\bar{u}_i^2$. The density of all the electrons but the ith is $\Sigma_{(k,k\neq i)}\bar{u}_k^2$ (where here, and always unless otherwise stated, all summations are assumed to be over all the electrons of the atom). The potential energy of the ith electron in this field, and in the field of the nucleus of charge Z units, is then $-Z/r_i+\Sigma_{(k,k\neq i)}\int(\bar{u}_k^2/r_{ik})dv_k$, where r_i is the distance of the ith electron from the nucleus, r_{ik} the distance between ith and kth. Thus the wave equation for this electron becomes[2]

$$\nabla_i^2 u_i+(\epsilon_i-2\sum_{(k,k\neq i)}\int(\bar{u}_k^2/r_{ik})dv_k+2Z/r_i)u_i=0 \qquad (1)$$

[2] Here and elsewhere we shall measure distances in terms of a_0, the radius of the first hydrogen orbit, and energies in terms of Rh. This accounts for the factor 2 in all potential energy terms.

Hartree finds u_i's and ϵ_i's so that these equations are satisfied for each i. Each equation is obviously that of an electron in a central field; and in each case he chooses the particular solution of the central field problem given by the quantum numbers he wishes to assign to the corresponding electron.

Next we inquire what differential equation is satisfied by the product of all the u_i's, which we shall call ψ: $\psi = u_1 \cdots u_n$. We have at once, multiplying Eq. (1) by all the other u's, recalling that each u_k is a function only of x_k, and then adding the equations so obtained,

$$\nabla^2\psi + \left(\sum_i \epsilon_i - \sum_{(i,k;i\neq k)} \int 2\bar{u}_k^2/r_{ik}\,dv_k + Z \sum_i 2/r_i \right)\psi = 0 \qquad (2)$$

This is an equation which, as we shall show, is not very different from the true equation for ψ, which is $H\psi = E\psi$, where

$$H = -\nabla^2 + \tfrac{1}{2} \sum_{(i,k;i\neq k)} 2/r_{ik} - Z \sum_i 2/r_i \qquad (3)$$

(where the factor $\frac{1}{2}$ is inserted because we wish each pair of electrons to be counted once, instead of twice, as the sum $\Sigma_{(i,k;i\neq k)}$ would give).

Having found the differential Eq. (2) satisfied by Hartree's function ψ, we can compute the matrix of H with respect to it by integrating the operator (3) over the function. That is, the component connected with a transition $\psi' \rightarrow \psi''$ is, using (2),

$$H'' = \int \psi' H \psi'' = \int \psi'\psi'' \left[\sum_i \epsilon_i + \tfrac{1}{2} \sum_{(i,k;i\neq k)} (2/r_{ik} - 2 \int 2\bar{u}_k''^2/r_{ik}\,dv_k) \right] \qquad (4)$$

We shall show the non-diagonal components of this matrix, at least those connected with one-electron transitions, to be very small. For to an approximation, in a one-electron transition, say of the jth electron, only u_j changes, the other u's remaining unchanged; u_j' and u_j'', on the other hand, are approximately orthogonal to each other, so that ψ' and ψ'' are orthogonal. We readily see that the only terms of Eq. (4) which survive are

$$H'' = \tfrac{1}{2} \sum_{(k,k\neq j)} \left(\int 4u_j' u_j'' u_k''^2/r_{jk}\,dv_{jk} - \int 4u_j' u_j'' \bar{u}_k''^2/r_{jk}\,dv_{jk} \right) \qquad (5)$$

Plainly this differs from zero only to the small extent to which $\Sigma_{(k,k\neq j)} \int u_k''^2/r_{jk}\,dv_k$ differs from $\Sigma_{(k,k\neq j)} \int \bar{u}_k''^2/r_{jk}\,dv_k$; a difference which we shall show later to be very small, appreciable in first order terms, but negligible in second order terms. Thus the second order energy, which involves squares of these non-diagonal components, is quite negligible. It is instructive to compare this result with what we should have if in the unperturbed wave function the mutual shielding effect of the electrons were not taken into account by Hartree's method. Then the last term of Eq. (5) would be absent, and the almost exact cancellation which we have here would not occur. From the nature of the cancellation in Eq. (5), it seems highly probable that Hartree's method is the best method using central fields that can be found, from the standpoint of making the non-diagonal terms of H small.

For comparison with Hartree's results, we wish, not the energy of the stationary state, but the ionization potentials, the differences between the energy of the atom and that of the ion with a particular electron removed. To do this, we must solve also for the energy of such an ionic state, and subtract. Following Hartree, we shall not assume the problem of the ion to be separately solved (except in the case of optical spectra, for which the procedure is somewhat different, and will be explained later). Rather we take as an approximate solution of the ionic problem the product of the atomic wave functions of all the electrons except that which is removed. This neglects the rearrangement of the orbits when one electron is removed, on account of the lost shielding of that electron. We may therefore expect this wave function to be a much less accurate solution of the ionic problem than the complete function is of the atomic problem; an expectation which is verified when we compute the energy, for now the non-diagonal terms of the matrix, and the second order term of E computed from them, are of an altogether larger order of magnitude than before.

The energy operator for the ion with the ith electron removed is

$$H^i = -\nabla^2 + \tfrac{1}{2}\sum_{(j,k;j\neq k;j,k\neq i)} 2/r_{jk} - Z\sum_{(j,j\neq i)} 2/r_j \tag{6}$$

where this ∇^2 does not include derivatives with respect to the coordinates of the ith electron. That is,

$$H - H^i = -\nabla_i^2 + \sum_{(k,k\neq i)} 2/r_{ik} - 2Z/r_i \tag{7}$$

This operator, averaged over the wave function in the proper fashion, will give the negative of the ionization potential which we desire. We should properly average H over the wave function of the atom, H^i over that of the ion; but as H^i does not involve the coordinates x_i in any way, the terms in u_i merely integrate to unity. Thus we may find the matrix of the ion by integrating H^i over the atomic wave function. Then

$$(H - H^i)'' = \int \psi'(-\nabla_i^2 + \sum_{(k,k\neq i)} 2/r_{ik} - 2Z/r_i)\psi'' dv \tag{8}$$

This may be put in different form by using Eq. (1); for from it

$$(-\nabla_i^2 + \sum_{(k,k\neq i)} 2/r_{ik} - 2Z/r_i)\psi'' = \left[\epsilon_i + \sum_{(k,k\neq i)}\left(2/r_{ik} - \int 2\bar{u}_k''^2/r_{ik}dv_k\right)\right]\psi''.$$

Thus

$$(H - H^i)'' = \int \psi'\psi'' dv\epsilon_i + \sum_{(k,k\neq i)} \int \psi'\psi''\left(2/r_{ik} - \int 2\bar{u}_k''^2/r_{ik}dv_k\right)dv \tag{9}$$

From Eq. (9), one can see to what extent Hartree's assumption is justified, that $-\epsilon_i$ measures the ionization potential of the ith electron. The

true ionization potential is determined from (9) as the sum of, first, the diagonal term; second, a combination of terms involving resonant interchanges between two electrons; third, second and higher order terms coming from products of non-diagonal terms. Now if the ψ's corresponding to different states, and to states with interchange of electrons, were orthogonal (as they nearly are), the first term of (9) would give just $-\epsilon_i$ for the ionization potential. Thus the error in Hartree's assumption comes principally from the second term. This term leads to contributions of the types mentioned earlier in the paper: (1) its diagonal terms are not zero, because $u_k''^2$ and $\bar{u}_k''^2$ are not the same; (2) its terms corresponding to resonant interchange of electrons are not zero, on account of the non-vanishing of $\int\psi'\psi''2/r_{ik}dv$; (3) its non-diagonal terms are not zero, resulting in a second-order term in the ionization potential. We see, however, that there is no large first order error coming from the use of an incorrect wave function for the ion; the process of averaging H^i over the wave function has made correction for this to the first order, only the second order error remaining. This is an instructive example of the value of the perturbation method of averaging H over an unperturbed orbit. The average, say, of the potential energy over the incorrect wave function would show considerable errors, on account of the excessive size of the outer shells as described by the incorrect wave function; but the average of the kinetic energy compensates this, to the first order, leaving an error of smaller order in the whole energy.

3. In investigating Hartree's method more closely, we next try to estimate the size of the various errors discussed above. In the present section we shall compute the first-order terms in the ionization potential. First is the diagonal term. This, from (9), is

$$(H-H^i)''=\epsilon_i+\sum_{(k,k\neq i)}\int u_i^2dv_i\int 2(u_k^2-\bar{u}_k^2)/r_{ik}dv_k \qquad (10)$$

The second term of (10), arising from the fact that u_k^2 is not spherically symmetrical, contains many terms which cancel each other, and in some cases it is strictly zero. For, as Unsöld[3] has shown, and as Hartree mentions, in any closed shell, the total distribution is spherically symmetrical. Thus if we write this term as $\int u_i^2dv_i\Sigma_{(k,k\neq i)}\int 2(u_k^2-\bar{u}_k^2)/r_{ik}dv_k$, and take the sum over all the electrons of a closed shell not including the ith electron, we shall have zero. The only contribution, then, comes from the other electrons in the same shell with the ith electron. Now the charge of these electrons, increased by that of the ith, must add to make a spherical shell, by what we have just said; thus they by themselves have charge in excess of the average where the ith electron is deficient, and have a deficiency where the ith has excess charge. Thus the density represented by $\Sigma_{(k,k\neq i)}(u_k^2-\bar{u}_k^2)$ is negative where the ith electron has large density, and positive where the ith has small density. In computing the integral, then, the regions where r_{ik} is small, and the integrand is large, will make negative contributions to

[3] A. Unsöld, Ann. d. Phys., **85**, 355 (1927).

the integral, while those with small integrands will make positive contributions; as a result, the integral is negative. It then results in a decrease in ϵ_i or an increase in ionization potential.

In two important cases, the second term vanishes exactly. These are first the case of a valence electron outside closed shells (so that this error is not met in Hartree's calculation of optical terms); and second the case of an s electron, where the other electron in the same shell has exactly a spherically symmetrical distribution. Thus this term is not met in the K shell, or the L_1 or M_1. On the other hand, in the L_2 shell, and other similar ones, such a term would be present. To estimate its importance, it has been calculated for the 2_2 shell of Rb, using Hartree's values of the field. The actual wave functions are the function of r given by Hartree, multiplied by certain spherical harmonics of the angles. Taking account of them, we find that the second term of (10) is respectively—1/25 and—4/25 times 5.46 (in terms of Rh) for the transitions in which a 2_2 electron with $m=1$ or $m=0$ is removed from the L shell. The first term (1/25 or 4/25) comes from integration of the spherical harmonics, and is of course different in the two cases because the states with $m=1$ and 0 have different distributions of charge; the second term (5.46) comes from an integration over the functions of r, an integration which should give a result resembling the interaction energy of one 2_2 electron on itself (which, as Hartree states, is about 12 units), but should be decidedly smaller.

In addition to the diagonal terms of the matrix (9), there are other terms entering the first order energy, arising from resonant interchanges of pairs of electrons. Suppose one denote the matrix component of H, connected with an interchange of the mth and nth electron, as H_{mn}. Then one can show, by the group theory developed by Wigner, Hund, Heitler[4] and others, that for an atom consisting of closed shells of electrons, except for a possible excess or deficiency of one electron (the only kind we need consider), the first order energy is the diagonal term of the matrix, decreased by the sum of the H_{mn}'s for all pairs of electrons which have spins in the same direction. In the difference between the energy of atom and ion, then, will appear, with a negative sign, the sum of all terms H_{mn} connected with interchange of the electron which is removed, and other electrons with spins in the same direction. Thus we have for the first order ionization energy the diagonal term (10), already found, with additional correction for the resonance terms:

$$E-E^i=(H-H^i)''-\sum_{(k,k\neq i;\ \text{spin } k \text{ par. to spin } i)}H_{ik}. \tag{11}$$

The last term in (11), arising from resonant interchange of electrons, can be shown to be small, though not strictly zero, in several important cases. One has

$$H_{ik}=\int 2u_i'u_i''u_k'u_k''/r_{ik}dv_{ik} \tag{12}$$

[4] E. Wigner, Zeits. f. Phys., **40**, 883; **43**, 624 (1927).
F. Hund, Zeits. f. Phys., **43**, 788 (1927).
W. Heitler, Zeits. f. Phys., **46**, 47 (1927).

where u_i' and u_k'' mean the same function, but of different arguments, and similarly u_i'' and u_k' mean the same function, although different from the previous one. Obviously this term, then, can be large only for interaction between electrons whose wave functions overlap considerably. Now the K electrons on the one hand, and the valence electron on the other, do not spend any large fraction of their time in a region where there are other electrons; thus the interaction terms for them are small. There is no term for interaction of one K electron with the other, because their spins are antiparallel. For electrons between the two extremes, however—the L, M, N shells, etc.—the resonance terms can be of considerable importance. Naturally the largest terms of this kind will come from the interchange of two electrons in the same shell, for their wave functions differ only in the spherical harmonic part; for two electrons in different shells, the wave functions differ also in the function of r, so that these terms are less important. As an estimate, the resonance terms for a 2_2 electron of Rb, coming from interaction with other 2_2's, have been calculated. These prove to be the product of—9/25 or—6/25 (the first for the removal of an electron with $m=1$, the second with $m=0$) with the same quantity 5.46 found above.

The sum of the two first order correction terms, for the L shell of Rb, is thus $(-1/25-9/25)\times 5.46$ for an electron with $m=1$, or $(-4/25-6/25)\times 5.46$ for an electron with $m=0$; that is, in either case, $2/5\times 5.46=2.2$ units. We should expect the correct ionization potential of a 2_2 electron to be, then, what Hartree finds (about 137 units), increased by 2.2 units. As a matter of fact, Hartree's value itself is in almost perfect agreement with experiment; but this seems to be a coincidence, to judge from his other figures, and the errors seem to be of the order of one or two units, so that the value we have found appears to be of the actual order of the errors of Hartree's method. For M electrons, and others, we should naturally suppose the errors from these terms to be less than for L orbits (on account of the smaller interaction of an M electron on itself); thus it seems likely that the errors introduced by the extra terms in the first order energy are in any case of the order of magnitude of the discrepancy between Hartree's calculations and experiment. It does not seem to be true, however, that one improves the agreement with experiment by making these corrections.

One fact of great theoretical interest was met in the last paragraph: the fact that, when both sorts of first order corrections are taken into account, the ionization potential for either an electron of $m=1$ or $m=0$ is the same. This means that the ion has the same energy, whatever kind of 2_2 electron is missing from the completed shell. The ionized shell is degenerate, and degenerate in just the same way that a single 2_2 electron would be. It is this fact that leads to the result that the interaction of a shell lacking one electron with the spins is just like the interaction of a single electron with its spin, so that the L terms of x-rays are doublet terms. The degeneracy in this case, however, does not seem to be obvious, as it is with a single electron; one can see this by noting that the remaining electrons of the shell provide an axis in a definite direction, or by remembering the way in which the

interaction energy is built up, of terms which separately are different for the different values of m.

4. In the last section, we discussed the first order ionization potentials, and showed the extent of the error which Hartree makes in his assumption as to the value of these quantities. Now we must consider the remaining error, arising from the second order energy. In finding this, which is a quadratic term, it is not at once allowable to use the matrix components of $H-H^i$, from (9); we should rather find separately the non-diagonal components of the separate matrices for H and H^i, work out their individual second-order terms, and subtract. But as we saw earlier, the non-diagonal terms of H are small compared with those of H^i, so that the non-diagonal terms derived from (9) are essentially those of H^i itself. Since this appears with negative sign, we are justified in computing the second order energy in the usual way from the matrix of (9), except that we must use the opposite sign to the usual one. Thus we have, from ordinary perturbation theory,

$$(E-E^i)_2 = -\sum{}''\{(H-H^i)'\,''(H-H^i)''\,'/(E'-E'')\}. \tag{13}$$

In one other respect, this problem differs from the ordinary one of perturbation theory: the matrix of $H-H^i$ is not the integral of one given function over the wave functions; the function is different (on account of the term $\int 2\bar{u}_k''^2/r_{ik}dv_k$) for each stationary state. Closer examination shows that this is to be taken care of by using $\bar{u}_k'^2$ in each of the components occurring in (13).

In finding the matrix components $(H-H^i)'\,''$ from (9), one notes first that the essential contributions come from the second term of (9), since ψ' and ψ'' are practically orthogonal; next, only those transitions for which some other electron than the ith changes its quantum number, have large components. For if the ith alone changes, ψ' and ψ'' differ essentially only in having different factors u_i' and u_i''. The summation in (9) then is $\int u_i'u_i''dv_i\Sigma_{(i,k,i\neq k)}\int 2(u_k^2-\bar{u}_k^2)/r_{ik}dv_k$. On account of the small difference between the actual distribution of charge and a spherical distribution (a difference of zero if the ith electron is the valence electron) this is small. We then consider only transitions of the electrons other than the ith. If, say, the pth has a transition, we have

$$(H-H^i)'\,'' = \int u_i^2dv_i\int u_p'u_p''\left(2/r_{ip}-\int 2\bar{u}_p'^2/r_{ip}dv_p\right)dv_p \tag{14}$$

We shall be able to interpret this term better after considering the optical case, in which it has a simple meaning.

For the valence electron, Hartree proceeds somewhat differently from what he does in other cases. He does not carry through a calculation of his problem for each energy level; instead, he solves the problem of the ion, and uses the central field determined from it for the atomic computation, neglecting therefore the reaction of the valence electron on the ion. The second-order error in the problem then comes in the energy E of the atom,

rather than in the E^i of the ion. For this electron, then, we need make no change in (13) except to change the sign. With this change, we shall show that the term represents, in a somewhat unsatisfactory way, the energy change on account of polarization of the ion by the valence electron. To demonstrate this, we may most conveniently consider a non-penetrating orbit, in which u_i^2 is not appreciable except for large values of r_i. Then, since $\bar{u}_p'^2$ represents a distribution which is spherical, and is practically all inside the radius r_i, we have very closely

$$2/r_{ip} - \int 2\overline{u_p''^2}/r_{ip}dv_p = 2/r_{ip} - 2/r_i.$$

We can next expand $2/r_{ip}$ in series in $1/r_i$:

$$2/r_{ip} = 2/r_i + 2r_p \cos(r_i, r_p)/r_i^2 \cdots.$$

Since the first of these terms cancels, we have essentially the second left, giving

$$(H - H^i)'' = \int 2u_i^2/r_i^2 dv_i \int u_p' u_p'' r_p \cos(r_i r_p) dv_p. \tag{15}$$

Thus the second order energy is

$$(E - E^i)_2 = 1/2\left[\int 2u_i^2/r_i^2 dv_i\right]^2 \sum''\left\{2\left[\int u_p' u_p'' r_p \cos(r_i, r_p) dv_p\right]^2 / (E' - E'')\right\} \tag{16}$$

The second term is recognized as the polarizibility of the ion; the first is, not the average of $1/r_i^4$, as we should expect, but the square of the average of $1/r_i^2$ (the numerical factor 2 in $2/r_i^2$ arises from our units). With this difference, the term is just the sort of polarization term that Hartree wished, to explain the discrepancy between observation and experiment. It results, one notices, in a decrease of $E - E'$ (on account of the negative sign of all terms $E' - E''$) or an increase of ionization potential.

The fact that this introduces a polarization term depending on the square of the average of $1/r_i^2$, instead of on the average of $1/r_i^4$, is to be interpreted as an error inherent in the method. The effect depends on the distortion of the inner orbits by the valence electron; and since the wave function we use is one obtained by separation of variables, so that the function for the inner electrons must not depend on the instantaneous position of the valence electron, the distortion effect must be the average of that produced by the valence electron at the different points of its orbit, giving the average of $1/r_i^2$. Thus when we average the change of energy on account of this distortion, over the orbit of the valence electron, we find the other factor $1/r_i^2$. When one calculates, it is found that for the important optical orbits $(\overline{1/r_i^2})^2$

and $\overline{1/r_i^4}$ differ by about a factor of 2, so that this difference makes a considerable error in the method, even when carried to the second order. That the correct polarization energy involves $\overline{1/r}^4$ is shown by the success of Waller's[5] calculations for helium.

Having seen that the second order term for the valence electron refers to polarization, we can return to the case of the other electrons. There evidently the same physical situation exists, the term representing the polarization of the atom, now not by an outer electron, but by one inside it. Since the electron is so much closer the atom, it might seem that the $1/r^4$ term would make the effect very large; but it is easy to see, directly from (14), that after a variable electron penetrates a shell, the polarization energy of this shell does not increase much more when the electron approaches the nucleus. It is possible to estimate the size of the energy actually present in such a case, by approximating to the polarizibility of the various shells; and it is found that the total correction for this effect, for the inner electrons, is of the same order of magnitude as the corrections found in section 3; not only that, but they are of the opposite sign, making a decrease in ionization potential (on account of the fact that the summation in (13), which is itself negative, has a negative sign). Thus it seems actually possible that the two effects, the first order and second order corrections, partly cancel, and that Hartree's excellent agreement in the x-ray terms arises in this way. Whether this is true or not, we see that none of the corrections to Hartree's terms are really much larger than the order of magnitude of his discrepancies from experiment, so that his good agreement with observations is justified.

JEFFERSON PHYSICAL LABORATORY,
HARVARD UNIVERSITY,
May 31, 1928.

[5] I. Waller, Zeits. f. Phys., 38, 635 (1926).

THE NORMAL STATE OF HELIUM

By J. C. Slater

Abstract

An approximate wave function for normal helium is calculated, by using theoretically determined functions for the limiting cases of large and small r's and interpolating between them. The charge density computed from this wave function is in good agreement with that found independently by Hartree. The diamagnetism of normal helium is calculated, and agrees with observation within the experimental error. The repulsive forces between two helium atoms are calculated by the method of Heitler and London, and the attractive Van der Waals forces are roughly estimated from Wang's results with hydrogen. The potential curve so found gives a "molecular diameter" in agreement with experiment, and the minimum of the curve leads to approximately correct density and boiling point for the liquid.

THE present paper describes an attempt to find a fairly accurate wave function for the normal state of the helium atom, and to apply this to the computation of several properties of atomic helium, in particular to its diamagnetic susceptibility, and to the forces of repulsion between two normal helium atoms. The method adopted is practically that described in a previous paper:[1] when one electron is at a considerable distance, the other close up, the variables are assumed to be separable, the wave function being a product of an ionic function of the inner electron, and a hydrogen-like function of the outer one, the energy constant for the latter being taken from the experimental term value. When both electrons are close up, the function is taken to be a simple form, described in the previous paper, which the actual wave function approaches in the limit as the electrons both approach the nucleus. Between these two limits, simple interpolations are used. It is plain that the method is not one for calculating the energy of the normal state; we easily convince ourselves, however, that the experimental energy is the true characteristic number of the wave problem, by observing that the functions described above, for large and small r's, join much more smoothly than they would if a different energy value were assumed. The calculations were made before the writer saw Hartree's[2] paper, in which he obtains a charge density distribution for helium in quite a different way. The wave function found in the present paper is more complicated than Hartree's in the matter of the way in which it takes the interaction energy between electrons into account. But the charge density can be computed equally well from either method, and this permits a comparison of the present results with Hartree's. The discrepancies between the two are nowhere greater than one or two percent. This is highly satisfactory, both in that it verifies the present method and Hartree's, and also that

[1] J. C. Slater, Phys. Rev., **31**, 333 (1928).

[2] D. R. Hartree, Proc. Camb. Phil. Soc., **24**, p. 89, 1928.

it justifies us in believing this density distribution to be correct within a narrow limit of error. The other numerical results are also gratifying: the diamagnetic susceptibility agrees with the experimental value within a percent and a half, and the results for collisions of two atoms agree with experiment within the rather wide limit caused by uncertainties in the kinetic theory treatment of the imperfect gas problem.

1. The Wave Function

We assume that, for r_2 small, r_1 large, the wave function approaches $e^{-2r_2}\times$a function of r_1, the latter being that solution of the hydrogen problem which corresponds to the term value of normal helium (1.805 Rh), and remains finite at infinity. This function is easily found in a series expansion as the confluent hypergeometric function of Sugiura[3] and others. We seek a solution of Schrödinger's equation for the hydrogen problem in descending powers of r; the solution is

$$u=e^{-r/n^*}r^{(n^*-1)}(1+a_1/r+a_2/r^2\cdots)$$

where

$$a_n=-(n^*/2n)((n^*-n)(n^*-n+1)-k(k+1))a_{n-1}$$

$n^*=1/(-E)^{1/2}$, $E=$term value (in terms of Rh), $k=$azimuthal quantum number, and r's are expressed as multiples of the radius of the first Bohr orbit.

Putting in, for normal helium, $E=-1.805$ (the experimental value), $k=0$, we have $n^*=.745$, $a_1=.0707$, $a_2=-.00421$, $a_3=.00149$, etc. Thus our assumption for the wave function with r_1 large, r_2 small, is

$$e^{-2r_2}e^{-1.344r_1}r_1^{-.255}(1+.0707/r_1-.00421/r_1^2+.00149/r_1^3\cdots) \quad (1)$$

For the case when r_1 is small, r_2 large, we may interchange the arguments, since the function must be symmetrical in the coordinates of the two electrons.

When both r's are small, we take as the wave function

$$e^{-2(r_1+r_2)+1/2r_{12}} \quad (2)$$

This is the function introduced in the previous paper, and can be obtained as follows: we try to satisfy the wave equation as closely as possible at small r's by a function which is e raised to a linear combination of r_1, r_2, and r_{12}. By choosing the coefficients as in (2), we satisfy the wave equation as far as terms of the zero order in the r's, while with any other choice of coefficients, the errors are of the order of $1/r$.

We now introduce a small correction term in (2), to make it join on smoothly to (1) along the line in configuration space given by $r_2=0$. Along this line, $r_{12}=r_1$, so that (2) becomes $e^{-1.5r_1}$. The correction term which we now apply is a quadratic term in the exponent; we use the function $e^{-1.5r_1+\alpha r_1^2}$. The method of finding the value of α is shown in Fig. 1, where the quantities

[3] Y. Sugiura, Phil. Mag., Ser. 7, **4**, p. 498, 1927.

$d \log u/dr_1$ are plotted for both functions (1) and (2). The correction to (2) changes the curve from a horizontal straight line at 1.5 to a straight line with a slight slope. We naturally choose this line so that it is tangent to the curve (1), for then u'' as well as u' will join smoothly together. One sees graphically that this demands a tangent to curve (1) at about the point $r=3$. When one substitutes numerical values, this gives $\alpha=.0107$. By comparing with the curves of the function (1) for $E=1.70$ and 1.90, we see how much more easily the curve with the correct ionization potential, 1.805, joins on than any other would.

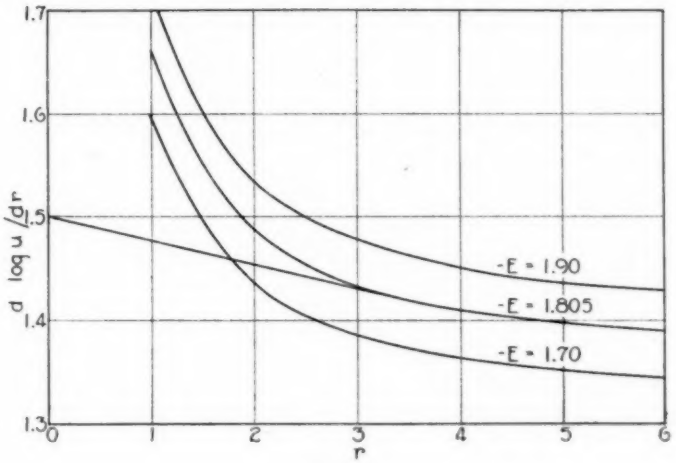

Fig. 1

Having equalized the slopes of the functions (1) and (2) at $r=3$, we must multiply one of them by a constant, so that the functions themselves will join smoothly. We find at once that we must multiply (1) by .8916. Then we have the following results: for $r_2=0$,

$$u=e^{-1.5r_1+.0107r_1^2} \quad \text{for } r_1<3$$

$$=.8916e^{-1.344r_1}r_1^{-.255}(1+.0707/r_1-.00421/r_1^2+.00149/r_1^3\cdots) \quad \text{for } r_1>3.$$

and the whole wave function can be written

$$u=e^{-2(r_1+r_2)+.5r_{12}+.0107(r_1^2+r_2^2)} \quad \text{for } r_1,\ r_2 \text{ small}$$

$$=.8916e^{-2r_2}e^{-1.344r_1}r_1^{-.255}(1+.0707/r_1-.00421/r_1^2+.00149/r_1^3\cdots)$$

$$\text{for } r_1>3,\ r_2 \text{ small}.$$

This function is not determined in detail everywhere; for we have not specified the way in which the two parts of it join, except along the lines $r_1=0$ and $r_2=0$. But this difficulty is not a serious one in most work demanding the function.

Having found a wave function, our next task is to normalize it. To do this, we require the integral of u^2 over the configuration space. The first step

is to integrate u^2 over the volume element of the coordinates of one electron. The result will be the charge density in the sense of Hartree; it is a function of one electron, by which we multiply any function of the coordinates of that electron, and integrate, to get the average of the corresponding function. It is therefore what is generally needed in applying the wave function to specific problems. In two limiting cases, it can be calculated directly; these are the cases where $r_1=0$, and where r_1 is very large. In the first case, we must square the function of r_2 which we obtain by setting $r_1=0$ in u (that is, $e^{-1.5r_2+.0107r_2^2}$ for small r_2, and the other function for large r_2) and integrate over dv_2. This can be carried out without great difficulty, by expanding in series when necessary, and the result is 4π (.07630). The second case, when r_1 is very large, is simpler: there u depends on r_2 only through the term e^{-2r_2}, so that the integration over dv_2 can be immediately carried out, yielding $\int u^2 dv_2=(4\pi/32)u^2(r_1,\ r_2=0)$. Thus in this limit, the integral is proportional to the square of the wave function for $r_2=0$; and it is natural to write in all cases $\int u^2 dv_2=f(r_1)u^2(r_1,\ r_2=0)$. The function f will then approach the value $4\pi/32$ for large r_1; on the other hand, it equals 4π (.07630) for $r_1=0$, a value roughly twice as great. Our problem can be formulated as that of finding $f(r_1)$ for intermediate r_1's.

To a certain degree of accuracy, we can approximate to $f(r_1)$ by assuming u to have the value (2), and actually carrying out the integration over the coordinates of the second electron. This can be done by using elliptic coordinates, and one finds

$$f(r_1)=2\pi\left[(4/15)^2(1-1/4e^{-5r_1})+(4/15)^3(1-e^{-5r_1})/r_1\right]$$

This function approaches $4\pi\ (2/27)=4\pi$ (.07407) rather than 4π (.07360) as the correct function does; this is because, in the integration, the term $e^{.0107r^2}$ in u was neglected. But more serious than this, it approaches quite a wrong value at infinity, $2\pi\ ((4/15)^2+(4/15)^3)=4\pi$ (.0355) rather than 4π (.03215). This is because the function (2) fails decidedly at large distances in the matter of the interaction energy of the electrons. Thus the function f found above can do no more than serve as a general guide in forming a function to approach the proper values at the limits of small and large r_1. It possesses one feature, however, which seems to be of importance: if we expand it about $r_1=0$, the expansion commences with the terms $4\pi(2/27)$ $(1-r_1\cdots)$. That is, the slope at the origin is numerically equal to the function; $f\ (r_1)$ starts off, in other words, as e^{-r_1}. Since $u^2(r_1,\ r_2=0)$ starts as e^{-3r_1} the integral, or $\int u^2 dv_2$ acts as e^{-4r_1}, which is the behavior of the solution of a central-field problem with a nuclear charge of 2 units. This of course is what Hartree's function does; it is of great interest that our solution does the same, and it seems as if this property were one to be retained in the final function f.

We wish, then, an interpolation formula for $f(r_1)$, reducing to 4π (.07630) for $r_1=0$, having a negative slope numerically equal to this at the origin, decreasing asymptotically to 4π (.03125), and having the general form of the function f found above. A function which satisfies all these demands is

the simple exponential interpolation formula $f=4\pi\ (.03125+.04504\ e^{-1.692r_1})$, where there are just enough conditions to determine the constants. Examination of the function shows that it reaches substantially its asymptotic value soon after r_1 passes outside the range of the second electron, a condition which the function should satisfy. Since it seems satisfactory in every way, we are justified in using it.

Taking the value of f just found, we may multiply it by $u^2(r_1,\ r_2=0)$ and obtain an approximation for $\int u^2 dv_2$. Then it is a simple matter to integrate over r_1; and the result is $\pi^2\ (.05233)=\int u^2 dv_1 dv_2$. To normalize our wave function, we must then divide by the square root of this, and the result is

$$\left.\begin{aligned} u&=1.392e^{-2(r_1+r_2)+.5r_{12}+.0107(r_1^2+r_2^2)} \quad \text{for } r_1,\ r_2<3\\ u&=1.241e^{-2r_2}e^{-1.344r_1}r_1^{-.255}(1+.0707/r_1\cdots) \text{ for } r_1>3,\ r_2 \text{ small}\\ u&=1.241e^{-2r_1}e^{-1.344r_2}r_2^{-.255}(1+.0707/r_2\cdots) \text{ for } r_2>3,\ r_1 \text{ small}\end{aligned}\right\} \tag{3}$$

These represent our estimate of the normalized wave function of normal helium. Similarly we have

$$\left.\begin{aligned}\int u^2 dv_2 &= .7604(1+1.440e^{-1.692r_1})e^{-3r_1+.0214r_1^2} \text{ for } r_1<3\\ &= .6048(1+1.440e^{-1.692r_1})e^{-2.688r_1}r_1^{-.510}(1+.1414/r_1-.0034/r_1^2\cdots)\\ &\qquad\qquad \text{for } r_1>3\end{aligned}\right\} \tag{4}$$

The function $\int u^2 dv_2$, given in (4), should be the density distribution of charge, in Hartree's sense; multiplied by 2 (on account of the two electrons of helium), it should give just his dZ/dr. In Table 1 we show a comparison of the values given by both methods; the resemblance is striking. The only difference is a slight tendency of the present function to emphasize the smaller r's at the expense of the larger. It is hard to say which function is to be preferred.

TABLE I.

r	dZ/dr present theory	dZ/dr Hartree	r	dZ/dr present method	dZ/dr Hartree
0	.000	.00	1.6	.468	.48
.1	.314	.30	1.8	.319	.33
.2	.851	.83	2.0	.216	.22
.3	1.307	1.28	2.2	.145	.15
.4	1.605	1.57	2.4	.095	.10
.6	1.745	1.73	2.6	.063	.06
.8	1.544	1.55	2.8	.041	.04
1.0	1.231	1.25	3.0	.026	.026
1.2	.924	.94			
1.4	.664	.68			

2. DIAMAGNETIC SUSCEPTIBILITY

Van Vleck[4] has shown the diamagnetic susceptibility of a monatomic gas to be given by $\chi=-(e^2L/6mc^2)\Sigma\bar{r}^2$ where the summation is the sum of all

[4] J. H. Van Vleck, Proc. Nat. Acad. Sci., **12**, 662 (1926); Phys. Rev. **31**, 598 (1928).

the r^2's of the various electrons, averaged over the orbit. We have $\overline{r_1^2} = \int u^2 r_1^2 dv_1 \; dv_2 = \int dv_1 r_1^2 \int u^2 dv_2$. This shows that we are to use the function (4) in computing such an average. Carrying out the integration, we find $\overline{r_1^2} = 1.1569$ (in terms of a_0^2). Since this also equals $\overline{r_2^2}$, we have $\Sigma \overline{r^2} = 2.3138$. Then $\chi = 1.853 \times 10^{-6}$. The experimental value of Wills and Hector[5] is 1.88×10^{-6}. The discrepancy is but $1\frac{1}{2}$ percent. Whether it is on account of experimental error, or from inaccuracy in the calculations, one cannot see. The uncertainty in the wave function indicated by the difference between the two functions of Table I would account for an error of about this magnitude. For comparison, we note that Wang's[6] calculation of χ, using Kellner's wave function, is 1.53×10^{-6}, with an error of 20%. The great advantage of the present function, in point of accuracy, is obvious.

3. Forces Between Atoms

Heitler and London[7] have discussed the repulsive forces between atoms, indicating that the electronic wave functions for two atoms near to each other must be taken as linear combinations of the wave functions of the individual atoms, and showing that the average of H over this combined wave function (giving the first order perturbation energy) results in a repulsive energy increasing rapidly as the atoms approach, in case each atom contains electrons only in closed shells. This is an interference effect of the waves of the two, becoming appreciable only to the extent to which the wave functions actually overlap, so that it decreases exponentially with the distance. In addition, Wang[8] has treated the second order perturbation energy between two hydrogen atoms, showing that it contains an inverse sixth power attractive energy. (The writer is indebted to Dr. H. A. Kramers for the information that this effect was discussed some time ago in lectures by Dr. Pauli). This term is, in a certain way, a Debye attraction of the variable electric moment of one atom (the variable terms are not zero, even in the normal state, although the diagonal term is) for the dipole which it induces in the other atom. The first of these terms gives the repulsion of atoms at close distances, resulting in their impenetrability; the second results in the Van der Waals attraction at large distances. The former can be calculated from the knowledge of the normal state alone; and this calculation is given in the present paper. It is unsatisfactory in some details, on account of the mathematical difficulty, but is probably a fairly accurate deduction from the assumed wave function. The other term, being a second order one, demands a knowledge of the other wave functions as well, so that no exact calculation is possible. We content ourselves with a rough estimate from Wang's value for hydrogen, taking account of the differing size and polarisibility (as determined experimentally) of helium. The results are in rough agreement with the values found from kinetic theory;

[5] Wills and Hector, Phys. Rev., **23**, 209 (1924); **24**, 418 (1924).
[6] S. C. Wang, Proc. Nat. Acad. Sci., **13**, 798 (1927).
[7] Heitler and London, Zeits. f. Physik, **44**, 455 (1927).
[8] S. C. Wang, Phys. Zeits., **28**, 663 (1927).

from the equilibrium position of two atoms under the attractive and repulsive forces, we can estimate the density and boiling point of the liquid; and from the distance to which atoms with the average temperature energy would approach, we compute a molecular diameter. These results are in as close agreement with experiment as would be expected, when we consider the various errors in the calculations.

We shall now consider the first order term in the interaction energy. The first step is to set up the correct unperturbed wave function. Let us suppose that the wave function for the atom a by itself, with the electrons 1 and 2 in it, is $u_a(1, 2)$. This is to be taken, say, as the function of r_1 and r_2 described in (3), where r_1 is the distance of the 1st electron from the nucleus a, etc. It is symmetric in the coordinates 1 and 2, so that $u_a(1, 2) = u_a(2, 1)$. Similarly for an atom b with electrons 3 and 4, the wave function is $u_b(3, 4)$. A conceivable unperturbed wave function for the problem of four electrons would be $u_a(1, 2)u_b(3, 4)$. But this is not the proper wave function. We have instead, if we assume the function in which the electrons 1 and 3 have their spin in one direction, 2 and 4 in the opposite direction, the combination which is anti-symmetric in the electron coordinates 1 and 3, and also in 2 and 4:

$$u_a(1,2)u_b(3,4)-u_a(1,4)u_b(2,3)-u_a(2,3)u_b(1,4)+u_a(3,4)u_b(1,2).$$

Now when we square the wave function, to use either for normalization or for integrating H, terms of three kinds arise: diagonal terms, as $u_a^2(1, 2)$ $u_b^2(3, 4)$; terms corresponding to the interchange of two electrons, one in each atom, as $u_a(1, 2)u_b(3, 4)u_a(1, 4)u_b(2, 3)$; and terms corresponding to the interchange of all four electrons, as $u_a(1, 2)u_b(3, 4)u_a(3, 4)u_b(1, 2)$. There are four terms of the first type, eight of the second (each with negative sign), and four of the third (with positive sign). The second type of term is large only in that part of configuration space in which an electron of each atom (here the 2d and 4th) have both considerable probability of being found; the third is large only where all four electrons are likely to be found at once. Thus, for a moderate separation of the nuclei, the second term varies, so to speak, directly as the amount of penetration of one atom by the other; the third as the square of this. For this reason, the latter is small, and we may neglect it in our approximate calculations. We thus have, if

$$I_1 = \int u_a^2(i,j)u_b^2(k,l)dv = 1 \text{ (by normalization of separate } u\text{'s)}$$

$$I_2 = \int u_a(i,j)u_b(k,l)u_a(i,l)u_b(k,j)dv$$

that the normalization integral is $4\ I_1 - 8\ I_2$. Similarly if H is the perturbation energy, and

$$H_1 = \int Hu_a^2(i,j)u_b^2(k,l)dv$$

$$H_2 = \int H u_a(i,j) u_b(k,l) u_a(i,l) u_b(k,j) dv$$

the integral of H is $4H_1 - 8H_2$. Thus the first order perturbation energy is $(H_1 - 2H_2)/(I_1 - 2I_2)$.

We first evaluate I_2. In carrying this out, we meet certain approximations which we must make in each such integral. The integrand is large only at points corresponding to arrangements of electrons in which two electrons, the jth and lth, have considerable probability of belonging to either atom. Since the atoms are assumed to be some little distance apart, this means that these two electrons must be in the region between the two nuclei, at a considerable distance from either nucleus. For the integrand to be large, then, the other two electrons, the ith and kth, must be fairly close to the ath and bth nucleus respectively. Thus in the essential region, $u_a(i, j)$ or $u_a(i, l)$ correspond to the case where electron i is close, electron j or l far away, with a corresponding situation for the u_b's. Then we can approximately use the forms, from (3),

$$u_a(i,j) = 1.241 e^{-2r_{ai}} e^{-1.344 r_{aj}} r_{aj}^{-.255} (1 + .0707/r_{aj} \cdots)$$

$$u_a(i,l) = 1.241 e^{-2r_{ai}} e^{-1.344 r_{al}} r_{al}^{-.255} (1 + .0707/r_{al} \cdots)$$

and similarly for the other u's. We can immediately integrate over dv_i (and similarly over dv_k), obtaining

$$\begin{aligned}\int u_a(i,j) u_a(i,l) u_b(k,j) u_b(k,l) dv_i dv_k \\ = (.6048)^2 e^{-1.344 r_{aj}} r_{aj}^{-.225} (1 + .0707/r_{aj} + \cdots) e^{-1.344 r_{al}} r_{al}^{-.255} \\ (1 + .0707/r_{al} \cdots) e^{-1.344 r_{bj}} r_{bj}^{-.255} (1 + .0707/r_{bj} \cdots) \\ e^{-1.344 r_{bl}} r_{bl}^{-.255} (1 + .0707/r_{bl} \cdots).\end{aligned}$$

Thus we have

$$I_2 = [.6048 \int e^{-1.344(r_{aj} + r_{bj})} (r_{aj} r_{bj})^{-.255} (1 + .0707/r_{aj} \cdots)(1 + .0707/r_{bj} \cdots) dv_j]^2$$

$$= \left[\int u_a u_b\right]^2 \text{ (for abbreviation)}$$

We make a further approximation, by neglecting all except the constant term, in the summations at the end. The remaining integral can be evaluated by using elliptical coordinates. If $R = r_{ab}$, $\lambda = (r_{aj} + r_{bj})/R$, $\mu = (r_{aj} - r_{bj})/R$, $\rho = 1.344\ R$, we have, since $dv = \pi/4\ R^3(\lambda^2 - \mu^2) d\lambda d\mu$ in these coordinates,

$$\int u_a u_b = .6048\pi/4R^3 \int\int e^{-\rho\lambda} (R/2)^{-.510} (\lambda^2 - \mu^2)^{.745} d\lambda d\mu$$

$$= .6765 R^{2.49} \int\int e^{-\rho\lambda} (\lambda^2 - \mu^2)^{.745} d\lambda d\mu,$$

where λ goes from 1 to ∞, μ from -1 to $+1$. The integration cannot be carried out directly. We therefore adopt an approximate method. We may write the integrand $e^{-\rho\lambda}(\lambda^2-\mu^2)^k$ with $k=.745$. Now the integration can be carried out exactly for integral values of k, and the result is a uniformly varying function of ρ and k. We find this for a number of values of k, and interpolate for $k=.745$. We have

$$\int u_a u_b = .6765R^{2.49}2e^{-\rho}/\rho[1] \quad \text{for } k=0$$

$$= .6765R^{2.49}2e^{-\rho}/\rho[2/3+2/\rho+2/\rho^2] \quad \text{for } k=1$$

$$= .6765R^{2.49}2e^{-\rho}/\rho[8/15+8/3\rho+32/3\rho^2+24/\rho^3+24/\rho^4] \text{ for } k=2, \text{etc.}$$

By plotting the coefficients of the powers of $1/\rho$ against k, we can interpolate for the coefficients for $k=.745$, and the result is

$$\int u_a u_b = .6765R^{2.49}2e^{-\rho}/\rho[.725+1.675/\rho+.20/\rho^2]$$

From this result, I_2 can be immediately found.

Next it is convenient to find H_2, since it involves the same sort of integrals as I_2. For this, we have, where H is the perturbation energy,

$$Hu_a(i,j)u_b(k,l) = [8/r_{ab}-4/r_{bi}-4/r_{bj}-4/r_{ak}-4/r_{al} + 2/r_{ik}+2/r_{il}+2/r_{jk}+2/r_{jl}]u_a(i,j)u_b(k,l).$$

We multiply by $u_a(i,l)u_b(k,j)$ and integrate over the ith and kth electrons. In this integration, the term $4/r_{bi}$ (or $4/r_{ak}$), multiplied by $e^{-4r_{ai}}$ (or $e^{-4r_{bk}}$) represents the potential of the spherical charge distribution $e^{-4r_{ai}}$ at the point b. Now we may reasonably say that b is entirely outside this distribution; for the distribution e^{-4r} decreases so much faster than that of the other electron, $e^{-2.688r}$, that although the latter distributions overlap appreciably in the region between nuclei, the former will not appreciably extend to the other nucleus. Thus in these terms, by the fundamental properties of the potential of spherical distributions, we may replace $4/r_{bi}$ (or $4/r_{ak}$) by $4/r_{ab}$. Similarly in the term $2/r_{ik}$, one electron is definitely attached to the one nucleus, the other to the other, without overlapping, so that we may replace this by $2/r_{ab}$. In the terms $2/r_{il}$, $2/r_{jk}$, one electron (the ith or kth) is definitely attached to one nucleus, the other wanders with greater freedom. By the same arguments used above, we may replace them to a good approximation by $2/r_{al}$, $2/r_{bj}$. Then we have approximately

$$H_2 = \int u_a(i,l)u_b(k,j)Hu_a(i,j)u_b(k,l)dv$$

$$= \int u_a(i,l)u_b(k,j)u_a(i,j)u_b(k,l)dv[2/r_{ab}-2/r_{al}-2/r_{bj}+2/r_{jl}]$$

The result is just as if we considered the interaction energy only of the pair of electrons in resonant interaction, concentrating the other electron of each atom at its nucleus.

In carrying out the integrations, we may now integrate over the ith and kth electrons as before. The first term gives $2\ I_2/r_{ab}$. The second and third unite to give $-4\int u_a u_b f(u_a u_b/r_{al})$ where $\int(u_a u_b/r_{al})$ is an abbreviation for

$$.6048\int e^{-1.344(r_{al}+r_{bl})}(r_{al}r_{bl})^{-.255}/r_{al}(1+.0707/r_{al}\cdots)(1+.0707/r_{bl}\cdots)dv_l.$$

The latter integral we evaluate much as we did $\int u_a u_b$. The result is approximately

$$\int(u_a u_b/r_{al}) = .6765R^{2.49}(2/R)(2e^{-\rho}/\rho)[1.15+.22/\rho].$$

The last term of H_2 is, after carrying out the integration over the ith and kth electrons,

$$2(.6048)^2\int(e^{-1.344(r_{aj}+r_{bj}+r_{al}+r_{bl})}/r_{jl})(r_{aj}r_{bj}r_{al}r_{bl})^{-.255}(1+\text{etc.})dv_j\,dv_l.$$

If it were not for the term raised to the power $-.255$, this would be essentially the same integral as that evaluated by Sugiura.[9] The presence of this term can be allowed for as with the other integrals, by letting $k=1-.255$, integrating for integral values of k, and interpolating. On account of the difficulty of this integration, even for integral k's, we content ourselves with a linear interpolation between $k=0$ and $k=1$. For $k=1$, the result is essentially the same as Sugiura's; we have the term

$$=(16/5)(.6765)^2R^{3.98}\rho^{-5}[-e^{-2\rho}(-25/8+23\rho/4+3\rho^2+\rho^3/3)$$
$$+(6/\rho)\{S(C+\log\rho)+S'E_i(-4\rho)-2(SS')^{1/2}E_i(-2\rho)\}]$$

where

$$S=(1+\rho+\rho^2/3)^2e^{-2\rho},\ S'=(1-\rho+\rho^2/3)^2e^{2\rho},\ C=.5772.$$

For $k=0$, by methods essentially similar to Sugiura's, we find

$$(16/5)(.6775)^2R^{3.98}\rho^{-5}[(5/2)\rho^2\{e^{-2\rho}/2(C+\log\rho)$$
$$-E_i(-2\rho)+e^{2\rho}/2E_i(-4\rho)\}].$$

We take as the result the linear interpolation between these two functions (which, when worked out, are not very different, so that the interpolation is not a doubtful one). By putting all these terms together properly, we find H_2.

[9] Y. Sugiura, Zeits. f. Phys., **45**, 484 (1927).

Finally we must evaluate H_1, the diagonal term. Since this is not a particularly large term, and since its calculation involves no particular difficulties, we merely state the result, which is

$$H_1 = e^{-2\rho}[2.10R^{-.510}(1+1/2\rho\cdots)-1.458R(.81+2.13/\rho\cdots)].$$

The second term preponderates, giving a negative energy. This term, however, is never of a size at all comparable numerically with H_2, which is positive, and results in a repulsion.

When we compute the first order energy of interaction, from the complicated formulas found above, it appears that it is a simple function of the distance, always repulsive, increasing very rapidly as the distance decreases. It is in fact possible to approximate very accurately to the complicated result by a simple exponential expression, without theoretical significance, but nevertheless very useful. This is the following: Potential of two helium atoms at distance $r =$

$$7.70\times10^{-10}e^{(-r(\text{cm})/.218\times10^{-8})} \text{ ergs},$$

where now we have expressed distances in centimeters, energy in ergs. This formula expresses the results of our calculations, with errors no greater than the other errors introduced in the method, for values of r between 1 $A°$ and large distances.

Now that we have derived the first order repulsive energy, we shall try to make a rough estimate of the second order attractive energy. Wang finds that, for two hydrogen atoms, this energy has a leading term of $-(243/28)(2/R^6)$ (where energy is in terms of Rh, distances in terms of a_0). He further interprets the constant as being of the nature of the polarizibility multiplied by the square of an electric moment (this moment representing the variable electric moment of the atom). We may then expect that very roughly the corresponding term of helium will be to the hydrogen term as the ratio of polarizibility, multiplied by the square of electric moment. Now the polarizibility of atomic hydrogen, as computed from the second order Stark effect by Waller,[10] is $.66\times10^{-24}$; for helium, as one can find it simply from measured dielectric constants and refractive indices, it is about $.213\times10^{-24}$. For the ratio of moments, we may roughly take the ratio of the linear dimensions of the atoms. Since the square of the linear dimensions of a shell is inversely proportional to the ionization potential, this means that the square of the moment for helium can be taken roughly 1/1.8 times as great as for hydrogen. Thus our rough estimate for this term is

$$-(243/28)(2/R^6)\times(.213/.66)\times(1/1.8) = -3.11/R^6.$$

Expressing energy in ergs, distances in centimeters, this is $-.67\times10^{-10}/(R/a_0)^6$. This figure is to be regarded as highly uncertain. One could with right say that, since helium has two electrons, hydrogen but one, it should

[10] I. Waller, Zeits. f. Phys., **38**, 635, (1926).

be doubled. On the other hand, one could argue that the square of the moment, which appears in the formula, should be proportional to the polarizibility, so that instead of 1/1.8 as a ratio we should have had another factor .213/.66, resulting in a term about half as great. Thus a factor of 2 either way is not impossible.

We have found the forces between two neutral helium atoms to consist of two terms, one repulsive, the other attractive:

$$\text{Energy} = 7.7\times10^{-10}e^{-2.43/(R/a_0)} - .67\times10^{-10}/(R/a_0)^6.$$

This function has a minimum at $R/a_0 = 5.6$, $R = 3.0\times10^{-8}$ cm. Its value at that point is -1.21×10^{-15} ergs. These figures may be brought into rough connection with the properties of liquid helium. This has a density of about .14, so that each atom of the liquid occupies a volume of $(3.62\times10^{-8})^3$ cubic centimeters. The distance apart in the liquid is then obviously of the order of the distance of equilibrium found above. The critical temperature is 5.2° Abs; the mean kinetic energy of a molecule at this temperature is 1.07×10^{-15} ergs, a quantity of the same order of magnitude as the energy of separation found above. Thus the equilibrium position which we have found seems to correspond with fair accuracy to that which must actually occur in the liquid. It must not be forgotten, however, that our results are subject to great error, particularly in the attractive term.

It is also possible to draw parallels between the potential which we have found and the "radius" of helium atoms as determined from kinetic theory. Various estimates of this quantity, given in Jeans' "Dynamical Theory of Gases," range from $.99\times10^{-8}$ cm, to 1.10×10^{-8} cm. The corresponding values of our energy function are 6.35×10^{-14} ergs and 1.84×10^{-14} ergs. These are the average kinetic energies of atoms at 309° Abs (or 36°C) and 90° Abs respectively. Thus the various distances represent the distances of closest approach of average atoms in the temperature range usually used; this is surely the only thing one could mean by a diameter of such a structure. This agreement is then satisfactory; it is also more sure than those for the liquid, for at the smaller distances used here, the attractive term in the energy is relatively less important.

JEFFERSON PHYSICAL LABORATORY,
HARVARD UNIVERSITY,
May 31, 1928.

ON THE QUANTUM THEORY OF ELECTRONIC IMPACTS[1]

By J. R. Oppenheimer*

Abstract

It is shown that the previous treatment of electronic collisions has been incomplete; the error consists in the neglect of terms in the solution which correspond to an interchange of the colliding electron with one of those in the atom. The corrected first order cross section for elastic collisions is evaluated by Dirac's method for atomic hydrogen and helium. The complete solution for hydrogen is set up by Born's method for hydrogen; it is shown that the elastic cross section becomes infinite, for low velocities, with the reciprocal of the velocity; it is further shown that the first order cross section reduces to that already obtained. For hydrogen this is a monotonically increasing function; for atoms with completely paired electrons the monotonic increase is broken by a minimum at velocities corresponding to about a volt; the higher the azimuthal quantum number of the paired valence electrons, the more marked the minimum, and the lower the voltage at which it occurs.

THERE are at present two methods of treating the collision of an electron with an atom. In the one calculation[2] one solves the transformation equation from the time to a set of constants of integration specifying the state of the atom and the components of momentum of the electron; and by choosing a solution which represents the atom initially in its normal state, and a free electron wave of unit intensity per unit time per unit area, one may obtain transition probabilities which give directly the cross section for an encounter of any specified type. In the second method[3] one obtains a solution of the stationary Schroedinger equation for the coupled system of atom and electron, combines the solutions to represent an incident wave of unit intensity per unit area impinging upon the unexcited atom, and interprets the scattered wave by means of a flux vector. In the former method one thus computes the rate of increase of the probability that the system is in the final state in question; in the second one finds the rate at which electrons leave the atom in this state; and since it follows from the normalization of the wave functions for this state that these two rates are equal,[4] the two methods are equivalent. The former method is more convenient for the estimation of first order cross sections; the latter for low velocity encounters, where the properties of the exact solution are important.

The first order problem has been solved explicitly for the collision of an electron with a hydrogen atom.[5] The cross section for elastic collision so

[1] For a preliminary account of this work see J. R. Oppenheimer, Proc. Nat. Acad. Sci. **14**, 261 (1928).

* National Research Fellow.

[2] P. A. M. Dirac, Roy. Soc. Proc. **A114**, 243 (1927).

[3] M. Born, Zeits. f. Physik, **38**, 803 (1926).

[4] J. R. Oppenheimer, Phys. Rev. **31**, 66 (1928).

[5] M. Born, Goett. Nach. 146 (1926); W. Elsasser, Zeits. f. Physik, **45**, 522 (1927).

obtained is a monotonic function of the electronic velocity, and increases uniformly to a finite limit—the gas kinetic cross section—as the velocity is diminished. This calculation would indicate that for hydrogen there should be no Ramsauer effect, and no secondary maxima in the angular distribution of the scattered electrons.

Before the development of the quantum mechanics, Elsasser suggested[6] that these effects might be interpreted as the diffraction by the atom of the long de Broglie waves of the electron, and predicted that the elastic cross section should vanish with the fourth power of the electronic velocity. This argument is, however, incorrect. In the first place, as we shall show, the atom does not behave, even for slow collisions, as a rigid body: all the atomic characteristics are excited. In the second place Mensing showed[7] that, even for an especially favorable atomic model, the cross section does not vanish in the limit; this is because the refractive index within the atom is not, as in the optical case, nearly a constant, but varies instead with the reciprocal of the velocity. In the course of this work we shall see that the cross section does not become infinite faster than the reciprocal of the velocity; it is not possible to prove that it remains finite nor that it vanishes.

All of the work on collisions has, however, been incomplete. Analytically, this incompleteness is the result of neglecting, in the former method of treating the problem, transitions to states in which atomic and impacting electrons are interchanged; and, in the latter method, the excitation of the continuous spectrum. If one does not neglect these effects, he finds that, for a given atom, there is not one, but a series of elastic cross sections, corresponding to wave functions of differing symmetry in the orbital coordinates of the electrons in the atom and the colliding electron. Thus for hydrogen there are two cross sections, one for symmetric waves, one for waves antisymmetric in the coordinates of the two electrons. In general all cross sections approach, for high velocity encounters, those computed with neglect of the resonance terms; for low velocities there are characteristic deviations, which make the angular distribution of the scattered electrons irregular, and the total elastic cross section pass, in certain cases, through a minimum, instead of increasing monotonically with decreasing velocity.

In this paper we shall first compute by the former of the two methods the first order cross section for encounters with a hydrogen atom. We shall then set up the general equations for the collision by the second method, and show how the solutions are to be interpreted physically. We shall investigate the behavior of the elastic cross section for extremely low velocities; and we shall also show that the equations lead to a first order cross section identical with that found by the former method. We shall apply this to obtain the first order cross sections for hydrogen and helium, although these are of no quantitative significance; for the calculation itself shows the first approximation to be inadequate for low velocity encounters, and the full

[6] W. Elsasser, Naturwiss, **13**, 711, 1925.
[7] L. Mensing, Zeits. f. Physik, **45**, 603, 1927.

calculations appear impossible. We shall indicate, however, the physical predictions to be made on the basis of the theory, and obtain a few qualitative results for more complex atoms.

2. If we neglect the interaction of the atom and electron, we may describe the system by giving numerical values to six first integrals: the quantum numbers of the atom n, k, m, and the three electronic constants, ν, θ, ϕ, which are defined in terms of the cartesian components of the electronic momentum by the relations:

$$\nu=(2Mh)^{-1}[p_x^2+p_y^2+p_z^2]\ ;\quad \theta=\tan^{-1}(p_x^2+p_y^2)^{1/2}/p_z\ ;\quad \phi=\tan^{-1}p_y/p_x, \quad (1)$$

where M is the reduced electronic mass. To each set of values of these six integrals we shall be able to assign two linearly independent wave functions; in particular these may be chosen respectively symmetric and antisymmetric in the coordinates of the two electrons. If they are so chosen, then a wave function initially symmetric will give rise, during the collision, only to symmetric waves; one initially antisymmetric will produce only antisymmetric waves: for the interaction energy is of course symmetric. If now one solves the transformation equation from this set of integrals to the time, he finds, for the first order cross sections[8]

$$\sigma_{nkm}(\nu',\theta,\phi)=(4\pi^2/h^2)\left|\,V_{\pm}(n,k,m,\nu',\theta,\phi)\,\right|^2 \quad (2)$$

where ν' and n are connected with the initial value of ν, ν say, by the relation $\nu-\nu'-R+Rn^{-2}=0$ where R is Rydberg's constant $2\pi^2Me^4/h^3$. Here $V_+(n, k, m, \nu', \theta, \phi)$ and $V_-(n, k, m, \nu', \theta, \phi)$ are the matrix components of the interaction energy for a transition from the initial wave function, which has

$$n=1,\ k=0,\ m=0,\ \nu=\nu,\ \theta=0$$

to a wave function with n, k, m, ν', θ, ϕ; and the wave functions are in the two cases respectively symmetric and antisymmetric.

These matrix components may readily be written down, although one cannot give explicitly the corresponding operator in coordinate space. If $\mathbf{r}_1$ and $\mathbf{r}_2$ are the vectors from the atomic center of gravity to the two electrons, and ψ_{nkm} the normalized hydrogen wave functions, and $\chi_{\nu\theta\phi}$ the normalized functions for the free electron, then the wave functions normalized to $d\nu$ are for the two cases respectively

$$\Psi^{\pm}_{nkm\nu\theta\phi}=2^{-1/2}\{\psi_{nkm}(\mathbf{r}_1)\chi_{\nu\theta\phi}(\mathbf{r}_2)\pm\psi_{nkm}(\mathbf{r}_2)\chi_{\nu\theta\phi}(\mathbf{r}_1)\} \quad (3)$$

Furthermore, the initial wave, properly normalized to represent a stream of unit intensity per unit area, is

$$2^{-1/2}\{\psi_{100}(\mathbf{r}_1)\eta_\nu(\mathbf{r}_2)\pm\psi_{100}(\mathbf{r}_2)\eta_\nu(\mathbf{r}_1)\} \quad (4)$$

[8] Here as in the following, the upper sign refers to the orbitally symmetric, the lower to the orbitally antisymmetric, solution.

with

$$\eta_\nu = (2\pi/\gamma)\cdot\chi_{\nu 00} = (h/Mv)\chi_{\nu 00} \tag{5}$$

where v is the initial electronic velocity.

With

$$V(\mathbf{r},\mathbf{r}') = -e^2/r + e^2/|\mathbf{r}|-\mathbf{r}'$$

the matrix components then become

$$2^{-1/2}\int d\mathbf{r}_1 \int d\mathbf{r}_2 \Psi^{\pm *}_{nkm\nu'\theta\phi}[V(\mathbf{r}_1,\mathbf{r}_2)\psi_{100}(\mathbf{r}_2)\eta_\nu(\mathbf{r}_1) \pm V(\mathbf{r}_2,\mathbf{r}_1)\psi_{100}(\mathbf{r}_1)\eta_\nu(\mathbf{r}_2)] = f \pm g \tag{6}$$

with

$$f(\nu',\theta,\phi) = \int d\mathbf{r}_1 \int d\mathbf{r}_2\, \psi^*_{nkm}(\mathbf{r}_1)\psi_{100}(\mathbf{r}_1)V(\mathbf{r}_2,\mathbf{r}_1)\chi^*_{\nu'\theta\phi}(\mathbf{r}_2)\eta_\nu(\mathbf{r}_2)$$

and

$$g(\nu',\theta,\phi) = \int d\mathbf{r}_1 \int d\mathbf{r}_2 \psi^*_{nkm}(\mathbf{r}_2)\psi_{100}(\mathbf{r}_1)V(\mathbf{r}_2,\mathbf{r}_1)\chi^*_{\nu'\theta\phi}(\mathbf{r}_1)\eta_\nu(\mathbf{r}_2)$$

so that we get for the elastic cross section

$$\sigma(\nu',\theta,\phi) = (4\pi^2/h^2)\,|\,f(\nu',\theta,\phi) \pm g(\nu',\theta,\phi)\,|^2 \tag{7}$$

An obvious difficulty may perhaps be mentioned here. The functions ψ are all orthogonal to each other, and so are the functions χ; but the ψ's are orthogonal to the χ's only in the sense of continuous spectra:

$$\lim_{\Delta\to 0}\int d\mathbf{r}\int_\Delta d\nu \chi^*_{\nu\theta\phi}(\mathbf{r})\cdot\psi_{nkm}(\mathbf{r}) \to 0$$

This is because ψ and χ satisfy different wave equations. The non-orthogonality is negligible for high velocities, but for slow encounters it may introduce a serious ambiguity. One may overcome this in principle by using in place of the χ's, the corresponding wave functions for the hyperbolic orbits of the hydrogen atom; and for high velocities this would give the same result as (7). But again for low velocities it would introduce a serious error into the first order cross section; for the two terms in the interaction energy which do in fact nearly neutralize each other would here be treated unsymmetrically; and the resulting cross section would turn out too large. We shall meet the same difficulty in a somewhat different form in 3.

By considering the secondary waves whose amplitude does not increase steadily with the time, one may solve the transformation equations correctly to a higher order; and the difficulty in the choice of proper orthogonal initial wave functions would then disappear. But this method is in practice less suited to the exact solution of the problem than that of Born.

3. The Schroedinger equation

$$[(h^2/8\pi^2M)(\Delta_1+\Delta_2)+h(\nu-R)+e^2/r_1+e^2/r_2-e^2/|r_1-r_2|]\Psi=0 \qquad (8)$$

has solutions of the form[9]

$$\sum_{nkm}\{u_{nkm}(r_1)\psi_{nkm}(r_2)\pm u_{nkm}(r_2)\psi_{nkm}(r_1)$$

$$+\int_0^\infty d\nu'\sum_{km}\{u_{\nu'km}(r_1)\psi_{\nu'km}(r_2)\pm u_{\nu'km}(r_2)\psi_{\nu'km}(r_1)\} \qquad (9)$$

where the $\psi_{\nu'km}$'s are the hyperbolic wave functions for the hydrogen atom, with energy $h\nu'$, and normalized to $d\nu'$, and where the u's satisfy

$$[(h^2/8\pi^2M)\Delta+h(\nu-R+Rn^{-2})]u_{nkm}(r)+K_{nkm}(r)=0 \qquad (10a)$$

and

$$[(h^2/8\pi^2M)\Delta+h(\nu-R-\nu')-\nu')+e^2/r]u_{\nu'km}(r)+K_{\nu'km}(r)=0 \qquad (10b)$$

Here

$$K_{nkm}(r)=\sum_{n'k'm'}V_{nkmn'k'm'}u_{n'k'm'}(r)+\int_0^\infty d\nu'\sum_{k'm'}V_{nkm\nu'k'm'}(r)u_{\nu'k'm'}(r)$$

$$K_{\nu'km}(r)=\sum_{\nu'k'm'}V_{\nu'kmn'k'm'}(r)u_{n'k'm'}(r)+\int_0^\infty d\nu''\sum_{k'm'}\{V_{\nu'km\nu''k'm'}(r) \qquad (11)$$

$$+(e^2/r)\delta_{mm'}\delta_{kk'}\delta(\nu'-\nu'')\}u_{\nu''k'm'}(r)$$

and

$$V^{n'}_{\nu'k'm'}{}^{n}_{\nu}{}_{km}(r)=\int dr'\overset{*}{\psi}{}^{n'}_{\nu'k'm'}(r')V(r,r')\psi^{n}_{\nu}{}_{km}(r')$$

If one considers a linear combination, ψ say, of the solutions (9), he sees that this involves some terms quadratically nonintegrable in r_1, some quadratically nonintegrable in r_2, and, for sufficiently large E, some quadratically integrable in neither r_1 nor r_2. Now for each pair of terms in ψ and ψ^* quadratically nonintegrable in r_1, there will correspond two waves in r_1-space, one approaching, the other receding, from the atom. One may then combine the solutions (9) with different u's in such a way that there is no ingoing wave in r_1-space to correspond to an excited or quadratically nonintegrable wave in r_2-space, and that the ingoing wave in r_1-space corresponding to the wave function of the unexcited atom in r_2-space represents a stream of electrons moving parallel to z, of $\frac{1}{2}$ electron per unit time per unit area. The incident wave will then have asymptotically the same form as that of

$$(2v)^{-1/2}\{\epsilon^{i\gamma z_1}\psi_{100}(r_2)\pm\epsilon^{i\gamma z_2}\psi_{100}(r_1)\} \qquad (12)$$

[9] Here as in the following, Σ_{nkm} indicates that the terms are to be summed over m from $-k$ to k, over k from 0 to $n-1$, over n from 1 to infinity. For Σ the term $n=1$ is omitted. Σ_{km} indicates summation over m as before, over k from 0 to infinity.

The corresponding solution (9) will then have, as we shall show, the asymptotic form

$$(2v)^{-1/2}\left\{\epsilon^{i\gamma z_1}\,\psi_{100}(r_2)\pm\epsilon^{i\gamma z_2}\,\psi_{100}(r_1)\right\}+\Gamma_{\pm}(\nu,\theta,\phi)\left\{(\epsilon^{-i\gamma r_1}/r_1)\psi_{100}(r_2)\right.$$
$$\left.\pm(\epsilon^{-i\gamma r_2}/r_2)\psi_{100}(r_1)\right\}+\sum_{nkm}{}'D_{\pm}(n,k,m,\nu',\theta,\phi)\left\{(\epsilon^{-i\gamma_n r_1}/r_1)\psi_{nkm}(r_2)\right.$$
$$\left.\pm\epsilon^{-i\gamma_n r_2}/r_2\cdot\psi_{nkm}(r_1)\right\}+\int_0^{\infty}d\nu''\sum_{km}F_{\pm}(\nu'',k,m,\nu',\theta,\phi)/r_1r_2\cdot\left\{\epsilon^{-i(\gamma' r_1+\gamma'' r_2)}\right.$$
$$\left.\pm\epsilon^{-i(\gamma' r_2+\gamma' r_1)}\right\}$$

with

$$\left.\begin{aligned}\gamma_n&=[\gamma^2-(8\pi^2MR/h)(1-n^{-2})]^{1/2}\\ \gamma'&=2\pi(2M\nu'/h)^{1/2}\\ \gamma''&=2\pi(2M\nu''/h)^{1/2}\end{aligned}\right\}\quad\left\{\begin{aligned}&;\ \nu'=\nu-R(1-n^{-2})\\ &\nu'+\nu''+R-\nu=0\end{aligned}\right\}\tag{13}$$

The constants D vanish for $\nu<3R/4$; the constants F vanish for $\nu<R$. The evaluation of the flux vector then gives for the cross section for elastic collision:

$$\sigma_0(\nu,\theta,\phi)=2v\,|\,\Gamma_{\pm}(\nu,\theta,\phi)\,|^2\tag{14}$$

for the cross section for excitation[10] to the state n, k, m:

$$(h\gamma_n/\pi M)\,|\,D_{\pm}(n,k,m,\nu',\theta,\phi)\,|^2\tag{15}$$

and for the cross section for ionization, in which the two electrons have the energies $h\nu'$ and $h\nu''$

[10] In a recent paper (Proc. Nat. Acad. Sci. **13**, 800, 1927) the collision problem was considered, to obtain an estimate of the cross section for excitation when the electronic voltage approaches the resonance potential, in order to prove that in this limit the polarization of the excited light tends to vanish. In this treatment the continuous spectrum of the atom was neglected; and the treatment is therefore as it stands invalid. If one considers the continuous spectrum, one may in fact show that the polarization will tend to fall far below its value given by the momentum rules; it does not appear possible to show in general that it vanishes. Perhaps we may state the physical grounds for the failure of the momentum rule in an elementary way: when, as in the derivation of the momentum rules, the effect of the atom on the motion of the electron after the collision is neglected, only those electrons with vanishing angular momentum will have, in the limit, an appreciable chance of being near the atom; conversely, in this limit, the electron will have no appreciable chance of carrying away angular momentum; and this, since the electron initially had no angular momentum about the direction of the electron beam, at once gives, by the conservation theorem, the momentum rules. But when the influence of the atom on the final wave function for the electron is taken into account—and it is of capital importance in the limit when the electronic voltage approaches the resonance potential, the situation is changed; for now an electron with finite angular momentum can be near the atom; conversely the electron can now take up, and in general will take up, momentum from the atom; and thus excitations forbidden by the momentum rule will occur. It may be added that this modification does not affect at all the second part of the paper quoted, which is concerned with the anomalous polarization of the intercombination lines.

$$(\gamma'\gamma''h^2/2\pi^2M^2)\,|\,F_{\pm}(\nu',k,m,\nu'',\theta,\phi)\,|^2 \tag{16}$$

In each case there is a cross section corresponding to waves initially symmetric, and one corresponding to waves initially antisymmetric, in the orbital coordinates of the electrons. We shall consider this solution in detail for the case $\nu<\frac{3}{4}R$.

For this case the wave

$$\sum_{nkm}u_{nkm}(\boldsymbol{r}_2)\psi_{nkm}(\boldsymbol{r}_1)+\int_0^\infty d\nu'\ \sum_{km}u_{\nu'km}(\boldsymbol{r}_2)\psi_{\nu'km}(\boldsymbol{r}_1) \tag{17}$$

will involve only one set of waves quadratically nonintegrable in r_2. For both $K_{nkm}(\boldsymbol{r}_2)$ and $K_{\nu'km}(\boldsymbol{r}_2)$ vanish as $r_2\to\infty$, since the V's fall off at least with $1/r$, and the u's are bounded uniformly in r. Thus the equations for the u's take the asymptotic form

$$\begin{aligned}&[\Delta+\lambda_n]u_{nkm}=0 \qquad &&\lambda_n=(8\pi^2M/h)(\nu-R+Rn^{-2})\\ &[\Delta+\lambda_{\nu'}+e^2/r]u_{\nu'km}=0 \quad &&\lambda_{\nu'}=(8\pi^2M/h)(\nu-R-\nu')\end{aligned} \tag{10c}$$

And for all the u's except u_{100} the parameter λ is negative; the corresponding solutions will therefore be uniformly quadratically integrable; only u_{100} will involve waves which extend to infinity.

Similarly, there will be only one set of waves quadratically nonintegrable in r_1. For in the first place all the functions for the discrete states, ψ_{nkm}, fall off exponentially. And although the functions $\psi_{\nu'km}$ are quadratically nonintegrable, the coefficients $u_{\nu'km}$ are uniformly bounded in ν and r_2 except in the immediate neighborhood of $\nu'=\nu$. To see this we may examine more closely the equations (10) for the u's. If we take the second term in the expression for $K_{\nu'km}$, we see that it is an improper integral; for in the nucleus for $\nu''=\nu'$, the term

$$\int d\boldsymbol{r}'\,|\,\psi_{\nu'km}(\boldsymbol{r}')\,|^2e^2/|\,\boldsymbol{r}-\boldsymbol{r}'\,|$$

does not exist. We may, however, modify the work to get rid of this difficulty. The physical reason for the modification will be made evident when we consider the interpretation of the waves. Let us expand the solution ψ in terms of the ψ_{nkm}'s, as before, but replace the $\psi_{\nu'km}$'s by the solutions $\phi_{\nu'km}$ of the differential equation

$$[(h^2/8\pi^2M)\Delta+h\nu'+(e^2/r)\epsilon^{-r/B}]\phi_{\nu'km}(\boldsymbol{r})=0 \tag{18}$$

where B is a large positive constant. Then

$$\lim_{B\to\infty}\phi_{\nu km}\to\psi_{\nu km}$$

$$\lim_{B\to\infty}\int d\boldsymbol{r}\,\psi^*_{nkm}(\boldsymbol{r})\phi_{\nu km}(\boldsymbol{r})\to 0$$

so that by going to the limit $B\to\infty$ in the final expressions for the cross sections, we shall obtain the solutions (9). For finite B the solutions will now have the $\phi_{\nu' km}$ in place of the $\psi_{\nu' km}$ in (9), the u's will be given by (10), and for the K's we shall have the proper integral

$$\int_0^\infty d\nu'' \sum_{k'm'} U_{\nu' km\nu'' k'm'}(\boldsymbol{r}) u_{\nu'' k'm'}(\boldsymbol{r}) \text{ with } U_{\nu' km\nu'' k'm'}(\boldsymbol{r})$$
$$= \int d\boldsymbol{r}' \phi_{\nu'' k'm'}(\boldsymbol{r}') \phi_{\nu' km}(\boldsymbol{r}') \{ -e^2/|\boldsymbol{r}-\boldsymbol{r}'| + (1-\epsilon^{-r_1/B}) e^2/r' \} \tag{19}$$

Now the inhomogeneous terms K will be bounded. And unless

$$\nu - R - \nu' = -R/e^2 \tag{20}$$

where l is integral, the inhomogeneous equations will have bounded solutions. But since

$$\nu - R - \nu' < -R/4$$

only for $l=1$ will the homogeneous equation be soluble, and only for this value of ν' will the amplitude of the solution of the inhomogeneous equation become infinite. The integral in (17) thus has the form

$$\int_0^\infty d\nu' \sum_{km} L_{\nu' km}(\boldsymbol{r}_2) \phi_{\nu' km}(\boldsymbol{r}_1) + \int_{\nu-\epsilon}^{\nu+\epsilon} d\nu' \sum_{km} h^{-1} (\nu-\nu')^{-1} \phi_{\nu' km}(\boldsymbol{r}_1) \psi_{100}(\boldsymbol{r}_2)$$
$$\int d\boldsymbol{r}' \psi^*_{100}(\boldsymbol{r}') K_{\nu' km}(\boldsymbol{r}') \tag{21}$$

where L is a function bounded in ν' and $\boldsymbol{r}_2$. Now the first term of (21) gives a wave in $\boldsymbol{r}_1$ which is quadratically integrable, since it is expansible in terms of the ϕ's with uniformly bounded coefficients. The second term gives at once

$$-\kappa_{\nu km} \phi_{\nu km}(r_1 - \pi i/2\gamma, \theta, \phi) \psi_{100}(\boldsymbol{r}_2) \tag{22}$$

with

$$\kappa_{\nu km} = 2\pi h^{-1} \int d\boldsymbol{r}' \, \psi^*_{100}(\boldsymbol{r}') \, K_{\nu km}(\boldsymbol{r}') \tag{23}$$

Now the ϕ's may be given asymptotically by

$$\phi_{\nu' km}(\boldsymbol{r}) = \phi_{\nu' km}(r, \theta, \phi) \sim (2/v)^{1/2} Y_{km}(\theta, \phi) \sin [\gamma r + \alpha(\nu', k)] \tag{24}$$

where θ and ϕ are the polar angles of the vector $\boldsymbol{r}$, the Y_{ps} are the normalized spherical harmonics of order p and degree s, and the α's are real constants depending upon B. Similarly

$$u_{100}(\boldsymbol{r}) \sim \sum_{km} Y_{km}(\theta, \phi)/r \cdot \{ B_{+km} \epsilon^{i(r_{km}+\gamma r)} + B_{-km} \epsilon^{i(r_{-km}-\gamma r)} \} \tag{25}$$

with the B's and τ's real. As we shall show, the B_{-km} and τ_{-km} may be determined in terms of the B_{+km} and τ_{+km} by the wave equation (10a). (See (36) and (37)). Further the κ's are determined in these terms by (19) and (23). Finally the remaining u's are determined; for the corresponding homogeneous equations have no solution, and the inhomogeneous terms depend only on the B's and τ's and κ's. For the case $\nu<3R/4$, then, the solution is completely given in terms of the two sets of constants B_{+km} and τ_{+km}; and these must be chosen to make the incident wave of the solutions (9) one of unit intensity per unit area:

$$B_{+km}\epsilon^{i\tau_{+km}}\mp v^{-1/2}\kappa_{\nu km}\epsilon^{i\alpha(\nu,k)}=(2v)^{-1/2}\gamma^{-1}\delta_{m0}(k+1/2)\epsilon^{(k+1/2)\pi i} \tag{26}$$

The scattered wave then becomes

$$\sum_{km}\Delta_{km}\left\{\epsilon^{-i\gamma r_1}/r_1\cdot\psi_{100}(\boldsymbol{r}_2)Y_{km}(\theta_1,\phi_1)\pm\epsilon^{-i\gamma r_2}/r_2\cdot\psi_{100}(\boldsymbol{r}_1)Y_{km}(\theta_2,\phi_2)\right\} \tag{27}$$

with

$$\Delta_{km}=B_{-km}\epsilon^{i\tau_{-km}}-B_{+km}\epsilon^{i\tau_{+km}-(k+1)\pi i}\mp v^{-1/2}\kappa_{\nu km}\epsilon^{-i\alpha(\nu,k)} \tag{28}$$

This yields at once the elastic cross section. Of this we have to show (a) that in the limit $v\to 0$ it grows in general with v^{-1}; and (b) that in first order it reduces to (7).

The physical interpretation of the waves (9), (13), is immediate. In spite of the fact that the atom cannot be excited or ionized by the collision without violation of the energy theorem, the wave functions for such excitation do not in general vanish identically; instead they fall off rapidly as the nonatomic electron recedes from the atom, so that the chance of finding the atom excited or ionized is only then considerable when another electron is in its immediate vicinity. The excitation is thus not permanent; during the collision the atom will make quantum jumps; but when the collision is over the atom will have returned to its normal state. The electron which is left in the normal state is not necessarily the same as was originally there; but since one has no way of distinguishing which was originally in the atom, it is physically meaningless to ask which has escaped.

The necessity for replacing the ψ's by the ϕ's in order to make the integral for the K's exist may be interpreted in this way: the hyperbolic wave functions $\psi_{\nu' km}$ are not a possible zero order approximation to the motion of the ejected electron; for this ejection only takes place when the atom is left neutral, and not ionized; and the hyperbolic wave functions do not approach, for infinite distance, a linear combination of the waves which represent the motion of an electron with the same energy in the field of a neutral atom. In the final results the limit $B\to\infty$ should exist.

Write

$$u_{100}(\boldsymbol{r})=\sum_{km}y_{km}(r)Y_{km}(\theta,\phi) \tag{29}$$

Then the equations for the y's are, with $\xi=\gamma r$,

$$(d/d\xi)(\xi^2 y_{km}'(\xi))+[\xi^2-k(k+1)]y_{km}(\xi)+\gamma^{-2}\xi^2 S_{km}(r)=0 \tag{30}$$

where

$$S_{km}(r)=\int d\phi \int d\theta \sin\theta Y_{km}^*(\theta,\phi)K_{100}(r,\theta,\phi)$$

and

$$\begin{aligned} K_{100}=V_{100100}\,u_{100}-\sum_{km}\kappa_{\nu km}V_{100\nu km}\,\psi_{100}+\sum_{nkm}{}'V_{100nkm}\,u_{nkm} \\ +\int_0^\infty d\nu' \sum_{km} V_{100\nu' km}\,L_{\nu' km} \end{aligned} \tag{31}$$

The solutions of (30) which remain finite for $\xi=0$ then satisfy

$$y_{km}=c_{+km}y_{+k}(\xi)+c_{-km}y_{-k}(\xi)+I_{km}(\xi) \tag{32}$$

with

$$\begin{aligned} &y_{+k}(\xi)=\xi^{-1/2}J_{k+1/2}(\xi)\ ;y_{-k}(\xi)=\xi^{-1/2}J_{-k-1/2}(\xi) \\ &I_{km}(\xi)=\gamma^{-2}\int_\infty^\xi dx\,G_k(x,\xi)S_{km}(x) \end{aligned} \tag{33}$$

and

$$c_{-km}=-\lim_{\xi\to 0}\left[I_{km}(\xi)\cdot y^{-1}{}_{-k}(\xi)\right] \tag{34}$$

and

$$G_k(x,\xi)=\begin{vmatrix} y_{+k}(x) & y_{+k}(\xi) \\ y_{-k}(x) & y_{-k}(\xi)\end{vmatrix}\cdot\begin{vmatrix} y_{+k}(x) & y_{-k}(x) \\ y'_{+k}(x) & y'_{-k}(x)\end{vmatrix}^{-1} \tag{35}$$

We shall see (45), (47) that I exists and vanishes for $\xi\to\infty$. The solution (29) then behaves asymptotically like (25) with

$$\begin{aligned} B_{\pm km}=(2\pi)^{-1/2}\gamma^{-1}\{\,|\,c_{+km}\,|^2+|\,c_{-km}\,|^2+2\,|\,c_{+km}\,c_{-km}\,|\,\epsilon^{(k+1/2)\pi i\pm\pi i} \\ \sin\left[\arg c_{+km}-\arg c_{-km}\right]\}^{1/2} \end{aligned} \tag{36}$$

and

$$\begin{aligned} \sin\tau_{\pm km}=(2\pi\gamma B_{\pm km})^{-1/2}\{\,|\,c_{+km}\,|\sin\left[\arg c_{+km}\right. \\ \left.\pm(k+1)\pi/2\right]+|\,c_{-km}\,|\cdot\sin\left[\arg c_{-km}\mp k\pi/2\right]\} \end{aligned} \tag{37}$$

The incident wave will thus represent a stream of unit intensity if $|c_{+km}|$ and $\arg c_{+km}$ are chosen so that (26) is satisfied. This shows that,[11] as $v\to 0$

[11] Here, as in the following, A is a fixed positive constant independent of r, v, k, m.

$$|c_{+km}|^2+|c_{-km}|^2<Av^{-1} \tag{38}$$

We shall now show that

$$|c_{-km}|<Av^{1/2} \tag{39}$$

for the case that $V_0=V_{100\,100}<Ar^{-2-\epsilon}$ i.e., that the atom has no dipole moment in its normal state. For in the first place

$$|V_{100nkm}|<A/r \tag{40}$$

Further, by (10) and (38)

$$|u_{nkm}|<v^{-1/2}Q(r)\ ;|L_{\nu km}|<v^{-1/2}Q(r) \tag{41}$$

where the Q's are bounded uniformly in v, and are, as we have shown, quadratically integrable in r. Further, as we shall show (57)

$$|\kappa_{\nu km}|<v^{-1/2}A\ ;\ V_{100\nu km}<A/r \tag{42}$$

Finally

$$|V_0 u_{100}|<v^{-1/2}Ar^{-2-\epsilon} \tag{43}$$

Thus by (31)

$$|S_{km}|<Av^{-1/2}r^{-1} \text{ for } v\leqq r_0 \tag{44}$$

$$|S_{km}|<Av^{-1/2}r^{-2-\epsilon} \text{ for } r>r_0 \tag{45}$$

But on the other hand it follows from the non-vanishing of the Wronskian and the expansions for the J's that

$$\lim_{\xi\to 0}\left[G_k(x,\xi)(y_{-k}(\xi))^{-1}\right] \left.\begin{array}{ll}<Ax \text{ for } x>x_0\\ <Ax^{2+k}(\ln x)^{\delta_{1k}} \text{ for } x\leqq x_0\end{array}\right\} \tag{46}$$

Hence

$$c_{-km}=\int_{\infty}^{0}T_{km}(x)dx \tag{47}$$

with

$$|T_{km}| \left.\begin{array}{ll}<Av^{-3/2}x^{1+k}(\ln x)^{\delta_{1k}} \text{ for } x\leqq x_0\\ <Av^{-1/2+\epsilon}x^{-1-\epsilon} \text{ for } x>x_0\end{array}\right\}$$

From this we find, uniformly in v

$$|c_{-km}|<Av^{1/2+k}(\ln v)^{\delta_{1k}} \tag{48}$$

as announced.

To estimate the κ's we may note first that the ϕ's remain uniformly bounded as $v\to 0$, and approach

$$A_k J_{2k+1}\left[(2\pi e/h)(2Mr)^{1/2}\right]\cdot Y_{km}(\theta,\phi)$$

Thus the matrix components $U_{\nu' k' m' \nu k m}$ exist, and remain uniformly bounded as $v \to 0$, satisfying

$$| U | < A/r \tag{49}$$

Further, from (41)

$$| u_{nkm} | < A v^{-1/2} ; | L_{\nu km} | < A v^{-1/2} \tag{50}$$

Thus

$$| \kappa_{\nu km} | < A v^{-1/2} \tag{51}$$

as used in (43).

Hence from (27) we find, uniformly in k and m, that if the $|c_{+km}|$ and the arg c_{+km} are chosen to satisfy (26)

$$| \Delta_{km} | < A v^{-1} \tag{52}$$

Thus

$$| \Gamma_{\pm}(\nu, \theta, \phi) | < A v^{-1} \tag{53}$$

and (14) gives for the cross section

$$\sigma_0(\nu, \theta, \phi) < A v^{-1} \tag{54}$$

If we had neglected the continuous spectrum, we should have found instead that σ_0 approached in the limit a finite constant independent of θ and ϕ, so that scattering became uniform over all angles. But this result is of no physical significance; and since we have used the properties of the wave functions to obtain the lowest upper limit for σ_0 that they in general permit, we must conclude that in general the cross section grows in accordance with (54).

When we evaluate σ_0 in first order, we may introduce several simplifications. In the first place we may neglect the influence of the scattered wave on the incoming wave, as this would give a term of second order. We may thus satisfy (26) by setting

$$c_{+km} = (\pi/v)^{1/2} \delta_{m0} (k + \tfrac{1}{2}) \epsilon^{(k+1/2)\pi i} \tag{55}$$

Further we may replace the ϕ's by the ρ's, defined by

$$\rho_{\nu km}(r) = \int d\phi \int \sin\theta d\theta Y_{km}^{*}(\theta, \phi) \chi_{\nu\theta\phi}(r) \tag{56}$$

(This amounts to setting $B = 0$), since the validity of the first order calculation depends upon neglecting the distinction between the ψ's and the χ's, and, as pointed out in 2, it is best to use the same functions for both electrons. (See further 4.) Finally we may evaluate K_{100} and $K_{\nu km}$ by giving the u's their initial values

$$u_{\nu km} = u_{nkm} = 0 \tag{57}$$

except

$$u_{100} = (2v)^{-1/2}\epsilon^{i\gamma z} = 2^{-1/2}\eta_\nu$$

Then (23) gives

$$\kappa_{\nu km} = 2^{1/2}\pi h^{-1} \int d\tau \int d\tau' \psi_{100}^*(\tau')\psi_{100}(\tau)\eta_\nu(\tau')\rho_{\nu km}^*(\tau)V(\tau',\tau) \tag{58}$$

and with (28), (23), (25), and (30) we get

$$\begin{aligned}\Delta_{km} = &-2\pi h^{-1}(2v)^{-1/2} \int d\tau \int d\tau' \,|\, \psi_{100}(\tau) \,|^2 \eta_\nu(\tau')\rho_{\nu km}^*(\tau')V(\tau',\tau) \\ &\mp 2\pi h^{-1}(2v)^{-1/2} \int d\tau \int d\tau' \psi_{100}^*(\tau')\psi_{100}(\tau)\eta_\nu(\tau')\rho_{\nu km}^*(\tau)V(\tau',\tau)\end{aligned} \tag{59}$$

Thus with (56)

$$\Gamma_\pm(\nu,\theta,\phi) = 2\pi h^{-1}(2v)^{-1/2}[-f(\nu,\theta,\phi) \mp g(\nu,\theta,\phi)] \tag{60}$$

which, with (14), gives

$$\sigma_0(\nu,\theta,\phi) = (4\pi^2/h^2)\,|\,f-g\,|^2 \tag{61}$$

in agreement with (7).

4. The quantitative estimation of these cross sections has no very precise significance. For the ρ's are a very bad approximation to the wave functions for the aperiodic motion of the electrons; they are not orthogonal to the ψ_n's; and they give a cross section which remains finite for $v=0$, whereas the true cross section presumably becomes infinite with v^{-1}. This may be shown to depend upon the fact that the ρ's approach zero for $v=0$, whereas the ϕ's and presumably the true functions, do not. Nor can one overcome this difficulty by using the ψ's or the ϕ's for the ρ's; in the former case the flux vector does not exist, and in the second case it depends essentially, in the first order calculation, upon B, and does not approach a limit when $B\to\infty$. These difficulties would disappear in a complete solution, but at present they appear analytically inevitable.

The qualitative characteristics of σ_0 are easy to obtain. The first term f is

$$f(\nu,\theta,\phi) = f(\nu,\theta) = -(e^2/8\pi R)\{[1+\nu/R\cdot\sin^2\theta/2]^{-1} + [1+(\nu/R)\sin^2\theta/2]^{-2}\} \tag{62}$$

and is just the term that gives Born's cross section. The second term cannot be written in closed form. For large v it is smaller than f, since

$$g < Av^{-5} \tag{63}$$

whereas f falls off only with the inverse square of v. For $v=0$ we have directly

$$\begin{aligned}g_0 = g(0,\theta,\phi) &= \int d\tau \int d\tau' \psi_{100}^*(\tau')\{-e^2/r' + e^2/\,|\,\tau-\tau'\,|\,\}\psi_{100}(\tau) \\ &= -3e^2/2\pi R = +6f(0,\theta)\end{aligned} \tag{64}$$

For fixed angle of deflection θ both f and g decrease monotonically with increasing v. Thus for each value of θ there is a value of v for which the two terms become equal. These values of v lie within a small range for which v corresponds to a few volts.

The symmetric cross section is always larger than Born's value. For large v it is nearly equal to this latter; for small v it is 49 times as great. It increases monotonically with decreasing v. The angular distribution of scattered electrons varies slowly with v, and there are no secondary maxima.

The antisymmetric cross section is much larger than Born's for $v=0$, and nearly equal to it for large v. But in the range in which the functions $f(\nu, \theta)-g(\nu, \theta)$ have their zeros, it will be smaller than Born's value; and because these values of v lie in a small range, the total cross section

$$\int d\phi \int \sin\theta d\theta \sigma_0(\nu,\theta)$$

has a minimum in this region. In this region also there are secondary maxima in the angular distribution of the electrons.

Had we taken for the normal state of the atom, a P or D, instead of an S, term, with wave function, say, respectively

$$\psi_{210}=\text{const}\,\epsilon^{-r/2a}r\cos\theta$$
$$\psi_{320}=\text{const}\,\epsilon^{-r/3a}r^2(3\cos^2\theta-1)$$

we should obtain analogous results. But since in this case

$$\begin{aligned} g&<Av^{-7} \\ g&<Av^{-9} \end{aligned} \tag{65}$$

for the two functions respectively, the second term will fall off more rapidly than for the S state, and the zeros of f-g will thus occur for lower values of v. And since they will also occur within a smaller range, the minimum in the total cross section will be more marked. Quite generally, the lower the position of the minimum, the sharper it will be. For θ enters the cross section only in the form $v\begin{pmatrix}\cos\theta \\ \sin\theta\end{pmatrix}$ so that, the lower the velocity, the slighter the dependence of f and g upon θ, and the smaller the range of velocities in which $f=g$.

5. If there were no electronic spin, we should have to take, to satisfy the exclusion principle, the orbitally antisymmetric solution for the collision of an electron with a hydrogen atom; and this would lead to a cross section which had a minimum as a function of v. But because of the electron spin the symmetric solution will occur with a third the weight of the antisymmetric one; so that the total first order cross section for atomic hydrogen is

$$(4\pi^2/h^2)\cdot(f^2+g^2-fg) \tag{66}$$

Now

$$f^2+g^2-fg\geq 3f^2/4\ ;\ f^2+g^2-fg\geq\tfrac{1}{2}(f^2+g^2) \tag{67}$$

The total cross section can thus never fall much under Born's value, and for low velocities it will be larger. Thus the theory leads to the prediction that atomic hydrogen, and probably the similar alkali atoms, should show no Ramsauer effect.

For other atoms we obtain different results. Thus for helium the orbital wave must be symmetric in two electrons—to correspond to the normal state of the atom—and cannot, by the exclusion principle, be symmetric in all three. The two non-combining wave functions corresponding to (3) turn out to be

$$\begin{aligned} &(a)\quad \psi(r_1,r_2)X_{\nu\theta\phi}(r_3)+\epsilon\psi(r_1,r_3)X_{\nu\theta\phi}(r_2)+\epsilon^2\psi(r_2,r_3)X_{\nu\theta\phi}(r_1)\\ &(b)\quad \psi(r_1,r_2)X_{\nu\theta\phi}(r_3)+\epsilon^2\psi(r_1,r_3)X_{\nu\theta\phi}(r_2)+\epsilon\psi(r_2,r_3)X_{\nu\theta\phi}(r_1) \end{aligned} \tag{68}$$

with $\epsilon=\frac{1}{2}(i-3^{-1/2})$

where $\psi(r,r')=\psi(r',r)$ is the wave function for the normal state of the atom.[12]

[12] The functions (68) may be used to compute the excitation probabilities for singlet and triplet atomic states; the final wave functions are for the two cases, e.g. in the system (a)

$$\psi_{\pm}(r_1,r_2)\chi_{\nu\theta\phi}(r_3)+\epsilon\psi_{\pm}(r_1,r_3)\chi_{\nu\theta\phi}(r_1)+\epsilon^2\psi_{\pm}(r_3,r_1)\chi_{\nu\theta\phi}(r_2)$$

with

$$\psi_{\pm}(x,y)=\pm\psi_{\pm}(y,x)$$

The cross section for the singlets becomes

$$\sigma_+=(4\pi^2/h^2)\left|\int\int\int dx\,dy\,dz\,\psi_+^*(x,y)\chi^*_{\nu\theta\phi}(z)\left\{\psi(x,y)y_\nu(z)\left[\frac{e^2}{|z-\chi|}+\frac{e^2}{|z-y|}-\frac{2e^2}{z}\right]-\psi(y,z)\eta_\nu(x)\left[\frac{e^2}{|x-y|}+\frac{e^2}{|x-z|}-\frac{2e^2}{x}\right]\right\}\right|^2$$

That for the triplets is

$$\sigma_-=(12\pi^2/h^2)\left|\int\int\int dx\,dy\,dz\,\psi_-^*(x,y)\psi(y,z)\chi_{\nu\theta\phi}(z)\eta_\nu(x)\left[\frac{e^2}{|x-y|}+\frac{e^2}{|x-z|}-\frac{2e^2}{x}\right]\right|^2$$

Neither of these vanishes identically. One may obtain a rough idea of the behavior of the cross sections by neglecting the coupling of the atomic electrons, and setting $\psi(x,y)=\psi_{100}(x)\,\psi_{100}(y)$,

$$\psi_+(x,y)=(1/2^{1/2})\{\psi_{100}(x)\psi_{nkm}(y)\pm\psi_{100}(y)\psi_{nkm}(x)\}$$

Then

$$\sigma_+=(8\pi^2/h^2)\,|\,L-\tfrac{1}{2}M-\tfrac{1}{2}N\,|^2;\qquad \sigma_-=(6\pi^2/h^2)\,|\,M-N\,|^2.$$

with
$$L=\int\int dx\,dy\,\psi^*_{nkm}(x)\psi_{100}(x)\chi^*_{\nu\theta\phi}(y)\eta_\nu(y)\left[\frac{e^2}{|x-y|}\right]$$

$$M=\int\int\int dx\,dy\,dz\,\psi^*_{nkm}(x)\,|\,\psi_{100}(y)\,|^2\psi_{100}(z)\chi^*_{\nu\theta\phi}(z)\eta_\nu(x)\left[\frac{e^2}{|x-y|}+\frac{e^2}{|x-z|}-\frac{2e^2}{x}\right]$$

$$N=\int\int\int dx\,dy\,dz\,\psi^*_{nkm}(x)\psi_{100}(y)\psi^*_{100}(x)\psi_{100}(z)\chi_{\nu\theta\phi}(z)\eta_\nu(y)\left[\frac{e^2}{|x-y|}\right]$$

Here L corresponds to transitions in which one atomic electron is excited; M to those in which one atomic electron is ionized, and the impacting electron is bound in the excited state; N to those in which one atomic electron is freed, and the other excited, and the impacting electron is caught in the normal state. Further

$$L<Av^{-4};\qquad M<Av^{-6};\qquad N<Av^{-8}$$

so that with increasing electronic velocity singlet excitation should predominate.

The first order cross section then is

$$(4\pi^2/h^2)\cdot|f_1-g_1|^2 \tag{69}$$

with

$$f_1=\int d\tau\int d\tau'\int d\tau''\,|\psi(\tau,\tau')|^2\chi_{\nu\theta\phi}^*(\tau'')\eta_\nu(\tau'')\left[-2e^2/r''+e^2/|\tau''-\tau'|+e^2/|\tau''-\tau|\right] \tag{70}$$

$$g_1=\int d\tau\int d\tau'\int d\tau''\psi(\tau,\tau')\psi(\tau,\tau'')\chi_{\nu\theta\phi}^*(\tau')\eta_\nu(\tau'')\left[-2e^2/r''+e^2/|\tau''-\tau'|+e^2/|\tau''-\tau|\right]$$

Here again f gives the classical cross section. And since (69) depends upon v and θ much as (7) does, the theory does give, for helium, a break in the monotonic rise of the cross section with decreasing v. In general we can say that the ratio of the true cross section to its "classical" value will pass through a minimum. Whether the cross section itself passes through a minimum, or merely shows a flattening, will depend upon the distribution of zeros of $f(v,\theta)-g(v,\theta)$. And this effect should occur for all atoms with paired electrons, and should not occur for an atom with an unpaired electron. Thus cadmium should show the break, and sodium should not. But these results are based upon the approximately hydrogenic character of the atomic wave functions, and are thus not directly applicable to molecules.

Since the minimum is more marked for P than for S, for D than for P terms, we should expect the effect to be more marked the higher the azimuthal quantum number of the paired valence electrons. And we should expect the minimum to occur for a lower voltage the higher the azimuthal quantum number

In conclusion it should be recalled that an adequate quantitative treatment of the collision problem involves a more complete solution of the equations (10) than can as yet, even in the simplest case of atomic hydrogen, be given.

NORMAN BRIDGE LABORATORY OF PHYSICS,
PASADENA, CALIFORNIA,
May, 1928.

POLARIZATION OF THE RESONANCE RADIATION FROM DEGENERATE SYSTEMS

By Frank C. Hoyt*

Abstract

The problem of resonance between light and an atom is treated by solving the wave equation through the method of variation of constants. It is found that an initial degeneracy is removed by the action of the light, and that there occur fluctuations between the two states involved. Calculation of the electric moment of the perturbed atom on the Schrödinger density hypothesis shows that when the incident light is linearly polarized the radiation has the same degree of polarization as though the atom were in a weak magnetic field parallel to the electric vector of the light. In the case of circular polarization this fictitious field is perpendicular to the plane of polarization. These results confirm the Heisenberg rule deduced from the correspondence principle.

THE problem of accounting for the characteristic polarization of the radiation excited by light which is in resonance with the principal absorption frequency of a gas has been much discussed on the basis of the older forms of the quantum theory.[1] It is well known that in the case of degenerate systems difficulties of a fundamental nature are encountered. These difficulties have been partially removed with the aid of the new mechanics, and Oppenheimer[2] has been able to deduce the Heisenberg[3] rule for the calculation of the degree of polarization with the use of the Dirac q-number theory for the radiation.

It is the purpose of the present paper to investigate how far it is possible to give an account of the observed phenomena on the basis of the Schrödinger wave mechanics, in which the radiation is described by means of the continuous oscillations of the wave function. In so far as we are concerned only with the calculation of the degree of polarization it would appear legitimate in most cases to neglect the complication introduced by taking into account the reaction of the atom on the radiation field, which is responsible for the damping and the finite life-time of stationary states.[4] The present calculations are accordingly made with neglect of this reaction, since we shall regard the radiation field merely as an external perturbation. The justification for such a procedure lies in the fact that it may be thought of as corresponding to excitation for a period of time very short compared to the life-time of an atom, during which the effect of damping is negligible. The degree of polarization of the emitted light may then reasonably be expected to be independent of the method of illumination.

* Fellow of the John Simon Guggenheim Memorial Foundation.

[1] Pauli, "Handbuch der Physik" Vol. XXIII.

[2] J. R. Oppenheimer, Zeits. f. Physik **43**, 27, (1927).

[3] W. Heisenberg, Zeits. f. Physik, **31**, 617, (1925).

[4] This reaction may be treated by the method of Dirac, Proc. Roy. Soc. **A114**, 243, (1927).

Method for the Treatment of Resonance Problems

The problem of resonance between an atom and a light wave has usually been discussed as a special case of scattering. Schrödinger,[5] however, has shown that the solution of the wave equation in the case of very near resonance must differ essentially from the approximation which is valid when the frequency of the light does not approach too nearly any absorption frequency of the atom. In particular he has shown, without actually giving the resonance solution, that "catastrophic" terms which become infinite in the classical theory because of a vanishing denominator cannot appear in the wave mechanics, even when no damping term is introduced. We shall show here that it is possible to obtain the desired solution in a simple way by means of the method of variation of constants developed by Dirac,[6] Born,[6] Schrödinger,[7] and Slater.[8]

We work with the Schrödinger wave equation in the form

$$\partial\psi/\partial t=(2\pi i/h)H[\psi], \tag{1}$$

where H is the operator corresponding to the Hamiltonian function. For the sake of simplicity we suppose that we have to do with a single electron only, which may be regarded as the "series" electron. In the presence of an external radiation field characterized by its scalar and vector potentials V and $\boldsymbol{A}$ the operator H becomes H_0+H_1 where

$$H_0=-(h^2/8\pi^2m)\nabla^2+eV_0$$
$$H_1=eV+(h/2\pi i)(e/mc)\boldsymbol{A}\cdot\nabla.$$

Here V_0 is the potential of an effective internal field. We denote vectors by heavy type, and ∇ stands for the gradient operator, so that ∇^2 is the usual Laplacian operator, and the scalar product $\boldsymbol{A}\cdot\nabla$ stands for $A_x\partial/\partial x+A_y\partial/\partial y+A_z\partial/\partial z$. The assumption of a single electron and an effective internal field is somewhat special, but any other assumption would involve uncertainties and unessential complications.

Let the unperturbed problem $H=H_0$ have the set of normalized characteristic functions $\psi_k e^{2\pi i\nu_k t}$ so that the ψ_k satisfy equation

$$H_0[\psi_k]=h\nu_k\psi_k \tag{2}$$

of which $E_k=h\nu_k$ are the characteristic values. It is convenient to take the ψ_k complex, so that they satisfy the condition of the orthogonality,

$$\int \psi_k\psi_l^*d\tau=\begin{matrix}0 & k\neq l\\ 1 & k=l\end{matrix}$$

where $d\tau$ is the volume element in three dimensional space, and the asterisk denotes the conjugate imaginary.

[5] E. Schrödinger, Ann. d. Physik **81**, 109 (1926).
[6] P. Dirac, Proc. Roy. Soc. **A112**, 674 (1926); M. Born, Zeits. f. Physik, **40**, 167 (1927).
[7] E. Schrödinger, Ann. d. Physik **83**, 956 (1927).
[8] J. C. Slater, Proc. Nat. Acad. Sci. **14**, 104 (1927).

The solution of the perturbed problem $H=H_0+H_1$ is then given in the form

$$\psi=\sum_{k=1}^{\infty}c_k\psi_k e^{2\pi i\nu_k t} \tag{3}$$

and the amplitudes or excitation constants c_k as functions of the time, are solutions of the set of (exact) differential equations

$$dc_k/dt=(2\pi i/h)\Sigma_l a_{kl}c_l e^{2\pi i(\nu_l-\nu_k)t} \tag{4}$$

$$a_{kl}=\int\bar{\psi}_k H_1[\psi_l]d\tau \tag{5}$$

obtained by substitution of (3) in (1). The quantities a_{kl} may be regarded as elements of a perturbation matrix.

We now consider perturbation by a monochromatic, elliptically polarized plane wave of frequency ν. Except in the case of very short wave-length the vector potential $\boldsymbol{A}$ at the center of the atom describes completely the light wave. For H_1 we may now write $(h/2\pi i)(e/mc)\boldsymbol{A}\cdot\nabla$ with

$$\boldsymbol{A}=\boldsymbol{C}e^{2\pi i\nu t}+\boldsymbol{C}^*e^{-2\pi i\nu t},$$

where $\boldsymbol{C}$ is a constant complex vector.

For the a_{kl} we now have

$$a_{kl}=(h/2\pi i)(e/mc)(\boldsymbol{C}e^{2\pi i\nu t}+\boldsymbol{C}^*e^{-2\pi i\nu t})\cdot\int\psi_k^*\nabla\psi_l d\tau.$$

By a simple transformation involving the fact that the ψ_k are solutions of (2) we find

$$\int\psi_k^*\nabla\psi_l d\tau=(4\pi^2m/h)(\nu_k-\nu_l)\int r\psi_k^*\psi_l d\tau, \tag{6}$$

where $\boldsymbol{r}$ is the radius vector from the center of gravity of the system. The complex integral on the right hand side has for its real part half the electric moment, calculated by the Schrödinger density hypothesis, of the oscillating part of the charge distribution resulting from the excitation of the kth and lth characteristic vibrations of the unperturbed atom. We use for this electric moment the notation

$$\boldsymbol{M}_{kl}=\int e\boldsymbol{r}\psi_k\psi_l^*d\tau,\quad(\boldsymbol{M}_{lk}=\boldsymbol{M}_{kl}^*). \tag{7}$$

If we further put $\nu_{kl}=\nu_k-\nu_l$ we may write the elements a_{kl} of the perturbations matrix in the following form:

$$a_{kl}=f_{kl}e^{2\pi i\nu t}+f_{lk}^*e^{-2\pi i\nu t}. \tag{8}$$

$$f_{kl}=-(2\pi i/c)\nu_{kl}\boldsymbol{C}\cdot\boldsymbol{M}_{kl}.^* \tag{9}$$

It is important to note that the a_{kl} are Hermitian (i.e., $a_{kl}=a_{lk}^*$), while the f_{kl} are so only when $\boldsymbol{C}$ is real. The perturbation Eqs. (4) now take the form

$$dc_k/dt=(2\pi i/h)\Sigma_l\left[f_{kl}c_l e^{2\pi i(\nu_{lk}+\nu)t}+f_{lk}^* c_l e^{2\pi i(\nu_{lk}-\nu)t}\right], \qquad k=1,2,\cdots\infty. \tag{4a}$$

These differential equations are exact, and apply equally well to a degenerate or non-degenerate system. It is convenient, however, to write them in a form which displays better the effect of degeneracy. To each characteristic value E_k let there correspond a set of characteristic functions ψ_{k1}, ψ_{k2}, $\cdots$, $\psi_{k\alpha_k}$. The complete set ψ_{ki}, $k=1, 2, \cdots\infty$, $i=1, 2, \cdots\alpha_k$ may be normalized and made orthogonal. All indices now become doubled, and in particular for f_{kl} we write

$$f(ki\,;lj)=-(2\pi i/c)\nu_{kl}\,\boldsymbol{C}\cdot\boldsymbol{M}(ki\,;lj). \tag{10}$$

To each characteristic function corresponds an "excitation constant" c_{ki} so that the perturbation Eqs. (4a) become

$$\begin{aligned} dc_{ki}/dt=(2\pi i/h)\sum_{l=1}^{\infty}\sum_{j=1}^{\alpha l}\{&f(ki\,;lj)c_{lj}e^{2\pi i(\nu_{lk}+\nu)t} \\ &+f^*(lj\,;ki)c_{lj}e^{2\pi i(\nu_{lk}-\nu)t}. \qquad k=1,2,\cdots\infty. \end{aligned} \tag{11}$$

For our problem we require the approximate form which these equations take when the frequency ν of the incident light coincides very nearly with some definite emission frequency, say $(E_m-E_n)/h=\nu_{mn}$, where $E_m>E_n$. Let us put

$$\nu_{mn}-\nu=\delta$$

and treat δ as a very small quantity. To a first approximation, when the $f(ki;lj)$ are not too large, we may neglect all terms in the sum on the right hand side of (11) for which the exponent of e is not of the order of magnitude of δ. It is clear that we are then neglecting terms which produce only rapid oscillations of small amplitude in the c_{ki} provided always

$$|f(ki\,;lj)|\ll h(\nu_{lk}\pm\nu),\quad \nu_{lk}\neq\nu_{mn}.$$

We may also think of this as a replacement of the c_{ki} by their average values over a period of time long compared to the period of any term except those with period $1/\delta$. It is now seen without difficulty that (11) reduces to the set

$$\begin{aligned} de_{m\rho}/dt&=(2\pi i/h)\textstyle\sum_\sigma f(m\rho\,;n\sigma)c_{n\sigma}e^{-2\pi i\delta t} \qquad \rho=1,2,\cdots,p \\ dc_{n\sigma}/dt&=(2\pi i/h)\textstyle\sum_\rho f(\overset{*}{m}\rho\,;n\sigma)c_{n\rho}e^{2\pi i\delta t} \qquad \sigma=1,2,\cdots,q \end{aligned} \tag{12}$$

The first set represents all equations resulting from (11) when $k=m$, the second those when $k=n$. We have written p and q for the "statistical weights," α_m and α_n; and replaced i, j by the indices ρ, σ, which we suppose have here the ranges 1 to p and 1 to q respectively. The remaining c's ($k\neq m, n$) suffer only small oscillations about their initial values. The effect of the resonance is thus, as we would expect, confined almost entirely to the

two characteristic vibrations (stationary states) with whose frequency difference the light is in resonance. Further, the amplitudes of the vibrations with frequency ν_m are coupled to those of frequency ν_n with a strength proportional to the electric moment of the oscillating charge density resulting from these two vibrations.

This set of equations is reduced by a simple transformation to a set of linear first order differential equations with constant coefficients. The matrix of the constants is Hermitian. To show this, let us make for the c's the transformation:

$$K_{m\rho}=c_{m\rho}e^{\pi i\delta t}, \quad K_{n\sigma}=c_{n\sigma}e^{-\pi i\delta t}. \tag{13}$$

At the same time we may regard the quantities $K_{m1}, K_{m2}, \cdots, K_{mp}, K_{n1}, K_{n2}, \cdots, K_{nq}$ as the components K_i of a vector $\boldsymbol{K}$ in space of $p+q$ dimensions. It is readily seen that the e exponents are eliminated by this substitution, and if we put Φ for the matrix of the constant coefficients we may write

$$d\boldsymbol{K}/dt=(2\pi i/h)\Phi\boldsymbol{K}$$

and all now depends on the form of the matrix Φ. If we put for simplicity $f_{\rho\sigma}$ for $f(m\rho; n\sigma)$ the matrix is at once seen to be:

$$\Phi=\begin{vmatrix}
h\delta/2 & \cdots & 0 & f_{11} & \cdots & f_{1q} \\
\vdots & & \vdots & \vdots & & \vdots \\
0 & \cdots & h\delta/2 & f_{p1} & \cdots & f_{pq} \\
f_{11}^{*} & \cdots & f_{p1}^{*}-h\delta/2 & & \cdots & 0 \\
\vdots & & \vdots & \vdots & & \vdots \\
f_{1q}^{*} & \cdots & f_{pq}^{*} & 0 & \cdots & h\delta/2
\end{vmatrix} \tag{14}$$

(diagonal matrix)

All that interests us for the present is that it is Hermitian, although the $f_{\rho\sigma}$ are not. Thus the solution reduces to a principal axis transformation. The substitution

$$K_i=\kappa_i e^{(2\pi s/h)\epsilon t}$$

leads to the usual secular equation, and the Hermitian property assures the reality of the roots.

The solution for the κ will be of the form

$$K_i = \sum_{j=1}^{p+q} A_j \kappa_{ij} e^{(2\pi i/h)\epsilon_j t},$$

where the A_j are arbitrary constants and the ϵ_j the $p+q$ roots of the secular equation which we assume are all distinct. The matrix of the κ_{ij} is that of the set of principal axis vectors $\kappa_{1j}, \kappa_{2j}, \cdots, \kappa_{p+q,j}$ which is orthogonal and may be normalized so that

$$\sum_r \kappa_{rj} \kappa_{rj'}^* = \begin{matrix} 0 & j \neq j' \\ 1 & j = j' \end{matrix} \tag{15}$$

The κ_{ij} are then completely determined, except as regards their phases. The solution for the constants $c_{m\rho}$ and $c_{n\sigma}$ is

$$\begin{aligned} c_{m\rho} &= \sum_j A_j \kappa_{\rho j} e^{2\pi i[(\epsilon_j/h)-(\delta/2)]t} \\ c_{n\sigma} &= \sum_j A_j \kappa_{\sigma j} e^{2\pi i[(\epsilon_j/h)+(\delta/2)]t}. \end{aligned} \tag{16}$$

By means of the A_j the solution may be made to fit initial conditions for the amplitudes. It will be recalled that the new frequencies ϵ_j/h depend on the intensity of the incident light and the electric moment vectors $\boldsymbol{M}$ of the unperturbed atom, as well as on δ. We shall not make use of the solution in this too general form to describe the properties of the radiation, since in special cases considerable simplification is introduced. However, from this form we may show two facts of some interest.

First, the degeneracy of the system is at least partially removed by the action of the light. In fact the situation is analogous to the removal of the degeneracy by a constant external field as discussed by Schrödinger[7] and Slater[8] except that the *two* initially degenerate characteristic vibrations are involved in place of one. On forming the wave function ψ it will be seen that the new characteristic values are $E_{mj} = E_m + \epsilon_j - h\delta/2$ and $E_{nj} = E_n + \epsilon_j + h\delta/2$ while the new characteristic functions are linear combinations of the old ones. That each characteristic value splits into $p+q$ is only a formal result, since in general the roots of the secular equation are multiple.

Secondly, there occurs here the type of fluctuation between the amplitudes of the characteristic vibrations which is always associated with resonance in quantum phenomena. Thus if we form the amplitude-squares $c_{m\rho} c_{m\rho}^*$ and $c_{n\sigma} c_{n\sigma}^*$ by means of Eqs. (16) they show the same type of multiply periodic fluctuations as in the above-mentioned work of Schrödinger and Slater, with the difference that here we have interchange between amplitudes belonging to two different characteristic values E_m and E_n. The fluctuational character of the changes follows from the constancy in time of the quantity $\Sigma_\rho c_{m\rho} c_{m\rho}^* + \Sigma_\sigma c_{n\sigma} c_{n\sigma}^*$ which is readily proved from the orthogonality relation (15). The frequencies of the fluctuations are of the form $[(\epsilon_j - \epsilon_{j'})/h] \pm \delta/2$

and their character depends on the nature of the solution of the secular equations, which is more readily investigated in special cases.

Excitation by Linearly Polarized Light

To apply the method just described we require certain properties of the electric moments of the unperturbed atom, which are readily established by the following semiempirical reasoning.

We may take for these electric moments their limiting values in the case of a vanishingly small magnetic field in an arbitrary direction. This is equivalent to choosing one of the infinitely many possible sets of unperturbed characteristic functions, and the final results are, of course, independent of this choice. At the same time we interpret ρ and σ as the magnetic quantum numbers (in the Landé scheme) of the upper and lower states. The empirically established rules for the polarization of the Zeeman components give us the necessary relations. Thus the polarization vector

$$\boldsymbol{P} = \int e\boldsymbol{r}\psi\psi^* d\tau$$

is made up of terms of the form,

$$2\mathcal{R}c_{m\rho}c_{n\sigma}{}^*\boldsymbol{M}(m\rho\ ;\ n\sigma)e^{2\pi i\nu_{mn}t},$$

where R stands for the real part of all that follows it. Then $\boldsymbol{M}$ must vanish when $\rho-\sigma$ is not 0 or ± 1 (selection rule). Further, if we take the z-axis in the direction of the magnetic field the light must be right circularly polarized in the sense of a positive rotation about the field when $\rho-\sigma=\pm 1$, left circularly polarized when $\rho-\sigma=-1$, and linearly polarized along Oz when $\rho-\sigma=0$. This will be the case only when

$$\begin{aligned} M_y(m,\rho\ ;\ n,\rho-1) &= -iM_x(m,\rho\ ;\ n,\rho-1) \\ M_y(m,\rho\ ;\ n,\rho+1) &= iM_x(m,\rho\ ;\ n,\rho+1) \\ M_x(m\rho\ ;\ n\rho)\neq 0,\quad & M_x(m\rho\ ;\ n\rho) = M_y(m\rho\ ;\ n\rho) = 0. \end{aligned} \tag{17}$$

The indices ρ and σ are of course no longer necessarily integers, and take negative as well as positive values. Their ranges are those of the magnetic quantum numbers in the Landé scheme. Relations very similar to these may be deduced from the properties of the tesseral harmonics of the wave equation, but the empirical basis is at present more certain.

We now consider the case where the incident light is linearly polarized. For the unperturbed characteristic functions it is most convenient to take those corresponding to an infinitely small magnetic field in the direction of the electric vector, which we take also as the direction of the z-axis. The coefficients of Eq. (9) are

$$\begin{aligned} f(m\rho\ ;\ n\sigma) &= -(2\pi i/c)\nu_{mn}c_z M_z{}^*(m\rho\ ;\ n\sigma) \\ &= \left| f(m\rho\ ;\ n\sigma)\right| e^{-2\pi i[\phi(m\rho;\,n\sigma)+1/4]} \end{aligned}$$

if we take C_z real and ϕ_z for the phase of M_z.

By virtue of the last Eq. of (17) the perturbation Eqs. (12) simplify at once to

$$dc_{m\rho}/dt=(2\pi i/h)f_\rho e^{-2\pi i\delta t}c_{n\rho}$$
$$dc_{n\sigma}/dt=(2\pi i/h)f_\sigma^* e^{2\pi i\delta t}c_{m\sigma},$$

where f_ρ stands for $f(m\rho;\ n\sigma)$. In the matrix Φ of (14) only one element remains in each row outside the diagonal. However, the equations may be solved directly without use of the general method, for we can pair them off into sets of two for each of which $\rho=\sigma=\lambda$. Each set is independent of the others. Thus only those excitation constants are coupled with each other which correspond to two states whose combination gives rise to light polarized in the same manner as the incident light. All others remain constant.

To obtain the solution we substitute in each set

$$c_{m\lambda}=\kappa_{m\lambda}e^{(2\pi i/h)(\epsilon-h\delta/2)t},\quad c_{n\lambda}=\kappa_{n\lambda}e^{(2\pi i/h)(\epsilon+h\delta/2)t}.$$

It is important to note that the range of λ is simply that of the magnetic quantum number of that state which has the smaller multiplicity in a magnetic field. The roots of the secular equation for ϵ are $\pm[|f_\lambda|^2+(h\delta/2)^2]^{1/2}$ and by means of the κ's the solution can be made to fit initial values for the c's. For these the obviously reasonable assumptions, when the atom is in the normal state, are, for $t=0$, all $c_{m\rho}=0$ while all $c_{n\sigma}$ equal each other. To find the solution corresponding to these conditions is a routine matter. It is

$$\begin{aligned}c_{m\lambda}&=c_n^0(if_\lambda/\epsilon_\lambda)e^{-\pi i\delta t}\sin 2\pi\epsilon_\lambda t/h\\ c_{n\lambda}&=c_n^0e^{\pi i\delta t}\{\cos 2\pi\epsilon_\lambda t/h+i[(h\delta/2)/\epsilon_\lambda]\sin 2\pi\epsilon_\lambda t)h\}\\ \epsilon_\lambda&=+[|f_\lambda|^2+(h\delta/2)^2]^{1/2}\end{aligned}\qquad(18)$$

where c_n^0 is the arbitrary initial value of any $c_{n\sigma}$. This gives for the amplitude squares

$$\begin{aligned}c_{m\lambda}c_{m\lambda}^*&=c_n^0c_n^{0*}(|f_\lambda|/\epsilon_\lambda)^2\sin^2(2\pi/h)\epsilon_\lambda t\\ c_{n\lambda}c_{n\lambda}^*&=c_n^0c_n^{0*}[\cos^2 2\pi\epsilon_\lambda t/h+(h\delta/2\epsilon_\lambda)\sin^2 2\pi\epsilon_\lambda t/h].\end{aligned}\qquad(19$$

The results may perhaps be most simply stated in the language of stationary states and transitions, in which the amplitude-squares represent the fractions of atoms in the corresponding states.

The Eqs. (18) show that only those states are excited which could be reached by absorption from the normal state *if the atom were in a magnetic field parallel to the electric vector of the light wave*. This implies of course that only those transitions can be produced by absorption which in emission give rise to light polarized in the same manner as the incident light.

The Eqs. (19) show in a simple form the fluctuations mentioned above in the general case, and we see that there occur oscillations of the atom between the upper and lower levels, with the same magnetic quantum number. After a quarter of the period h/ϵ_λ nearly all have reached the upper state, only a fraction $(h\delta/2)^2$ remaining behind. Thus it is only in the case

of exact resonance that there is a complete transition to the upper state. The order of magnitude of the periods is important, and introducing the electric vector of the light wave in place of the vector potential we find

$$\epsilon_\lambda/h \approx |f_\lambda|/h = (E_z/2h)\,|M_z(m\lambda\,;\,n\lambda)|\,.$$

The frequency thus depends on the intensity of the light. If we take for the intensity that of solar radiation we find that the period is of the order of magnitude of 10^{-7} sec, so that for the intensity at the center of an emission line, which is alone effective in producing the resonance radiation, this period may be taken as long compared to the life time of an excited atom. It is, however, doubtful whether this dependence on the intensity of light can be considered as correct, due to the classical way in which the radiation field was introduced.

We shall not consider further here the results for near resonance, but confine ourselves to exact coincidence $\delta = 0$. This assumption may be introduced as far back as Eq. (12) and exponential factors in e become unity. The perturbations of the amplitudes then take the very simple form

$$\begin{gathered} c_{m\lambda} = c_n{}^0 e^{-2\pi i\phi_\lambda} \sin 2\pi\epsilon_\lambda t/h, \qquad e_{n\lambda} = e_n{}^0 \cos 2\pi\epsilon_\lambda t/h \\ \epsilon_\lambda = |f_\lambda| = (E_z/2)\,|M_z(m\lambda\,;\,n\lambda)| \end{gathered} \tag{20}$$

in which ϕ_λ is the phase of $M_z(m\lambda;\,n\lambda)$.

We now form the polarization vector $\boldsymbol{P}$ after computation of $\psi\psi^*$ from (3) and (20), finding at once

$$\boldsymbol{P} = N \sum_\lambda \sum_{\lambda'} 2 \sin 2\pi\epsilon_\lambda t/h \cos 2\pi\epsilon_{\lambda'} t/h \; \mathcal{R}\boldsymbol{M}(m\lambda\,;\,n\lambda') e^{2\pi i(\nu t - \phi_\lambda)},$$

where $N = c_n{}^0 c_n{}^{0*}$. Only that part of $\boldsymbol{P}$ which oscillates with nearly the frequency ν of the incident light has been retained. The sine and cosine terms represent oscillations with periods very long compared to the life time of an excited atom, so that we may write the polarization in the approximate form,

$$\boldsymbol{P} = (2\pi/h) N t E_z \sum_\lambda \sum_{\lambda'} |M_z(m\lambda\,;\,n\lambda)|\, \mathcal{R}\boldsymbol{M}(m\lambda\,;\,n\lambda') e^{2\pi i(\nu t - \phi_\lambda)} \tag{21}$$

It is essential for the interpretation of this result to remember that the index λ has the range of the magnetic quantum number of that state with the smaller multiplicity, while λ' ranges over the magnetic quantum number of the lower state.

We may now compare our results with the predictions of the above-mentioned Heisenberg rule. It will be recalled that this rule, deduced from the correspondence principle, states that in the case of excitation by linearly polarized light in the absence of an external field, the resonance radiation will be the same as though the atom were excited in a very weak magnetic field parallel to the electric vector of the incident light. Now we have already seen, in connection with the interpretation of Eqs. (18), that the excitation

which our calculations give is just that to be expected, on the basis of older forms of the theory, in such a magnetic field. This is also apparent from Eq. (21) if due regard is taken of the restricted range of the index λ. Here we have calculated the spontaneous emission on the Schrödinger density hypothesis, and it is seen to be made up of components corresponding to all possible combinations with the normal state of those upper states excited according to the above rule. Further, the intensity of each component will be proportional to the Einstein B of the transition by which its initial state is reached, on account of the factor $|M_z(m\lambda; n\lambda)|$. This again is in agreement with the interpretation of the Heisenberg rule in the older theory.

In other respects also, the expression for the electric polarization given by Eq. (21) appears to be satisfactory. Thus in the linearly polarized components (P_z) the arbitrary phases cancel out, and we have a phase difference of 90° between the incident light and the resonance radiation. This is as in the classical theory when there is a damping term, however small. On the other hand, in the case of the circular components, the phase relations with the incident light as well as between the various components are entirely arbitrary. This incoherence of the circular components with the incident light would appear to be necessary in order that they should not disturb the dispersion. Their incoherence with each other means that they appear as separate circular components in opposite directions and do not combine to a single linear component. This is in agreement with the observations on the polarization.

It cannot be claimed, however, that we have obtained a completely satisfactory theory of resonance radiation, for it is well known that the density hypothesis used here does not lead to an adequate description of the spontaneous radiation. Thus when there is present on energy level between the two which are in resonance the present theory gives zero intensity for the radiation due to combination of this level with the upper resonance level, unless this intermediate level is initially escited. Even if it is feebly excited the calculated intensity would obviously be much too small, since it is proportional to the product of the squares of the excitation coefficients of the two levels involved, though there is no reason to believe that the present theory would not give the degree of polarization correctly. The same difficulty in the interpretation of $\psi\psi^*$ as electric density is encountered in the theory of scattering and dispersion. As Klein[9] has shown, it is possible to obtain the correct intensities in the Kramers-Heisenberg formula only with the aid of correspondence principle considerations of a statistical nature. It may be said, however, that all these uncertainties are due to the lack of a complete theory of radiation from the standpoint of pure wave mechanics, while we are concerned here only with the removal of those difficulties connected with the space degeneracy. When there is an initial degeneracy due to the presence of equivalent electrons in the outer shell, as in mercury, special considerations might be required.

[9] O. Klein, Zeits. f. Physik **41**, 407 (1927).

Excitation by Circularly Polarized Light

In this case the Heisenberg rule requires that we replace the magnetic field parallel to the electric vector by one perpendicular to the plane of polarization of the light. Corresponding to this our perturbation equations take their simplest form, with only one element in each row outside the diagonal in Φ, when for the unperturbed characteristic functions we choose those for such a field. This will be seen from the form of the coefficients and the relations (17). If we take the xy-plane as that of the electric vector and suppose for definiteness the light to be right circularly polarized ($C_z=0$, $C_y=-iC_x$) Eq. (10) gives

$$f_{kl}=-(2\pi i/c)\nu_{kl}C_x[M_x^*(kl)-iM_y^*(kl)],$$

and by (17) we find as the only non-vanishing coefficients in Eqs. (12) those of the form

$$f(m,\lambda\,;\,n,\lambda-1)=-(2\pi i/c)\nu_{mn}\;2C_xM_x^*(m,\lambda\,;\,n,\lambda-1),$$

so that for exact resonance we are led to pairs of equations in which $\rho=\sigma+1=\lambda$ that may be written

$$dc_{m\lambda}/dt=(2\pi i/h)f_{\lambda,\lambda-1}\,c_{n,\lambda-1}$$
$$dc_{n,\lambda-1}/dt=(2\pi i/h)f_{\lambda,\lambda-1}{}^*c_{m,\lambda}$$

with $f_{\lambda,\lambda-1}=f(m,\lambda;\,n,\lambda-1)$. Each $c_{m\lambda}$ is thus coupled only with $c_{n,\lambda-1}$ and all amplitudes not thus coupled remain constant. This coupling is again between those vibrations whose combination gives light polarized in the same manner as the incident light—here right circularly.

These equations are solved directly by an exponental substitution and with the same initial conditions as before we find for the electric moment of the perturbed atom

$$P=(4\pi/h)NtE_x\sum_\lambda\sum_{\lambda'}\left|\;M_x(m,\lambda\,;\,n,\lambda-1)\;\right|\;\mathfrak{R}\boldsymbol{M}(m\lambda\,;\,n\lambda')e^{2\pi i[\nu t-\phi_x(m,\lambda;n,\lambda-1)]}.$$

The interpretation is clear by analogy to the case of linear polarization, and the Heisenberg rule is again confirmed.

For elliptic polarization the actual solution is complicated by the fact that each amplitude will be coupled to two others, but there is no difficulty in principle.

In a further paper it is hoped to apply the method here developed to the problem of excitation in a magnetic field and the attendant phenomenon of rotation of the plane of polarization.

It is a pleasure for the author to acknowledge his indebtedness to Prof. E. Schrödinger for valuable suggestions throughout the course of the work, and to Prof. N. Bohr for the privilege of discussing with him the general problems here involved.

Berlin,
May, 1928.

ELECTRONIC STATES AND BAND SPECTRUM STRUCTURE IN DIATOMIC MOLECULES. VII. $^2P \rightarrow {}^2S$ AND $^2S \rightarrow {}^2P$ TRANSITIONS

By Robert S. Mulliken

Abstract

A survey is made of the varied empirical structure-types to be expected for $^2P \rightarrow {}^2S$ and $^2S \rightarrow {}^2P$ bands, and examples of these types are discussed individually. In agreement with Kemble's theory, the arrangement of the rotational levels in the ^2P state changes continuously with the parameter $\Delta E/B$ (ΔE = electronic doublet separation), and these changes are responsible for a large part of the observed variations in band structure. Fig. 1 and Table I show how the arrangement of the ^2P levels changes with $\Delta E/B$, and Figs. 2—5 show, for the MgH, OH, HgH, and NO γ bands, how observed branches are related to energy levels. In Table II, data on ΔE and B are listed for a number of molecules. The mode of variation of the arrangement of the rotational levels in ^2P states appears to be in striking agreement with the quantitative formulas of Hill and Van Vleck. For example, if $\Delta E/B = +2$, their equation becomes formally identical with the Kramers and Pauli formula which holds exactly for the ^2P state of CH.

A *consistent notation*, as proposed in VI of this series, is given here for the known branches of the MgH, CaH, OH, ZnH, CdH, HgH, and NO bands; this notation has already been applied to the OH and BO bands (Kemble, Jenkins) and to CH λ3900. A more or less detailed discussion is given of the spectra mentioned, especially MgH and OH; some term values are given for ^2P and ^2S states of MgH, CaH and OH.

In the bands just mentioned, band-structure and missing lines show good agreement with theory. In the cases where $|\Delta E/B|$ is small for the ^2P state (CH, MgH) there is agreement with the case b intensity theory (six main branches, four weak satellite branches). As $|\Delta E/B|$ increases, the satellite branches get stronger, and two new branches become evident. This tendency first appears distinctly in OH, where the satellite branches, although very weak, are much too strong for Hund's case b, and where a previously unclassified very weak branch is found to be one of the two new branches just mentioned. As $|\Delta E/B|$ increases still further, the six weak branches finally become equal to the other six in intensity. This metamorphosis has also been discussed by Hulthén. The observed relations, in particular the equality of intensity of the six "weak" and the six "strong" branches when $|\Delta E/B|$ is very large, appear to be in excellent agreement with the quantitative intensity formulas of Hill and Van Vleck.

A conclusion of interest for the empirical study of $^2P \rightarrow {}^2S$ and $^2S \rightarrow {}^2P$ bands is the following: in four-headed bands of these types the *first* head should always be weaker than the rest unless $|\Delta E/B|$ is large, and should disappear if $|\Delta E/B|$ is near zero.

Intensity relations in $^2P \rightarrow {}^3S$, $^2P \rightarrow {}^1S$, and other types of bands are briefly discussed for the case that one electronic state falls under Hund's case a, the other under his case b; some predictions are made.

Introduction: General Survey of Structure and Intensity Types in $^2P \rightarrow {}^2S$ and $^2S \rightarrow {}^2P$ Bands

THE present and the previous paper (VI)[1] of this series resulted from an attempt to explain in detail a number of spectra which, according to

[1] R. S. Mulliken, Phys. Rev. 30, 785 (1927); for discussion of magnetic and nuclear kinetic energy relations cf. pp. 793–6.

Hund's theory of molecular electronic states,[2] must be classified as $^2S \rightarrow {}^2P$ and $^2P \rightarrow {}^2S$ transitions,[3] but which exhibit great variety in the obvious features of their structure. These spectra differ especially in regard to (1) the forms of the rotational energy functions which must be assumed to account for the forms of the observed branches, (2) intensity relations, as shown especially by the number of strong branches, which is sometimes six, sometimes twelve, sometimes apparently eight. The explanation of these differences must be sought in variations in the doublet separations and other related characteristics of the ^2S and especially in those of the ^2P states involved.

The object of the following paragraphs is to make a brief qualitative survey of the types which are to be expected theoretically for the structure of bands of the class here considered. This makes it easier to understand the individual examples which are discussed in the later sections of the paper.

Form of rotational terms of ^2P state as a function of $\Delta E/B$. First we consider the possible forms of the rotational energy terms $F_1(j)$ and $F_2(j)$ of the ^2P state. As Kemble has shown, these forms depend essentially on the parameter $\Delta E/B$,[5] where ΔE is the energy-difference between parallel and antiparallel orientations of s with respect to σ_k,[6] and B is the familiar coefficient of the main rotational energy term (both ΔE and B are to be understood below as measured in wave-numbers). For our survey of types we have then to investigate how $F_1(j)$ and $F_2(j)$ behave as a function of $\Delta E/B$. The complication that each level of the F_1 and F_2 sets is really a narrow doublet (σ-type doubling) need not concern us for the present.

If $|\Delta E/B|$ is large, and j not too large, we have Hund's case a. Positive ΔE gives a normal ^2P state, which we shall call ^2P_n, negative ΔE an inverted ^2P, or ^2P_i, state. If $\Delta E \sim 0$, or if j is very large, we have Hund's case b. For intermediate values of $\Delta E/B$ or j there are intermediate cases. The various distinctive cases may be classified according to the notation of Table I, in which the main characteristics of the $F(j)$ functions are given for each such case. The meaning of the notation (e.g., $^2P_{nab}$) should be obvious. The relations given in Table I can all be deduced from the qualitative considerations given in VI (cf. ref. 2, pp. 793–6), together with Kemble's quantitative formulas.[4,7] The same results also follow from the beautiful

[2] F. Hund, Zeits. f. Physik, **36**, 657 (1926); **42**, 93 (1927).

[3] Cf. R. S. Mulliken, Phys. Rev. **29**, 642–3 (1927).

[4] E. C. Kemble, Phys. Rev. **30**, 387 (1927).

[5] $\Delta E/B$ is Kemble's function P. *In general*, $P = A/2Bs^2$, the magnetic energy being $A \cos\theta$, θ being the angle between s and σ_k. Evidently, $\Delta E = 2A$. For $s = \frac{1}{2}$ as in the present case, P reduces to $2A/B$ or $\Delta E/B$.

[6] ΔE is approximately equal in Hund's case a to the observed separation between the lowest F_1 and F_2 levels, but is more difficult to specify in case b, especially in view of the loss of the old literal interpretation of the geometrical relation of σ_k, l, and s in the new quantum mechanics. But cf. Hill and Van Vleck.[7a]

[7] Kemble's results are not in the form of closed formulas applicable to all cases, hence the qualitative considerations of VI are used here, supplemented by the conclusions expressed in Kemble's Eq. (23). But cf. ref. 7*a*.

TABLE I. *Term-form as a function of j for ^2P states, for various values of the parameter $\Delta E/B$. (Footnote numbers here refer to the notes at the bottom of this page.)*

Value of $\Delta E/B$	*Term-form*[1,4]	*Form of ΔF's*[1,3,4]	*F and ΔF relations for moderate j.*[5]	
+large ($^2P_{na}$)	$B[j(j+1)-\sigma_i^2]$, $\sigma_1=\frac{1}{2}, \sigma_2=1\frac{1}{2}$ (cf. note 2)	$\Delta_1F(j)=2B(j+1)$ $\Delta_2F(j)=4B(j+\frac{1}{2})$	$F_2(j)-F_1(j+1)=$Const. $>>>0$	$\Delta F_2(j)\backsim\Delta F_1(j)$
>about +10 (+10 is about middle of $^2P_{nab}$ region, which begins at $\Delta E/B=+4$)	$B_i^*[j(j+1)]+\cdots$, with $B_2^*>B>B_1^*$	$\Delta_1F_i(j)=2B_i^*(j+1)+\cdots$ $\Delta_2F_i(j)=4B_i^*(j+\frac{1}{2})+\cdots$	$F_2(j)-F_1(j+1)>>0$, but diminishing with increase of j (cf. note 6)	$\Delta F_1(j+1)>\Delta F_2(j)>\Delta F_1(j)$
+2 (middle of $^2P_{nba}$) region)[7]	$B[\{(j+\frac{1}{2})^2-\sigma_k^2\}^{\frac{1}{2}}\mp\epsilon]^2$, $\sigma_k=1$, $\epsilon=\frac{1}{2}$	Not simple[7]	$F_2(j)-F_1(j+1)<0$; $F_2(j)-F_1(j)>0$ (cf. note 6)	$\Delta F_2(j)>\Delta F_1(j+1)$
$\backsim$0(^2P_b)	$B[j_k(j_k+1)-\sigma_k^2]$, with $j_k=j\pm\frac{1}{2}$	$\Delta_1F(j_k)=2B(j_k+1)$ $\Delta_2F(j_k)=4B(j_k+\frac{1}{2})$	$F_2(j)-F_1(j+1)=0$; $F_2(j)-F_1(j)>0$	$\Delta F_2(j)=\Delta F_1(j+1)$, i.e. $\Delta F_2(j_k)=\Delta F_2(j_k)$
$-$($^2P_{iab}$)	$B_i^*[j(j+1)]+\cdots$, with $B_2^*>B>B_1^*$	$\Delta_1F_i(j)=2B_i^*(j+1)+\cdots$ $\Delta_2F_i(j)=4B_i^*(j+\frac{1}{2})+\cdots$	$F_2(j)-F_1(j+1)>>0$, but diminishing with increasing j(cf. note 6)	$\Delta F_1(j+1)>\Delta F_2(j)>\Delta F_1(j)$
$-$large ($^2P_{ia}$)	$B[j(j+1)-\sigma_i^2]$, $\sigma_1=1\frac{1}{2}, \sigma_2=\frac{1}{2}$. (cf. note 2)	$\Delta_1F(j)=2B(j+1)$ $\Delta_2F(j)=4B(j+\frac{1}{2})$	$F_2(j)-F_1(j+1)=$Const. $>>>0$	$\Delta F_2(j)\backsim\Delta F_1(j)$

Notes for Table I. (1) The term-form as given is of course incomplete in that small terms in j^4, etc. have been omitted. The j and j_k values in the term-formulas are those of the new mechanics: j = half-integral, j_k = integral, for ^2P.

(2) Although the B^* values should become practically identical for the F_1 and F_2 states as case *a* is approached (large $|\Delta E/B|$), a small real difference in B values might be expected ultimately to develop if ΔE becomes very large.

(3) By definition (cf. I of this series) $\Delta_2F(j)=F(j+1)-F(j-1)$, while $\Delta_1F(j)=F(j+1)-F(j)$.

(4) It will be noted that Δ_2F should be approximately of the form $C\tau$, with τ = integral or half integral, except in certain regions of small positive values of $\Delta E/B$. When this is the case, the absolute j or j_k numbering, as well as the minimum values of j or j_k, can be determined at once from the empirical Δ_2F's (if τ = integral, we know $\tau=j+\frac{1}{2}$, while if τ = half-integral, $\tau=j_k+\frac{1}{2}$,—cf. note 1 above). This method is still good even when B^* differs considerably from B, but finally fails in the region of small positive $\Delta E/B$ values already mentioned; this region extends a considerable distance[7c] toward case $^2P_{nab}$, from case ^2P_b. Here ΔF_2 is no longer even approximately a linear function of j or j_k (cf. the cases of CH λ3900 in VI, and of MgH, below), and other criteria must be used. In border-line cases (CaH, OH), the relation $\Delta_2F=C\tau$ is only roughly fulfilled, but can be used subject to confirmation by other methods.—Similar relations hold for Δ_1F (cf. note 3).

(5) The relations given in the last column hold for Δ_1F's as well as for Δ_2F's, at least if σ-type doubling is neglected.

(6) In the fourth column, the differences $F_2(j)-F_1(j+1)$ in the intermediate cases $^2P_{nab}$, $^2P_{nba}$, and $^2P_{iab}$, tend toward zero as j increases; cf. ref. 7*b* for exact formula; but this formula is subject to correction for the effects of the magnetic field developed by rotation (cf. Kemble, ref. 4, top p. 395).

(7) For the relations in this case, cf. discussion of CHλ3900 in VI. The Kramers and Pauli term-form here now proves to be exactly the form which Hill and Van Vleck's formula[7b] assumes for $\Delta E/B=+2.00$.

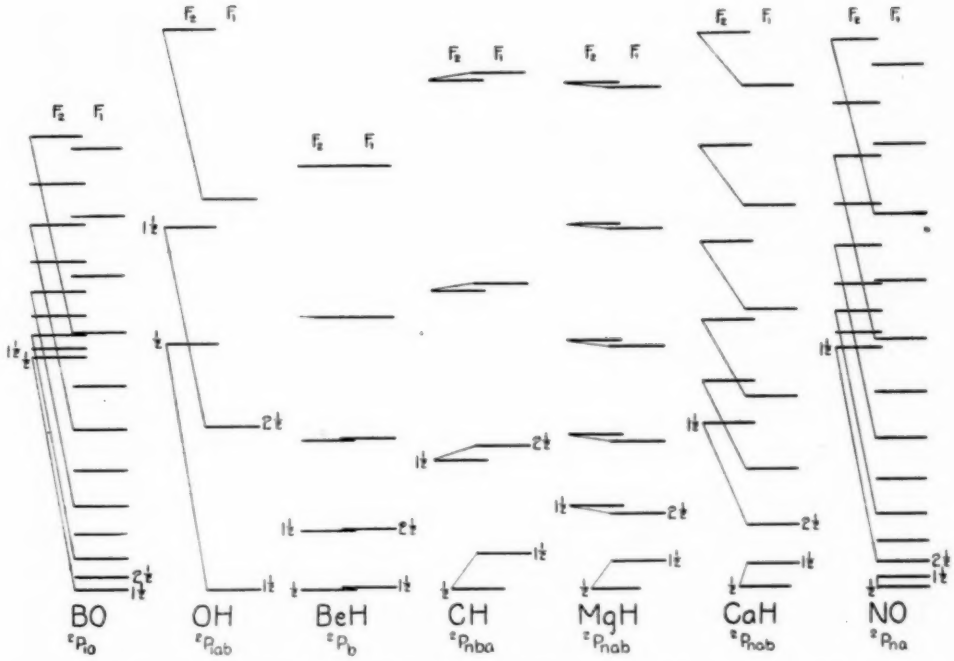

Fig. 1 shows, on a uniform scale, with the lowest level placed at zero in each case, the arrangement and spacing of the rotational levels of a number of ^2P states having a variety of values of ΔE and B (cf. Tables I and II for more complete data and explanation of designations such as $^2P_{iA}$, $^2P_{nba}$). The numbers opposite some of the levels are j values. The spacings of the levels are for the vibrational quantum number $n=0$, except that in the case of NO they are for $n=4$. F_1 and F_2 levels which would in case b correspond to the same value of j_k are indicated by slanting connecting lines. The level $F(\frac{1}{2})$, which is classified as $F_2(\frac{1}{2})$ for negative values of $\Delta E/B$, soon becomes obviously associated with the F_1 levels as $\Delta E/B$ becomes increasingly positive, and is then naturally classified as $F_1(\frac{1}{2})$. The level $F(\frac{1}{2})$ is accordingly represented in Fig. 1 as shifting gradually from the F_2 set to the F_1 set of levels.[7d] The reader may find it of interest to compare and correlate the varying patterns of levels shown in Fig. 1 with the varying relative orientations and interaction energies of the σ_k and s vectors. A discussion of the latter will be found in ref. 1 (cf. Fig. 1 and pp. 793–6) and in ref. 4. The $F_1(j)$ and $F_2(j)$ data used are mainly quantitative data which either are given in this paper (MgH, CaH) or have been obtained in obvious ways with the help of published ΔF data (BO, ref. 11; OH, Dieke, ref. 31; NO, ref. 41). For BeH, the spacings of the levels have merely been estimated roughly by assuming $F(j_k)=7.82[j_k(j_k+1)-\sigma_k^2]$, the value $B=7.82$ having been obtained from Petersen's value of the moment of inertia (Abstract 86, April 1928 meeting of Am. Phys. Soc.); the separations $F_1(j+1)-F_2(j)$ here are very small and not yet accuratey known, and the spacings are exaggerated. In Petersen's BeH bands, (cf. also Watson, Abstract 85), the type of transition is not certain, but probably either the initial, or the final, state is ^2P, and since $B'\sim B''$ in these bands, the above representation should be not far wrong.

[7c] At $\Delta E/B=+4$ (boundary of $^2P_{nba}$ and $^2P_{nab}$ regions), according to Hill and Van Vleck's formula,[7b] the term form is the same as for $\Delta E/B=0$; hence near *both* these points we expect $\Delta_2 F\backsim C\tau$, with $\tau=$ half-integral. But inside each of the regions $^2P_{nba}$ and $^2P_{nba}$ (cf. CH, with $\Delta E/B=+2$, and MgH, with $\Delta E/B\backsim 6$), $\Delta_2 F$ is no longer even approximately of the form $C\tau$.

[7d] In Hill and Van Vleck's formula[7b], $F(\frac{1}{2})$ must be classified as $F_2(\frac{1}{2})$ from $\Delta E/B=-\infty$ to $+2$, and as $F_1(\frac{1}{2})$ for $\Delta E/B>+2$.

work of Hill and Van Vleck[7a] who, with the new quantum mechanics, have recently obtained a closed formula giving the energy quantitatively throughout the entire range of $\Delta E/B$ values.[7b].

The changing associations and spacings of the rotational levels as $\Delta E/B$ is varied can best be understood with the help of Fig. 1, in which observed levels are shown for a number of *actual examples* of ^2P states; these examples are individually discussed below, or elsewhere. The gradual shift of the $F(\frac{1}{2})$ level (cf. refs. 2 and 4) from its association with the F_2 levels in $^2P_{ia}$ and ^2P_b states to association with the F_1 levels in $^2P_{na}$ states is especially well shown.

TABLE II. *Examples of ^2P states arranged according to $\Delta E/B$ values.*

Case	Molecule	ΔE	B_1*	B_2*	B	$\Delta E/B$	Bands	Diagram
$^2P_{na}$	HgH	3683	6.56	6.61	6.58	+560	$P\rightarrow S$	Fig. 4
	CdH	1001	5.96	6.03	5.99	+169	$P\rightarrow S$	(Type of Fig. 4)
	NO	124	1.675	1.724	1.70	+73	$S\rightarrow P$	Figs. 1, 5.
	ZnH	330	7.15	7.47	7.3	+45	$P\rightarrow S$	(Type of Fig. 4)
	NO	33	1.070	1.168	1.12	+29	$P\rightarrow P$	(Data, ref. 9)
	CaH	80	4.09	4.49	4.3	+19	$P\rightarrow S$	Fig. 1
$^2P_{nab}$	MgH	35	—	—	6.1	+5.7	$P\rightarrow S$	Figs. 1, 2.
$^2P_{nba}$	CH	28.4	14.19		14.19	+2.00	$S\rightarrow P$	Fig. 1; and Ref 2, Fig. 3.
$^2P_{iab}$	OH	−127	16.60	20.56	18.47	−6.9	$S\rightarrow P$	Figs. 1, 3.
	CN	−54	—		(1.6)	(−34)	$P\rightarrow S$	
	CO^+	−126	—		(1.6)	(−79)	$P\rightarrow S$	(BO type)
$^2P_{ia}$	$B^{11}O$	−126	1.383	1.412	1.40	−90	$P\rightarrow S$	Fig. 1 and ref. 11

Notes for Table II. (1) The data on ΔE and B^* can be found mainly in the following references: ZnH, CdH, HgH, ref. 8; NO (data from β bands), ref. 9; CaH, ref. 10; MgH, see following detailed treatment for references; CH, ref. 2; OH, see below; CN, CO^+, ref. 10a; $B^{11}O$, ref. 11. The ΔE values used (except for CH and MgH) are merely the empirical values of the interval between the lowest F_1 and the lowest F_2 level, and are perhaps not the most appropriate[6]; the ΔE values given for MgH and CH are so chosen as to make the experimental F data fit Hill and Van Vleck's formula[7b] (cf. Table I, note 7).

(2) The B values given are mostly averages of the B_1* and B_2* values; they should then be moderately accurate, according to Kemble's work[4] on OH.

(3) Under "Bands" is recorded the type of transition ($^2S\rightarrow{}^2P$ or $^2P\rightarrow{}^2S$) in which the given ^2P state has been observed.

(4) Under "Diagram" a reference is given to a figure showing the observed energy levels and transitions (cf. discussion of "Line and level types," below); unless otherwise stated, the figure is to be found in the present paper.

[7a] E. L. Hill and J. H. Van Vleck, Phys. Rev., **32,** 250, 1928. The writer is greatly indebted to Prof. Van Vleck for the opportunity to examine this work before publication. Unfortunately this was not possible before receipt of the proof of the present paper, so that use of Hill and Van Vleck's results could be made only incompletely, in minor changes and additions in the proof.

[7b] Cf. Eq. (27) of Hill and Van Vleck. λ of Hill and Van Vleck is the same as $\Delta E/B$ here. The j_1 and j_2 rotational states of Hill and Van Vleck are respectively identical with the F_2 and F_1 states of the present and previous papers of this series.

[8] R. S. Mulliken, Proc. Nat. Acad. Sci., **12,** 151 (1926).

[9] F. A. Jenkins, H. A. Barton, and R. S. Mulliken, Phys. Rev. **30,** 150 (1927).

[10] E. Hulthén, Phys. Rev. **29,** 97 (1927).

[10a] For data on CO^+ and CN, cf. R. S. Mulliken, Phys. Rev. **26,** 571 (1925). The value of B for CN is estimated by means of the rule that ω_0/B is roughly a constant for the various electronic states of one molecule (R. Mecke, Zeits. f. Physik, **32,** 823, 1925).

[11] F. A. Jenkins, Proc. Nat. Acad. Sci. **13,** 496 (1927). The separation of the F_1 and F_2 sets of levels in Jenkins' Fig. 1 is not to scale.

The changing order of corresponding F_1 and F_2 levels in passing through the $^2P_{nba}$ neighborhood, from $F_2(j) > F_1(j+1)$ to $F_1(j+1) > F_2(j)$ and back, is also clearly shown.

Further information concerning the ^2P states of Fig. 1, and others, is given in Table II. The divergence of B_1^* from B_2^* (cf. ref. 4 and Table I for the meaning of these coefficients), in agreement with Kemble's theory, for intermediate values of $\Delta E/B$, is well shown by the data in Table II. The fact that, in agreement with Kemble's theory, $\Delta E/B$ and not ΔE is the parameter which determines the behavior of a ^2P state for a given range of j values, will be evident if one compares OH and BO (or CaH and NO) in Fig. 1 and in Table II. For the physical reason behind this fact, reference may be made to Kemble's paper. The same fact is also shown in the existence of a continuous variation of intensity relations, in $^2P \rightarrow {}^2S$ and $^2S \rightarrow {}^2P$ bands, as the parameter $\Delta E/B$ changes. These intensity relations are discussed in the following paragraphs.

Intensity relations and number of branches as a function of $\Delta E/B$ *of* ^2P *state.* The intensity relations in $^2P \rightarrow {}^2S$ and $^2S \rightarrow {}^2P$ transitions can be predicted by means of the theoretical equations given in VI, if $|\Delta E/B|$ is small for the ^2P state, so that both initial and final state fall to a good approximation under Hund's case *b*. The theory then predicts six strong branches accompanied by four satellite branches of very low intensity.

When $|\Delta E/B|$ is large for the ^2P state, the latter falls under Hund's case *a*, while the ^2S state, as always,[12] falls under case *b*. For such a mixed (*a*,*b*) transition, neither the intensity theory for case *a* transitions (cf. III of this series[13]) nor that for case *b* transitions as given in VI, is applicable. Empirically, however, it is found that as $|\Delta E/B|$ increases there is a gradual transition from the case *b* type with six strong branches (example CH λ3900, with $\Delta E/B = 2.0$) to a type with twelve strong branches (HgH bands, with $\Delta E/B = 560$). In the MgH, OH, and CaH bands ($\Delta E/B \sim +5.7$, -6.9, and $+19$ respectively), the intensity relations of case *b* are still essentially true, there being only six strong branches. But in the OH bands—presumably also in the MgH and CaH bands, but these are less well known—the four satellite branches, whose intensity in case *b* should fall to negligible values as j_k increases, have an appreciable, although still very small, intensity even for large values of j. Also, in OH, at least one new branch makes its appearance, in low intensity. In the ZnH bands ($\Delta E/B \sim +45$) the four satellite branches are perhaps nearly half as strong as the six main branches,[14] and are accompanied by two about equally strong new branches; these (one of which corresponds to the new branch in OH) are branches which in case *b* should be completely absent because they would involve $\Delta j_k = \pm 2$. In the NO γ, BO α, and CdH bands ($\Delta E/B \sim +73$, -90, and $+169$, respectively), the six weaker branches make further gains, and in HgH ($\Delta E/B = +560$) they are approximately equal in intensity to the other six branches. It is

[12] Cf. R. S. Mulliken, Phys. Rev. **30**, 138 (1927).
[13] R. S. Mulliken, Phys. Rev. **29**, 391 (1927).
[14] E. Hulthén, Zeits. f. Physik **45**, 335 (1927).

evident that in the limit of very large $|\Delta E/B|$ the intensities depend on Δj and not at all on Δj_k, j_k having now completely lost its rôle as a quantum number. The twelve observed strong branches represent merely all the possible combinations between ^2P and ^2S levels which satisfy the rule $\Delta j = 0, \pm 1$.

The above relations have been sketched in two preliminary abstracts,[15] and also in a paper by Hulthén.[14] Hulthén has given a partial explanation of them in terms of the correspondence principle. Van Vleck and Hill[7a] have now given theoretical intensity formulas good for the whole range of values of $\Delta E/B$. These have not yet been tested for intermediate values of $|\Delta E/B|$, but agree with the observed relations for very large $|\Delta E/B|$ as in HgH, hence presumably also for the intermediate values.

Throughout the entire range of $\Delta E/B$ values for the ^2P state, σ-type doubling exists for the latter, but on account of certain typical selection rules which evidently remain valid throughout, is prevented from increasing the number of branches. Without these selection rules, one would expect twelve strong branches for small $\Delta E/B$, twenty-four for large $\Delta E/B$. In the OH bands, to be sure (cf. detailed discussion below), certain additional branches are found which run counter to these rules, but they are very weak.

Apparent eight-branch bands of $^2S \rightarrow {}^2P$ and $^2P \rightarrow {}^2S$ types. In certain cases where $|\Delta E/B|$ is large there appear to be only eight instead of twelve branches (BO α bands, CO^+ comet-tail, red CN, NO γ bands). This condition has been shown previously[17] to result from an almost exact coincidence of F_1 and F_2 levels of the ^2S state. The reason this reduces the apparent number of branches from twelve to eight will be clear from a study of diagrams such as Figs. 2–4 below and Fig. 1 of Jenkins' paper on the BO α bands.[11] Essentially, the four satellite branches ${}^QR_{12}$, ${}^PQ_{12}$, ${}^RQ_{21}$, and ${}^QP_{21}$ coalesce each with its corresponding main branch.

The two branches (${}^{PP}P_{12}$ and ${}^{RR}R_{21}$) which correspond to $\Delta j_k = \pm 2$ never coalesce with other branches. Thus when there is coalescence of main and satellite branches the total number of visible independent branches is eight if $|\Delta E/B|$ is large enough to bring out the P_{12} and R_{21} branches (examples, BO α and NO γ bands); otherwise it is six (examples, CH, MgH bands).—As Hulthén has shown,[14] approximate coincidence of F_1 and F_2 levels of the ^2S state occurs in molecules for which ΔE (not $\Delta E/B$) is small in the ^2P state.

Survey of line and level types in $^2P \rightarrow {}^2S$ and $^2S \rightarrow {}^2P$ bands. The possible empirical types of $^2P \rightarrow {}^2S$ and $^2S \rightarrow {}^2P$ bands may be classified according to (*a*) whether the ^2P state is initial or final, (*b*) the sign and magnitude of $\Delta E/B$ of the ^2P state, (*c*) whether or not the F_1 and F_2 levels of the ^2S state are practically coincident. The structure of such bands, and the com-

[15] R. S. Mulliken, Phys. Rev. **29**, 921*A* (1927); **31**, 310*A* (1928).

[16] Cf. II, IV, and especially VI of this series, and theoretical papers of Hund (Zeits. f. Physik **42**, 111, 1927) and of R. de L. Kronig (Zeits. f. Physik **46**, 814, 1928).

[17] R. S. Mulliken, Phys. Rev. **28**, 1218–20 (1926); cf. also F. Hund, Zeits. f. Physik **42**, 99 (1927), and E. Hulthén, ref. 10.

bination relations, combination defects, missing lines, and so on, are much more readily understood with the help of diagrams of rotational energy levels and transitions than in any other way. Hence it seems desirable that such diagrams should be on record for the band-types likely to be found most frequently in practise. Diagrams for a number of representative examples are therefore given in the figures of the present paper, and others are available elsewhere (cf. references in Table II under "Diagram").

The following points may be helpful to the reader in studying these examples: (1) *In all cases* the possible branches are limited to the following: P_1, Q_1, R_1, P_2, Q_2, R_2 (strong branches always); ${}^{Q}R_{12}$, ${}^{P}Q_{12}$, ${}^{R}Q_{21}$, ${}^{Q}P_{21}$ (satellite branches, very weak if $\Delta E/B$ is small, strong if it is large); ${}^{PP}P_{12}$, ${}^{RR}R_{21}$ (absent if $\Delta E=0$, strong if $\Delta E/B$ is large). The notation is that of VI, extended in the case of the last two branches to indicate, by RR or PP, that these branches would correspond in case b to $\Delta j_k=\pm 2$. (2) In ${}^2P\rightarrow{}^2S$ transitions the allocation of given-named satellite branches to main branches is different than in ${}^2S\rightarrow{}^2P$ transitions, e.g., ${}^{P}Q_{12}$ is satellite to P_1 in ${}^2P\rightarrow{}^2S$, but to P_2 in ${}^2S\rightarrow{}^2P$ transitions. (3) The value of j for the first line in any given-named branch differs in many cases for ${}^2P\rightarrow{}^2S$ and ${}^2S\rightarrow{}^2P$, often also (because of the shift of $F(\frac{1}{2})$ from the F_1 to the F_2 series of levels) for an inverted as compared with a normal ${}^2P$ state. (4) For an inverted case a ${}^2P$ state like that in BO the F_1 levels and F_2 levels respectively correspond to ${}^2P_{1\ 1/2}$ and ${}^2P_{1/2}$ electron states, whereas for a *normal* case a ${}^2P$ state as in NO or HgH, they correspond to ${}^2P_{1/2}$ and ${}^2P_{1\ 1/2}$ electron states respectively.

Prediction of Intensity Relations for ${}^3P\rightarrow{}^3S$ and Other Transitions

The present section is a digression from the discussion of ${}^2P\rightarrow{}^2S$ and ${}^2S\rightarrow{}^2P$ transitions. It is, however, an outgrowth of the material of the previous section, and rounds out the discussion of intensity relations given in the papers of this series.

In ${}^3P\rightarrow{}^3S$ bands, nine strong main branches and a number of weak satellite branches are expected if the ${}^3P$ state falls under Hund's case b. The theoretical intensities could be calculated, if desired, by the methods used in V and VI.[17a] The NH bands as analyzed by Hulthén and Nakamura[18] are an example of this type. Here $|\Delta E|$ is roughly 60, B$\sim$15, hence $|\Delta E/4B|$, which for triplet states[5] takes the place of $\Delta E/B$ for doublet states, has approximately the value 1. With increasing values of $(\Delta E/4B)$ in the ${}^3P$ state in ${}^3P\rightarrow{}^3S$ and ${}^3S\rightarrow{}^3P$ transitions, we may, by analogy with ${}^2P\rightarrow{}^2S$ and ${}^2S\rightarrow{}^2P$ bands, expect to find increasing intensity of satellite branches. For large $|\Delta E/4B|$ we may then perhaps expect the appearance in high intensity of all the branches, 24 in number, which conform to the rule $\Delta j=0,\ \pm 1$ and to the selection rules of σ-type doubling.[17a]

Similar considerations doubtless apply to other bands, such as ${}^4P\rightarrow{}^4S$, involving combinations of P and S states. Presumably they apply,[17a] even in cases not involving S states, whenever one state falls under Hund's case a,

[17a] Cf. also ref. 7*a*.

[18] E. Hulthén and S. Nakamura, Nature, Feb. 12, 1927.

the other under Hund's case *b*. We have in general three limiting cases to consider: (1) Both states fall under case *a*; (2) one state falls under case *a*, the other under case *b*; (3) both states fall under case *b*. The predicted strong branches are the same for case (1) as for case (3), but in case (1) satellite branches should be strictly absent, while in case (3) such branches should be present in low intensity.[19] In well-developed case (2) the satellite and certain other branches presumably become intense. The NO β bands ($^2P \rightarrow {}^2P$) agree in their intensity relations[20] with case (1), although the $\Delta E/B$ values ($+29$ for the initial, $+73$ for the final state) suggest that a tendency toward case (2) might have been observed.

For an intersystem combination such as $^3P \rightarrow {}^1S$, it is not clear what is to be expected. The fact that ^1S may be classified under either case *a* or case *b* makes it difficult to decide how it should behave here. At any rate, the maximum possible number of branches satisfying $\Delta j = 0, \pm 1$ is nine, in three groups, $^3P_2 \rightarrow {}^1S$, $^3P_1 \rightarrow {}^1S$, $^3P_0 \rightarrow {}^1S$. The objection might be raised that σ changes by 2 in $^3P_2 \rightarrow {}^1S$, but this objection probably is not valid, since σ is merely the sum of σ_k and σ_s and is not important as a quantum number. Empirically it appears, from what is known of the band structure, that all the levels $^3P_2$, $^3P_1$, and $^3P_0$ combine with ^1S in the Cameron CO bands.[21,22]

The MgH Bands

Structure and interpretation: general. The green MgH bands, first measured by Fowler[23] and later classed by Heurlinger[24] with the OH bands as typical doublet bands, have more recently been remeasured and analyzed by Watson and Rudnick.[25,26] That the bands are actually due to MgH is satisfactorily shown, in confirmation of other evidence, by the isotope effect.[25,26]

[19] In case (1) the Hönl and London intensity formulas (cf. ref. 13) are applicable, supplemented by Hund's selection rule $\Delta\sigma_s = 0$ (cf. Hund, ref. 1, 1926, and IV of this series: Phys. Rev. **29**, 637, 1927). In case (3), Eqs. (8)–(13) of VI apply.

[20] F. A. Jenkins, H. A. Barton, and R. S. Mulliken, Phys. Rev. **30**, 175 (1927).

[21] Cf. R. T. Birge, Phys. Rev. **28**, 1157 (1926).

[22] But in the red Na_2 bands, which are also thought to be $^3P \rightarrow {}^1S$, each band appears to have only one head, suggesting a limitation to $^3P_1 \rightarrow {}^1S$ (cf. R. Ritschl and D. Villars, Naturwiss., **16**, 219, 1928). No reason is evident for such a contrast between the CO and the Na_2 bands, since $\Delta E/B$ is probably of the same order of magnitude in both.

It is possible that this anomaly can be avoided as follows. The green Na_2 bands ($^1P \rightarrow {}^1S$) and the red bands have a common final ^1S state which on dissociation gives two unexcited (^2S) Na atoms. The initial state of both green and red bands gives on dissociation a ^2P and a ^2S atom (F. W. Loomis, Phys. Rev. **31**, 323, 1928). Now there are four molecular states which are theoretically derivable from a ^2P and a ^2S atom, namely ^3P, ^3S, ^1P, and ^1S. Thus it is possible that the initial state of the red bands may be ^1S (or ^3S) rather than ^3P, so that the bands are $S \rightarrow {}^1S$. Certain features of the bands seem to be in disagreement with this suggestion, however, according to a private communication from Professor Loomis. The question can probably be settled only by a detailed analysis.

[23] A. Fowler, Phil. Trans. Roy. Soc., **209A**, 447 (1909).

[24] T. Heurlinger, Dissertation Lund, 1918.

[25] W. W. Watson and P. Rudnick, Astrophys. J. **63**, 20 (1926).

[26] W. W. Watson and P. Rudnick, Phys. Rev. **29**, 413 (1927).

Each band has three pairs of branches P_1, P_2; Q_1, Q_2; R_1, R_2. Pairs of lines such as $P_1(m)$ and $P_2(m)$, in the notation used by previous workers, form rather narrow doublets which slowly become narrower as m increases. These characteristics are exactly those expected for a case b $^2S \rightarrow {}^2P$ or $^2P \rightarrow {}^2S$ transition. The missing lines and the forms of the Δ_2F''s and Δ_2F'''s give evidence (see below) that the transition is $^2P \rightarrow {}^2S$; data on the relative intensities of the P, Q, and R branches, which would give further support to this classification, are not recorded by Watson and Rudnick.

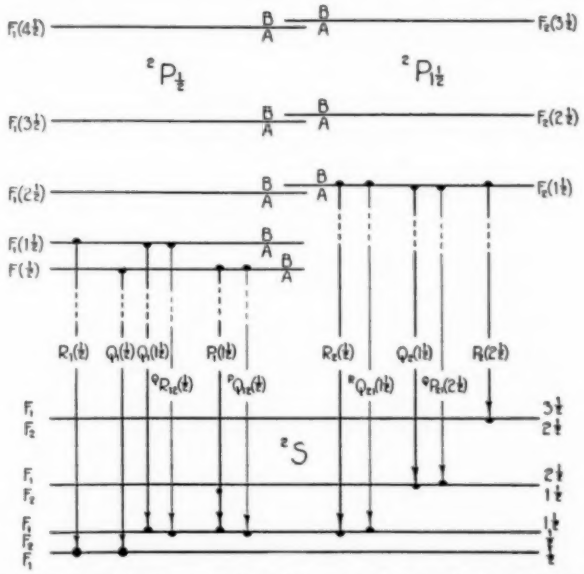

Fig. 2. *Lowest rotational levels, and first line of each branch, for MgH* λ5211 (0, 0 *band*). The levels are drawn to scale from the F' data of Table III (but cf. note *a* of Table III in regard to the level $F_2(1\frac{1}{2})$), and (cf. text, p. 399) from the equation $F''(j_k) = 5.710\, j_k(j_k+1)$. The σ-type doubling is negligibly small on the scale employed, and is shown only by the use of double designations for the levels. Similar remarks apply to the ρ-type doubling in the ^2S levels. On account of the absence (within experimental error) of doubling in the ^2S levels, each satellite branch (light vertical lines in Fig. 2) coincides with one of the main branches (strong vertical lines). The way in which the doublets observed in the spectrum are related to the rotational levels can be seen by drawing additional lines in Fig. 1; e.g. $R_1(1\frac{1}{2})$ forms a doublet with $R_2(\frac{1}{2})$, $Q_1(2\frac{1}{2})$ with $Q_1(1\frac{1}{2})$; $P_1(3\frac{1}{2})$ with $P_2(2\frac{1}{2})$. It may be noted that if the ^2P level $F(\frac{1}{2})$ were here classified as $F_2(\frac{1}{2})$ rather than as $F_1(\frac{1}{2})$, the designations of the lines $Q_1(\frac{1}{2})$, $P_1(1\frac{1}{2})$, and $^PQ_{12}(\frac{1}{2})$ would be altered, to $^RQ_{21}(\frac{1}{2})$, $^QP_{21}(1\frac{1}{2})$, and $Q_2(\frac{1}{2})$. The designations for the ^2P levels of the CH molecule, in VI, were made on the basis of the classification of $F(\frac{1}{2})$ as $F_2(\frac{1}{2})$.[7d]

The observed six branches can be quantitatively explained by the system of energy levels shown in Fig. 2, together with the usual selection rules (cf. VI). The observed branches are evidently the "main" branches, four of them presumably with superposed weak satellite series (these should be unresolved, since $F_1''(j+1) \sim F_2''(j)$ for the ^2S state (see below)). Watson and Rudnick report, without giving data, that there are also independent weak satellite series; these may perhaps correspond to the irregular satellites

in OH which run counter to the selection rules of σ-type doubling. By good luck, the designations P_1, Q_1, R_1, P_2, Q_2, and R_2 used by previous workers can be adopted here without change. The m numbering previously used is, however, to be replaced, by means of the following relations: in the P_1, Q_1, and R_1 branches, $m=j_k''+1=j''+\frac{1}{2}$; in the P_2, Q_2, and R_2 branches, $m=j_k''+1=j''+1\frac{1}{2}$. The j' and j_k' numberings follow, since we know Δj and Δj_k ($\Delta j=\Delta j_k$ here) for each branch.

The relations shown in Fig. 2 are essentially the same as those in CH λ3900 (cf. Fig. 3 of VI[1]), except that (*a*), the change from a $^2S\rightarrow{}^2P$ to a $^2P\rightarrow{}^2S$ transition produces characteristic changes in respect to the first lines of the various branches, and (*b*), in MgH, evidently because of the greater value of $\Delta E/B$, the ^2P $F(\frac{1}{2})$ level is now obviously associated with the F_1 set of levels and so is naturally classed as $F_1(\frac{1}{2})$ rather than as $F_2(\frac{1}{2})$, whereas in CH the classification as $F_2(\frac{1}{2})$ seems the more natural.[7d]

Intensity anomaly in P_2, Q_2, and R_2 branches. According to the intensity theory for case *b*,[1] the lines of the P_2, Q_2 and R_2 branches should be somewhat weaker—approximately in the ratio of the mean j values—than corresponding lines[27] of the P_1, Q_1, and R_1 branches. This of course gives asymptotic equality of intensity of doublet components for high j values. The observed relations are in agreement with these predictions, except that the intensity inequality for low j values is more pronounced than expected; in fact, the first line of each of the branches P_2, Q_2, and R_2 (involving in each case $F_2'(1\frac{1}{2})$) is so weak as to have escaped observation.[25] The CaH bands (see below), with a larger $\Delta E/B$, show a similar but less marked weakness of the early F_2 lines, none of them being too weak to observe except in the Q_2 branch; in molecules with larger values of $\Delta E/B$ the anomaly is no longer noticeable. The explanation of these anomalies is not evident, but they are presumably characteristic of the transition from a case *b* to a case *a* ^2P state.

Empirical justification of interpretation given. While the system of energy levels shown in Fig. 2, plus the selection rules there assumed, is *sufficient* to account for the observed band structure and is in agreement with the theory, it is desirable to show so far as possible that the interpretation given is empirically, with a minimum of theory, a *necessary* one. This requires the investigation of various combination relations.

Empirically, "internal" combination relations such as

$$[RQ_i''\equiv R_i(j)-Q_i(j+1)]=[QP_i''\equiv Q_i(j)-P_i(j+1)]=\Delta_1F_i''(j) \tag{1}$$

and

$$[RQ_i'\equiv R_i(j)-Q_i(j)]=[QP_i'\equiv Q_i(j+1)-P_i(j+1)]=\Delta_1F_i'(j) \tag{2}$$

with $i=1$ or 2, are very nearly, but not quite, fulfilled (cf. ref. 25, Table I, and ref. 26); RQ_i'' etc. here are merely abbreviations for $R-Q$, etc. In explanation of these slight combination defects, Watson and Rudnick assumed, in analogy to Dieke's interpretation of the OH bands, the existence of a fine-scale doubling in all the initial, ^2P, levels (cf. Fig. 2), such that P_i, Q_i, and R_i branches have common final levels, but that the Q_i branches come from slightly displaced levels (F_{iA}' levels) as compared with the P_i and R_i branches (F_{iB}' levels).

In order to justify this scheme empirically, it is necessary to show, (*a*), that P_i, Q_i, and R_i branches actually have common final levels; (*b*), that P_i and R_i branches have common initial levels. This can be done only by means of "external" combination relations, i.e., the demonstration of suitable equalities between sets of combination differences obtained from three

[π] Corresponding lines have equal j_k values and form the obvious doublets of ref. 25.

different bands such as (n_a', n_a''), (n_a', n_b''), (n_b', n_a''). Watson and Rudnick have measured and analyzed the (0, 0), (1, 0), (1, 1), and (0, 1) bands, but unfortunately give wave number data only on the λ5211 (0, 0) band. These are supplemented by a few sets of combination differences from the other bands. The equality,—within experimental error, but not altogether satisfactory (cf. Table II of ref. 26),—of combination differences $Q_1(j)-P_1(j)$ in the (0, 0) and (0, 1) bands furnishes (cf. Fig. 2) the desired verification of the assumption that $P_1(j)$ and $Q_1(j)$ have a common final state. No published evidence is available to show that $R_1(j)$ has also the same final state, nor that $P_2(j)$, $Q_2(j)$, and $R_2(j)$ have a common final state, nor that $P_i(j+2)$ and $R_i(j)$ have a common initial state. Watson and Rudnick indicate, however, that they have tested such relations, and in ref. 26 they give sets of Δ_2F' and Δ_2F'' values for λ5211 which presuppose the validity of such relations.

The fact that the P_1, Q_1, and R_1 branches belong together, and share neither initial nor final states with the likewise coherent P_2, Q_2, and R_2 branches, is only very incompletely established by the published data.

Assignments for j and j_k cannot be made here on the basis of the term forms alone, since the ΔF values of the initial state are not of a simple type (cf. F' data of Table III). The form of the ΔF's of the final state shows, however—cf. below— that this is the ^2S state. If then we agree that the observed lines are "main branch" lines, the restrictions $j' \leqslant \frac{1}{2}$, $j'' \leqslant \frac{1}{2}$, $\Delta j = 0, \pm 1$ are sufficient to determine the j and j_k values for the P_1, Q_1, and R_1 branches, and to show that the subscript 1 is rightly used here. The assignments for the P_2, Q_2, and R_2 branches readily follow, if the obvious doublets are interpreted as is required for a $^2P \rightarrow {}^2S$ transition in which the ^2P states closely approach case b for high j values.

Rotational terms of final (^2S) *states.* Assuming, in spite of the incomplete empirical justification, that the interpretation given in Fig. 2 is correct, we can investigate some of the quantitative relations of F_1 and F_2 terms. Watson and Rudnick's Δ_2F'' values for λ5211[26] are of the form $F_i''(j_k+1) - F_i''(j_k-1) \sim 4B(j_k+\frac{1}{2})$, with $B \sim 5.71$ and $j_k = 1, 2, 3, \cdots$ (except that $j_k = 1$ and 2 are missing for F_2). This corresponds to $F_i''(j_k) = Bj_k(j_k+1) + \cdots$, with $j_k = 0, 1, 2, \cdots$, as expected for a ^2S state. The F_1'' values are probably slightly greater than the corresponding F_2'' values, since the Δ_2F_1'' values appear to be slightly greater,[28] although not surely to an extent beyond experimental error, than the Δ_2F_2'' values.

Initial (^2P) *states; comparison of* F_1 *and* F_2 *terms.* Knowing the F'' values, values of F_1' and F_2' can be determined as illustrated by the following examples (cf. Fig. 2 for justification): $F_{iB}'(2\frac{1}{2}) = R_i(1\frac{1}{2}) + F_i''(1\frac{1}{2})$; $F_{iA}'(2\frac{1}{2}) = Q_i(2\frac{1}{2}) + F_i''(2\frac{1}{2})$, with $i = 1$ or 2. The F'' values can be obtained by calculation from the equation $F_1''(j+1) = F_2''(j) = 5.710j_k(j_k+1)$, where $j_k = j+\frac{1}{2}$; the use of this equation, for low j values, is probably more accurate than an attempt to determine individual F_1'' and F_2'' values from the experimental data. It is found that the F' values obtained in the manner indicated fulfil the relation $F_{iA}' = F_{iB}'$ within experimental error for *low values* of j. We need therefore here distinguish only F_1' and F_2' levels. Averaging the F' values obtained from P_1, Q_1, and R_1 branches, or from P_2, Q_2, and R_2 branches, the results are as given in Table III; the table can readily be extended to larger j values, if desired. Although too much weight should not be

[28] The Δ_2F_1'' values are to be found in ref. 26, Table II (Part *a*, "low-frequency components"); the Δ_2F_2'' values are given in part *b* of this table ("high-frequency components"), which can be extended to higher m values by using the data of Table I of ref. 26.

attached to the exact figures given, on account of the uncertainty of the calculated F'' values used, the data of Table III show unmistakably that $F_2'(j) > F_1'(j+1)$, by an amount which diminishes at first as j increases.

TABLE III. *Initial terms for MgH bands.*

j	$F_2'(j)$	$\Delta_1F_2'(j)$	$F_1'(j+1)$	$\Delta_1F_1'(j+1)$	$F_2'(j)-F_1'(j+1)$
$-\frac{1}{2}$			19,273.28	14.21	
$\frac{1}{2}$			19,287.49	25.03	
$1\frac{1}{2}$	[19,318.0]	[35.3]	19,312.52	36.90	[5.5]
$2\frac{1}{2}$	19,353.34	48.43	19,349.42	48.87	3.92
$3\frac{1}{2}$	19,401.77	60.41	19,398.29	61.04	3.48
$4\frac{1}{2}$	19,462.18	72.64	19,459.33	73.08	2.85
$5\frac{1}{2}$	19,534.82		19,532.41		2.41

(*a*) Lines involving $F_2'(1\frac{1}{2})$ have not yet actually been observed; the values given for this level have been estimated by means of Hill and Van Vleck's formula.

(*b*) The same $F_2'(j)-F_1'(j+1)$ values can also be obtained directly from the doublet separations $P_1(j+1)-P_2(j)$, $Q_1(j+1)-Q_2(j)$, etc.

This involves the assumption $F_2''(j)\sim F_1''(j+1)$, which was also made in calculating Table III. If this holds for high values of j, we may conclude that $F_2'-F_1'$ asymptotically approaches values of about 1.35 and 1.8 for the A and B sub-levels, respectively, since according to Watson and Rudnick,[26] the doublet separations for high j values in the Q branches approach the limiting value 1.35, and in the P and R branches approach the value 1.8.

(*c*) For high values of j, $\Delta F_2'(j)$ and $\Delta F_1'(j+1)$ become asymptotically equal (cf. Δ_2F' values in Table II of ref. 26).

The small, positive, values of $F_2'(j)-F_1'(j+1)$ indicate that the magnetic energy difference in favor of the F_2' term slightly exceeds the kinetic energy difference in favor of the F_1' terms, i.e., we are just on the case *a* side of the region (cf. discussion in VI, pp. 793–96), typified by the ^2P state of CH, where $F_1 > F_2$. The form of the F''s for MgH (cf. the Δ_1F' values in Table III) does not closely approximate any of the cases of Table I, but the relations $F_2(j) > F_1(j+1)$ and $\Delta F_1(j+1) > \Delta F_2(j) > \Delta F_1(j)$ expected for $^2P_{nab}$ of Table I are fulfilled; the ^2P state of MgH may be said to lie near the $^2P_{nba}$ boundary of $^2P_{nab}$. *At* this boundary ($\Delta E/B = +4$), according to Hill and Van Vleck's formula, the doublets $F_2(j)$, $F_1(j+1)$ should have zero separation for all values of j, the first two F_1 levels, however, not forming doublets. MgH is evidently not far from this case (cf. Fig. 2.). Approximate calculations indicate that the F' values of Table III can be accurately represented by Hill and Van Vleck's formulas[7b] if $\Delta E/B \sim 5.7$ and $B = 6.1$.

Initial (^2P) *states: comparison of* F_{iA} *and* F_{iB} *terms.* As can be seen by a study of Fig. 2, the differences $RQ_i''-QP_i''$ and $RQ_i'-QP_i'$, which represent "combination defects" (cf. Eqs. (1) and (2) for meaning of symbols), should satisfy Eq. (3)

$$RQ_i''-QP_i''=RQ_i'-QP_i'=[F_{iB}'(j+1)+F_{iB}'(j)]-[F_{iA}'(j+1)+F_{iA}(j)] \quad (3)$$

From Table I of ref. 25, it can be seen that for λ5211, $RQ_i''-QP_i''$ is approximately zero up to about $m=10$, then increases to about $+0.8$ for $m=18$ and beyond.[29] Hence, we conclude, $F_{iB}'(j)-F_{iA}'(j)\sim 0.4$ for $m \geqq 18$. This is

[29] The $RQ_1''-QP_1''$ values for λ5622 (Table I of ref. 25), which should agree within experimental error with those for λ5211, since both bands have the same initial states, are *negative* for low values of j. This discrepancy may probably be attributed to errors of measurement.

confirmed by a study of the data in Table I of ref. 26, which also show that $F_{2B}'(m) > F_{2A}'(m)$ by somewhat larger amounts than in the case of F_1'. For low values of j, as we have seen previously, $F_{iA}' = F_{iB}'$ within experimental error.

The CaH Bands

Structure and interpretation. Hulthén[10] has measured and analyzed red CaH bands belonging to two systems, which he designates A and B. In each he has investigated two bands, "A" and "A'," "B" and "B'," which are probably (0,0) and (1,1) bands. The B bands are $^2S \rightarrow {}^2S$. The A system bands each have six branches, and are closely analogous to the green MgH bands, except that the doublets (P_1P_2, etc.) are much more widely separated at low j values, corresponding to a larger $\Delta E/B$. Hulthén shows that for the A band the misssing lines in the P and R branches agree with $F_1'(\frac{1}{2})$ and $F_2'(1\frac{1}{2})$ as the lowest $^2P_{1/2}$ and $^2P_{1\ 1/2}$ levels, respectively; for the A' band the exposure was too weak to detect the lines corresponding to the lowest j values. The first lines of the P_2, Q_2, and R_2 branches, as in MgH, are abnormally weak as compared with the case b theory, but the effect is less marked than in MgH, except perhaps in the Q_2 branch. Hulthén makes no mention of possible satellite branches, but did not make an exhautive study.

Hulthén shows (cf. his Table VI) that the same set of Δ_2F_i'' values is obtainable from the P_i and R_i branches of the A band as from those of the B band ($i = 1$ or 2); similarly for the A' and B' bands. If we agree that the branches which look like P and R really have $\Delta j = \pm 1$, the j' and j'' numberings and F_1 and F_2 designations for both A and B systems now follow, from the specification that j' cannot be less than $\frac{1}{2}$ in the B bands. As shown in V of this series, the resulting assignment for the B bands is in agreement with the intensity theory for $^2S \rightarrow {}^2S$ transitions. The Δ_2F_i' values for the A bands can now be calculated (Hulthén's Table VII). Strictly, these Δ_2F_i' values should be checked by combination relations, such as could be obtained by measuring a (1,0) or (0,1) A band, but from the general theory for $^2P \rightarrow {}^2S$ bands there can be little doubt that they are correct.

From the general theory, Hulthén's Q_1 and Q_2 branches are likewise doubtless correctly designated, but in the absence of data on a (1,0) or (0,1) band, their relation to the other branches is not empirically verified. "Internal" combination relations corresponding to the Eqs. (1) and (2) given above for MgH seem to be not even approximately fulfilled, so that even a probable assignment of j values cannot be made in the Q branches.[30] These difficulties indicate that interesting results would be obtained in

[30] As Hulthén states, the assignment made in his Table II and III is very uncertain. It seems likely that the j numbering in Q_1 should be increased by unity for the A band, but not for the A' band, and that a new first line should be added in the A band, but that the first line given in the A' band should be dropped. Even with these changes, the combination defects are large for the lowest values of j. They decrease for higher values of j, but show irregular variations. Apparently $F_{1A}'(j) - F_{1B}'(j)$ is large for the lowest j values, then decreases. In the Q_2 branches the difficulties are, if anything, worse.

respect to the relation of F_{iA}' and F_{iB}' states if the correct numbering were determined by measurements on a (1,0) or (0,1) band.

Hulthén's designations of the branches and band-lines agree with those used here, except that the j values need to be reduced by $\frac{1}{2}$ unit if they are to agree with the quantum mechanics numbering.

Term values of initial and final states. Taking $F_1''(\frac{1}{2})$ as the zero of energy, the Δ_2F'' values show that $F_i''(j_k)=4.225j_k(j_k+1)\pm 0.0225j_k+\cdots$, with the plus sign for F_1, the minus sign for F_2; j values can be obtained from the relation $j=j_k\pm\frac{1}{2}$. The F'' equation gives the following calculated F'' values: $F_1''(1\frac{1}{2})=8.47$, $F_2''(\frac{1}{2})=8.43$; $F_1''(2\frac{1}{2})=25.39$ (observed, 25.37); $F_2''(1\frac{1}{2})=25.31$, etc. Assuming these calculated values to be correct, F_B' values can be obtained as follows: $F_{1B}'(\frac{1}{2})=P_1(1\frac{1}{2})+F_1''(1\frac{1}{2})$; $F_{1B}'(1\frac{1}{2})=R_1(\frac{1}{2})$; $F_{2B}'(1\frac{1}{2})=R_2(\frac{1}{2})+F_2''(\frac{1}{2})$; $F_{2B}'(2\frac{1}{2})=R_2(1\frac{1}{2})+F_2''(1\frac{1}{2})$; from these by the use of Δ_2F' values from Hulthén's Table VII the F_B''s for higher j's can be built up (the method can be seen by examining, e.g., Fig. 2). Some of the F_B' values so obtained are given in Table IV. On account of the uncertainty as to the j numbering for the Q branches,[30] F_A' values cannot be given with confidence.

TABLE IV. *F_{iB} terms for ^2P state of CaH, from A bands.*

j	$F_2'(j)$	$\Delta_1F_1'(j)$	$F_1'(j+1)$	$\Delta_1F_1'(j+1)$	$F_2'(j)-F_1'(j+1)$
$-\frac{1}{2}$			14,394.35	12.45	
$\frac{1}{2}$			14,406.90	20.74	
$1\frac{1}{2}$	14,479.01	22.54	14,427.64	28.88	51.37
$2\frac{1}{2}$	14,501.55	31.39	14,456.52	36.97	45.03
$3\frac{1}{2}$	14,532.94	40.24	14,493.49	45.18	39.45
$4\frac{1}{2}$	14,573.18		14.538.67		34.51
$18\frac{1}{2}$	16,028.67	164.99	16,027.13	165.95	1.54
$19\frac{1}{2}$	193.66	172.41	193.08	173.81	0.58
$20\frac{1}{2}$	366.07	180.31	366.89	181.23	−0.82
$21\frac{1}{2}$	546.38		548.12		−1.74
$30\frac{1}{2}$	18,495.54	251.08	18,505.53	251.63	−9.99
$31\frac{1}{2}$	746.62	257.41	757.16	258.35	−10.54
$32\frac{1}{2}$	19,004.03	263.69	19,015.51	264.30	−11.48
$33\frac{1}{2}$	267.72		279.81		−12.09

The relations shown in Table IV may be taken as fairly typical of a $^2P_{nab}$ state. For low j values, $\Delta_1F_1(j)\sim\Delta_1F_2(j)$, showing an approach to the case a relation $\Delta_1F_1(j)=\Delta_1F_2(j)$—cf. Table I, $^2P_{na}$. Both Δ_1F's, furthermore, correspond (cf. Table I, especially note 4) to F's of the form $F_i=C_i+B_i^*[j(j+1)]+\cdots$, with $B_1^*=4.09$, $B_2^*=4.49$ for the A band, and with j values which agree with and confirm those assigned above on quite other grounds. Thus, $\Delta_1F_1'(\frac{1}{2})\sim 8.18\times 1\frac{1}{2}$; $\Delta_1F_1'(1\frac{1}{2})\sim 8.18\times 2\frac{1}{2}$, etc., in agreement with the expected relation $\Delta_1F_i(j)\sim 2B_i^*(j+1)$—cf. Table I.

For large j values, $\Delta_1F_2'(j)\sim\Delta_1F_1'(j+1)$, approaching the case b relation (Table I, ^2P_b) $\Delta_1F_2(j)=\Delta_1F_1(j+1)$. But for all values of j, $\Delta_1F_1(j+1)>\Delta_1F_2(j)>\Delta_1F_1(j)$ is fulfilled as expected. Table IV shows the interesting fact that the relation $F_2(j)>F_1(j+1)$ which holds for low j values is reversed beyond $j=19\frac{1}{2}$; possible causes of such a reversal are discussed in Note 6 of

Table I. This reversal corresponds to the fact that $\Delta_1 F_1(j+1)$ remains appreciably greater than $\Delta_1 F_2(j)$ for large j.

The OH Bands

The $^1S \rightarrow {}^2P$ OH bands[31] are the classical example of Heurlinger's "bands with doublet series." They will be considered next because in respect to observed branches and intensity relations—and $|\Delta E/B|$—they constitute an important transition case between the CaH and ZnH bands, although in other respects they fall outside the series of metal hydrides. The fact that the bands are due to OH rather than OH^- or H_2O or H_3O^+ is definitely shown by their doublet character, which shows that their emitter has an odd number of planetary electrons.

Using data of Grebe and Holtz[31] and of Watson,[31] on the (0,0), (1,0), (1,1) and (2,1) bands, Dieke[31] has tested the combination relations and obtained the $\Delta_2 F'$ and $\Delta_2 F''$ values. Assuming only that the obvious Q, R, and P branches really correspond to $\Delta j = 0, \pm 1$, and that the lowest of a set of ^2S levels is always single, Dieke's analysis makes it possible to construct, with assurance of its empirical correctness, the system of energy levels shown in Fig. 3. The missing lines (cf. Table VI) give proof that the lowest levels of each set are as shown.

Final (^2P) *states.* On comparing the arrangement of the ^2P levels of OH and CaH in Fig. 1, there is at first sight a marked similarity: the levels in each case fall naturally into two sets, one of which begins at a considerable distance above the other. Closer examination discloses an important difference: in OH the nth level of the lower set approaches the nth level of the upper set as j increases, while in CaH the $(n+2)$nd level of the lower set approaches the nth of the upper set. This difference suggested to the writer that the ^2P state is *inverted* in OH (cf. Fig. 1). Kemble[4], and Hill and Van Vleck,[7b] have now shown that the observed behavior in OH is exactly that to be expected theoretically for an inverted ^2P, while the observed relations in CaH (and MgH) correspond to those expected for a normal ^2P state. As will be shown in the last part of this section, j' and j'' values, F_i' and F_i'' designations, and the inverted character of the ^2P state, are now *empirically* assured, assuming only that Δj is limited to $0, \pm 1$, by the discovery[15] of combination relations obeyed by a seventh (non-satellite) branch in the OH bands. This gives valuable support to Kemble's theory, since it can be shown that, in the absence of the new evidence and the theory, an assignment of j values corresponding to a *normal* ^2P state could have been made without contradiction of the rule $\Delta j = 0, \pm 1$ just as well as the assignment corresponding to an inverted ^2P.

[31] L. Grebe and O. Holtz, Ann. der Phys. **39**, 1243 (1912); T. Heurlinger, Dissertation Lund, 1918; R. Fortrat, J. de phys. **5**, 20 (1924); W. W. Watson, Astrophys. J. **60**, 145 (1924); G. H. Dieke, Proc. Acad. Sci. Amsterdam, **28**, 174 (1925); R. T. Birge, Chapter IV, part 5d, of National Research Council Report on Molecular Spectra in Gases; D. Jack, Proc. Roy. Soc. **115A**, 373 (1927) and **118A**, 647 (1928); E. C. Kemble, ref. 4.

As Kemble has shown,[4] the form of the $\Delta_2 F''$'s (cf. Dieke, l.c.[31]) is approximately that derivable from a term-form $F_i''(j) = B_i^*[j(j+1) - \sigma_i^2] + \cdots$, with $j = 1\frac{1}{2}, 2\frac{1}{2}, \cdots$ for the $F_1(^2P_{1\,1/2})$ levels and $j = \frac{1}{2}, 1\frac{1}{2}, \cdots$ for the $F_2(^2P_{1/2})$ levels, and $B_1^* = 16.60$, $B_2^* = 20.57$. With increasing j, the F_1 levels approach the corresponding F_2 levels but do not pass them as in CaH, at least not in the observed range. Kemble finds in fact that the rate of approach is somewhat *less* than that calculated from his equations, and suggests that this is due to the rotationally induced magnetic field tending here to make $F_2(j) > F_1(j+1)$.[32] A similar effect but with opposite sign may perhaps explain why $F_1(j+1)$ passes $F_2(j)$ in CaH.

TABLE V. *Revised Notation for* OH *Bands.*[a]

New Old[b]	$P_1(1\frac{1}{2})$ $P_2(2)$	$Q_1(1\frac{1}{2})$ $Q_2(2)$	$Q_1A_1B(1\frac{1}{2})$ $\sigma Q_2(2)$ of Watson		$^QP_{21}(1\frac{1}{2})$ $F_1(2) - f_2'(\frac{1}{2})$ *Sat.* $Q_2(2)$	$R_1(1\frac{1}{2})$ $R_2(2)$	$^RQ_{21}(1\frac{1}{2})$ $\sigma R_2(2)$ *Sat* $R_2(2)$	$^{RR}R_{21}(1\frac{1}{2})$ (Previously undesignated)
New Old[b]	$^{PP}P_{12}(1\frac{1}{2})$ (Unknown)	$P_2(1\frac{1}{2})$ $P_1(3)$	$^PQ_{12}(\frac{1}{2})$ $P_1(2)$	$^PQ_{12}(1\frac{1}{2})$ $\sigma P_1(3)$ or Sat. $P_1(3)$	$Q_2(\frac{1}{2})$ $Q_1(2)$	$Q_2A_2B(\frac{1}{2})$ $\sigma Q_1(2)$ of Watson	$^QR_{12}(\frac{1}{2})$ Sat. $Q_1(2)$	$R_2(\frac{1}{2})$ $R_1(2)$
New Old[b,c]	$F_1'(\frac{1}{2})$ $F_2(1)$	$F_2'(\frac{1}{2})$ $F_1(2)$	$F_1A''(1\frac{1}{2})$ $f_2'(2)$	$F_1B''(1\frac{1}{2})$ $f_2(2)$	$F_2A''(\frac{1}{2})$ $f_1'(2)$	$F_2B''(\frac{1}{2})$ $f_2'(2)$		

Notes. (*a*) The j'' numbers given correspond to the *predicted* first line in each branch, but are not intended to imply that this line has been recorded in the case of every branch.

(*b*) The old notation and (*m*) numbering originated with Heurlinger. Satellite notation has been used with varying degrees of explicitness by Heurlinger, Fortrat, Dieke and Watson.[31]

(*c*) The old F, f, f' term notation is that given by Dieke. Dieke's supposed state $F_1(2)$, involved in his line $P_1(2)$, is really identical, according to the present interpretation, with his $F_2(1)$.

TABLE VI. *Predicted and observed j'' values for first lines in* OH *branches.*

Branch	(2, 0) *band*	(1, 0) *band*	(2, 1) *band*	(0, 0) *band*	(0, 1) *band*	*Predicted j''*
P_1	$1\frac{1}{2}$	$1\frac{1}{2}$	$1\frac{1}{2}$	$1\frac{1}{2}$	$1\frac{1}{2}$	$1\frac{1}{2}$
Q_1	$1\frac{1}{2}$	$(1\frac{1}{2})$	$1\frac{1}{2}$	$(1\frac{1}{2})$	$1\frac{1}{2}$	$1\frac{1}{2}$
R_1	$1\frac{1}{2}$	$1\frac{1}{2}$	$3\frac{1}{2}$	$1\frac{1}{2}$	$1\frac{1}{2}$	$1\frac{1}{2}$
P_2	$(1\frac{1}{2})$	$(1\frac{1}{2})$	$1\frac{1}{2}$	$1\frac{1}{2}$	$1\frac{1}{2}$	$1\frac{1}{2}$
$^PQ_{12}$	$\frac{1}{2}$	$(\frac{1}{2})$	$\frac{1}{2}$	$\frac{1}{2}$	$\frac{1}{2}$	$\frac{1}{2}$
Q_2	$(\frac{1}{2})$	$(\frac{1}{2})$	$\frac{1}{2}$	$\frac{1}{2}$	$\frac{1}{2}$	$\frac{1}{2}$
R_2	$(\frac{1}{2})$	$\frac{1}{2}$	$2\frac{1}{2}$	$\frac{1}{2}$	$\frac{1}{2}$	$\frac{1}{2}$
$^{RR}R_{21}$	–	$1\frac{1}{2}$	–	$1\frac{1}{2}$	–	$1\frac{1}{2}$

Notes. (1, 0) and (2, 1) bands (λ2811), data of Watson[31]; (0, 0) band (λ3064), data of Grebe and Holtz[21]; (2, 0) and (0, 1) bands (λλ2608 and 3428), data of Jack.[31] Values given in parenthesis are inconclusive because of superposition of other lines. The apparent disagreement in the R branches of the (2, 1) band is doubtless a result of the weakness of these branches (cf. Table VIII).

Notation. The interpretation of the OH bands given by Kemble and the writer necessitates a *reversal of the subscripts 1 and 2*, as compared with the designations introduced by Heurlinger, in order to bring the notation into

[32] This effect is probably even greater than appears in Kemble's Fig. 4, since the empirical curves in his Fig. 4 are based on the use of his Eq. (43), which assumes that the F' doublet separations, in the ^2S initial state (cf. Eq. (4) above), are negligible.

harmony with the scheme proposed in VI. The change seems desirable, in spite of temporary confusion which may result, because it makes possible uniform designations for analogous branches in all spectra corresponding to the same type of electron jump. Table V shows the old and new notation for the OH bands.

Term values for initial (^2S) states. For the initial states, Dieke's Table II[31] shows unquestionably that (in the present notation, which is the reverse of Dieke's—cf. Table V), $\Delta_2F_1' > \Delta_2F_2'$ from the beginning. Hence, assuming in accordance with the theory for ^2S states that the lowest ^2S state is the single level $F_1'(\frac{1}{2})$, the relation $F_1'(j+1) > F_2'(j)$ holds. The quantitative relation for the rotational energy, for the vibrational state $n'=0$, is approximately

$$F'(j_k) = 16.85[j_k(j_k+1)] \pm 0.11 j_k \tag{4}$$

This gives for $F_1(j_k) - F_2(j_k)$, for $j_k = 1, 2, 3, \cdots$ the calculated values 0.22, 0.44, 0.66, $\cdots$.

Comparison of F_{iA}'' and F_{iB}'' terms (σ-type doubling in ^2P states). From Fig. 3 it will be seen that the following relations should hold:

$$[R_i(j) - Q_i(j+1)] - [Q_i(j) - P_i(j+1)] = [F_{iA}''(j) + F_{iA}''(j+1)] - [F_{iB}''(j) + F_{iB}''(j+1)] \cong 2[F_{iA}''(j+\tfrac{1}{2}) - F_{iB}''(j+\tfrac{1}{2})] = 2\delta_{AB}F_i''(j+\tfrac{1}{2}) \tag{5}$$

The last equality in Eq. (5) merely *defines* the quantity $\delta_{AB}F_i(j)$.

While this method does not give exact individual values of the doublet intervals, it should give a good idea of the mode of variation of σ-type doublet separations as a function of j. Values of $\delta_{AB}F_i''(j)$ could also be obtained directly from data on Q_i branches and their Q_{iAiB} satellites (see later section) by means of the relation:

$$\delta_{AB}F_i''(j) = Q_{iAiB}(j) - Q_i(j). \tag{6}$$

TABLE VII. *Doublet intervals in σ-type doubling for ^2P levels in OH.*

$j+\frac{1}{2}$	$\delta_{AB}F_1''(j+\frac{1}{2})$	$\delta_{AB}F_2''(j+\frac{1}{2})$	$j+\frac{1}{2}$	$\delta_{AB}F_1''(j+\frac{1}{2})$	$\delta_{AB}F_2''(j+\frac{1}{2})$
1		−0.11	11	+5.10	+3.40
2	+0.12	−0.18	12	+6.15	4.11
3	0.31	−0.19	13	7.03	4.66
4	0.56	−0.06	14	7.74	5.50
5	0.98	+0.21	15	8.94	6.53
6	1.35	+0.49	16	10.03	7.31
7	2.12	0.79	17	11.24	8.34
8	2.69	1.28	18	12.26	9.44
9	3.45	1.85	19	13.36	10.31
10	4.28	2.52	20	14.52	11.49
			21	15.93	

Note. The above values were obtained from Dieke's Table I as follows: the subtraction $[R_1'(m) - Q_1'(m+1)] - [Q_1'(m) - P_1'(m+1)]$, in Dieke's notation, was performed for λ3064 and for λ2811, and the average of these results was taken as $2\delta_{AB}F_2''(j+\frac{1}{2})$, with $j+\frac{1}{2} = m-1$ (cf. Table V for key to changes of notation). Similarly, an average value of $2\delta_{AB}F_1''(j+\frac{1}{2})$ was obtained from $[R_2'(m) - Q_2'(m+1)] - [Q_2'(m) - P_2'(m+1)]$, with $j+\frac{1}{2} = m$ in this case. Division of each result by two gave the values listed above.

But the less direct method of Eq. (5) seems preferable, because the data available for use in Eq. (6) are not very satisfactory.

Table I of Dieke's paper gives differences of the type R-Q, Q-P, etc., required for use in Eq. (5). Using Dieke's values and performing the necessary subtractions, the results given in Table VII are obtained. The different behavior of the F_1'' and F_2'' levels, and the reversal of sign for low values of j in the F_2 levels, are noteworthy. The data on MgH show indications of similar behavior, except that the rôles of the F_1 and F_2 levels appear to be interchanged, and that the observed effects are much smaller.

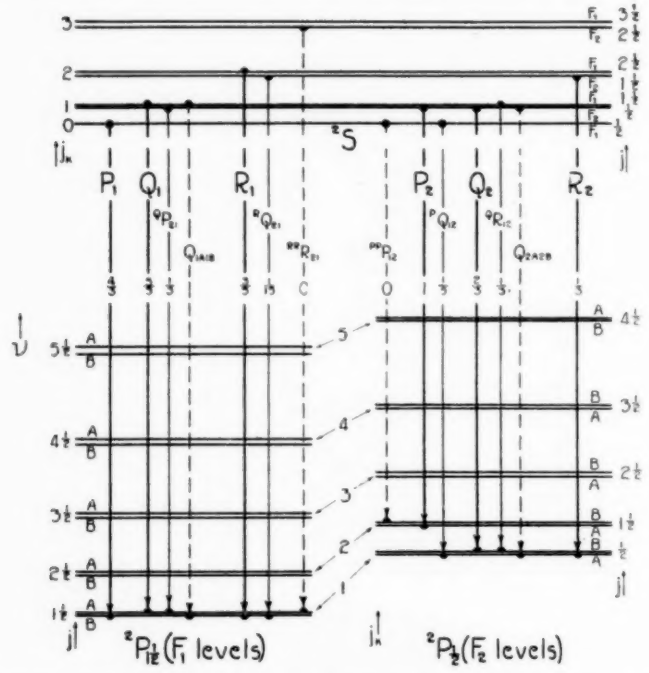

Fig. 3. *Lowest rotational levels of each electronic state, and first line of each branch, with its theoretical intensity as calculated for case b from Eqs.* (14)–(22) *of* VI, *for* OH λ2811 (1, 0 *band*). The rotational levels are drawn to scale, making use of the ΔF data of Dieke,[31] except that all doublet separations are exaggerated (cf. Table VII for numerical data on ^2P level doubling). The strong full vertical lines represent main branches, the weak full vertical lines, normal satellite branches. Two of the broken vertical lines represent branches which would be forbidden in case *b*: of these $^{RR}R_{21}$ is known, but $^{PP}P_{12}$ is not yet known. The other two broken lines represent weak satellite branches which violate the ordinary selection rules of σ-type doubling. The j_k values given for the ^2P state are those which would be appropriate in case *b*, although for the lowest rotational levels in OH, which are near case *a*, they have little real meaning.

Intensity relations and first lines. Intensities predicted by the equations[2] corresponding to Hund's case *b*, for the first line of each of the various main and satellite branches, are given in Fig. 3. The observed first lines, including the satellite line $^PQ_{12}(\frac{1}{2})$, are within the errors of determination exactly as predicted (cf. Table VI). Both predicted intensities and first lines, incidentally, are the same as in CH λ3900.

Some of the observed intensities recorded by Watson and Jack for four of the OH bands are given in Table VIII. The major intensity relation $Q>P>R$ characteristic of $S\rightarrow P$ transitions (cf. III, IV, and VI of this series) is obviously fulfilled. Another predicted relation for case b (cf. Eqs. (14)–(22) of VI) is that for small values of j, $R_1>R_2$, $Q_1>Q_2$, $P_1>P_2$ for the members of each doublet, with asymptotic equality of intensity of doublet components for large j. These relations are on the whole fulfilled, but there is evidence that the inequalities for low j are more pronounced than expected in the case of the R branches, but are less pronounced than expected, or even reversed, in the P branches. The satellite branches (see below) show unpredicted relatively high intensity. Also, an additional R branch is present which should not appear at all in case b. These various departures from the case b intensity relations may be attributed to the fact that the ^2P state is well on the way toward case a. The observed agreement is on the whole surprisingly good.

TABLE VIII. *Observed intensity relations in OH bands.*

$j-\frac{1}{2}$	$R_1(j+1)$	$R_2(j)$	$Q_1(j+1)$	$Q_2(j)$	$P_1(j+1)$	$P_2(j)$	$R_1(j+1)$	$R_2(j)$	$Q_1(j+1)$	$Q_2(j)$	$P_1(j+1)$	$P_2(j)$
	λ2811 (1, 0) band (data of Watson[31])						λ2875 (2, 1) band (data of Watson[31])					
0	3	0	*	*	5	*	–	–	7	2	2	0
1	4	2	9	5	5	*	–	–	9	5	5	5
2	4	*	9	6	6	9	*	0	*	4	*	*
3	4	4	10	7	8	9	*	4	8	8	*	7
4	*	4	10	*	8	9	6	*	*	8	7	8
5	*	*	*	10	9	9	*	0	8	*	*	8
6	4	*	10	10	9	8	*	*	8	*	7	6
	λ2608 (2, 0) band (data of Jack[31])						λ3428 (0, 1) band (data of Jack[31])					
0	6	*	8	*	5	*	6	0	7	5	1	5
1	7	3	10	*	9	8	2	*	6	8	9	5
2	8	4	9	8	8	9	5	1	7	9	5	8
3	7	5	10	*	9	9	3	2	7	9	5	8
4	6	8	9	9	9	9	2	2	7	8	6	5
5	7	5	10	9	9	7	0	5	7	5	5	*
6	4	*	*	9	8	7	10	10	9	5	2	*

Note. Data for higher values of j can be found in Watson's and Jack's papers.

Satellite series. The satellite branches in OH, first noted by Heurlinger and later extensively investigated by Fortrat, have been shown by Dieke to correspond to combinations (cf. Fig. 3) between the same levels which are needed to explain the main branches (cf. Table VI for Dieke's notation). It is only because of their abnormally high intensity, and because of the comparatively large $F_1'-F_2'$ values in the ^2S state (cf. Eq. (4), which permit resolution of the satellite from the corresponding main lines, that it is possible to establish the existence of the satellite series.[32a] This was not possible for CH λ3900 or MgH, for both of which $F_1(j+1)-F_2(j)$ for the ^2S state is small even for large j.

[32a] This statement is not intended to apply to the abnormal satellite series (see below) which violate the selection rules of σ-type doubling.

For the P and R branches, the satellites are exactly those expected: R_2 and P_1 have no satellite series, R_1 and P_2 each have one, according to Fortrat's data on the λ3064(0,0) band (*l.c.*,[31] Tables II and IV). The recorded lines of the P_2 satellite series in ${}^{P}Q_{12}$ extend from $j''=2\frac{1}{2}$ to $j''=12\frac{1}{2}$. According to Fortrat (*l.c.*,[31] top p. 23) ${}^{P}Q_{12}(2\frac{1}{2})$ is of equal intensity with the corresponding main line $P_2(2\frac{1}{2})$. Successive satellite lines show increasing intensity,[33] but with a less rapid increase than in the main branch, followed by falling intensity beyond ${}^{P}Q_{12}(6\frac{1}{2})$; the last satellite line detected was ${}^{P}Q_{12}(12\frac{1}{2})$, while the main branch was followed to $P_2(26\frac{1}{2})$. The intensities in the ${}^{P}Q_{12}$ branch are evidently much greater than those predicted for case b (cf. VI, Eq. (19), and Fig. 3 of VII), but they nevertheless still show a marked tendency toward the predicted case b behavior of falling off inversely as j_k.—According to the present interpretation, the previously supposed first line of the P_1 branch is really ${}^{P}Q_{12}(\frac{1}{2})$, there being no corresponding main line. The apparent absence of ${}^{P}Q_{21}(1\frac{1}{2})$ is evidently due merely to a lack of resolution from the corresponding main line $P_1(1\frac{1}{2})$; the calculated separation is 0.26 wave numbers.—In the ${}^{R}Q_{21}$ branch (satellite of R_2), the recorded lines extend from $j''=1\frac{1}{2}$ to $j''=4\frac{1}{2}$,[34] with recorded intensities falling from 3 to 1; the predicted first line ${}^{R}Q_{21}(\frac{1}{2})$ falls on an R_2 line.

Each of the Q branches is accompanied by more than one satellite series. In the case of the Q_2 branch, satellite lines of the expected type (${}^{Q}R_{12}$) appear to be present up to $j''=11\frac{1}{2}$ or $12\frac{1}{2}$. In the Q_1 branch, the expected satellites (${}^{Q}P_{21}$) extend to at least $j''=6\frac{1}{2}$. In both cases, the intensity rises to a maximum for a low value of j, then falls (cf. Fortrat, *l. c.*, p. 26–7).

In addition, as Dieke[31] and Watson[35] have shown, there are Q satellite branches which in the present notation (cf. VI) are Q_{2A2B} and Q_{1A1B}. These branches, unlike the other satellites, extend to fairly large j values, i.e., the intensity distribution as a function of j is similar to that in the main branches. They constitute the only known cases where the σ-type doubling selection rules for Q branches ($A\rightarrow A$ or $B\rightarrow B$), which also hold for ${}^{Q}P$ and ${}^{Q}R$ branches, and which are probably associated with $\Delta j_k=0$, rather than with $\Delta j=0$, are broken through.

The satellite series given above do not exhaust Fortrat's data; especially in the Q_1 branch (Q_2 of Fortrat) there are many additional unexplained satellite lines. Dieke has concluded that some of these belong to a ${}^{Q}P_{2A1B}$ branch (combination F_1-f_2 in Dieke's notation), but a recalculation of the expected positions from Eq. (4) and Table VII seems not to justify this conclusion. Further, ${}^{Q}P_{2A1B}$ would hardly be expected in measurable intensity, since it bears to the already weak satellite branch ${}^{Q}P_{21}$ the same relation as the weak branch Q_{1A1B} to the strong branch Q_1. One might,

[33] Fortrat's statement to this effect seems to be partially contradicted by his recorded intensities (Table II), which are, beginning with Q_{12} ($2\frac{1}{2}$), 3, 3, 2,—, 2, 1,—, 1, 1, 1, 0.

[34] Additional lines up to $j''=8\frac{1}{2}$, recorded by Fortrat, fail to fulfill the proper combination relations.

[35] W. W. Watson, Nature, Jan. 30, 1926: new measurements on Q_{1A1B} and Q_{2A2B}.

however, expect to find additional weak branches, violating the σ-type doubling selection rules, as satellites of the strong P and R branches.

Identification of seventh non-satellite branch in OH *bands.* Watson has given data[31] on a previously undescribed weak series of lines associated with the λ3064 OH band. This series starts near the λ3064 head, and extends to λ3021 where it forms an additional head. Jack has subsequently found and measured an analogous branch in the λ2811 band.

It is natural to suppose that this very weak head is analogous to one of the outlying heads in the four-headed type of $^2S\rightarrow{}^2P$ or $^2P\rightarrow{}^2S$ bands of which the NO γ and the BO α bands are examples. In such bands, one of the four heads is formed either by the ${}^{PP}P_{12}$ or by the ${}^{RR}R_{21}$ branch, both of which should be absent for a case b ^2P state. Since the intensity relations in the OH bands are close to those of case b, such branches should be very weak, but in view of the strength of the satellite series (cf. above), they might well be of detectable intensity. We shall then assume that the OH branch in question is an ${}^{RR}R_{21}$ branch, and proceed to test the correctness of this assumption by means of combination relations.

From Fig. 3 it will be seen that the following relations should hold:

$$\begin{aligned}{}^{RR}R_{21}(j) &= F_2'(j+1) - F_{1A}''(j) = [F_2'(j-1) - F_{1A}''(i)] \\ &\quad + [F_2'(j+1) - F_2'(j-1)] = {}^{Q}P_{21}(j) + \Delta_2 F_2'(j) \qquad (7)\end{aligned}$$

From experimental data on the ${}^{Q}P_{21}$ lines and on the $\Delta_2 F_2'$ values, we should be able to predict the positions of the ${}^{RR}R_{21}$ lines. The ${}^{Q}P_{21}$ branch is, however, unfortunately a weak satellite branch, for which the data are fragmentary and uncertain. By making a slight use of the theory, we can, however, calculate the positions of the ${}^{Q}P_{21}$ lines fairly accurately from data on the corresponding main branch (Q_1) together with estimated values of $[F_1'(j) - F_2'(j-1)]$; according to Fig. 3 and Eq. (4)—noting that $j = j_k \pm \frac{1}{2}$ in Eq. (4)—we have

$${}^{Q}P_{21}(j) = Q_1(j) - [F_1'(j) - F_2'(j-1)] = Q_1(j) - 0.22(j - \tfrac{1}{2}). \qquad (8)$$

Hence we expect with considerable accuracy

$${}^{RR}R_{21}(j) = Q_1(j) + \Delta_2 F_2'(j) - 0.22\ (j - \tfrac{1}{2}) \qquad (9)$$

The value 0.22, from Eq. (4), refers to the state $n' = 0$, and so is applicable to the prediction of the ${}^{RR}R_{21}$ series for the λ3064(0,0) band. For the λ2811(1,0) band, a corresponding value for the state $n' = 1$ should be used. There are, however, so many superpositions of lines in Watson's data on the λ2811 band that no accurate estimate of this coefficient can be made, and we shall merely assume that the same value is applicable for $n' = 1$ as for $n' = 0$.

Table IX shows that the positions of the observed lines of the ${}^{RR}R_{21}$ branch are in satisfactory agreement with the calculated positions, thus confirming our assumption. The small differences between observed and

calculated values are not surprising, since the observed and calculated values involve data of different observers, and since the assumption $F_1'(j) - F_2'(j-1) = 0.22(j-\frac{1}{2})$ is not known to be more than approximately true.

TABLE IX. *Calculated and observed positions of lines of* $^{RR}R_{21}$ *branch. (calculations according to Eq.(9))*

	λ3064 (0, 0) *band*			λ2811 (1, 0) *band*		
$j+\frac{1}{2}$	Calc'd ν	Obs'd ν (Watson)	Int.	Calc'd ν	Obs'd ν (Jack)	Int.
2	32,643.42	32,643.39	8	35,622.08*	35,621.67	10
3	694.45	694.52	8	666.46*	666.65	10
4	745.10	744.61	7	708.32	708.29	10
5	793.07	792.80	6	746.80	746.59	10
6	838.62	838.44	5	780.93*	780.48	9
7	881.60*	881.18	4	809.98*	809.82	8
8	920.76*	920.61	4	834.37	834.20	7
9	956.68	956.57	3	853.35*	853.60	6
10	988.58	988.47	2	867.25	867.36	5
11	33,016.68	33,016.53	1	875.24	876.63?	—
12	040.14	040.11	0	877.15*	876.63	4
13	059.36	059.16	–	872.98*	873.28	4
14	074.10	073.54	–	863.24*	862.60	3
15	083.90	083.79	0	847.11*	846.41*	2*
16	089.00			823.00	823.16*	1*
17	088.94	088.92	1*d*	793.26	793.16*	1*
18	083.85	083.79		756.17	756.56*	0*
19	073.09	073.54				
20	056.92					

Notes. The data used in the calculations are from the following sources: λ3064 band, Q_1 data from Fortrat, Δ_2F_2' values as given by Dieke (cf. his Table II), from data of Grebe and Holtz; λ2811 band, Q_1 data from Watson, Δ_2F_2' values as given by Dieke (Table II) from data of Watson. For the convenience of the reader in case he desires to refer to these data, it may be noted that in terms of the old notation $Q_1(j)$ of Eq. (9) becomes $Q_2(m)$ of Fortrat or $Q_2'(m)$ of Watson, with $m=j+\frac{1}{2}$, while $\Delta_2F_2'(j)$ becomes $\Delta F_1(m-1)$ of Dieke, with $m-1=j+\frac{1}{2}$. The observed wave-numbers for the R_{21} branch are from Watson, *l.c.*,[31] p. 158, for λ3064; Jack, 1927 paper,[31] p. 389, for λ2811. The intensities given have only *relative* significance, and this only within each band.

It will be noted (cf. Table IX) that each $^{RR}R_{21}$ branch begins, as expected (cf. Fig. 3), with $^{RR}R_{21}(1\frac{1}{2})$. According to the data in Table IX, the intensity reaches a maximum at about the second line, then falls off steadily. This is in accordance with the fact that this branch corresponds to a strong transition for a case *a* ^2P state (cf. HgH) but to a forbidden transition for a case *b* ^2P state; for the lowest values of j, the ^2P state is close to case *a*, but steadily approaches case *b* as j increases. It is of interest to note that the phenomenon of an early intensity maximum followed by rapid falling off is more pronounced here than in the legitimate satellite branches (cf. above); this difference is probably correlated with the fact that the satellite branches are merely very weak but not forbidden in case *b*.

In view of the presence of a weak $^{RR}R_{21}$ branch in the OH bands, the presence of a weak $^{PP}P_{12}$ branch may be predicted. This should perhaps be stronger than the R_{21} branch, but must be less favorably situated for observation, since it should be in the midst of the strong branches, while the R_{21} branch occupies an isolated position (cf. reproduction in Jack's 1927 paper[31]).

ZnH, CdH, AND HgH BANDS

Interpretation. The interpretation of the ZnH, CdH, and HgH bands has been discussed previously by Hulthén, Kratzer,[36] and the writer.[37] The interpretation given previously by the writer assumed what would now be called a $^2P_{na}$ initial and a ^2S final state.

The ^2P terms were written in the form $F_1',_2(^2P_i) = B_i[(j^2-\sigma_i^2)^{1/2} \mp \epsilon]^2 + \cdots$, with $\sigma_i \sim \frac{1}{2}$ or $1\frac{1}{2}$ for $^2P_{1/2}$ or $^2P_{1\ 1/2}$, and with $\mp\epsilon$ corresponding to F_1' and F_2'. The use of $\mp\epsilon$ implied ρ-type doubling like that of the ^2S state, but we must now of course interpret it as σ-type doubling. The term-form (cf. following paragraph in regard to data on term values) may now perhaps

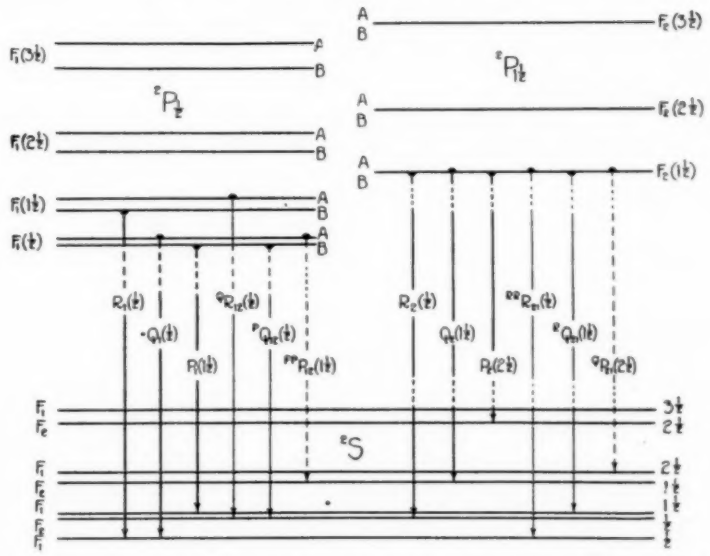

Fig. 4. *Lowest rotational levels, and first lines of each branch, for HgH* (0, 0) *bands* λ3500 ($^2P_{1\frac{1}{2}} \rightarrow {}^2S$ *sub-band*) *and* λ4017 ($^2P_{\frac{1}{2}} \rightarrow {}^2S$ *sub-band*). The $^2P_{1\frac{1}{2}}$, $^2P_{\frac{1}{2}}$, and ^2S sets of levels are all drawn to the same scale from Hulthén's data (cf. paragraph in the text on "Term Values of HgH)." Because of space limitations, however, the $^2P_{1\frac{1}{2}}$ and $^2P_{\frac{1}{2}}$ sets of levels could not be drawn in their true relative positions; the $^2P_{1\frac{1}{2}}$ levels shown are actually all much higher than the $^2P_{\frac{1}{2}}$ levels shown. Strong vertical lines, weak vertical lines, a nd dashed vertical lines respectively indicate branches which in case *b* would be main, satellite, and forbidden branches. *All* these branches are strong in HgH.

best be expressed for low values of j as $F_{i\alpha}'(j) = B_i^*[j(j+1)-\sigma_i^2] \pm \delta j + \cdots$, where $i=1$ or 2 and $\alpha = A$ or B, with $\sigma_1 = \frac{1}{2}$ (F_1 or $^2P_{1/2}$ terms) and $\sigma_2 = 1\frac{1}{2}$ (F_2 or $^2P_{1\ 1/2}$ terms); $+\delta j$ goes with $\alpha = A$, $-\delta j$ with $\alpha = B$, hence $F_A(j) > F_B(j)$: cf. Fig. 4. In this formula, δ is practically zero[38] for the $^2P_{1\ 1/2}$ states for all three molecules; but for the $^2P_{1/2}$ states $\delta \sim 0.02\ B_1^*$ for ZnH, $0.06\ B_1^*$ for CdH, and $0.19\ B_1^*$ for HgH, corresponding to a large-scale σ-type

[36] A. Kratzer, Ann. der Physik, **71**, 89 (1923).

[37] R. S. Mulliken, Proc. Nat. Acad. Sci. **12**, 151 (1926); also E. Hulthén, ref. 14.

[38] The existence of any doubling at all in the F_2 states is shown only in the case of certain perturbed lines in HgH (cf. E. Hulthén, Zeits. f. Physik **32**, 32, 1925, and H. Ludloff, Zeits. f. Physik, **34**, 485, 1925).

doubling, especially in HgH. It is hardly necessary to say that the difference between B_1* and B_2*, previously interpreted as caused by a real difference in moments of inertia, is now to be explained by Kemble's theory.

Term values of HgH. Hulthén in his 1925 paper has given a complete list of term values for HgH, for both ^2S states (cf. his Table 8) and ^2P states (cf. his Table 7: his $n=0$ and $n=1$ belong to the $^2P_{1/2}$, his $n'=0$ and 1 to the $^2P_{1\ 1/2}$ terms). His term values are based on the assumption $F_1(\frac{1}{2})=9.8$ for the lowest ^2S level and should all be lowered by 9.8 if one wishes to take $F_1(\frac{1}{2})$ as the zero of energy, as is natural in the present state of the theory. At the end of Table X is given a key for translating Hulthén's notation into that used here.

The arrangement of the energy levels, and their relation to the observed branches, are shown for HgH in Fig. 4.

Notation. A revised notation for the ZnH, CdH, and HgH bands, in harmony with that proposed in VI, is given in Table X, together with earlier notations of various authors. It is to be hoped that no further changes will be needed.

TABLE X. *New and old notations for first line of each branch in* ZnH, CdH, *and* HgH *bands*

Present	$R_1(\frac{1}{2})$	$^QR_{12}(\frac{1}{2})$	$Q_1(\frac{1}{2})$	$^PQ_{12}(\frac{1}{2})$	$P_{11}(1\frac{1}{2})$	$^{PP}P_{12}(1\frac{1}{2})$	
Birge[31] 1927	$R^-(1)$	$R^+(1)$	$Q^\mp(1)$	$Q^\pm(1)$	$P^-(2)$	$P^+(2)$	
Mulliken[37] 1926	R_1	R_2	Q_1	Q_2	P_1	P_2	$^2P_{1/2}\rightarrow S^2$
Hulthén[39] 1923–5	R_2	R_1	Q_2	Q_1	P_2	P_1	
Kratzer[36] 1923	R_1	R_2	Q_2	Q_1	P_1	P_2	
Hulthén 1922	R_1	R_2	R_3	P_3	P_2	P_1	
Present	$^{RR}R_{21}(\frac{1}{2})$	$R_2(\frac{1}{2})$	$^RQ_{21}(1\frac{1}{2})$	$Q_2(1\frac{1}{2})$	$^QP_{21}(2\frac{1}{2})$	$P_2(2\frac{1}{2})$	
Birge[31] 1927	$R^-(1)$	$R^+(1)$	$Q^\pm(2)$	$Q^\mp(2)$	$P^-(3)$	$P^+(3)$	
Mulliken[37] 1926	R_1	R_2	Q_1	Q_2	P_1	P_2	$P_{1\ 1/2}\rightarrow ^2S$
Hulthén[39] 1923–5	R_2	R_1	Q_2	Q_1	P_2	P_1	
Kratzer[36] 1923	R_1	R_2	Q_1	Q_1	P_1	P_2	
Hulthén 1922	R_1	R_2	R_3	P_3	P_2	P_1	

Notes. (a) In regard to the earliest series notation, that of Liese, cf. Hulthén, Diss. Lund 1923, p. 34.

(b) The numbers in parentheses are the same for all the old notations as for that of Birge, and so have not been repeated.

	^2P *levels*			^2S levels	
Present	$F_{1A}(\frac{1}{2})$	$F_{1B}(\frac{1}{2})$	$F_2(1\frac{1}{2})$	$F_1(\frac{1}{2})$	$F_2(\frac{1}{2})$
Hulthén 1925	$F_1(1)$	$F_2(1)$	$F(2)$	$F_2(1)$	$F_1(1)$

Note. Hulthén's notation is that used in his Tables 7 and 8 of ref. 39 (1925 paper); cf. paragraph on "Term Values" above.

Intensity relations. As already noted in the first section of this paper, the satellite and forbidden branches of case *b* show a progressive increase in intensity in the series ZnH, CdH, and HgH, until in HgH all branches are about equally strong, according to data of Hulthén.[39] This last result is in

[39] E. Hulthén, Dissertation Lund 1923, and Zeits. f. Physik **32**, 32, 1925. In HgH the $^2P_{1\frac{1}{2}}\rightarrow ^2S$ branches as a whole are much weaker (Hulthén, cf. footnote 9 of ref. 37) than the $^2P_{\frac{1}{2}}\rightarrow ^2S$ branches, but this effect may be attributed to the conditions of excitation: the $^2P_{\frac{1}{2}}$ levels as a whole might naturally be more readily excited than the much higher-lying $^2P_{1\frac{1}{2}}$ levels.

complete agreement with the theory of Hill and Van Vleck. ZnH is an interesting transition case. Here in the orthodox branches P_i, Q_i, and R_i the major intensity relation $Q>R>P$ characteristic of a $P\rightarrow S$ transition is found.[40] Similar relations exist in the unorthodox branches, which are, however, on the whole, only about half as intense as the orthodox. An interesting point is that the unorthodox branches reach a maximum intensity at a much smaller value of j than the orthodox branches. This is to be explained by the fact that for large values of j case b is being approached. A similar phenomenon is noted in the OH bands (cf. above).

NO Bands

NO γ *bands*. The NO γ bands, whose structure (eight branches) has been analyzed by Guillery,[41] show the features expected for a $^2S\rightarrow{}^2P_{nab}$ transition in which the doublets $F_1(j+1)$ and $F_2(j)$ of the ^2S levels are (within the experimental accuracy) unresolved. Table XI shows the relation of Guillery's notation to the present notation, and Fig. 5 shows the relations which exist between rotational levels and observed branches.

TABLE XI. *Revised notation and predicted first lines for NO γ bands.*

Present	$P_1(1\frac{1}{2})$	$Q_1(\frac{1}{2})$	$Q_1(1\frac{1}{2})+{}^QP_{21}(1\frac{1}{2})$	$R_1(\frac{1}{2})+{}^RQ_{21}(\frac{1}{2})$	${}^{RR}R_{21}(\frac{1}{2})$	$\}{}^2S\rightarrow{}^2P_{1/2}$
Guillery	$P_2(1)$	$Q_2(1)$	$Q_2(2)$	$R_2(2)$	$R_2'(3)$	
Present	${}^{PP}P_{12}(1\frac{1}{2})$	$P_2(1\frac{1}{2})+{}^PQ_{12}(1\frac{1}{2})$	$Q_2(1\frac{1}{2})+{}^QR_{12}(1\frac{1}{2})$	$R_2(1\frac{1}{2})$		$\}{}^2S\rightarrow{}^2P_{1\,1/2}$
Guillery	$P_1(1)$	$Q_1(2)$	$R_1(3)$	$R_1'(4)$		

Since for the lower ^2P state of NO, the value of $\Delta E/B$ is near that in ZnH (cf. Table II), we may expect similar intensity relations. The observed relations[41] may be summarized as follows: $[Q_2+{}^QR_{12}]>[Q_1+{}^QP_{21}]>[R_1+{}^RQ_{21}]>[P_2+{}^PQ_{12}]\sim P_1>>{}^{PP}P_{12}>R_2>{}^{RR}R_{21}$. Because of the coalescence of the satellite branches with corresponding main branches, the individual intensities cannot be determined in all cases, but the comparatively low intensity of the unorthodox ${}^{PP}P_{12}$ and ${}^{RR}R_{21}$ branches is evident. The observed intensities appear also to agree with the general relation $Q>P>R$ expected for an $S\rightarrow P$ transition. The rather surprising contrast $R_2<<R_1$ which apparently exists finds to some extent a parallel in the OH bands (cf. Table VIII) and elsewhere.

So far as can be judged from the data,[41] the observed first lines in the various branches are in reasonable agreement, taking into consideration the experimental difficulties, with those predicted in Table XI. In several cases one or two unpredicted lines are assigned by Guillery at the beginning of a branch, but in nearly all such instances, the lines in question are lines which also fit in other series.

[40] E. Hulthén, Diss. Lund, 1923, p. 26.

[41] M. Guillery, Zeits. f. Physik, **42**, 121 (1927).

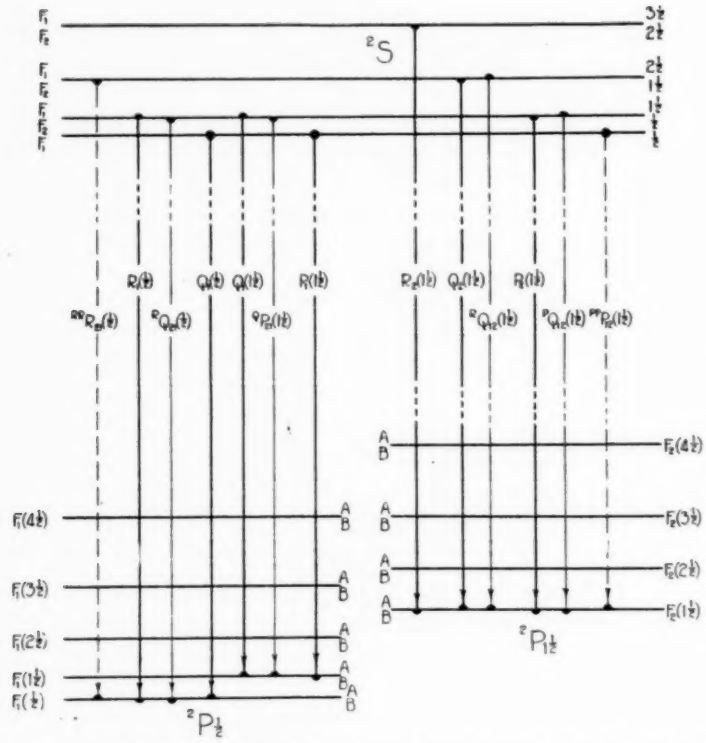

Fig. 5. *Lowest rotational levels, and first lines of each branch, for NO γ band* λ2721 (0, 4 *band*). The levels are drawn to scale with the help of Guillery's Δ_2F data.[41] The relative positions of the ^2S, $^2P_{1\frac{1}{2}}$, and $^2P_{\frac{1}{2}}$ *sets* of levels are, however, not to scale. Doublet separations are all negligible on the scale used, and are shown only by the double designations of the levels. Because of the vanishing ^2S level separations, the satellite branches (light vertical lines) coincide with four of the main branches (heavy vertical lines).

σ-type doubling. According to Guillery's data, the following relations hold.[42,43]

$$R_{21}(j)-R_1(j)\sim Q_1(j+2)-P_1(j+2)<R_1(j+1)-Q_1(j+1) \tag{10}$$

$$R_2(j)-Q_2(j)\gtrsim P_2(j+2)-P_{12}(j+2)<Q_2(j+1)-P_2(j+1) \tag{11}$$

The inequalities indicated in these equations are very slight, especially those in Eq. (11), where it is possible that they represent nothing more than experimental error. Eq. (10) shows (cf. Fig. 5 and Ref. 44) that the relation $F_{1A}''(j)>F_{1B}''(j)$ holds, and from the original data we find $F_{1A}''(j)-F_{1B}''(j)\sim 0.01j''$. Similarly from Eq. (11) and the original data we find $F_{2A}''(j)\geqq F_{2B}''(j)$, the inequality, if any, being very slight.

[42] In Guillery's notation, Eqs. (10) and (11) may be expressed as follows: $c\sim b<a$, where $c=R_i'(m+1)-R_i(m)$, $b=Q_i(m+1)-P_i(m)$, and $a=R_i(m+1)-Q_i(m)$; $i=1$ in her Table 5, 2 in her Table 6.

[43] To avoid confusion, only one symbol has been used even for branches which consist of two superimposed branches: e.g. $R_1(j)$ is intended to imply $R_1(j)$ plus $^RQ_{21}(j)$; all this should be clear from Fig. 5 and Table XI.

NO β *bands*. In the NO β bands ($^2P \rightarrow {}^2P$, with the same final state as the γ bands), the notation which has been used previously[9] is entirely in agreement with the system proposed in VI. The branches observed in these bands are exclusively ordinary *main* branches.

In the NO β bands, the lines of the $^2P_{1/2} \rightarrow {}^2P_{1/2}$ sub-band are doublets of spacing approximately $0.0146j$ (cf. ref. 7, p. 169); assuming $F_{1A}''(j) - F_{1B}''(j) \sim 0.01j''$ from the γ bands, we get $|F_{1A}'(j) - F_{1B}'(j)| \sim 0.025j'$ or $0.005j'$; the two possibilities given, and the order of the A and B levels, cannot be distinguished empirically. In the $^2P_{1\ 1/2} \rightarrow {}^2P_{1\ 1/2}$ band, the lines are single, indicating, since $F_{2A}''(j) \sim F_{2B}''(j)$, that $F_{2A}'(j) \sim F_{2B}'(j)$.

Other Spectra (CN, BO, CO^+)

Intensity relations. The ^2P states of CN, CO^+, and BO form a series with increasing negative values of $\Delta E/B$ (cf. Table II). The values of $\Delta E/B$ here are of the same order of magnitude as those for ZnH and NO, and one therefore expects to find intensity relations in the $^2P \rightarrow {}^2S$ bands of CN, CO^+, and BO similar to those in the ZnH and NO γ bands.

Only the BO α bands have been satisfactorily analyzed in detail.[11] In his analysis of these bands, Jenkins has used a notation conforming with the scheme suggested by the writer in VI. Here, as in the NO γ bands, the ^2S levels $F_1(j+1)$ and $F_2(j)$ are unresolved, hence the four satellite branches coincide with the corresponding main branches. As we should expect from the value of $\Delta E/B$, the unorthodox branches $^{RR}R_{21}$ and $^{PP}P_{12}$ appear to be distinctly weaker than any of the other branches.

Similar intensity relations exist in the CO^+ comet-tail bands: according to data of Baldet[45] on one of these bands, the intensities of the branches (after altering Baldet's notation to conform with that of the obviously analogous BO α bands) are in the order $[Q_2 + {}^QP_{21}] > [Q_1 + {}^QR_{12}] > [R_2 + {}^RQ_{21}] > [P_1 + {}^PQ_{12}] > R_1 \sim P_2 > {}^{RR}R_{21} > {}^{PP}P_{12}$. The characteristic relation $Q > R > P$ of $P \rightarrow S$ transitions is here also evident.

Intensities of heads. The occurrence of four distinct heads (or six, if the ^2S levels are widely split as in HgH) is typical of both $^2P \rightarrow {}^2S$ and $^2S \rightarrow {}^2P$ bands, in all cases where $|\Delta E|$ or $|\Delta E/B|$ of the ^2P state is large enough to make sensible a division into $^2P_{1/2} \rightarrow {}^2S$ and $^2P_{1\ 1/2} \rightarrow {}^2S$ or $^2S \rightarrow {}^2P_{1/2}$ and $^2S \rightarrow {}^2P_{1\ 1/2}$ sub-bands. It so happens that the first of the four heads, numbering the latter in order in the direction of shading, is always formed by the $^{RR}R_{21}$ branch if the bands are shaded toward the red, and by the $^{PP}P_{12}$ branch if they are shaded toward the violet; this is true whether the ^2P state

[44] As can best be seen with the help of Fig. 5, noting especially the equality $F_1'(j+1) = F_2'(j)$, the following relations are true: $[c \equiv R_{21}(j) - R_1(j)] = \Delta_1 F_1'(j+1) - \delta_{AB}(j)$; $[b \equiv Q_1(j+2) - P_1(j+2)] = \Delta_1 F_1'(j+1) - \delta_{AB}(j+2)$; $[a \equiv R_1(j+1) - Q_1(j+1)] = \Delta_1 F_1'(j+1) + \delta_{AB}(j+1)$. Here $\delta_{AB}(j)$ mean $F_A''(j) - F_B''(j)$. The experimental relation $c \backsim b$ shows that $\delta_{AB}(j) \backsim \delta_{AB}(j+2)$; we may then take $(c+b)/2$ as practically equal to $\delta_{AB}(j+1)$. The following relation should then hold: $(a-c) \backsim (a-b) \backsim [a-(b+c)/2] = 2\delta_{AB}(j+1)$. Thus from the quantities a, b, c of Guillery's tables,[42] values of $\delta_{AB}(j)$ can be estimated for the F_1'' levels. A similar treatment applies to the quantities in Eq. (11), with the conclusion given in the text.

[45] Cf. F. Baldet, Compt. Rend. **180**, 820 (1925): Thèse Paris 1926.

is initial or final, normal or inverted, as the reader can prove to his own satisfaction by drawing diagrams for all the possible cases. The second and fourth heads are always formed by strong (main plus satellite) branches, the third by a main branch. Thus the relative intensity of the first as compared with the other heads should be an index of $|\Delta E/B|$.

The expected relations are well shown in the series OH, CN, CO^+, BO. Since the P,S bands of these molecules are all shaded toward the red, the first head in each is an ${}^{RR}R_{21}$ head. In OH this is relatively extremely weak and was long unrecognized (cf. above, "seventh non-satellite branch in OH bands"). In CN, it is much stronger than in OH, but is still much weaker than the other three heads.[46] In CO^+ and BO, the first head, while weaker than the other three, is comparable with them in intensity.[11,45]

σ-type doubling in BO. As Jenkins has shown, the relations $F_{1B}'(j) = F_{1A}'(j)$ and $F_{2B}'(j) > F_{2A}'(j)$ hold in BO; in the latter case, the doublet separation is approximately $0.026j$, from the data of ref. 11, Table 1.

WASHINGTON SQUARE COLLEGE,
NEW YORK UNIVERSITY,
June 5, 1928.

[46] Cf. photographs of A. Fowler and H. Shaw, Proc. Roy. Soc. **86A**, 118 (1912).

BAND SPECTRA IN THE EXTREME ULTRA-VIOLET EXCITED BY ACTIVE NITROGEN

By Harold P. Knauss

Abstract

To determine the amount of energy available in active nitrogen for the excitation of spectra, a vacuum grating spectrograph was used to observe spectra between 2500 and 1000A excited in certain gases in the afterglow. The gases were mixed with glowing nitrogen obtained by flowing nitrogen through a discharge tube containing an oscillatory discharge. H_2, O_2, N_2, CO and NO were studied, of which only CO and NO showed bands in the region mentioned.

NO bands excited by active nitrogen.—In addition to the β and γ bands of NO characteristic of the afterglow, a progression was found belonging to another system with the same final levels, i.e., levels associated with the normal electronic state of the molecule. The initial level, identified from published absorption data as an electronic state with zero vibration, is designated as level C, and the new system, as the δ band system of NO. The 0–0 δ-band is at 1915.7A, corresponding to 6.44 volts.

CO bands excited by active nitrogen.—A few bands of the fourth positive group of CO were obtained in the afterglow, corresponding to the excitation of vibration states $n'=1$ to 6 of electronic level A. The total energy of these levels is from 8.2 to 9.0 volts.

Mechanism of excitation by active nitrogen.—The results are discussed in the light of a possible mechanism of excitation proposed by Birge. It is assumed that atoms of nitrogen can combine to form an excited diatomic molecule if the encounter is such that the energy of formation and the relative kinetic energy of the atoms go over into electronic, vibrational, and rotational energy of the molecule. Such encounters will be rare, because both energy and momentum must be conserved in the recombination; therefore the active modification will have a relatively long life. On formation, the molecules have 11.4 ± 0.3 volts of energy; part of this is lost immediately by radiation of the α group bands, leaving from 9 to 10 volts in a configuration which is strongly metastable with respect to the normal electronic state. This metastable molecule is considered responsible for the excitation of spectra in the afterglow.

Introduction

E. P. LEWIS in 1900[1] called attention to the fact that discharge tubes containing nitrogen exhibit a glow which may under suitable conditions persist for a considerable time after the discharge is cut off; later[2] he showed that the afterglow excites spectra in gases or vapors mixed with it. The chemical activity of the afterglow was emphasized by Strutt,[3] who suggested that atoms of nitrogen recombining to form molecules might be responsible for the phenomenon. Recent attempts[4,5] to check this hypothesis spectrally have sought a connection between the heat of dissociation of nitrogen, known

[1] E. P. Lewis, Astrophys. J. **12**, 8 (1900).
[2] E. P. Lewis, Astrophys. J. **20**, 49 (1904).
[3] R. J. Strutt, Proc. Roy. Soc. **85A**, 219 (1911).
[4] Ruark, Foote, Rudwick, and Chenault, J. Optical Soc. Am. **14**, 17 (1927).
[5] Okubo and Hamada, Phil. Mag. **5**, 372 (1928).

to be 11.4 ± 0.3 volts,[6] and the energy content of the levels found excited in the afterglow. The quartz prism spectrographs used are subject to the limitation that wave-lengths corresponding to energy changes of more than seven volts (1800A) are not transmitted by the prisms, and only the observation of transitions between excited states can establish the occurrence of excitation to higher levels. To observe transitions between levels above seven volts and the normal unexcited level, a vacuum grating spectrograph or a fluorite prism instrument is required.

The present investigation was undertaken to study spectra excited in the afterglow, beyond the limits of quartz, and to determine whether the entire association energy of nitrogen, 11.4 volts, is available for the excitation. The apparatus used and the results obtained with various gases are described in the following sections. No evidence was obtained of excitation higher than nine volts in the materials selected, and in the discussion which concludes the paper, a mechanism of excitation is suggested to account for the results obtained.

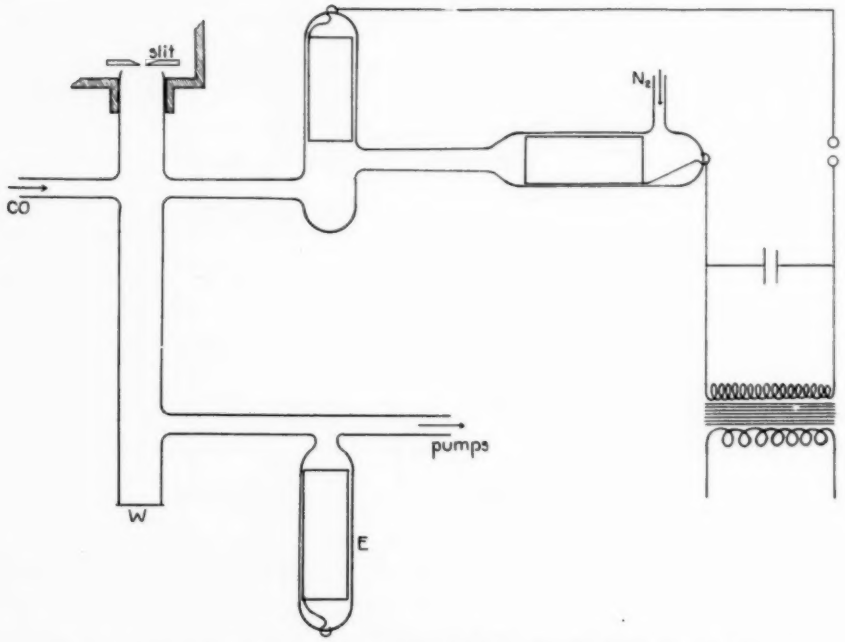

Fig. 1. Apparatus for observing spectra of gases excited in active nitrogen.

Apparatus

The spectrograph used was designed by Hopfield and built in the department shop. A brass receiver contains a grating of one meter radius, ruled at the National Physical Laboratory, in England, and giving a dispersion of about 17.6 A/mm. Sealed to the receiver, and communicating with the interior through the slit, was the tube in which the gas to be excited was

[6] H. Sponer, Zeits. f. Physik, **34**, 622 (1925).

mixed with active nitrogen. The arrangement is indicated in Fig. 1, which shows the slit of the spectrograph at one end of the viewing tube, a Pyrex window *W* at the opposite end, and the side tubes admitting the gas under test (marked CO in the figure) and active nitrogen respectively. The electrical connections indicated produce an oscillatory discharge through the L shaped discharge tube, which is placed so that light from the discharge is not reflected or scattered to the slit. The auxiliary electrode *E* is used in connection with one of the others to obtain an ordinary 60 cycle discharge through the viewing tube, yielding emission spectra for comparison purposes.

Commercial nitrogen from a steel cylinder was passed over hot copper to reduce the oxygen content, and over P_2O_5 to remove moisture, and admitted to the discharge tube at the point shown through a torsion capillary valve due to Hopfield.[7] The flow was maintained by pumps exhausting at the point indicated. Another pair of pumps in parallel was connected to the receiver of the spectrograph, thereby maintaining about the same pressure (about 2 mm) on both sides of the slit, and limiting the entry of active gas into the receiver to that which diffused through the slit.

The films used were either Schumann films prepared according to the method developed by Hopfield,[8] or commercial films treated with paraffine oil to obtain sensitivity in the extreme ultra-violet by fluorescence. There was little to choose between the two types, because the quicker response of the oiled films was counteracted by their readiness to fog. Exposures with the oiled films ran up to 22 hours, and with the Schumann films, to 48 hours.

The slit was made 0.25 mm wide to decrease the time of exposure required for the appearance of bands. The NO bands appeared distinctly with exposures of two hours on oiled film, or five hours on Schumann films.

Nitrogen

The known energy levels[9] of nitrogen are shown in Fig. 2. The constants of the normal unexcited state are known from the $a_1 - X$ transitions, measured by Birge and Hopfield.[10] The exact position of level *A* in the diagram is uncertain, since no connection has been found between *X* and any of the levels *A*, *B*, *C*, or *D*, which are inter-related in the first, second, and fourth positive groups of nitrogen. Accordingly, their position is assigned as a result of measurements on the energy of excitation by electron impact, combined with spectroscopic observation, made by Sponer.[6] During her stay in Berkeley, she also photographed the afterglow[11] with the grating used in the present work, running exposures up to 60 hours, in the hope of

[7] J. J. Hopfield, J. Optical Soc. Am. **12**, 391 (1926).

[8] J. J. Hopfield, Phys. Rev. **20**, 573 (1922).

[9] See "Molecular Spectra in Gases," Bulletin 57 of the National Research Council. Fig. 2, above, embodies results that have been obtained since the preparation of Fig. 26, p. 244 of the Bulletin.

[10] Birge and Hopfield, Nature **116**, 15 (1925).

[11] H. Sponer, Proc. Nat. Acad. Sci. **13**, 100 (1927).

finding the predicted $A-X$ bands. No such bands appeared. Since then the grating has been inverted and refocused, and the diaphragms in the receiver have been readjusted, to obtain a speed possibly three or four times greater than before. Under the new conditions, a 48 hour exposure still failed to show either the known a_1-X or the expected $A-X$ bands. Her work on absorption in N_2, which yielded the Birge-Hopfield bands (a_1-X), has since been carried further by Hopfield[12] with the result that new levels have been found, but nothing involving the levels A, B, C, or D.

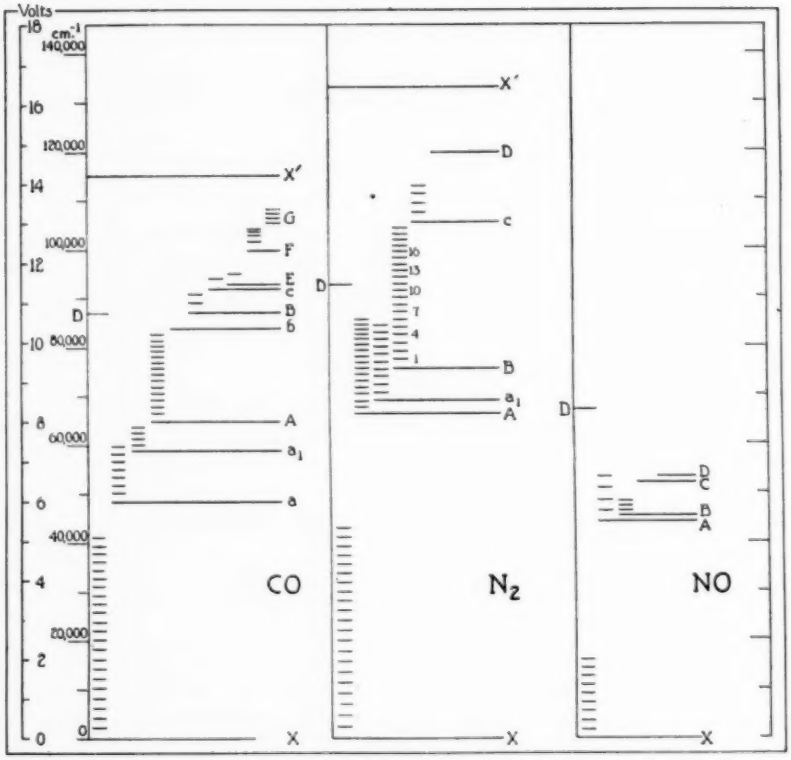

Fig. 2. Electronic and vibrational levels of CO, N_2, and NO.

The absence of the $A-X$ combinations indicates a high degree of metastability for the A level, and therefore has a direct bearing on the problem of the afterglow. The afterglow is characterized by the presence of certain bands, the α group, belonging to the first positive system, which arise from transitions to vibration states of electronic level A. Because the latter is metastable, the molecules cannot lose the electronic energy by radiation, but must return to the unexcited state by giving up the energy in second type collisions, or at the walls of the vessel.

[12] J. J. Hopfield, Abstract No. 89, Washington Meeting, American Physical Soc. Apr. 1928.

Certain bands of the second positive group ($C-B$) are associated with the afterglow according to Ruark, Foote, Rudwick, and Chenault,[4] who worked with an electrodeless discharge at low pressures. These may have appeared because of a defect in the operation of the sectored disk which was used to hide the discharge, as suggested by Okubo and Hamada,[5] or if the effect was real, the occurrence of excitation to the C level at 13 volts could be explained as a four volt excitation of a metastable molecule carrying nine volts of energy. The non-appearance of the bands in the work of Okubo and Hamada might be due to the fact that they used a continuous flow method with pressures 100 times as great as those used in the electrodeless discharge method. In the present work, certain transitions of this system appeared on the afterglow films with intensities varying from film to film, but no critical study was made to decide whether these bands were due to stray discharge, to light reflected or scattered from the discharge tube, or to the afterglow proper.

Hydrogen

The first excited electronic level of the hydrogen molecule has been shown by Dieke and Hopfield[13] to have an energy of 11.1 volts. Excitation to this level should be possible in the afterglow if 11.4 volts are available. Repeated attempts were made to obtain the molecular spectrum of hydrogen in the afterglow, but it failed to appear on any of the films. A comparison spectrum picture made at the pressure maintained for the afterglow experiments showed that the mixture of nitrogen and hydrogen in the receiver was transparent in the region under investigation. Both electrolytic hydrogen and the commercial product were employed, and the rate of admission was varied from the slowest, which left the appearance of the glow unchanged, to the most rapid, which almost quenched the visible glow.

Oxygen

While the electrolytic generator was in service, it was easy to reverse the current and obtain oxygen. The comparison spectrum showed no bands in the region investigated under the conditions available, and a short trial exposure in the afterglow also gave no bands below 2000A. Since oxygen absorbs light very strongly in this region, no further attempt was made to use it.

Nitric Oxide

If any oxygen is present with the nitrogen in a discharge, NO is formed, and the characteristic β and γ bands of NO are observed in the afterglow. They correspond to transitions from electronic levels B and A respectively to X. (See Fig. 2.) A progression of bands belonging to another system with the same final states was observed, the data for which are given in Table I.

[13] Dieke and Hopfield, Zeits. f. Physik **40**, 299 (1926) and Phys. Rev. **30**, 400 (1927).

TABLE I. *Delta bands of NO observed in active nitrogen.*

I*	$n'-n''$	λ (Head)	ν, cm^{-1}	$\Delta\nu$, obs	$\Delta\nu$, calc**	obs−calc
1	0–0	1913	52,274			
				1947	1874.4	+73
2	0–1	1987	50,327			
				1831	1846.6	−11
3	0–2	2062	48,496			
				1811	1818.9	− 8
4	0–3	2142	46,685			
				1822	1791.1	+31
3	0–4	2229	44,863			
				1760	1763.4	− 3
2	0–5	2320	43,103			

* The 0–0 γ-band has an intensity of 6 on this scale.
** From formula for vibrational levels of the normal state.

The bands degrade toward the violet, and the measurements given are for the heads. Since the 0−0 band appears only faintly, because of self-reversal, and is difficult to measure accurately, the most probable value for its frequency is obtained indirectly by adding the known $\Delta\nu$ to the frequency of the 0−1 band, yielding 52,201 cm^{-1} or 1915.7A, and placing the energy at 6.44 volts. This new system of afterglow bands is designated here as the δ band system of NO, and the initial level, the *C* level.

The level here found in emission is responsible for the absorption band found by Leifson[14] at 1910.6A. The discrepancy of 5A is due in part to the fact that Leifson's measurements were of the middle of the band, and those given here are of the heads. The width of the slit (0.25 mm) used in the present work tends to exaggerate the difference. Although Leifson grouped some of his absorption bands into series, the band at 1910.6A is not among them. Further work on the analysis of NO bands is under way in this laboratory.

CARBON MONOXIDE

Since carbon monoxide has a number of electronic levels between 6 and 12 volts (see Fig. 2), it was selected as the next gas to try. The gas was generated by the action of sulphuric acid on ammonium oxalate and was stored over water. It was passed through concentrated KOH solution to remove CO_2, dried with P_2O_5, and run through a liquid air trap and a torsion capillary valve into the afterglow.

Great difficulty was experienced in obtaining CO bands in the far ultraviolet in the afterglow. Two exposures, made with oiled films, contained very faint impressions of bands in the region in question, but attempts to obtain the bands more strongly with longer exposures resulted simply in fogging the films. The faintness of the results leaves open the possibility that the bands observed are not actually an afterglow phenomenon. However, comparison with a CO emission spectrum on the same film shows that the distribution of intensities is different, and that the bands of the third positive

[14] S. W. Leifson, Astrophys. J. **63**, 73 (1926).

group, which are very strong in the emission spectrum, are definitely absent in the afterglow. Furthermore, analysis shows that the bands which appear are related in a manner consistent with the argument of a special type of excitation.

These facts are exhibited in Table II. Only the bands observed in the afterglow are listed, some thirty additional bands which appeared in the comparison spectrum being omitted. The wave-length measurements, made on the comparison spectrum, are uncertain by ± 2A because the impressions

TABLE II. *Fourth positive group of CO excited in afterglow.*

1 λ	2 *I*, comp.	3 *I* in N_2	4 λ*	5 $n'-n''$*	6 *I**
1410	1	6	1409.0	6–1	2
1464	2	0	1463.7	4–1	3
1493	1	2	1493.8	3–1	3
1496			1497.8	6–3	3
1528	4	0	1527.6	5–3	3
1542	5	0	1542.2	3–2	5
1558	5	10	1559.3	1–1	5
				4–3	
1574	5	8	1576.5	2–2	4
				5–4	
1597	1	9	1597.4	0–1	3
			1596.1	6–5	1
				3–3?	
				3–4	5
1648	0	7	1648.2	6–6?	
1653	1		1653.3	0–2	4
1669	1	5	1669.9	1–3	6
1792	2	4	1792.6	1–5	10d
1810	1	3	1811.0	2–6	10d
2171	1	1	2173.3	5–13	8
				1–10?	
2194	1	1	2195.0	2–11	6
			2196.9	6–14	8

* See reference 15
d = double

obtained on oiled film are not sharply defined, particularly with a slit as wide as the one used here. In column 2 intensities on an arbitrary scale from 1 to 5 are given for the bands of the comparison spectrum. In column 3 intensities in the afterglow are indicated on a quite different scale: the strongest band is arbitrarily called 10, the others being numbered serially in the order of decreasing intensity. Several bands about which there might be some doubt are listed as of 0 intensity.

The quantum designation of each of the observed bands is known from the analysis by Birge.[15] In column 4 are shown the wave-lengths as listed by Birge, alternative interpretations being suggested for a few of the bands because of the uncertainty of the present measurements. The quantum assignments made by Birge, and the intensities as listed by him, are given in columns 5 and 6 respectively.

[15] R. T. Birge, Phys. Rev. **28**, 1157 (1926).

It will be seen that the initial vibration states which are present run from 1 to 6, carrying total energies from 8.2 volts to 9.0 volts. The absence of the bands of the third positive group $(b-a)$ indicates that the b level, carrying 10.35 volts of energy, is not excited.

Discussion

Reference has already been made to the suggestion of Strutt[3] that recombining atoms might be responsible for the characteristics of the afterglow. Attention was diverted from this hypothesis by a paper of Saha and Sur[16] which applied the theory of collisions of the second kind[17] and ascribed the activity to an excited nitrogen molecule, with an energy which they estimated at 8.5 volts. Birge[18] pointed out that the α group of the afterglow was known to belong to the first positive system of nitrogen, with an initial level estimated to be at about 11.5 volts. The energy was checked within ± 0.3 volts by Sponer's excitation potential measurements.[6] The electronic levels, both initial and final, of the first positive group of nitrogen, are "floating," i.e., no spectral connection between these levels and the normal level has been observed, therefore no spectral determination of the energy has been possible. Birge at that time suggested that the long life of the afterglow required the hypothesis that the initial level is for some reason metastable.

Meanwhile measurements on the rate of decay of the afterglow by Angerer[19] indicated that two activated entities are involved in each elementary process of light emission. Sponer[6] revived the atomic hypothesis, and sought to account for the long life of the afterglow by assuming that a triple collision is necessary to make recombination possible. In so doing, she referred to the case of hydrogen as studied by Bonhoeffer[20] where it was shown that atoms can recombine only at the walls, or in a triple collision including some third body that is capable of taking up the energy given out in recombination. In terms of this mechanism, then, a pair of nitrogen atoms colliding simultaneously with a third body, say a nitrogen molecule, can unite and give up the energy of association, 11.4 volts. Accordingly, the entire 11.4 volts might be available for excitation, and the process should be very efficient if the third body has energy levels at just under 11.4 volts.

Subsequent work of Bonhoeffer and Kaminsky[21] showed results in definite contradiction to the triple collision hypothesis. On keeping the partial pressure of active nitrogen constant, but increasing the partial pressure of N_2, the luminosity decreased, instead of increasing as required by the triple impact theory.

The analogy with hydrogen breaks down at a vital point. In hydrogen, the first excited electronic level[13] at 11.1 volts is far above the energy of

[16] Saha and Sur, Phil. Mag. **48**, 421 (1921).
[17] Klein and Rosseland, Zeits. f. Physik. **4**, 46 (1921).
[18] R. T. Birge, Nature **114**, 642 (1924).
[19] E. Angerer, Physik. Zeits. **22**, 97 (1921).
[20] K. F. Bonhoeffer, Zeits. f. Phys. Chem. **113**, 199 (1924).
[21] Bonhoeffer and Kaminsky, Zeits. f. Elektrochemie **32**, 536 (1926).

association, at 4.42 volts.[22] In nitrogen, on the other hand, the electronic levels A, a_1, and B are lower than the energy of association at 11.4 volts, and vibration-rotation levels are present which have total energies nearly equal to that value, so that spontaneous recombination with the formation of an excited molecule is possible. Since both energy and momentum must be conserved in such a process, the recombination can occur only in the rare cases where the relative kinetic energy of the atoms plus the potential energy is equal to the total energy of some particular quantum state in which the angular momentum of the molecule is equal to the angular momentum of the pair of atoms before collision. Some small tolerance must be assumed in such a process, otherwise the probability would be vanishingly small, and the life of the active state would be almost indefinite.

The assumption that recombination occurs in this manner offers an explanation of the long life of the afterglow. Birge[23] has shown that other afterglow phenomena, such as the variation of luminosity with temperature, can be described readily in terms of this mechanism. Bonhoeffer and Kaminsky's results have been considered by Bernard Lewis,[24] who shows that a two-body collision between atoms of nitrogen leads to results in agreement with their observations.

It is well known that the α bands characteristic of the afterglow are simply a set of bands selected from the first positive band system of nitrogen. The initial states represented are vibration levels 10, 11, and 12 of electronic level B, and the final states are vibration levels 5 to 8 of electronic level A, the observed bands lying in the green, the yellow, and the red. The emission of these bands, according to Birge, occurs immediately after recombination. Since the final levels are associated with electronic state A, which is strongly metastable, the molecules are thus left with considerable energy which cannot be lost directly by radiation, but which is available for the excitation of other atoms or molecules. It is possible to estimate the energy of these metastable molecules, by combining Sponer's data on excitation potentials[6] with spectral data[9] on the α bands. Assuming 11.4 volts to be the energy of the initial level 11, the energies of the final states run from about 9.0 to 9.5 volts. If the α bands extend into the infra-red, as might be inferred from the ordinary band spectrum of nitrogen, higher final levels would occur as well, up to say 10 volts. All of these values are uncertain within ± 0.3 volts, the experimental error of the excitation potential determinations. The most probable energy, corresponding to the most intense member of the α group, is 9.33 volts.

It should be noted that not all of this energy must necessarily be given up in a second type collision. Some of it may be lost by radiation in the infra-red with the loss of a quantum of vibrational energy. On the other hand, the molecule may be able to retain vibrational energy while returning to its normal electronic state in a second type collision. Thus the possibilities

[22] R. T. Birge, Proc. Nat. Acad. Sci. **14**, 12 (1928).

[23] R. T. Birge, unpublished work.

[24] B. Lewis, Phys. Rev. **31**, 314 (A) (1928) and J. Amer. Chem. Soc. **50**, 27 (1928).

for excitation of other spectra are much greater than in the case of metastable atoms, and the richness of spectra excited in the afterglow is explained.

However, there is reason to believe that excitation of particular levels does not always occur, even though it is possible from considerations of energy alone. Thus Okubo and Hamada[5] find a level of mercury at 9.51 volts excited in the afterglow, but the next at 9.65 unexcited. This may mean that the energy available is less than 9.65 volts (which would be consistent with the mechanism discussed here) or that the 9.65 volt level has characteristics which prevent it from taking over the energy of a metastable nitrogen molecule.

The bands found in CO with 8.2 to 9.0 volts of energy receive somewhat less than the predicted maximum energy from the afterglow. The probable explanation for this has been given above. In the case of NO, it is possible that the β, γ and δ bands are a recombination phenomenon, since it is apparent from the energy diagrams (Fig. 2) that the metastable nitrogen molecule carries energy sufficient to dissociate NO.

Conclusion

Since the experimental evidence of this and other researches is that atoms and molecules in the afterglow are excited readily with energies up to nine volts, and probably not above 9.5 to 10 volts, the conclusion may be drawn that the excitation is caused by a nitrogen molecule in one of a series of metastable states carrying the corresponding energy. The view that atoms of nitrogen combine to form an excited molecule responsible first for the emission of α bands and later for the excitation of other spectra is thus supported by the results obtained in these experiments.

It is a pleasure to acknowledge the guidance received from Professor J. J. Hopfield and Professor R. T. Birge in carrying out this investigation.

Department of Physics,
University of California,
April, 1928.

THE FLUORESCENCE AND ABSORPTION OF A MIXTURE OF MERCURY AND ZINC VAPORS

By J. G. Winans*

Abstract

It was observed that light from the aluminum spark of wave-length below 2000A excited vapor distilling from slightly amalgamated zinc, causing the emission of the first triplet of the sharp series of zinc, but excited neither the non-distilling vapor nor that distilling from pure zinc. The same kind of mercury-zinc mixture showed a continuous absorption from 2050 to <1850A in distilling but not in stagnant vapor. The stagnant vapor and pure zinc vapor show in addition to the absorption lines of zinc three new absorption bands. Two of these correspond to absorption bands in cadmium. The absorption spectrum of mercury alone is also studied and shown to be different from that of zinc amalgam. The fluorescence excited by the aluminum spark is emitted by 2^3S zinc atoms which may have been produced either through absorption by HgZn molecules and dissociation into excited zinc and normal mercury atoms or through collisions of the second kind between normal zinc atoms and excited HgZn molecules.

EXPERIMENTS by Franck, Cario, and others have shown that mixtures of gases illuminated by light which only one gas will absorb may emit a fluorescence light, the spectrum of which shows lines characteristic of both gases. In mixtures of monatomic gases, atoms of one gas absorb energy from the incident radiation and excite the atoms of the other gas through collisions of the second kind. The gas mixture then contains excited atoms of both gases and these atoms emit the fluorescence light. Such experiments are known for mixtures of mercury vapor with thallium, silver, cadmium, lead, bismuth, indium, sodium,[1] and zinc[2] vapors.

In a mixture of mercury and zinc, the sharp triplet of zinc ($2^3P_{2,1,0}-2^3S$) was excited by light from an aluminum spark which did not coincide in wave-length with absorption lines in either mercury or zinc. It was assumed that at the pressures used the 1849 absorption line of mercury was sufficiently broad to include the 1854 line of aluminum but later experiments on absorption spectra in similar mercury-zinc mixtures have shown that the 1849 line does not extend to 1854. The fluorescence excited by the aluminum spark can not then be explained by the simple process which holds for monatomic gas mixtures. To ascertain the processes involved a study has been made of the fluorescence in a mercury-zinc mixture and in pure zinc, and of the

* National Research Fellow in Physics.

[1] J. Franck and P. Jordan, Anregung von Quantensprungen durch Stösse p. 210–232.

[2] J. G. Winans, Phys. Rev. **30**, 1 (1927).

absorption spectrum in a mercury-zinc mixture, zinc, mercury, and a mercury-cadmium mixture.

1. Fluorescence of a Mercury-Zinc Mixture

The fluorescence tube is shown in Fig. 1. A condensed spark between electrodes of aluminum, iron, nickel, cadmium, or copper served as the source. In preparation, the fluorescence tube was evacuated to less than 10^{-6} mm and baked out at 650°C for over ten hours. Some zinc was then distilled in, a slight amount of mercury vapor was allowed to enter, and the tube was sealed off at a temperature near 650°C. The correct amount of mercury was obtained by heating a small reservoir of mercury, attached to the vacuum system 12 cm from the tube, over boiling water for five minutes before sealing off.

With the condensed aluminum spark as source and part *B* slightly hotter than part *A*, fluorescence was observed at temperatures over 450°C. The

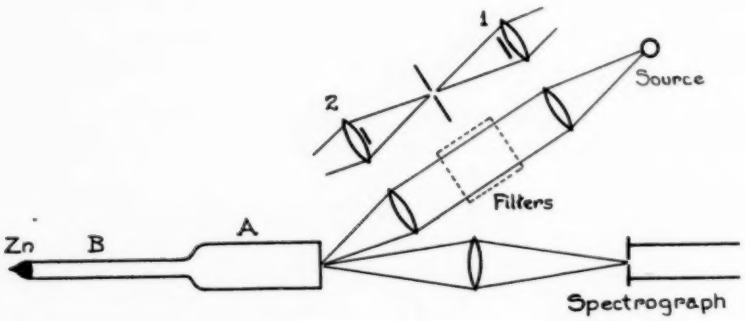

Fig. 1. Diagram of apparatus showing the arrangement for filtering the light. When desired, the lenses could also be arranged as shown at 1 and 2 with a system of diaphragms for the focal isolation of certain wave-lengths.

spectrum showed the sharp triplet of zinc ($2^3P_{2,1,0}-2^3S$) 4810, 4722, 4680 and much scattered light. The scattered light was eliminated when the lenses were arranged for focal isolation with diaphragms as in Fig. 1, 1 and 2, and focussed so that the exciting light contained only wave-lengths below 2000A. The fluorescence excited by this light showed also only the sharp triplet of zinc. When only one lens was used in the path of the exciting light, the fluorescence was sufficiently intense to be observed visually through a Hilger D1 glass spectrograph. The following observations were made.

1. The sharp triplet was excited with about the same intensity by light from condensed sparks of iron, cadmium, nickel, and aluminum when the temperature of *B* was greater than that of *A* and over 500°C. Light from the copper spark gave only very faint fluorescence.

2. When the window was heated by a blow torch, the fluorescence disappeared but reappeared as soon as the window had cooled slightly.

3. When the temperature of *A* was greater than that of *B*, no fluorescence resulted.

Of the sources tried, only those sparks which had strong lines below 1860 excited strong fluorescence and then only when there was an opportunity for evaporation of vapor near the window. In the first observation, distilling vapor resulted from the evaporation of small drops of metal which had condensed on or near the window. Heating the window for observation 2 prevented this condensation and evaporation, and only stagnant vapor was present.

2. Absorption Spectrum of a Mercury-Zinc Mixture

A quartz absorption cell 18.7 cms long was prepared with a mixture of mercury and zinc in the same way as the fluorescence tube, and mounted in a furnace as shown in Fig. 2. Nitrogen was passed continuously through the furnace and spectrograph during exposure to sweep out the air, and so eliminate the absorption due to oxygen. A condensed spark between aluminum electrodes gave a good continuous spectrum extending from 1840–7000A (see Fig. 3, No. 1). The spark gap had electrodes 0.4 cm in diameter

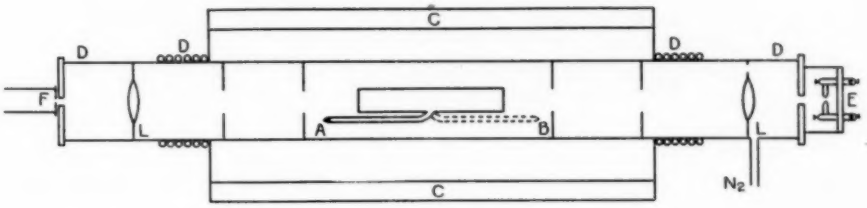

Fig. 2. *E*, aluminum spark; *C*, furnace; *F*, spectrograph; *D*, water cooling.

0.2 cm apart and was operated from a 1 KW., 17000 volt transformer connected in parallel with a 1 mfd condenser. A small E31 Hilger quartz spectrograph focussed for the region from 1850–2300 was used with Schumann plates.

With the absorption cell as in Fig. 2 *A* so that one window was cooled by the nitrogen stream, an absorption band appeared at temperatures greater than 160°C when the temperature was rising. This band extends continuously from λ2050 to wave-lengths less than 1850 and is especially strong for wave-lengths below 1860. The band limits are shown at *a-b* Fig. 3, Nos. 2 and 3. As the temperature and vapor pressure of the zinc increased, the limits of this band remained the same. The absorption line $2138(1^1S-2^1P)$ broadened symmetrically with pressure to a width of over 100A at 4.0 cms. The breadth of this line roughly indicated the pressure.

When the temperature of the furnace was falling or when the absorption cell was arranged as in Fig. 2 *B*, the absorption band from 2050–<1850 was no longer observed. Fig. 3, No. 3 *a-b* shows the absorption band observed

with increasing temperature and No. 4 shows the absorption with falling temperature. The vapor absorbs the aluminum spark lines 1854 and 1862 when the temperature is rising, but transmits these lines when the temperature is falling; the pressure as indicated by the width of 2138 at *e* was nearly the same in both cases. The temperature changed at the rate of about three degrees per minute.

The effect of the nitrogen stream in the arrangement of Fig. 2 *A* was to make the body of the cell cooler than the stem in which the zinc was contained. Zinc then condensed on the walls of the cell and later re-evaporated with further heating to give distilling vapor in the light path. On cooling or with the arrangement of Fig. 2 *B* only stagnant vapor was present. The

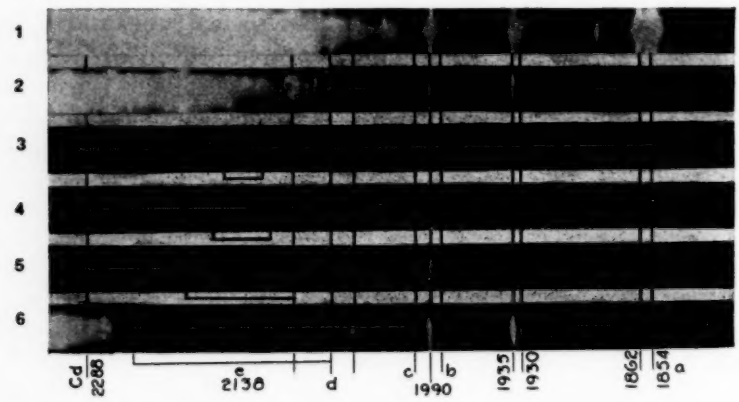

Fig. 3. (1) Aluminum spark (2) Absorption spectrum of distilling zinc amalgam vapor at 160°C (3) Absorption spectrum of distilling zinc amalgam vapor at 570°C. (4) Absorption in stagnant zinc amalgam vapor at 600°C. (5) Absorption in zinc at 670°C. (6) Absorption in zinc at about 720°C.

conclusion is that vapor distilling from the metal in a mercury-zinc mixture shows a continuous band absorption from 2050–<1850 which is not observed in stagnant vapor. The resolving power was not sufficient to detect any fine structure.

3. Absorption Spectrum of Zinc

The absorption cell was prepared as in the previous cases except that no mercury was introduced. The absorption spectrum of zinc with no mercury was the same in distilling and stagnant vapor, and was identical with that observed in stagnant vapor over zinc amalgam, except that the absorption lines 1849 and 2536 of mercury were absent. The band from 2050–<1850 was not observed.

Three absorption bands appear at pressures over 9 mm (590°C). At 35.6 mm (667°C) one band extends from about 1900 to wave-lengths below 1850, one from 1997 to 2006, and the other from a sharp edge at 2064.2 to a diffuse edge at 2072. Edges were measured at the position at which the

background intensity was estimated to have been reduced by one-half. With increased pressure the band at 1900 broadened slightly toward longer wave-lengths, the 1997–2006 band broadened a little in both directions and the 2064 band broadened only toward longer wave-lengths. With increased pressure the 2138 line broadened symmetrically until it overlapped the 2064 band on its short wave-length side, after which it broadened only toward longer wave-lengths. Fig. 3, Nos. 5 and 6 show the absorption of pure zinc at two pressures. Bands appear at *a*, *c*, *d*, and *e* (2138 line). At the higher pressure *d* and *e* are overlapped but have retained a sharp edge at *d*. The band at 1900 is similar in appearance to that found in distilling zinc amalgam. These are, however, two distinct bands, for the one at 1900 appears both in distilling and stagnant vapor, but only at pressures over 9 mm (590°C); the zinc amalgam band 2050 − <1850 appears only in distilling vapor at temperatures over 160°C.

4. Absorption Spectrum of Mercury

The same cell, 18.7 cms long, was prepared in the same way with mercury. For some of the observations on mercury and cadmium a hydrogen discharge tube similar to that described by Lambrey and Chalonge[3] was used as a source and photographs were taken with a medium size (E2) Hilger quartz spectrograph on Cramer contrast plates.

The absorption spectrum of mercury was the same in distilling and stagnant vapor. With increasing pressure of mercury, the 1849 line appeared at 1.2 mm (130°C) and widened into a band extending toward longer wave-lengths. At 4.2 mm (160°C) the band at 2540 appeared as a narrow line and broadened toward longer wave-lengths with increasing pressure. At 96.3 mm (260°C) the band at 2345 appeared and broadened only toward shorter wave-lengths until at 1400 mm (393°C)* it met the 1849 band at a wave-length of 2277. The three sets of flutings associated with the 2345 and 2540 bands observed by Rayleigh[4] in distilling vapor were observed in this experiment in stagnant vapor.

5. Absorption Spectrum of a Mercury-Cadmium Mixture

The absorption cell was prepared as in 1 with a mixture of cadmium and mercury. In the only case tried, too much mercury was admitted so that the 1849 absorption band of mercury overlapped the region in which the band analogous to that observed in the mercury-zinc mixture should lie. The cadmium bands corresponding to two of the bands found in pure zinc were, however, observed. At 83 mm (600.2°C) the band corresponding to the one from 1997–2006 in zinc extends from λ2120 to 2130 and the other correspond-

[3] M. Lambrey and D. Chalonge Comptes rendus **184,** 1057 (1927).

[4] Rayleigh, Proc. Roy. Soc. **A116,** 702 (1927).

* Vapor pressures from International Critical Tables v3 p. 205–6 and Landolt and Börnstein Physialkische Chemische Tabellen 5th ed. p. 1338.

ing to the 2064.2 band in zinc extends from 2208.7 to longer wave-lengths. With increasing pressure, this latter band appears first at 2211 and broadens toward longer wave-lengths till it overlaps the 2288 line. The 2288 line broadens nearly symmetrically with pressure until it meets the 2211 band at about λ2225, after which it broadens only toward longer wave-lengths. At 186 mm (654°C) the band formed from the union of 2288 and 2211 extends from 2207.1 to about 2530 terminating in a series of flutings on the long wave-length side. At 186 mm the other cadmium band limits are 2118-2130A. The flutings and the band at 2211 were first observed by Mohler and Moore[5] and the one from 2120–2130 was found by Jablonski.[6]

6. Discussion

Absorption and fluorescence of a mercury-zinc mixture. The appearance of an absorption band in vapor distilling from slightly amalgamated zinc and its failure to appear in stagnant vapor shows that distilling vapor contains some molecules which are not present in stagnant vapor. Since this absorption band was not observed in either zinc or mercury alone, it must be attributed to a compound of the two. It will be assumed to be HgZn. These HgZn molecules must distill out of the metal and later be dissociated by thermal impacts. This would require that the energy of dissociation be very low.

The appearance of fluorescence in a mercury-zinc mixture in distilling vapor but not in stagnant vapor indicates that the fluorescence is associated with the absorption of light by HgZn molecules. This view is strengthened by the fact that the 2^3S zinc atoms which emit the fluorescence possess an energy corresponding to a wave-length of 1862 and the HgZn absorption band showed especially strong absorption in this region.

To produce these 2^3S zinc atoms, HgZn molecules may absorb light of wave-length below 1862 receiving enough energy to dissociate into 2^3S zinc atoms and normal mercury atoms or the molecules may reach a fairly stable excited state through absorption of light near 1860 and later transfer their energy to normal zinc atoms through collisions of the second kind. The experiments described here offer no means of determining what percentage of the fluorescence is due to each process.

Many observers have found that the visible band-fluorescence of mercury can be excited only when the mercury is distilling. Wood and Voss[7] have recently shown that this is due to the sweeping away of impurities such as water and hydrogen by the vapor stream. In stagnant vapor the impurities are assumed to destroy the excited mercury molecules through collisions of the second kind so that no fluorescence results.

[5] F. L. Mohler and H. R. Moore J.O.S.A. **15**, 74 (1927).
[6] A. Jablonski, Zeits. f. Physik **45**, 878 (1927).
[7] R. W. Wood and V. Voss, Jour. Frank. Inst. **205**, 486 (1928).

This explanation can not be applied to the fluorescence in a mercury-zinc mixture for both the fluorescence and the corresponding absorption band were observed in distilling but not in stagnant vapor. One would not expect purification by distillation to introduce a new absorption band but if distilling vapor contained molecules which did not exist in stagnant vapor, such a band should appear.

Absorption and fluorescence of cadmium. Kapuscinski[8] found that greater pressures were required to obtain the sharp triplet ($2^3P_{2,1,0}-2^3S$ λλ5086, 4800, 4678) in fluorescence in pure cadmium than when a trace of mercury was present and Power[9] observed that the sharp triplet of cadmium was excited in fluorescence only when the vapor was distilling. Both used spark sources of light. The conditions of Power's experiment were such that the tube probably contained a slight amount of mercury. The fluorescence of the sharp triplet in these experiments is very likely due to unstable HgCd molecules which exist only in distilling vapor. The process of excitation would be the same as that described above for a mercury-zinc mixture. The existence of unstable HgCd molecules in distilling vapor was suggested also by MacNair[10] to explain the emission of the mercury line 2536 in vapor distilling from a mixture of mercury and cadmium illuminated by light of wave-length 2288.

Jablonski[6] has associated the fluorescence of the sharp triplet of cadmium with absorption of light in the cadmium band 2120–2130. He makes the hypothesis that two cadmium atoms at the instant of collision absorb light of wave-length 2120–2130 and separate as one excited and one normal atom. The kinetic energy of the colliding atoms is added to the energy of the light to produce the excited atom. This process should occur equally well in pure cadmium or cadmium with a trace of mercury, and in distilling or stagnant vapor but the fluorescence in these cases is markedly different. This process, however, may account for the fluorescence in pure cadmium at high pressure and temperatures.

Conclusions. These experiments lead to the conclusion that fluorescence in gas mixtures may occur in several ways. In a mixture of zinc and mercury illuminated by light from a spark or arc the zinc atoms may be excited through collisions of the second kind with excited mercury atoms, or with excited HgZn molecules, or may result from the absorption and dissociation of HgZn molecules into excited zinc and normal mercury atoms. These processes will also account for the emisssion in fluorescence of the cadmium lines 5086, 4800, 4678 by a mixture of cadmium and mercury.

Wood and Kinsey[11] have assumed the same processes to account for the

[8] W. Kapuscinski, Nature **116**, 863 (1925) Zeits. f. Physik **41**, 214 (1927).

[9] A. D. Power, Phys. Rev. **26**, 761 (1925).

[10] W. A. MacNair, Phys. Rev. **29**, 677 (1927).

[11] R. W. Wood and E. L. Kinsey, Phys. Rev. **31**, 793 (1928).

excitation of the *D* lines in mixtures of hydrogen, nitrogen, or air with sodium by light of wave-length 5100–5250A.

Compounds like HgZn may exist in other gas mixtures and should be considered in the explanation of their fluorescence. Wood and Guthrie[12] and later Waring[13] have found absorption bands in mixtures of mercury and thallium which were not observed in either mercury or thallium alone.

In conclusion I wish to express my thanks to Dr. K. T. Compton for permission to carry out this work in Palmer Physical Laboratory. I also wish to thank Professors K. T. Compton and L. A. Turner for their helpful suggestions.

PALMER PHYSICAL LABORATORY
PRINCETON UNIVERSITY
June 4, 1928.

Note added in proof: The absorption spectrum of pure cadmium has been found to be the same as that described above for a mercury-cadmium mixture. The asymmetrical broadening with pressure, over 60 mm, of the 2288 line from a constant short wave-length edge near 2208, must be attributed to cadmium and not to HgCd molecules. No absorption lines or bands were observed in cadmium between 2120 and 1860, at pressures less than 60 mm in a 32 cm absorption cell.

[12] R. W. Wood and D. V. Guthrie, Astrophys. J. **26**, 41 (1907).
[13] R. K. Waring, Nature **121**, 675 (1928).

ABSORPTION BANDS IN THE SPECTRA OF MIXTURES OF METALLIC VAPORS

By R. K. Waring

Abstract

Evidence of the existence of HgTl molecules in the vapor state.—It is shown by experiment that at a given temperature the amount of thallium in the vapor state is increased by adding mercury vapor. This indicates definitely that thallium-mercury molecules are formed.

Absorption bands of HgTl molecules.—In a mixture of thallium and mercury vapors a number of bands appear in absorption which are to be attributed to the HgTl molecule. In no case was the resolving power sufficient to show structure. Asymmetric broadening of the atomic Tl lines and of the Cd line 2288 due to Hg vapor has been observed. Two possible explanations are discussed: broadening due to a superimposed molecular band, and broadening due to transfer of kinetic energy by collisions.

Absorption bands of InCd molecules.—Absorption bands due to InCd molecules were observed in mixtures of In and Cd vapors at temperatures of 400°, 500° and 800°C. Their short wave-length limits are tabulated. A few showed traces of their structure but the resolving power was not sufficient to make measurements possible.

IN 1908 Wood and Guthrie[1] studied the ultra-violet absorption spectra of mixtures of metallic vapors. They found that the spectrum of a mixture of thallium and mercury contained bands which were not present in the spectrum of the vapor of either pure metal. They also found that the presence of mercury vapor caused the atomic lines of thallium and of cadmium to broaden asymmetrically. In addition, there appeared to be evidence that the presence of mercury vapor permitted the vaporization of thallium at temperatures lower than any at which its presence could be detected by its optical absorption when mercury was not present, but the absorption bands seen under this condition, which do not appear with mercury vapor alone, must be attributed to a molecule (probably HgTl), and not to atomic thallium. The effect alluded to above might perhaps be classified as a solution of thallium in mercury vapor, analogous to similar phenomena described by Wood in the case of potassium iodide and alcohol vapor.[2]

The question now presents itself as to whether the mercury atoms attach themselves to thallium atoms in the vapor state (for a few must be present even at the low temperatures), and by thus lowering the partial pressure of the thallium vapor, permit more vapor to leave the metal which, in its turn, unites with the mercury, or the mercury atoms unite with the thallium atoms at the surface of the metal, the amalgam molecule then going into the vapor phase. The present investigation was undertaken for the purpose of con-

[1] Wood and Guthrie, Astrophys. J. **29**, 211 (1909).
[2] Wood, Phil. Mag. **41**, 423 (1896).

firming and extending these results, and studying the observed phenomena from the viewpoint of the theory of band spectra, which has been developed in recent years.

Preliminary Experiment

As a preliminary experiment an investigation was made to see whether it could be shown by non-optical methods that the volatilization of thallium was assisted by the presence of mercury vapor. Two identical Pyrex U-tubes of 15 cc capacity were evacuated, baked, and sealed off. One U-tube contained a piece of thallium in one branch, and a small amount of mercury in the opposite branch. The other U-tube contained a piece of thallium in one branch, and nothing in the opposite branch. The tubes were placed together in a vertical furnace with their ends down, and heated to 600°C. When equilibrium had been reached, a blast of cold air was directed against the branches which had not originally contained thallium, causing an immediate condensation of the contents. The blast was kept on for 30 seconds, after which the tubes were removed from the furnace and allowed to cool. The tubes were then opened and an analysis for condensed thallium was made.

Tihe branch which had contained mercury yielded one-half a milligram of thallum, while the branch which had been empty yielded no thallium. The experiment was repeated, using larger tubes and an improved method of analysis. This time the branch which had contained mercury yielded 5.3 mg of thallium, and the branch which had been empty yielded 0.5 mg of thallium.

The chemical analysis offered difficulties because of the small amount of thallium involved. The method finally adopted consisted in introducing some mercury into the branch of the tube to be tested for thallium, and then oxidizing the thallium with air under a known volume of standardized sulphuric acid. The thallic hydroxide formed is immediately dissolved by the acid so that the amount of thallium can be calculated from the amount of acid used, which, in turn, is determined by titration. The process may be represented as follows:

$$4Tl + 3O_2 = 2Tl_2O_3$$
$$2Tl_2O_3 + 6H_2O = 4Tl(OH)_3$$
$$4Tl(OH)_3 + 6H_2SO_4 = 2Tl_2(SO_4)_3 + 12H_2O$$

The method was tested with known amounts of thallium, and it was found that for small amounts of thallium the test consistently showed less thallium than was really present. For example, when 10 mg of thallium was used, and air was bubbled through the acid for 15 hours, the test showed 7 mg of thallium. While this seems very rough, it is sufficient for the purpose since, in the last actual experiment, the yields of condensed thallium from the two branches of the two U-tubes were 0.5 mg, and 5.3 mg, respectively.

This result indicates that more thallium exists in the vapor condition when mercury is present. It was realized that such a result might be due to lack of uniform temperature throughout the furnace, so care was taken to

obtain a uniform temperature. The amount of mercury present was so small that it was entirely volatilized at 600°. When the mercury was condensed by means of the air blast it might have swept the thallium vapor along with it to such an extent as to increase the amount of thallium which was condensed, but this process could not possibly increase the amount of condensed thallium from 0.5 mg to 5.3 mg. Thus, the experiment seems to indicate quite definitely that thallium-mercury molecules were formed.

Winans[3] has found bands in the absorption spectra of vapor freshly distilled from a mercury-zinc amalgam which do not appear in the spectra of the stagnant vapor. He attributes the bands to a zinc-mercury molecule, and it would seem likely that the molecule is formed in the amalgam and soon dissociates when in the vapor state. In the case of thallium there is no evidence as to whether the molecule is formed at the surface of the solid thallium or in the vapor.

Experimental Procedure

The metals to be studied were placed in a quartz tube which was then evacuated, baked, and sealed off. Tubes were used from 10 to 15 cm long, and from 1 to 2 cm in diameter. At first flat quartz windows were sealed on the ends of the tube, but later it was found that quite satisfactory results were obtained by blowing a bulb on each end of the tube. If the quartz was blown rather thin the transmission was good. In the ultra-violet a quartz spectrograph of one meter focus was used, while in the visible a one meter concave grating, and a 21 foot plane grating spectrograph were employed. Hammer Special plates were used for the photography of the ultra-violet, and Panchromatic for the visible. The source of light in the ultra-violet was the continuous background of the cadmium spark, while in the visible the carbon arc was used. The usual procedure was to place the source of light about 50 cm from the slit of the spectrograph, and focus on the slit by means of a quartz lens placed about 10 cm from the source. The light then passed through the absorption tube, which was contained in a platinum wound furnace. The furnace was fitted with auxiliary heating units at each end in order to prevent condensation on the windows of the tube. The maximum temperature attainable was 1200°C.

Absorption Spectra of Mixtures of the Vapors of Thallium and Mercury

The ultra-violet absorption of pure thallium was photographed at temperatures between 200°C and 800°C. The following lines appeared: $2^2P_1 - 3^2S_1$ (2316A); $2^2P_1 - 2^2S_1$ (2580A); $2^2P_1 - 1^2S_1$ (3776A); $2^2P_1 - 4^2D_2$ (2380A); $2^2P_1 - 3^2D_2$ (2768A). The first three of these lines appeared at 700°C, and the last two at 600°C. In addition a very faint trace of a line at about 3230A appeared at about 400°, but its intensity did not increase at higher temperatures. Later on in the work, with a different tube and a different sample

[3] Winans, Phys. Rev. **31**, p. 710 (April, 1928).

of thallium, this line again appeared, and in addition, two very faint lines at about 3221 and 3241. These lines were also observed by Wood and Guthrie.

A number of tubes were next tried which contained 20 parts thallium to one part mercury, and one tube which contained 15 parts thallium to one part mercury. In every case the amount of mercury was 8 mg. Considerable difficulty was encountered because of the corrosive action of the thallium on the quartz windows which would eventually become opaque to ultra-violet light. It is interesting to note that this effect was always encountered when mercury was present, but never caused any trouble when the tube contained only thallium. With these tubes it was found that all the thallium lines came out at a lower temperature (roughly 100°) than with pure thallium. This is caused, at least in part, by the broadening of the lines due to the presence of the mercury vapor. The extremely faint lines observed with thallium at 3221, 3230 and 3241 now appeared at about 400°, as bands about 3A wide, sharp on the side of short wave-length, and shaded toward the visible. They broadened slightly with increasing temperature. Two other bands also appeared, one at about 3100 and one at about 2510. Both bands were somewhat faint but quite broad.

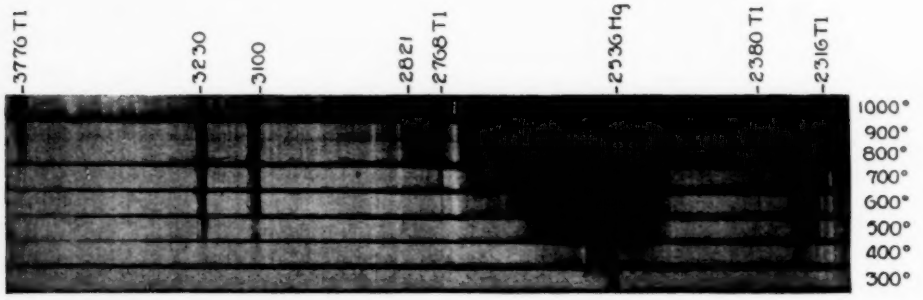

Plate I.

A tube was next prepared containing 132 mg of thallium and 100 mg of mercury. (It may be mentioned that in all cases the mercury was completely volatilized at temperatures, above 600°, while in no case was much of the thallium volatilized.) In this case all of the absorption lines and bands came out much stronger than in previous cases, and a number of new lines and bands appeared (Plate I). Table I gives a list of the absorption with this tube (temperature 900°C) omitting the absorption bands due to pure mercury vapor. The wave-lengths are accurate to a few tenths of an Angstrom,except where a question mark follows the recorded value. In no case was the resolving power sufficient to show the structure of any of the bands. All of the unclassified lines are faint and will probably not be visible in the reproduction included in this article. It is thought probable that many, or all, of the "unclassified lines" are very narrow bands. Wood and Guthrie observed a number of narrow bands in this region when they used very high vapor pressures.

TABLE I. *Wave-lengths of absorption bands and lines in a mixture of thallium and mercury vapors.*

Bands	Thallium Lines
3244? (diffuse limit) 3240.3 (sharp limit)	$2^2P_1-3^2S_1$ (2316) $2^2P_1-1^2S_1$ (3776) very broad $2^2P_1-4^2D_2$ (2380) very broad
3235? (diffuse limit) 3231.7 3230.5 (sharp limit)	$2^2P_1-3^2D_2$ (2768) very broad $2^2P_1-3^2D_2$ (3519) narrow
	$2^2P_2-3^2D_2$ (3539) narrow $2^2P_2-4^2D_3$ (2918) narrow
3226.1? (diffuse) 3221.3 (sharp)	Unclassified lines
3127? (diffuse) 3098? (diffuse)	3382.9? 3280.9 3323.7 3279.7? 3311.4 3270.5
2822.4? (diffuse) 2819.3? (diffuse)	3309.2 3263.9
2510? (a broad band which merges with the mercury band at 2536)	3300.1 3252.0? 3298.4 3205.9? 3292.3 3193.8? 3290.0

The band from 3230.5 to 3235 has a very narrow region at 3231.7 where the absorption is not as strong as in the rest of the band. From the appearance of the plate it seems probable that there are in reality two superimposed bands in this region.

At 700° a faint band appeared, extending from the short wave-length side of the atomic thallium absorption line 2380 to about 2375. As the temperature was raised this band rapidly became stronger and extended toward the long wave-lengths. At 800° it had attained a width of about 20A. It was sharp on the side of shorter wave-lengths and shaded towards longer wave-lengths. A similar effect was noted in the case of the line 3776 except that the band first appeared on the long wave-length side of the atomic line. Still greater broadening was observed at 2768, this band attaining a width of 40A at 900°C. No information is available as to the broadening of the lines 2580 and 2316 as they were masked by mercury absorption.

The visible spectrum was now examined for absorption, the only result being the observation of the thallium line $2^2P_1-1^2S_1$ (5350A) (Plate II-a). This line appeared at about 800°, and broadened more toward the long wave-lengths than toward the short in the same manner as the lines previously discussed. The fact that the line did not appear at a lower temperature is to be expected since 2^2P_2 is about 0.9 volts above the normal orbit of thallium 2^2P_1.

The question of the broadening of the atomic lines seems most worthy of discussion, but in this paper it will only be treated briefly since the available data are not sufficient to give a definite explanation of the phenomenon. It seems fairly certain that thallium-mercury molecules of some sort exist and that the absorption bands previously mentioned, that do not coincide with atomic lines, are the result of absorption by these molecules.

In the case of the broadening of the atomic lines, two explanations present themselves. The first is that the apparent broadening is really a superimposed molecular band, the molecule having a weak bond so that the band is not much displaced from the position of the atomic line. The fact that no fine structure appears is not surprising since both mercury and thallium atoms have very large mass.

The chief objection to the explanation is that Frayne and Smith[4] and others have observed with pure thallium a similar broadening of the atomic lines which originate on the 2^2P_1 orbit. All the lines observed in the present investigation, except $2^2P_2-1^2S_1$ (5350) originate on this level. Frayne and Smith heated thallium in a tube with open ends and could reach a temperature of 2000°C.

It has been suggested by Oldenberg[5] that, if an atom absorbs a light quantum at the instant in which it collides with another atom, it may be possible for the quantum energy and part of the kinetic energy of the colliding atoms to act together to excite the absorbing atom. This would mean that a light quantum of smaller energy than the excitation energy would be absorbed; that is, the atomic line would broaden toward longer wave-lengths as the temperature of the vapor is increased. If it is further postulated that a quantum of greater energy than the excitation energy can be absorbed at the instant of a collision, and the excess energy transferred to kinetic energy of the colliding atoms, a broadening towards the shorter wave-lengths will result. It follows that the short wave-length limit of the broadening should be independent of temperature and pressure, that the long wave-length limit should increase with increasing temperature, and that the intensity of the absorption should increase with the number of collisions, that is, with the pressure.

Under the conditions used in these experiments the pressure increases with the temperature. Hence, it should be expected that with increasing temperature (and pressure) the line would broaden steadily towards the long wave-lengths, but that on the short wave-length side the broadening would be constant, the intensity of the entire absorption increasing. This is just the effect which is actually observed.

In order to choose between the two alternatives, molecular band or collision broadening, additional data are needed. If the temperature should be increased at constant density, the absorption should get fainter if it is molecular in origin, since the molecules would dissociate more rapidly at a higher temperature, while, if the effect is due to collisions, the intensity should be proportional to the number of collisions, that is, to the square root of the absolute temperature. Photographs were actually taken under these conditions, but the temperature range at constant density was not sufficient to cause noticeable changes in the intensity of absorption.

[4] Frayne and Smith, Phys. Rev. **27**, p. 23 (1926).
[5] Oldenberg, Zeits. f. Physik **47**, p. 184 (Feb., 1928).

INDIUM-CADMIUM

In using a tube containing indium with cadmium present as an impurity a series of bands was observed (Plate II-b). It seems probable that these bands are due to indium-cadmium molecules. A few of the bands showed

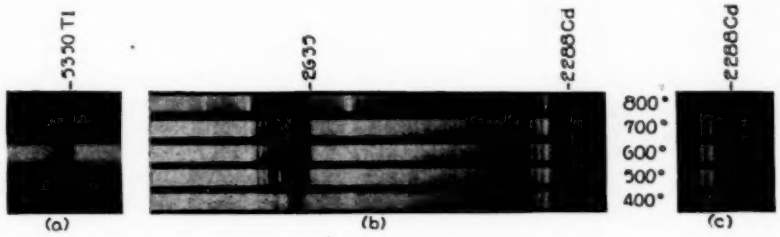

Plate II.

traces of their structure, but not clearly enough to enable measurements to be made. The bands were sharp at the short wave-length limit and shaded towards the visible. At temperatures above 400° the bands near the limit of the series merged so that the absorption appeared continuous. Table II gives the wave-lengths of the short wave-length limits of all the bands that could be measured at three different temperatures. It was impossible to

TABLE II. *Short wave-length limits of bands observed in mixture of indium and cadmium vapors.*

400°	500°	800°	800°
2652.8	[2640.1	[2634.6	2333.4
2661.4	{	{	2339.7
2672.1	{	{	2341.9
2684.2	[2685.8	[2690.6	2346.1
			2347.2
	2693.9	?	2352.9
			2353.4
2695.0	2694.6	[2694.2	
	2705.5	{	
2707.1	2711.6	[2712.4	
2718.1	2717.6	2717.0	
		2717.9	
	2728.2	2728.2	
2729.9	2729.8?	2729.8	
	2739.7?	2739.7	
	2741.1?	2741.1	
		2751.3	
	2752.8	2753.0	
		2776.3	
		2787.9	
		2800.2	

make very accurate measurements but the recorded values are correct to within a few tenths of an Angstrom. The approximate limits of the apparently continuous absorption are given in brackets. Another series of bands observed on the same plates (Plate II-b) is recorded in the last column in the table.

A band about 0.7A wide with both limits sharp appeared at 600°. It extended from 2333.6A to 2337.3A. A very faint diffuse band about one Angstrom wide appeared at 700°. The wave-length of the center of this band was about 2338.5A. With increasing temperature the intensity of both bands increased, but neither band broadened appreciably.

The cadmium line 2288 was absorbed and broadened symmetrically with increasing temperature (Plate II-b). The cadmium line 3261 also appeared at the higher temperatures, but was very faint. When a little mercury was added the line 2288 broadened more toward the long wave-lengths exactly as described by Wood and Guthrie (Plate II-c), while the line 3261 appeared stronger but did not broaden much. Further discussion of the results obtained with indium and cadmium will be postponed until more data are available.

I wish to take this opportunity of thanking Professor R. W. Wood for proposing this problem, and for offering many valuable suggestions while the work was in progress. I also wish to express my gratitude to Professor K. F. Herzfeld for the encouragement and valuable advice which he has given me.

THE JOHNS HOPKINS UNIVERSITY
May, 1928.

POLARIZATION OF RESONANCE RADIATION IN MERCURY[1]

By Harry F. Olson

Abstract

$1^1S_0-2^3P_1$ of mercury excited by plane polarized light shows incomplete polarization both in the absence and in the presence of a weak field parallel to the electric vector. The amount of initial polarization depends upon the relative intensities of the hyperfine structure lines in the exciting light. The polarization with various relative orientations of field and light vector and the variation of polarization with field intensity in weak fields may be interpreted successfully by means of a semi-classical model, with proper relative intensities parallel and prependicular to the light vector, rotating after excitation with an angular velocity $geH/2mc$ and emitting a damped wave. From curves connecting depolarization, rotation of maximum of polarization, etc., with field intensity α, the damping constant, has been found to be 1.02 ($\pm$0.02) 10^7 sec^{-1}.

IT has been found, in agreement with recent results of von Keussler,[2] that the behavior of the polarization of mercury resonance radiation in weak magnetic fields may be completely accounted for by a simple resonator rotating with the angular velocity of the Larmor precession and emitting a damped wave. The simple isotropic oscillator however is not an adequate model; it is necessary to assume that excitation of the oscillator by plane polarized light gives rise to a certain amount of radiation in the plane perpendicular to the electric vector of the exciting light. Since the $1^1S_0-2^3P_1$ line shows a 3/2 normal Zeeman pattern it might be expected that the isotropic oscillator would suffice as a model. That it does not is due to the peculiar behavior of the outer two hyperfine structure lines as shown by Ellett[3] and McNair. The three remaining hyperfine structure lines behave in accordance with the predictions of the theory of the anomalous Zeeman effect for a $1^1S_0-2^3P_1$ line.

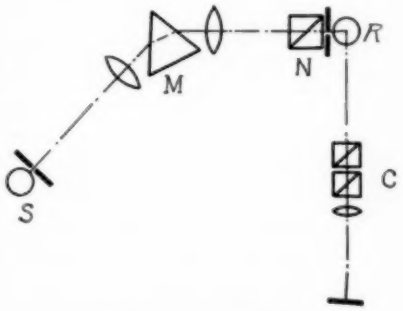

Fig. 1. Arrangement of apparatus.

The behavior of the isotropic oscillator as a model for the phenomena in question has been discussed by Eldridge[4] and Breit.[5] The introduction of the non-isotropic oscillator involves no more than a slight alteration of the constants

[1] Read at the Chicago Meeting of the American Physical Society, November 26, 1926. Publication has been withheld to check the discrepancy with von Keussler's results for the mean life of the excited atom.

[2] von Keussler, Phys. Zeits. **27**, p. 313 (1926).

[3] Ellett and McNair, Phys. Rev. **31**, p. 180 (1928).

[4] Eldridge, Phys. Rev. **24**, p. 234 (1924).

[5] Breit, Jour. of Opt. Soc. **10**, p. 439 (1925).

of their equations for the case discussed by them, and their analysis of course leads at once to the equations for other relative orientations of light vector, magnetic field and direction of observation.

The arrangement of apparatus is shown in Fig. 1 where S is a water-cooled quartz mercury arc, M a monochromator, N a nicol prism for polarizing the exciting light in any azimuth, C two Wollaston prisms and a camera with a quartz lens. The familiar Cornu method of determining polarization was used. This involves no assumption as to the density-exposure relations save that two adjacent areas exposed simultaneously to the same intensity for the same length of time will show equal blackening. Densities were measured on a microphotometer and from a series of exposures at intervals of 30′ for the relative setting of the two Wollaston prisms the positions of exact equality could be obtained quite accurately.

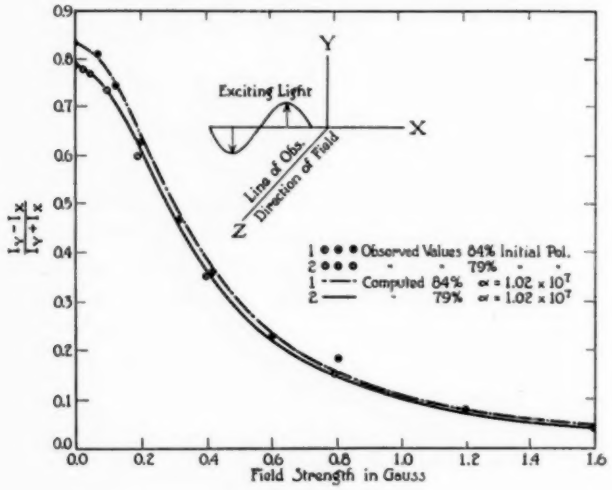

Fig. 2.

The results and their comparison with the curves calculated for the model discussed above are best presented graphically. Fig. 2 is for the case discussed by Eldridge[4] and by Breit[5] and examined experimentally by Wood[6] and Ellett and by von Keussler.[2] Curve 2 was taken with the arc operating on 3.5 amperes which gave an initial polarization of 79 percent. Curve 1 was taken with another arc operating on 1 ampere. This source gave an initial polarization of 84 percent. Operating this latter arc on 0.4 amperes approximately 86 percent initial polarization was obtained. The intensity under these circumstances is very feeble and not suitable for making the large number of observations required for a curve.

The different initial polarizations apparently are due to a change in the relative intensity of the hyperfine structure lines of the exciting light. As Ellett[3] and McNair have shown the incomplete polarization of λ2537 in the absence of an external field is due to the behavior of the outer two hyper-

[6] Wood and Ellett, Phys. Rev. **24**, p. 342 (1924).

fine structure lines. A change in the intensity of these lines relative to the other three will obviously alter the initial polarization.

The same value of the damping constant α is obtained for both types of excitation. This shows either that the three central components suffer the same change in intensity with the two types of excitation or that the mean lives[7] of the three components are the same.

The curve in Fig. 3 is for the relative orientations of light vector, magnetic field and direction of observation represented in the same figure. The rela-

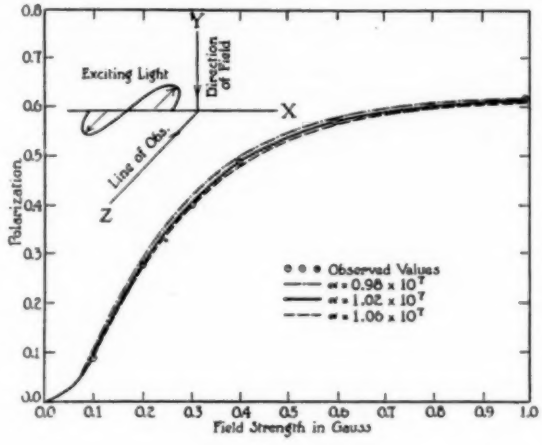

Fig. 3.

tion between polarization and intensity of magnetic field is given by the equation.

$$P=\frac{15}{23+2(2\alpha mc/geH)^2}$$

where α is the damping constant or reciprocal of the mean life of the excited atom. The three curves of Fig. 3 are drawn for values of α of 0.98, 1.02, 1.06×10^7 sec.$^{-1}$ respectively, and it is evident that its value is very nearly 1.02×10^7 sec.$^{-1}$, as given by Wien[8] from canal-ray experiments but differing somewhat from that of von Keussler[2] who obtained 0.88×10^7 sec.$^{-1}$ from his curve similar to Fig. 2 above.

The reason for the discrepancy between the writers observations and those of von Keussler is not evident. There are three possibilities, (a) error in measurement of polarization, (b) error in measurement of magnetic fields, (c) a real difference whose explanation might be sought in different relative intensities of the hyperfine structure components. Referring to (a) it might be said that von Keussler used a photoelectric method of measuring polarization and the writer the Cornu method mentioned above. There seems no

[7] Observations made in this laboratory using a Lummer-Gehrcke plate indicate that the mean life for these components is the same.

[8] Wien, Ann. d. Physik **73**, p. 483 (1924).

possibility of a systematic error in either method of the magnitude required to account for the difference. In fact under similar circumstances of excitation the same initial values of polarization are observed.

The possibility of error in the value of the magnetic field was eliminated by using two sets of Helmholtz coils. Results obtained with the two were in complete agreement. The ammeters used in measuring the current were checked against standard instruments.

There remains the third possibility. This would require that the values of $geH\tau/2mc$ should not be the same for the three central hyperfine structure components, so that different relative intensities of these components might give rise to different "average" values of τ. As stated in note 7 this seems improbable.

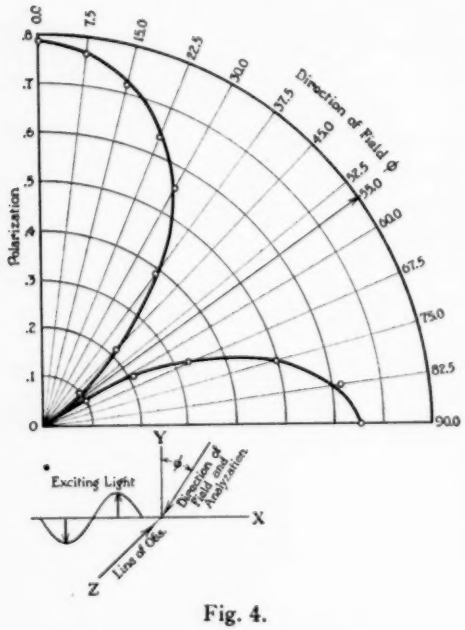

Fig. 4.

It might be pointed out that the displacement of the curve in Fig. 3 for a small change in α is greater than that of Fig. 2, in the range of polarization from 25 to 55 percent where the measurements of polarization are the most accurate.

The curve in Fig. 4 represents the variation of polarization for the various orientations of a fairly intense field (100–200 gauss). Here again the observed values are seen to lie quite well on the curve given by the equation and the angle of zero polarization[9] is 55 within a rather small experimental error.

$$P=\frac{7.5\cos^2\phi-3.75\sin^2\phi}{9.5\cos^2\phi+5.75\sin^2\phi}$$

In conclusion the author wishes to express his thanks to Professor A. Ellett for his advice during the progress of the work.

HALL OF PHYSICS,
UNIVERSITY OF IOWA,
April 21, 1928.

[9] Van Vleck, Proc. Nat. Acad. Sci. 11 p. 612 (1925). Also Eldridge, reference 4.

COMPARISON OF MEASUREMENTS OF CRITICAL POTENTIALS OF MERCURY VAPOR

By J. C. Morris, Jr.

Abstract

The critical potentials of Hg vapor were examined with a tube constructed to permit use of a number of different methods. For detecting critical potentials other than those of ionization, the *Hertz method* proved much the most satisfactory. Of the 13 critical potentials found below ionization, 10 have definite spectroscopic interpretation and the remaining 3, which are probably due to mercury molecules, confirm similar values reported by Miss Messenger. The *partial current method* of Franck and Hertz showed less resolving power, but otherwise gave good agreement with the Hertz method. The *Franck and Einsporn method* gave peculiar results, suggesting that it detected only photoelectric effects and not metastable atoms, and that the failure to show the other critical potentials was due to features of tube design which eliminated inelastic impacts in the region around the filament where space charge acts to limit emission.

Compton's method for studying ionization proved very satisfactory since no effects of other types of inelastic impacts were detected. Three *ultra-ionizing potentials* at 10.65, 11.34, 11.78 were found in good agreement with Lawrence, although the present results do not show the regions of maximum ionization probability near these values, as reported by him. An attempt to test the molecular origin of these high ionizing potentials led to negative results.

Introduction

IN THE study of the various energy states to which a neutral atom or molecule may be raised by supplying energy by an electron impact, a number of basically different methods have been developed for the detection, measurement, and classification of these energy levels. Results with various gases and vapors have indicated that the most suitable method varies with the gas or vapor employed. The apparatus described in this paper was designed to be used according to a number of the previously employed methods, and by simple changes in the connections the method could be changed. A comparison of the results obtained using the different methods should show that the observed values of critical potentials are compatible and should indicate which is the most suitable for measuring critical potentials of any particular type.

Measurement of the radiating potentials can be made according to the partial current method of inelastic impacts as employed by Franck and Hertz,[1] the modified Lenard method as employed by Franck and Einsporn,[2] and the Hertz,[3] method for inelastic impacts. Ionizing and non-ionizing potentials can be distinguished in the manner employed by Davis and

[1] Franck and Hertz, Phys. Zeits. **17**, p. 409 (1916).
[2] Franck and Einsporn, Zeits. f. Physik **2**, p. 18 (1920).
[3] Hertz, Zeits. f. Physik **18**, p. 307 (1923).

Goucher[4] or by a modification of the method employed by Compton.[5] Ionization and ultra-ionization potentials can be measured by the detection of positive ions in a chamber similar to that employed by Mackay.[6] This report deals with the results obtained with mercury vapor.

Apparatus

The construction of the tube is shown in Figure 1. Electrons from the filament F are accelerated to H by a variable, measured, electromotive force. Some of these electrons passing through the gauze G_1 enter the field free space S where a number of them will collide with the atoms or molecules present. The sides of the cylindrical electrode H about S are made of gauze as are the coaxial grids G_2 and G_3. The plate P is cylindrical, coaxial with the grids

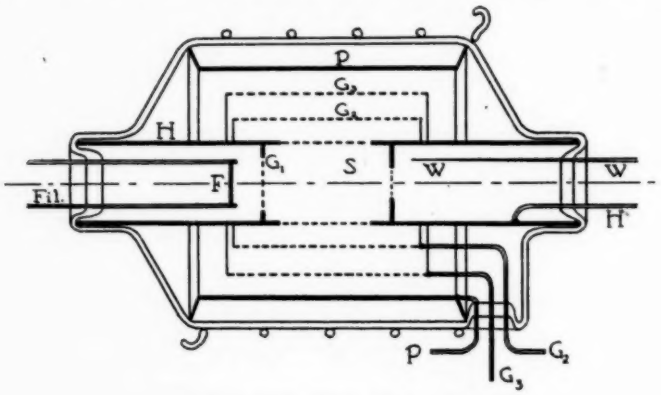

Fig. 1. Construction of the tube.

and mounted at some distance from the sides of the containing glass vessel. In the final form of the tube all metal parts mentioned thus far except the filament are of nickel. In an early experimental tube an aluminum plate was used. Filaments of molybdenum and of tungsten were used at first but later a Wehnelt cathode was employed with greatly improved results. The electrode W is a thin platinum wire mounted in H as shown and removed as far as possible from any direct radiation from S. The purpose of the coil of a few turns of heavy wire wound around the tube will be explained later. The usual precautions of "baking-out" and degassing the metal parts were observed.

The accelerating potential was varied uninterruptedly by steps (0.02 to 0.1 volt) and measured by a voltmeter checked against a potentiometer. In all cases the electron emission from the filament was measured and the observed effect divided by the emission thereby giving readings proportional to the effect of a constant electron stream. The effects produced by the electron bombardment—photoelectric, production of positive ions, etc.—were measured electrically by high sensitivity electrometers or galvanometers.

[4] Davis and Goucher, Phys. Rev. **10**, p. 101 (1917).
[5] Compton, Phil. Mag. **40**, p. 553 (1920).
[6] Mackay, Phil. Mag. **46**, p. 828 (1923).

With most of the readings a null method was employed whereby the electrometer or galvanometer was returned to zero by a counter electromotive force applied by a Leeds and Northrup potentiometer. The readings of the potentiometer are in these cases proportional to the currents being measured. In all cases where scale readings were employed the instrument was calibrated.

Franck and Hertz Method

With the tube connected as shown in Figure 2 it may be used to measure critical potentials by the partial current method of inelastic impact as in the work of Franck and Hertz.[1] The accelerating potential was varied in steps of 0.1 volt while the retarding potential was kept fixed at a value of 0.5 volt which was found to be best after trying values from 0.1 to 1 volt.

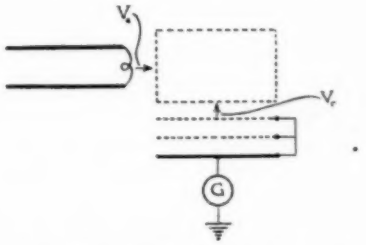

Fig. 2. Connections to give critical potentials by the method of Franck and Hertz.

Mercury vapor was used at pressures corresponding to temperatures from 150°C to room temperature, best results being obtained at the latter temperature. Figure 3 shows the curve obtained and the expected values of critical potentials. The method of determining the correction to be applied to the accelerating potential was as follows. A search was made in the neighborhood of 5 volts for indications of two critical potentials differing from each other by 0.2 volt corresponding to the known critical potentials at 4.7 and 4.9 volts. These were found and the accelerating potential scale was shifted to bring these peaks to the correct value, requiring a shift of about 0.6 volt. The success in accounting for the observed peaks when so corrected justifies the method.

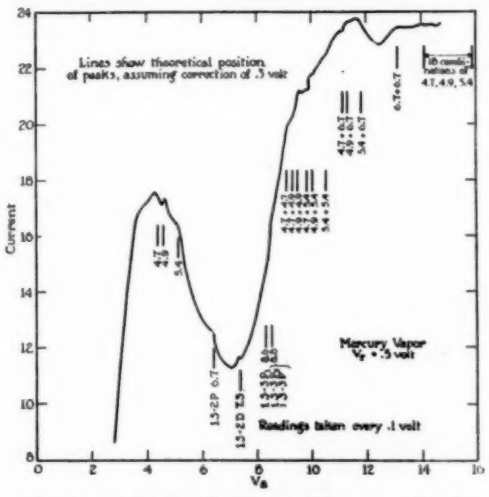
Lines show theoretical position of peaks, assuming correction of .5 volt
Mercury Vapor
Readings taken every .1 volt
Current
V_a

Fig. 3. Critical potentials of Hg vapor by the method of Franck and Hertz.

While the peaks and bulges observed are in general accounted for it is obvious that this method is hardly suited to serve for accurately locating the critical potentials, especially above eight volts, where the effects of superposition render any separation impossible.

Franck and Einsporn Method

Using similar connections but employing a retarding potential of twenty volts or more the tube was prepared to detect critical potentials according to the method of Franck and Einsporn.[2]

The impact of electrons with atoms in S may: (1) Produce positive ions by ionization of the atom; (2) Excite the atom, *i.e.*, leave the atom in a state of abnormally large energy. Some of these states may be metastable and persist for a finite time; others will be such that the atom spontaneously returns to its normal state with the emission of radiation of frequency ν given by the equation $eV = h\nu$.

The production of radiation, metastable atoms, or positive ions in the space S may be detected with this apparatus. The metastable atoms will in part drift by diffusion and reach the plate where at least a certain proportion will by a mechanism not clearly understood cause the ejection of an electron. Radiation will if of sufficiently high frequency cause photo-electric emission from the plate. Positive ions having diffused through the gauze sides of S will be drawn to P by the applied field V_R. Any one of these effects will produce an electron current from the plate, but will give no clue to the particular cause. As described later the minimum ionizing potential may be determined by independent means, leaving the effects produced by electrons having less than ionizing energy to be explained as being due to either metastable atoms or radiation. Messenger[7] has devised a method for separating these two effects.

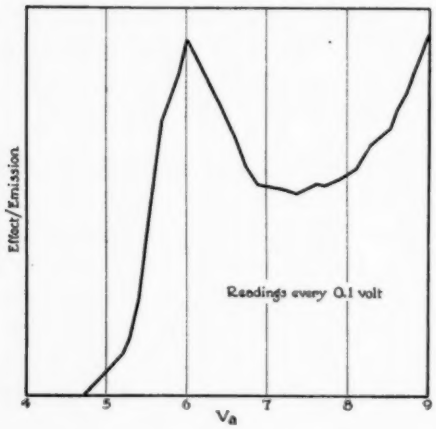

Fig. 4. Critical potentials of Hg vapor by the method of Franck and Einsporn.

The curves obtained were all rather erratic, but all of the general type shown in Figure 4, not showing the numerous breaks expected between 4.7 and 10.4 volts.

Although it was impossible to reproduce these curves with any degree of exactness even for successive runs, the general shape of the curves was preserved, the peak always being present more or less strongly, but at no time was it possible to detect any structure to the curve even when a Wehnelt cathode burned at very low temperatures was employed. The height of the peak varied very much from run to run—at times being five times as high as the subsequent part of the curve, at other times it was represented by only a flattening of the curve.

The function of the coil about the tube is as follows. When connected to a source of high frequency current such as is employed with an induction furnace, it heats the Plate P to a red heat. Such treatment seems to increase the photoelectric sensitivity of the plate, probably by a purely cleaning action. This treatment did not affect the shape of the curves subsequently obtained except perhaps to accentuate the peak a trifle.

[7] Helen A. Messenger, Phys. Rev. **28**, p. 962 (1926).

Changes of pressure of the mercury vapor from that corresponding to 150°C to room temperature did not affect the shape of the curves, but conditions were more steady at room temperature.

A comparison of the general shape of these curves and those of the intensity of the 2537 line plotted against the energy of the exciting electron, as given by White[8] and Crozier,[9] shows a striking similarity, sufficient to warrant the hypothesis that the curves here obtained indicate only the photoelectric effects with little or no contribution due to metastable atoms. If one regards the curves here obtained in this light, they may be thought of as representing jointly the effects of the 2537 line as indicated in the work of White[8] and Crozier[9] and that of the 1849 which, while coming in at 6.7 volts, is not intense until about 7.5 or 8 volts. This last fact was shown by the work of Messenger[7] by removing the effects of metastable atoms from the observations. This was done by shielding the plate with quartz filters which, while transparent to radiation, prevented the diffusion of metastable atoms to the plate.

Why the effect of metastable atoms should have been absent in the present experiments is not clear. The only significant difference in design of the tube used and those tubes in which the effects of metastable atoms have been observed is that the detecting plate is here parallel to the direction of the bombarding stream of electrons while in the other cases the plate was perpendicular to the electron stream. However, there seems to be no reason why the uncharged, metastable atoms should have any greater tendency to diffuse in one direction rather than in another.

Considering the possibility that the present unexpected results were due to the fact that the apparatus was unusually sensitive to photoelectric action and that the effect of the metastable atoms was being relatively masked, it was decided to make a run when the photoelectric sensitivity was unusually low. By avoiding the conditions for optimum photoelectric sensitivity (especially clean, degassed surfaces, etc.) the effect on the detecting system was reduced to 1/60 of its previous value, but a run made under these conditions showed no difference from other runs. However, this negative result is not very significant for with no definite knowledge of the mechanism whereby metastable atoms cause the ejection of electrons from a plate with which they come in contact, it is quite possible that this phenomenon may be in part photoelectric and that any reduction of the photoelectric sensitivity of the detecting plate would reduce the effects due to radiation or metastable atoms by the same factor.

Various detecting systems consisting of plate, one or two of the grids, and plate and grids together were tried all giving the same results. This precludes the possibility that the metastable atoms had been filtered out by the grids.

[8] D. R. White, Phys. Rev. **28,** p. 1123 (1926).

[9] Wm. D. Crozier, Paper No. 20 Presented at the meeting of the American Physical Society, Chicago, Ill., November, 1927. The writer is indebted to Mr. Crozier for a copy of his results.

In discussing these results Professor Franck has pointed out that in the original experiments by Franck and Einsporn it was possible to note the critical potentials as breaks in a curve showing the primary electron emission plotted against accelerating potentials. This was also observed in the work of Messenger but was not observed in the present experiments, although looked for. The explanation of this difference probably lies in the fact that the filament was so close to the accelerating gauze that at the pressure of mercury vapor employed the probability of a collision between an electron and mercury atom in this space was very low, so that there was no variation in the limiting effect of space charge due to inelastic impacts of electrons in this region.

The correction to be applied to the accelerating potential scale was determined by measuring the minimum ionizing potential (the value of which is known from spectroscopic data to be 10.4 volts) by the method to be described later and applying the correction to the accelerating potential scale required to bring the observed value to 10.4 volts. The correction necessary was of the order of 0.6 volt and checked the corrections made in the manner described under the Franck and Hertz method.

Hertz Method

Using again a small retarding potential of 0.1 volt and arranging switches so that this could be made 0 or 0.1 volt at will, and plotting the difference of the galvanometer readings for these two cases as ordinate against the accelerating potential as abscissa, the tube was used according to the Hertz[3]

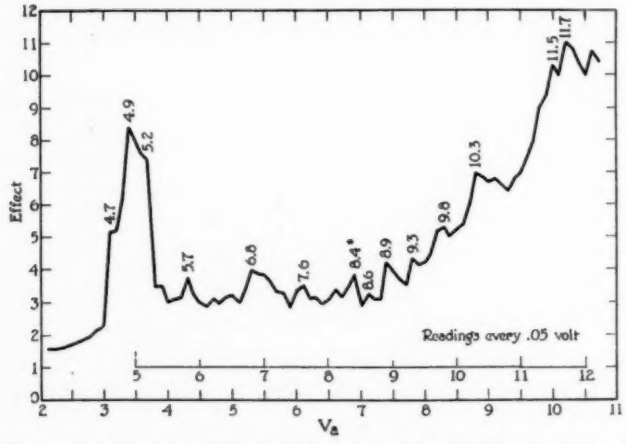

Fig. 5. Critical potentials of Hg vapor by the Hertz method.

method for determining the critical potentials of inelastic impacts. This was by far the most efficient method of all used for determining critical potentials below ionization. Figure 5 shows a set of the results obtained with this method and gives the values of the more prominent potentials noted. The accompanying table shows the interpretation placed on the various potentials. The curves obtained with this method could be reproduced without difficulty.

The curves were taken at various temperatures from 100°C to room temperature, best results being obtained at the latter temperature. The correction to be applied to the accelerating potential scale was determined in the manner described under the Franck and Hertz method.

Distinguishing Ionizing from Non-Ionizing Potentials

For the purpose of distinguishing radiating from ionizing potentials either the Davis and Goucher method or a modification of the Compton may be used. The latter method as employed in these experiments consists in using as collector alternately the large photoelectrically sensitive plate P and the small platinum wire W (shielded from radiation from S) as the collecting electrode. In the first case the ratio of the intensity of the effects produced by radiation to those produced by ionization would be relatively high compared to the same ratio when using the wire collector. In fact with Hg vapor no effect was obtained using the small wire collector below 10.4 volts showing that no critical potentials below that value could be termed ionizing potentials.

Table I. *Results obtained using Hertz method.*

Pot. observed (volts)	Interpreted from Theory	Calculated from Theory	Remarks
4.7	$1^1S-2^3P_0$	4.66	Metastable state
4.9	$1^1S-2^3P_1$	4.86	2537
5.2			5.25 obs. by Messenger
5.4	$1^1S-2^3P_2$	5.43	Metastable state
5.7	2^3P_0	5.73	Ionization of metastable excited atom
6.8	1^1S-2^1P	6.67	
7.6	1^1S-2^3S	7.69	
8.1			8.0 and 8.05 obs. by Messenger
8.4			8.35 obs. by F. & E.
			8.3 obs. by Messenger
8.6	$1^1S-3^3P_{0,1}$	8.58	
8.9	1^1S-3^1P	8.79	
	$1^1S-3^3D_{1,2,3}$	8.82	
	1^1S-3D	8.80	
	$1^1S-3^3P_2$	8.80	
9.3	$2(1^1S-2^3P_0)$	9.32	Successive impact
9.8	$2(1^1S-2^3P_1)$	9.8	Successive impact
10.3	1^1S	10.39	Ionization
	6.7+4.9		
11.5	6.7+4.7		

As both these methods are purely qualitative no curves are here given.

Ionizing Potentials

The minimum ionizing potential can be roughly determined by observing the upward break in the plate current-plate potential curve, caused by the partial neutralization of space-charge by positive ions. This method is suitable for only the roughest of determinations even when the curves are plotted in the manner suggested by Langmuir,[10] and employed by Found[11]

[10] Langmuir, Phys. Rev. **2**, p. 457 (1913).

[11] Found, Phys. Rev. **16**, p. 41 (1920).

Using this method the ionizing potential of mercury could be shown to be in the neighborhood of 10.5 volts.

The most interesting phase of this experiment was the determination of the ionizing and ultra-ionizing potentials of mercury vapor by the more accurate method suggested in the preceding section.

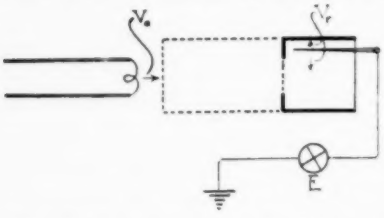

Fig. 6. Connections for obtaining the ionizing and ultra-ionizing potentials in Hg vapor.

Figure 6 shows the connections employed. It is to be noted that an electron current from the wire W might be due to photoelectric emission from the wire due to radiation, metastable atoms diffusing to the wire, or positive ions drawn to the wire by the applied retarding field. But as the wire is of platinum, is of small area, and is shielded from direct radiation the first two of the causes indicated above will have little or no opportunity to contribute to the electron current from the wire. This is born out by experiment, and the curves obtained represent ionization currents only.

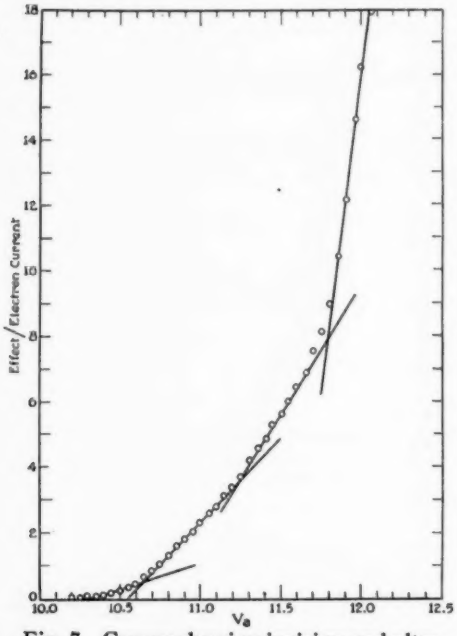

Fig. 7. Curves showing ionizing and ultra-ionizing potentials in Hg vapor.

When first tried using a molybdenum filament, the curve obtained was fairly smooth and showed only an uncertain suggestion of breaks above the minimum ionizing potential as had been reported by Lawrence.[12] In a further effort to locate these breaks a Wehnelt filament so nicked as to be an almost equipotential source was employed and burned at such a temperature that only the slightest redness was observable. Taking these precautions to reduce the velocity distributions of the bombarding electron stream, the curve shown in Figure 7 was obtained showing critical potentials above the minimum ionizing potential. The values of these critical potentials check closely those obtained by Lawrence. Unlike the curves obtained by him the probability of ionization appears from these curves to be proportional to the excess of energy of the electron over the amount required to produce this state. The constant of proportionality is measured by the slope of the curve. The relative value of the constant of proportionality after each break is as follows:

[12] Lawrence, Phys. Rev. **28**, p. 945 (1926); Lawrence, Jour. of the Franklin Institute. p. 91 (July 1927).

Critical Potential	10.4	10.65	11.34	11.78
Constant of Proportionality	0.36	1.03	1.54	8.00

The constant of proportionality for each type of ionization as measured by the difference of slope before and after each break are to each other as follows:

Critical Potential	10.4	10.65	11.34	11.78
Constant of Proportionality	.36	.67	.51	6.5

The curves showing this linear relationship between excess electron energy and number of positive ions formed extend over a range of only a few volts and hence this conclusion is in no wise at variance with the fact that the probability of ionization reaches a maximum at about 125 volts as shown in the work of Compton and Van Voorhis.[13]

Considering the possibility that these ultra ionizing potentials were of a molecular origin, the experiment was tried in superheated vapor at higher temperatures. Since the energy of dissociation of a mercury molecule is but slightly larger than the mean kinetic energy of a molecule at room temperature, a slight increase in temperature should greatly decrease the relative concentration of molecules to atoms, and curves taken at elevated temperatures should show critical potentials of molceular origin less prominently. No such effect was noted in the case of these ultra ionizing potentials.

The results obtained employing the various methods as has been described, are all compatible with each other and the results given for each method indicate its value for determining the critical potential of any type.

The writer wishes to acknowledge his indebtedness to the members of the Physics Department, especially to Professor K. T. Compton who suggested the problem and under whose guidance the work was carried out. He is also indebted to Professor Webb and Miss Messenger of Columbia University, for opportunity to discuss with them some of the problems which have arisen during the course of the work.

PALMER PHYSICAL LABORATORY,
PRINCETON, N. J.
June 2, 1928.

[13] K. T. Compton and C. C. Van Voorhis, Phys. Rev. **26**, p. 436 (1925).

IONIZING POTENTIALS OF METHANE, ETHANE, ETHYLENE, AND ACETYLENE

By J. C. Morris, Jr.

Abstract

After preparation and purification by the most approved methods, the gases *methane*, *ethane*, *ethylene* and *acetylene* were introduced into an ionization tube of the Mackay type and their ionization potentials measured. The calibration of the apparatus was made with the aid of Hg vapor and He gas as standards. The values found are: methane 14.4 volts, ethane 12.8 volts, ethylene 12.2 volts, acetylene 12.3 volts, and are believed to be correct within 0.2 volt.

THE method devised by Mackay[1] to measure ionizing potentials, having been found satisfactory for use with polyatomic gases, was employed with methane, ethane, acetylene, and ethylene.

The tube used was similar in all respects to the one used by Mackay except that it was slightly larger, giving a larger electron emission and hence larger positive ion currents. For description of the apparatus and method of taking measurements the reader is referred to the papers of Mackay mentioned above. Mercury vapor and helium were used as standards for calibration purposes, the ionizing potential of mercury being taken to be 10.4 volts and that of helium as 24.5 volt.

The gases employed were prepared as follows:

Methane: Methane was prepared by heating a mixture of sodium acetate and soda lime. The gas evolved was passed through concentrated caustic potash solution and then through concentrated sulfuric acid. The gas was then liquefied and allowed to evaporate, the middle third being kept for the purposes of the experiment.

Ethane: The gas was prepared by the action of the zinc-copper couple on ethyl iodide. The gas evolved was passed through alcohol and then through concentrated sulfuric acid. The gas was then liquefied with liquid air and allowed to evaporate, the middle third being kept for the purposes of the experiment.

Ethylene: The gas was generated by the reaction of ethyl alcohol with concentrated sulfuric acid. The gas evolved was passed through concentrated caustic soda solution to remove CO_2 and SO_2 and then through concentrated sulfuric acid. The gas was then liquefied with liquid air and allowed to evaporate, the middle third being kept for the purposes of the experiment.

A tank of the best commercial ethylene being available, some of this gas was purified in the manner described above and used in some of the measurements. No difference could be detected in the ionizing potential of this gas and the gas prepared.

[1] Mackay, Phil. Mag. **46**, p. 828 (1923); Phys. Rev. **24**, p. 319 (1924).

Acetylene: Acetylene from a commercial tank was purified by passing through water, silver nitrate solution, caustic soda solution, and concentrated sulfuric acid. The gas was then solidified and allowed to sublime the middle third being kept for the purposes of the experiment.

A number of measurements were taken with each gas and the values obtained averaged after correcting for initial velocity and contact difference of potentials by comparison with helium and mercury vapor as standards.

The values obtained are given in Table I.

TABLE I. *Ionization potentials of methane, ethane, ethylene and acetylene.*

Gas	Ioniz. Pot. observed (volts)	Previously reported values (volts)	Observer
Methane	14.4	9.5	Hughes & Dixon[2]*
		13.5	Mayer[3]*
		12.5	Pietsch[4]
		13.9	Hughes & Klein[5]
		14.4–15.2	Glockler[6]
		14.58	Pietsch & Wilcke[7]
Ethane	12.8	10.	Hughes & Dixon[2]*
Ethylene	12.2	9.85	" " "
Acetylene	12.3	9.95	" " "

* These investigations were made prior to knowledge of the distinction between ionizing and radiating critical potentials.

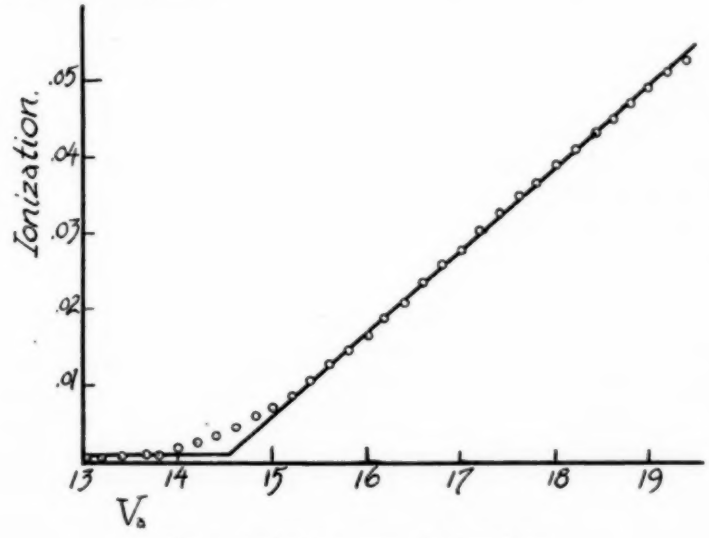

Fig. 1. Ionization curve for methane.

The curves shown are typical examples of the curves obtained with this method. The method employed has the disadvantage that there is a con-

[2] Hughes and Dixon, Phys. Rev., **10,** p. 495, 1917.
[3] F. Mayer, Ann. d. Phys. (4) **45,** p. 1, 1914.
[4] E. Pietsch, Dissert. Berlin 1926, S34.
[5] Hughes and Klein, Phys. Rev., **23,** p. 450, 1924.
[6] Glockler, Journ. Amer. Chem. Soc., **48,** p. 2021, 1926.
[7] Pietsch and Wilcke, Zeits. f. Phys. **43,** p. 342, 1927.

siderable velocity distribution among the electrons of the bombarding stream and some critical potentials may not have been detected. It is believed that these values are the principal ionizing potential to within 0.2 volt.

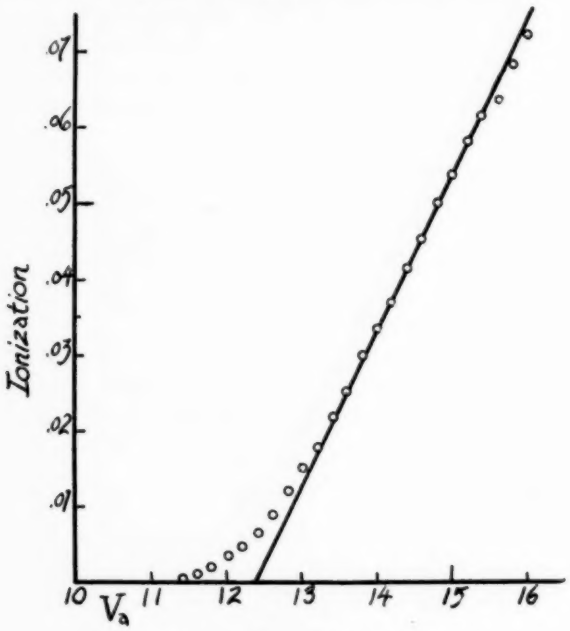

Fig. 2. Ionization curve for acetylene.

The writer wishes to express his appreciation to Dr. C. A. Mackay under whom this work was begun and to Professor K. T. Compton for assistance during the course of these measurements.

PALMER PHYSICAL LABORATORY,
PRINCETON, N. J.
June 2, 1928.

ABSORPTION COEFFICIENT OF SLOW ELECTRONS IN MERCURY VAPOR

By T. J. Jones*

Abstract

Absorption coefficient of Hg vapor for electrons with energies from 0.5 volts to 400 volts.—An account is given of measurements by two different methods of the absorption coefficient α in mercury vapor for electrons with energies of 0.5 volts up to 400 volts. The experiments described in the first part of the paper were made by Ramsauer's method, in which a homogeneous electron beam is obtained by bending the electrons through a series of slits suitably arranged in a magnetic field. The second part of the paper deals with experiments made by an arrangement which gave a fairly homogeneous beam of electrons without the use of a magnetic field. In each method the fraction of the initial electrons which traversed a given distance through the vapor without suffering collision was measured, and this enabled α to be calculated. The results obtained by the two different methods were found to be in fair quantitative agreement. The absorption coefficient increased continually as the energy of the electrons was reduced down to 0.5 volts. No evidence was obtained of the sharp decrease in α for electrons slower than 3 volts as reported by Beuthe. The results when compared with those obtained by former workers were found to be in fairly good agreement with those of Maxwell over the whole range of electron energies and with those of Brode at the lower energies.

WHEN a beam of electrons is projected into a monatomic vapor or gas, some of the electrons are removed by the gas atoms and so disappear from the original beam. This removal is effected by the scattering of the electrons and also by the formation of negative ions.

The effective area of an atom which is instrumental in removing an approaching electron from the beam can be calculated from the kinetic theory formula

$$N = N_0 e^{-\alpha x p} \tag{1}$$

where N_0 is the number of electrons initially present in the beam, N is the number remaining after traversing a distance x in the gas, p is the pressure of the gas (in mm) and α is the effective area, or absorption coefficient, of all the atoms in 1 cc at 1 mm pressure and 0°C. On dividing α by 3.6×10^{16} the mean effective area of a single atom is obtained. The reciprocal of the absorption coefficient α is the electronic mean free path at unit pressure and 0°C.

Absorption coefficients for slow electrons in mercury vapor have been measured by R. B. Brode,[1] L. R. Maxwell[2] and H. Beuthe.[3] Brode and Maxwell found that α increased rapidly as the velocity of the electrons was

* Commonwealth Fellow.

[1] R. B. Brode, Proc. Roy. Soc. **109A**, p. 937 (1925).

[2] L. R. Maxwell, Proc. Nat. Acad. Sci. **12**, p. 509 (1926).

[3] H. Beuthe, Ann. d. Physik **84**, p. 949 (1928).

diminished, down to velocities as low as 0.5 volt. Their results agree fairly well in the low velocity regions but for the higher velocities Brode's values of α are much smaller than those of Maxwell. Beuthe studied by the Ramsauer method the behavior of the absorption for electrons with velocities less than 7 volts, and found that as the velocity decreased, α increased to a maximum at about 3 volts and then diminished rapidly until at 1 volt it was 1/6 of its maximum value. Mercury in this connection behaved like the rare gases.[4] R. Minkowski,[5] also, has obtained evidence of a maximum absorption for very slow electrons in mercury vapor.

The present investigation was made in order to obtain further information on the behavior of the absorption coefficient for the faster electrons (this being necessary because of the considerable disagreement in the values obtained by Brode and by Maxwell at the higher velocities) and also to confirm if possible Beuthe's discovery of the Ramsauer effect in mercury vapor. The general procedure in determining α was to accelerate a beam of electrons from a thermionic source into a region where they collided with atoms of mercury vapor. For each value of the accelerating voltage and for different vapor pressures, the fraction of electrons which traversed a given distance in the gas without being removed from the beam was measured. These data were sufficient to enable α to be calculated from Eq. (1). Two entirely different experimental arrangement were employed in the work and this paper is accordingly divided into two parts.

The first part describes experiments made with a method similar to that devised by Ramsauer, in which the electron stream was resolved by an arrangement of slits suitably placed in a magnetic field so that a nearly homogeneous beam passed through the vapor. The experiments described in the second part were made with a simpler apparatus in which a fairly homogeneous electron beam was obtained without the use of magnetic fields.

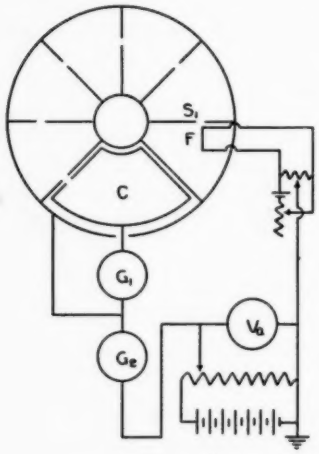

Fig. 1.

Part I

Apparatus and method. The apparatus and electrical connections are depicted in Fig. 1. The former was made of copper parts constructed so that they could be rigidly fastened together without the use of solder.

A preliminary experiment with an ionization gauge showed that, at the low pressures employed in this work, the vapor pressure of mercury was not influenced by the presence of copper. The filament F was a thin tungsten strip placed 1 cm from the slit S_1 which was crossed by several fine wires to serve as a grid. All the slits were rectangular, 1 mm wide and 1 cm

[4] C. Ramsauer, Ann. d. Physik **64**, 513 (1921).
[5] R. Minkowski, Zeits. f. Physik, **18**, 258 (1923).

long, mounted on a circle of radius 2.6 cm. A porton of the electron stream which passed through the grid was deflected through the slits by a magnetic field and finally collected in the Faraday cage C. The opening into this cage had slightly greater dimensions than those of the other slits. The slit system and the cage C were completely enclosed in a copper box so that electrons could not enter C except through the slits. The radius in a magnetic field H of an electron which has been accelerated through a potential difference of V volts is given by $r=3.37\ V^{1/2}/H$. In these experiments a solenoid 17 cm in diameter and 100 cm long was used to bend the electrons.

The total electron emission, J, from the filament was measured on a low-sensitivity galvanometer, G_2, and the initial current starting around through the slits was assumed to be proportional to this total current. (This procedure for measuring the initial current was employed by Brode[6] in measurements of the absorption coefficients of the rare, and other, gases.)

Those electrons which were not deflected from the initial beam were measured by the high sensitivity galvanometer, G_1. The length of path traversed by the beam before entering the collector C was 10.9 cm. To enable the temperature of the vapor in the space about the electron beam to be measured, a thermometer was placed in the tube with its bulb resting upon the copper box containing the slits. The pressure of the mercury vapor in the tube was varied by controlling the temperature of a mercury vapor trap, situated between the tube and the mercury diffusion pumps. This trap was always maintained at temperatures lower than the temperature of the tube, thus eliminating the possibility of condensation of mercury about the apparatus. Knudsen's[7] values of the vapor pressure of mercury at different temperatures were used in evaluating α. The procedure in making the measurements and calculating α was as follows.

The accelerating potential, V_a, was set at a given value and the magnetic field varied until the current, I, through the galvanometer, G_1, was a maximum. This value of I and the corresponding value of the total emission J were noted. A set of such corresponding values of I and J were taken for different accelerating potentials and a given vapor pressure. The pressure was then changed and for the same values of V_a as before, I and J were again noted.

At pressure p_1 and an accelerating voltage V, let I_1 be the current to the collector C and J_1 the corresponding filament emission, then

$$I_1=KJ_1e^{-\alpha xP_1+\beta}$$

Here K is the constant of proportionality between the initial current and the total emission, while β is a term to account for absorption of electrons by residual gas atoms. It is assumed that K is independent of the vapor pressure and also that β remains constant over the period in which a "run" is taken. Thus at a vapor pressure p_2

$$I_2=KJ_2e^{-\alpha xP_2+\beta}$$

[6] R. B. Brode, Phys. Rev. **25**, 636 (1925).
[7] Knudsen, Ann. d. Physik **29**, 179 (1909).

and therefore

$$\alpha=\frac{2\cdot 3026}{(p_2-p_1)}\log_{10}\left(\frac{I_1}{I_2}\cdot\frac{J_2}{J_1}\right)$$

p_1 was always the vapor pressure corresponding to 0°C (0.00017 mm) while p_2 took on different values up to about 0.0015 mm. Because of the heating due to the filament the temperature inside the apparatus was considerably higher than that of the vapor trap, and as the dimension of the tubes connecting these two regions were small compared with the molecular free paths a correction for thermal effusion was applied. This correction is a simple matter, the pressure in the apparatus being to the pressure in the trap as the square root of the ratio of the absolute temperature.

Results and discussion. The results of the measurements are given in Fig. 2 where the absorption coefficient is shown as a function of the electron energy

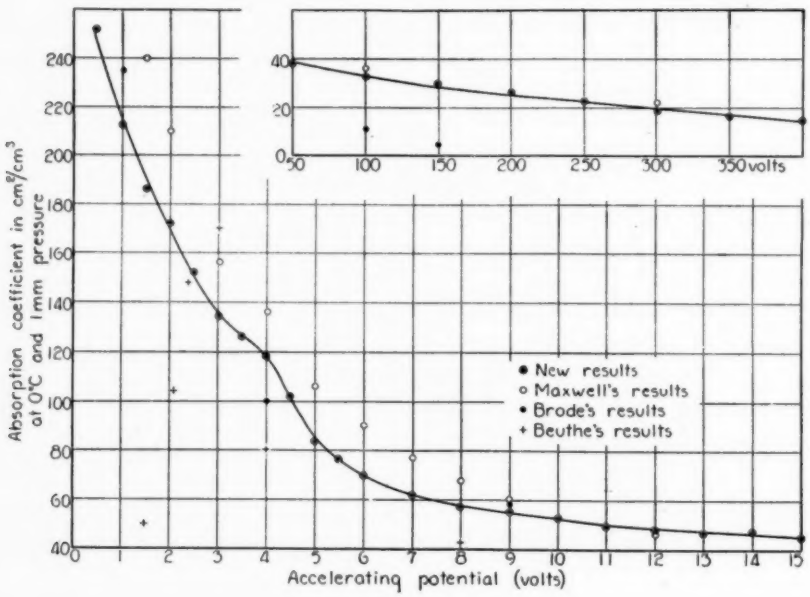

Fig. 2.

in volts. Each point on the curve is the mean of several values of α obtained at that voltage all of which differed from the mean by less than four percent. For purposes of comparison some of the values of α obtained by the other investigators are also shown.

When the accelerating voltage, V_a, was small, the determinations of α were found to be independent of the vapor pressure (over the limited range employed in this work) and also of the total filament emission if this did not exceed 10^{-4} amps. However, when V_a was greater than about 10 volts, consistent values of α could only be obtained by using the lowest possible filament emission and by keeping this emission constant, as the pressure is

varied, for each set of readings pertaining to a given value of V_a. The erratic results at higher filament emissions were probably attributable to disturbances in the space charge conditions about the filament, and consequently in the initial electron beam, by the ionization of the vapor. The effect of these disturbances would evidently be minimized and perhaps eliminated by the precautions observed in getting consistent values of α.

If this explanation is correct it is difficult to see why Brode[6] did not also experience the same difficulties in his experiments with a similar apparatus, especially when using argon for which the efficiency of ionization is almost as high as in mercury vapor. However, he used considerably higher pressures than were employed in this work, so that it was possible that the disturbing space charge effects were constant at the different pressures. Should this be the case, the computed values of α would be free from errors due to these effects.

It would seem that most of the troubles would have been avoided had the apparatus been constructed so that the initial electron current could be measured directly instead of by assuming it to be proportional to the filament emission. Beuthe's apparatus (which in other respects was similar to that used here) enabled this to be done; yet he experienced great difficulties which were only evaded by the use of low pressures.

The values of α shown in Fig. 2 are believed to be free from any appreciable errors at the lower electron energies but it is conceded that the precautions taken for obtaining *consistent* results when the electron energies were greater than 10 volts might not necessarily give *accurate* values of the absorption coefficient.

It is interesting to compare the results with those obtained by the other workers. At the lower energies there is a fairly good agreement as to general features and order of magnitude with the results of Brode and Maxwell, which were obtained by very different experimental arrangements. The significance of the small change in slope of the curve at about 4 volts is not understood. Maxwell, who also observed the same effect, attributed it to a change in the nature of the scattering, but it might equally well be due to an increase in the formation of negative ions. Beuthe's results, in spite of the essential similarity of his method with the one used in this research, show surprising differences. There is no indication of a continued decrease in the absorption coefficient below 3 volts as observed by Beuthe while above 3 volts his results agree with the present ones in order of magnitude alone. A short note added to Beuthe's paper by F. Krüger points out that the maximum in the absorption at 3 volts may not be a characteristic of the vapor, but due to some peculiarity in the electron beam itself.

It is difficult to understand why such a profound change in the absorption for slow electrons, if it really exists, had not been noticed previously in some of the many experiments dealing with electronic collisions in mercury vapor. Minkowski,[5] it is true, observed a small decrease in α for electrons slower than 1 volt but his experiments were indirect and capable of other interpretations.

At the higher velocities the values of α shown in Fig. 2 are in fair agreement with Maxwell's and differ considerably from those of Brode. As Maxwell has pointed out, there is probably a considerable source of error in Brode's measurements because of the emission of secondary electrons from the collectors in his apparatus.

Summing up, the results obtained in this work confirm reasonably well those obtained by Maxwell, and do not show the Ramsauer effect for mercury as reported by Beuthe.

PART II

Measurement of the absorption coefficient by another method. The apparatus and electrical circuits used in this determination of the absorption coefficient are shown diagrammatically in Fig. 3. Electrons from the electron "gun" A were accelerated into the chamber B where some of them after colliding with mercury atoms were deflected from the initial beam. The remainder passed on into the Faraday cylinder C and were measured by galvanometer G_2. The total initial current entering B was measured by G_1. Both G_1 and G_2 were high-sensitivity galvanometers.

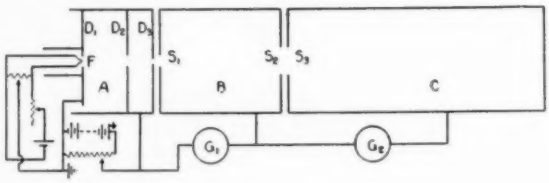

Fig. 3.

The chamber B was 5.2 cm long, 5 cm in diameter, and was lined on the inside with nickel gauze so as to make it a more efficient collector of the scattered electrons. The openings S_1 and S_2 were 4 mm and 1 cm in diameter respectively.

It was important that the Faraday cylinder C completely absorbed all the incoming electrons. To insure this, C was made 12 cm long and 5 cm wide while the aperture S_3 was 1.1 cm in diameter. Experiment showed that the cylinder acted as a perfect absorber of electrons.

The initial electron beam going through chamber B had to be fairly narrow, homogeneous, and of sufficient intensity to allow the currents in G_1 and G_2, at the lower accelerating potentials, to be measured accurately.

For producing such a beam, the electron "gun" A was designed. The filament F, consisting of a small loop of tungsten wire, just projected through a hole of 2 mm diameter in the earthed plate D_1. The middle of the filament was also earthed by the usual procedure of connecting the two ends to a high resistance and earthing an intermediate point.

The accelerating grids D_2 and D_3 were circular plates connected together, each 5 cm in diameter with circular openings 2 mm in diameter at their centers. D_1 and D_2 were 2 cm apart while D_3 was 1 cm from D_2. The edges

and sides of the holes in the grids were coated with lamp black to diminish secondary electron emission.

All the metal parts of the apparatus were of nickel, and were thoroughly outgassed both before assembling and after mounting in the Pyrex tube in which the measurements were made. This tube was placed with its axis parallel to the earth's magnetic field.

With liquid air surrounding the mercury vapor trap, measurements of the velocity distribution of the electron beam were made and the results for accelerating potentials of 5, 15, and 30 volts are shown in Fig. 4. It is seen

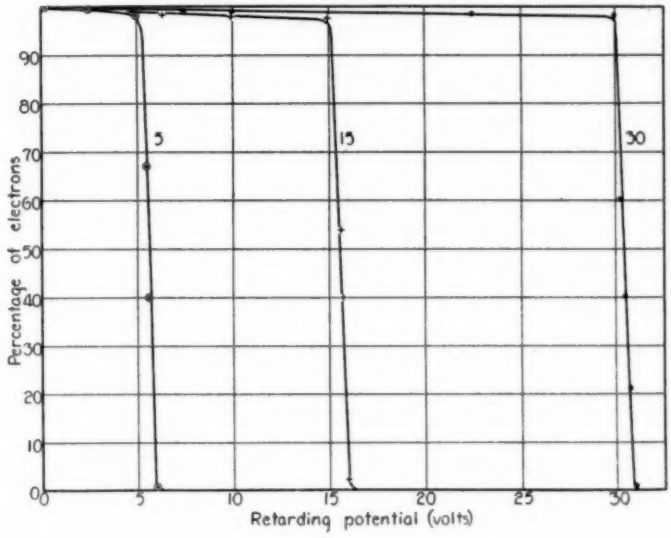

Fig. 4.

that at each voltage about 97 percent of the electrons are transmitted with the full velocity. Because of the initial thermal velocity of the electrons when they leave the filament and also the voltage drop along the filament a sharp upper limit to the velocity in the beam cannot be attained, unless the beam is magnetically analyzed as in the previous experiment. Measurements were also made of the current reaching the walls of the cylinder B when there was no vapor in the tube and it was found that the current was always less than 1 percent of the current collected by C. This indicated that the electron beam was narrow and also that the Faraday cylinder C was an efficient collector of electrons. Currents of the order 10^{-7} amps were obtainable from the gun even at potentials as low as a volt.

The procedure in determining α was the same as that described in Part I. Thus if J_1 and J_2 were the initial currents (indicated by G_1) at pressures p_1 and p_2 while the corresponding currents measured by G_2 were I_1 and I_2, then

$$\alpha=\frac{2\cdot 3026}{x(p_2-p_1)}\log_{10}\left(\frac{I_1}{I_2}\cdot\frac{J_2}{J_1}\right)$$

A possible source of error lay in the fact that electrons scattered through small angles would be able to pass through S_2 and be collected among the unscattered electrons in C. The magnitude of this error depended upon the solid angle subtended by S_2 at the place of collision and also upon the angular distribution of the scattered electrons. Assuming a uniform distribution of scattering the error in α due to this cause was negligible.

In Fig. 5, the absorption coefficient is shown as a function of the accelerating potential in volts. Some of the values obtained in the previous work are also include for purposes of comparison. The present results are consistently higher than those obtained in Part I, but exhibit the same general features. Thus the values of α continue to increase for values of the accelerating potential down to 0.5 volt.

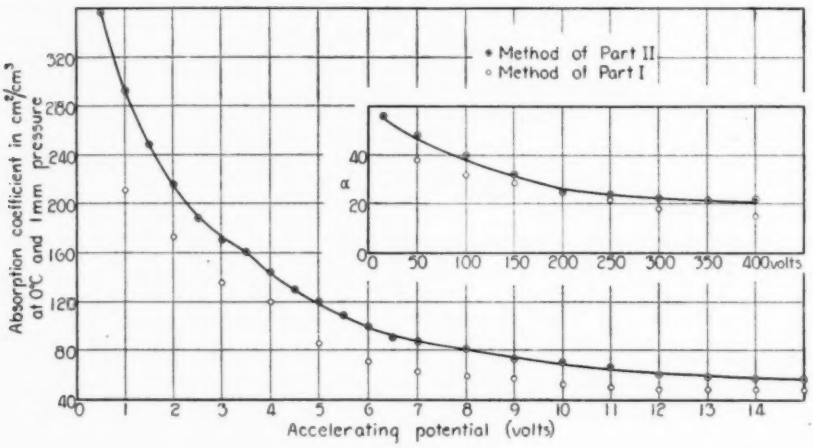

Fig. 5.

In the Ramsauer method a collision is defined more completely than by the method described in this part, as the latter does not measure collisions in which the electrons lose energy without having their direction appreciably changed. The values of α obtained by the Ramsauer arrangement should accordingly be somewhat larger than the others. The present experiments however indicate the reverse of this. A comparison of the results obtained in other gases by the Ramsauer method and by methods similar to the one here described shows that there is no appceciable difference between them.

In conclusion, the writer wishes to thank Professor H. A. Erikson for extending the facilities of the Laboratory at Minnesota, and also Professor J. T. Tate for his interest and helpful suggestions during the investigations. The work was done while the author was a Commonwealth Fellow.

PHYSICS DEPARTMENT,
UNIVERSITY OF MINNESOTA,
June 30, 1928.

THE SCATTERING OF POSITIVE IONS FROM A PLATINUM SURFACE

By Ronald W. Gurney

Abstract

The velocity and intensity of positive ions scattered at various angles from a metal surface have been measured by allowing the ions scattered from a heated platinum target to pass through slits into the electric and magnetic analysing fields of a positive ray box. The source, oxide catalyst emitting potassium, caesium, or lithium ions, could be rotated round the target, so that the latter could be bombarded from any angle. When the target was brought to a red heat the intensity of scattering was markedly increased, presumably because of the removal of a layer of adsorbed gas.

Velocity distribution. With a homogeneous initial beam the ions scattered at a given angle are nearly homogeneous in velocity. But the energy retained by the ions varies continuously with the angle of incidence, rising from 20 percent of the initial energy to over 80 percent as grazing incidence is approached. The velocity of ions scattered from a cold target on which an adsorbed layer has formed is much less, the energy retained rising to only 40 percent of the initial energy near grazing incidence.

Angle distribution. A separate apparatus was used to explore the intensity of scattering in all directions, by means of a collector which could be rotated around the source. For angles of incidence near the normal the intensity of scattering is very small or even zero, but increases with increasing angle of incidence. The most intense scattering takes place in a forward direction, the number of particles which suffer large deflections being small. Thus for a fixed angle of incidence the number of particles scattered in a direction normal to the target is very small or even zero, but increases steadily with increasing angle of reflection.

Critical energy. The intensity of scattering varies greatly with the energy of the incident ions, rising to a sharp maximum at about 40 volts. This critical energy for intense scattering is found to be the same for caesium, potasium, and lithium ions.

THE scattering from solid surfaces of particles of small momentum has been investigated by Davisson with Kunsman and Germer[1] who studied electrons, and by Ellett and Olson[2] who examined slow atoms of cadmium, mercury, sodium and hydrogen. In the experiments to be described here the scattering of particles of comparatively high momentum has been examined.

In an apparatus set up to investigate ionization of gases by fast positive ions it was found impossible to get rid of primary ions, which, after being scattered about from the metal sheath which lined the walls of the tube, found their way into the positive ray box intended for the analysis of the products of ionization. The original experiment was therefore postponed, and a target set up to examine this intense scattering. The velocities and distribution of alkali ions scattered from a heated strip of platinum foil have been measured by allowing the scattered ions to pass through slits into the electric and magnetic fields of a positive ray box of the Dempster type as

[1] Davisson and Kunsman, Phys. Rev. **22,** 242 (1923); Davisson and Germer, Phys. Rev. **30,** p. 705 (1927).

[2] Ellett and Olson, Phys. Rev. **31,** p. 312 (1928).

used by Smyth, Brasefield and others. While these experiments were in progress some work on the scattering of positive ions was reported by G. E. Read,[3] whose results differed in many points from the results which the writer had obtained. Read did not employ magnetic analysis to determine the velocity distribution of the ions, but allowed the scattered ions to impinge on a metal plate which could be rotated around the target. A simple apparatus, similar to his but with greater resolving power, was accordingly set up to investigate the points of difference. The results obtained are in agreement with those found with the positive ray box.

Apparatus

The first apparatus is shown in Fig. 1. An accelerating voltage applied between the catalyst oxide source, *O*, and the surrounding copper box, *B*, directed a stream of positive ions at the target *T*. The source and box were

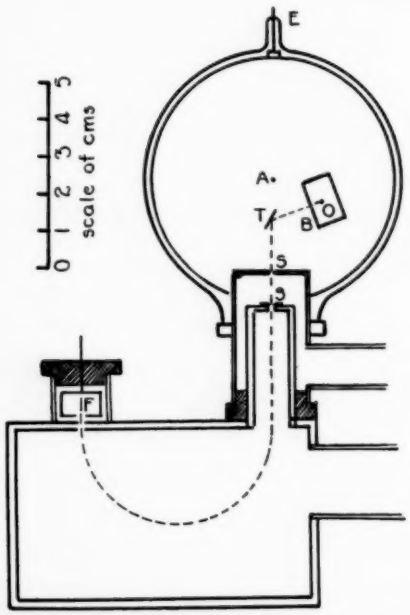

Fig. 1. Diagram of first apparatus.

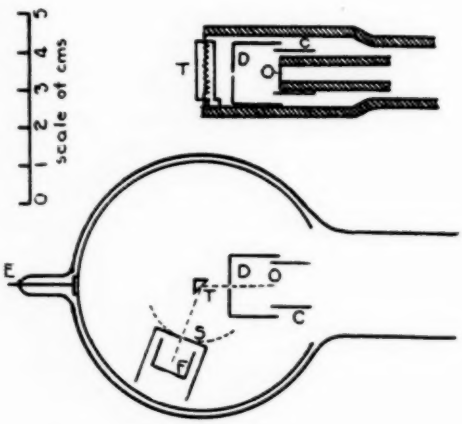

Fig. 2. Diagram of a second apparatu s.

mounted on a ground glass joint so that the target could be bombarded from any angle. It should be noted, however, that for a given orientation of the target the angle of reflection could not be varied. The ions scattered vertically downwards passed through the slits *S*, *S* into the positive ray box, where the magnetic field could be made to bring them around into the Faraday cylinder *F*, which was connected to a Compton electrometer.

The source of ions was a catalyst oxide of the type used by Kunsman,[4] containing a small amount of either potassium, lithium, or caesium and de-

[3] Read, Phys. Rev. **31**, p. 155 (1928).

[4] Kunsman, Jour. of Phys. Chem. **30**, 525 (1926); Barton, Harnwell, and Kunsman, Phys. Rev. **27**, 749 (1926).

posited on a platinum filament, which was held taut by a small molybdenum spring. The glass tube was lined with platinum foil, supported by the electrode E, which was put in electrical contact with the upper slit of the positive ray box. The target, a strip of platinum foil, through which a heating current could be passed, was held taut by a steel spring which took up the extension of the strip when the latter was brought to a red heat. The stray field of the electromagnet was compensated by a current passed through coils wound round the experimental tube.

The second apparatus is shown in Fig. 2. The face of the nickel drum D was pierced by a hole of 0.4 mm radius. At 12 mm from this was the source O, a speck of Kunsman oxide catalyst, on a short platinum filament. An accelerating voltage applied between the source and the drum directed a stream of ions at the target T; this was a piece of platinum welded to a nickel tube of triangular cross-section down the center of which ran a tungsten heating spiral. The source, drum and target were all mounted on one four-lead stem that could turn in a ground glass joint around ODT as axis. The drum, the target, and one end of the tungsten heating spiral were all welded to the same lead. Welded to one of the leads which supported the source was an additional cylinder C which protected the source from stray fields from the leads. The nickel parts were all outgassed by means of the induction furnace before assembling.

The collector was a small nickel box F, enclosed in a shield S, the front face of which was pierced by a circular hole of 0.6 mm radius. The lead supporting the collector was connected to the electrometer and was surrounded by a nickel tube, to which the shield S was welded. The glass tube was lined with a platinum foil supported by the electrode E; both this and the shield S were maintained at earth potential.

The collector could be moved around the target about a horizontal axis by turning the ground stem on which it was mounted. To explore the particles scattered in all directions we require to rotate the collector about another axis, at right angles to this first one. Since the initial beam was directed down the axis of the other ground joint, on which the target too was rigidly mounted, it is clear that turning this joint is exactly equivalent to moving the collector around the target about a vertical axis. In this way the whole hemisphere may be explored for a given angle of incidence, in contrast to the first apparatus.

An important plane is that which contains the initial beam and the normal to the target at the bombarded point. For if the beam of ions were a beam of light, the reflected beam would always lie in this plane, which we may call the meridian plane. It is clear that the collected beam lies in this plane when the target is parallel to the horizontal axis around which the collector moves. In the previous tube the collected beam was kept permanently in this plane, but in this second apparatus the collected beam could be in any plane passing through the direction of the incident beam.

Procedure and Results

Several results emerged almost as soon as the work started. In the first place, with a homogeneous initial beam the ions scattered at a given angle are nearly homogeneous in velocity, but this velocity retained by the ions varies continuously with the angle of incidence. In the second place, both the number of ions scattered and the proportion of the velocity retained by them are decidedly greater when the target is heated, but are independent of the temperature of the target when it is at least red hot. Presumably this results from the removal of a layer of adsorbed gas (e.g. grease vapour), which re-forms in a few minutes on allowing the target to cool, as described later.

The experiments which we will now describe in detail were taken with a heated target unless otherwise specified. All the curves shown in the diagrams in this paper were taken with the first apparatus, excepting those in Figs. 7 and 8.

With 1.0 ampere exciting current flowing through the coils of the magnet potassium ions of 65 volts energy are bent around by the magnetic field to enter the Faraday cylinder. The velocity distribution of the scattered ions is determined by finding how many volts applied between the slits S, S of the positive ray box are required to bring up the energy of the scattered ions to 65 volts. Thus for example when the voltage applied between the slits was 22 volts, the rate of deflection of the electrometer gave the number of particles which were scattered at the selected angle with 43 volts energy. (The velocities of fast ions could be determined by using a retarding instead of an accelerating field.) In any one determination of velocity distribution the following conditions were kept constant: A. Type of ion; B. Condition of target; C. Velocity of incident beam; D. Angle of incidence; E. Angle of reflection (for ions collected); F. Angle from the meridian (for ions collected).

The *velocity distribution* is found always to be a sharp peak, showing that the ions coming off at a given angle are nearly homogeneous in velocity. On comparing these peaks (Fig. 3) with peaks taken with the initial beam fired directly at the slits, it is found that they are but little wider, showing that the number of ions differing from the most probable velocity by more than one or two volts is small.

Change of velocity distribution with angle of incidence. If all the above conditions are kept constant except the angle of incidence, and the velocity-distribution is determined for various angles of incidence, a group of sharp peaks is obtained such as Fig. 3.

It is clear that the ions scattered at the selected angles differ not only in intensity but also in energy. The energy of the incident ions was 35 volts. The peak taken for incidence at 84° from the normal lies at 34 volts, so that the energy of its ions is $(65-34)=31$ volts. The peak taken at 44° incidence lies at 53 volts, hence its energy is at $(65-53)=12$ volts; i.e. the ions have lost about 23 volts, yet the peak is very little wider than the other in which the ions have lost 4 volts.

These energies of the scattered ions are plotted in Fig. 4, together with similar curves for other initial speeds, but all for the same selected angle of reflection. The points plotted for initial energies of 60 volts and 25 volts were derived from families of peaks similar to those shown in Fig. 3. In the case of 60 volt ions it will be seen that peaks were found in which the ions retained more than 50 volts or less than 10 volts. Yet such a large loss of energy as 50 volts is not accompanied by a great increase in the width of the peak; if the most probable energy retained by the ions is ten volts,

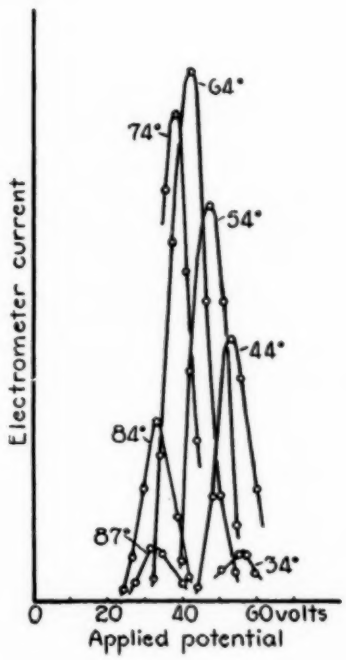

Fig. 3. Abscissas are volts applied between the slits of the positive ray box. Ordinates are intensity in arbitrary units. Initial energy of potassium ions was 35 volts. The selected angle of reflection was 66° from the normal.

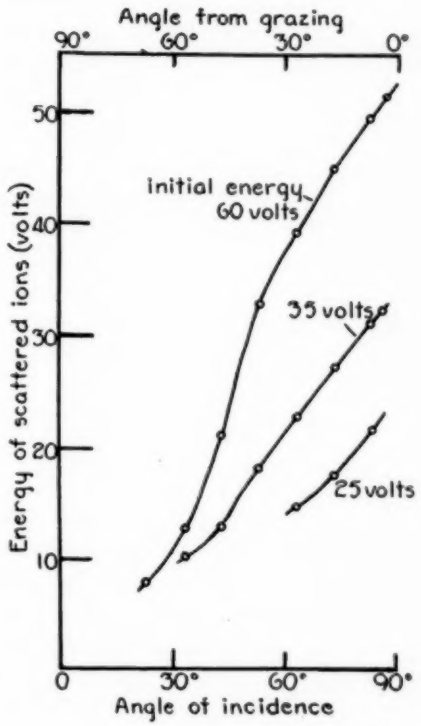

Fig. 4. Ordinates give the most probable energy of the scattered ions. Abscissae are angles of incidence. Selected angle of reflection was 66° from the normal.

most of the particles will lie in the range 10 ± 4 volts, having lost 50 ± 4 volts of energy.

Similar curves have been taken with ions of energies too great to be shown in Fig. 4. Curves almost identical with these have also been taken with lithium ions.

Variation of intensity with angle of incidence. The slits of the positive ray box, the upper 0.2 mm and the lower 0.4 mm wide, defined a narrow wedge-shaped volume, from which alone particles could reach the box. The

target was set accurately across this narrow solid angle by turning the ground-glass joint on which it was mounted, and whose axis was at A, Fig. 1. The orientation of the target was determined by introducing a pea-lamp into the positive ray box; the light reflected from the target formed an image of the slit on the copper box, B.

The incident beam was wide, and was intended to flood the target uniformly. The target was wide, but only a strip of width d, subtended by the slits, is operative. The width d subtends an angle ω at the source (Fig. 5), which varies from a maximum at normal incidence to zero at edge-on incidence. The angle ω is proportional to the cosine of the angle of incidence, and if the intensity of scattering were independent of the angle of incidence, the measured intensity would be proportional to this quantity, being a maximum at normal incidence.

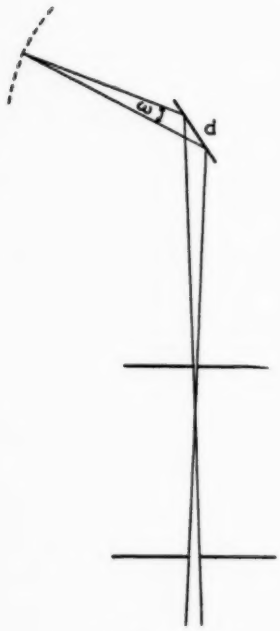

Fig. 5.

Instead of this, the intensity of scattering is found to be very low when the angle of incidence approaches normal.[5] Thus the observed intensity of scattering is a maximum for some intermediate angle of incidence, passing towards zero both for normal incidence and (by necessity) for edge-on incidence as ω tends to zero. This is shown by any family of peaks such as Fig. 3. The intensity obtained from these and similar peaks is plotted in Fig. 6 where each point represents the area of such a peak. The maximum occurs approximately at the specular angle, but we shall see that this is fortuitous. The question at once arises as to whether the observed decrease towards zero as edge-on incidence is approached is due to a factual decrease in the intensity of scattering, or whether it is due entirely to the decrease of ω. If we divide the intensity at each point by the corresponding value of ω, we find that, so far from decreasing, the curve continues to rise as edge-on incidence is approached. This means that the smaller the deflection (at the target) which the ions have suffered the more plentiful they are, since on increasing the angle of incidence the particles scattered at the selected angle have been deviated less. But the deduction of this result is not conclusive, since the rate at which the observed intensity falls to zero at edge-on incidence must depend on the finite width of the source, etc.

Variation with angle of reflection. The angle of reflection of the collected beam for which the curves in Fig. 6 were taken was 66° from the normal, (angle from grazing 24°). Now if reflection of the ions were approximately

[5] In studying the electron emission from metals under slow positive ray bombardment Jackson (Phys. Rev. **28**, 524, 1926) found that the intensity of reflection of potassium ions from various metals is for normal incidence "certainly less than 2 percent and may be zero."

specular, as reported by Read, we should expect to obtain for 66° incidence a smaller intensity, if we set the target to give some selected angle of reflection other than 66°. On the contrary, it was found that 75° reflection with 66° incidence gave a greater intensity than before, again suggesting that the particles are scattered in a forward direction.

To investigate this the second apparatus with movable collector was set up, as described above. The type of intensity curve for fixed incidence but varying angle of reflection as the collector was moved around the target in the meridian plane, is shown in Fig. 7. The scattered ions are found to be scattered in a forward direction in agreement with the results obtained with the previous apparatus. A similar curve was obtained with lithium ions.

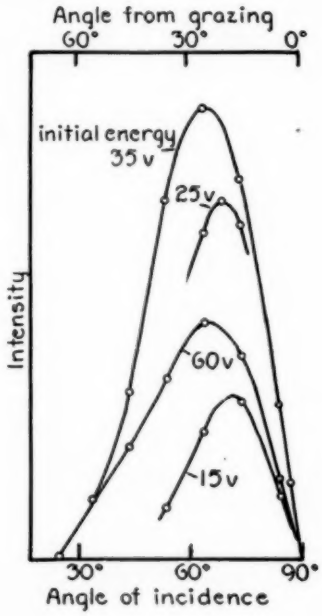

Fig. 6. Selected angle of reflection 66°.

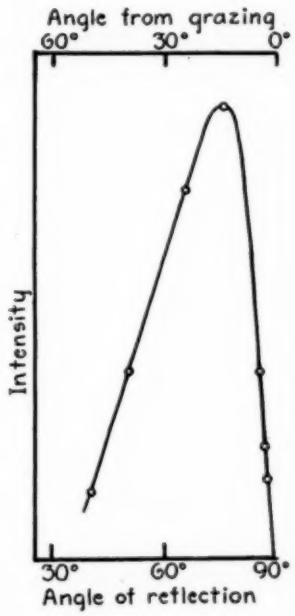

Fig. 7. Angle of incidence 46°. Initial energy of potassium ions 40 volts.

The position of the specular angle was accurately determined by turning the collector until the light from the glowing source after reflection from the target fell on the hole in the shield enclosing the collector. At this angle the intensity in Fig. 7 is seen to be small. It seems likely that if a smoother target could be used, the intensity would be found to fall still more suddenly to zero at the grazing angle.

The absence of specular reflection is obvious when we measure the intensity on either side of the meridian plane. Curve 1 in Fig. 8 shows the intensity on either side of the meridian when the collector had been set at the specular angle. The scattering extends through the whole 180 degrees. It is clear that when the collector is below the horizontal, i.e. when the collected beam makes more than a right angle with the incident beam, par-

ticles can no longer be collected through 90° on either side of the meridian. For at a smaller angle than this the collector will pass below the plane of the target, and disappear below the horizon. Thus the curve 2 in Fig. 8 is of necessity restricted, this curve having been taken through the peak in Fig. 7. The curves in these Figs. 7 and 8 are the only curves in this paper taken with the simple apparatus; the rest were all taken with the positive ray box.

Adsorbed layer on a cold target. Suppose that with the positive ray box we make a setting on the top of a peak, (by which we mean set the value of the electric field between the slits to bring the maximum yield to the Faraday cylinder). If we then turn off the heating current through the target, the

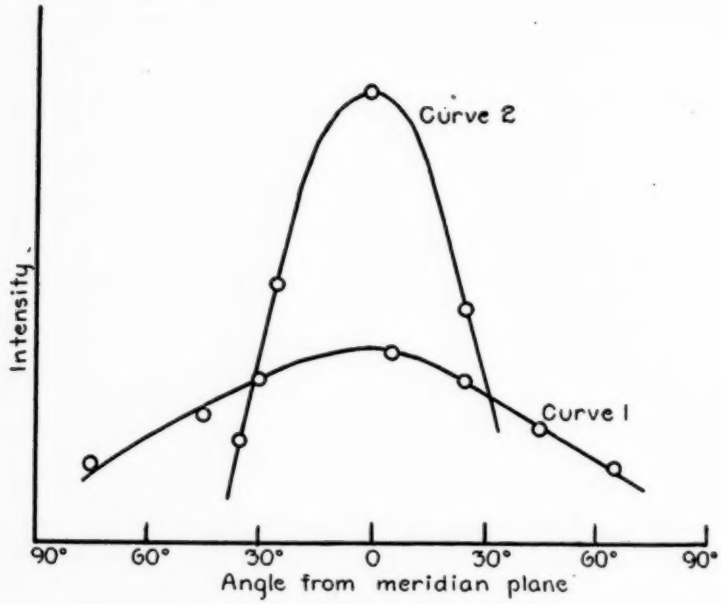

Fig. 8. Angle of incidence 46°. Initial energy 40 volts. Curve 1. Angle of reflection 44°. Curve 2. Angle of reflection 77°.

number of ions immediately falls off as shown in Fig. 9. Read took his measurements a few seconds after turning off the heating current, and states that the results were approximately the same as for a hot target. This was presumably because his method did not pay attention to the velocity of the scattered ions. For the rapidity of the fall in the first few seconds is due partly to the rate of decrease in the number of ions scattered, and partly to their rapid decrease in energy, which prevents them from traversing the magnetic field to the Faraday cylinder.

Curves similar to those in Figs. 3, 4, and 6 were obtained with an adsorbed layer, except that in this case the intensity was about one-eighth of that from a heated target, and the energy retained by the ions about one-half; i.e. the energy retained rose to 40 percent of their initial energy near grazing in-

cidence, instead of about 80 percent. Read stated that with his apparatus a cold target became after a few minutes completely ineffective as a reflector.

We will consider the rate of contamination first by potassium and then by residual vapour. The number of ions in one microampere is less than 10^{13} per second. The number of ions passing through the slit and reaching the target must have been less than 10^{10}. If the atomic radius is 10^{-8} it will require 10^{16} atoms to form a unimolecular layer over unit area, or 10^{15} atoms to cover one-tenth of this area. It is clear that the formation of a layer of alkali from the beam of incident ions would be extremely slow, even if a large proportion of them adhered to the cold target.

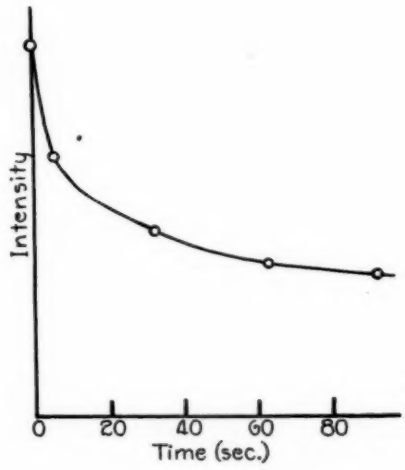

Fig. 9. Abscissae show the time elapsed since the heating current through the target was cut off.

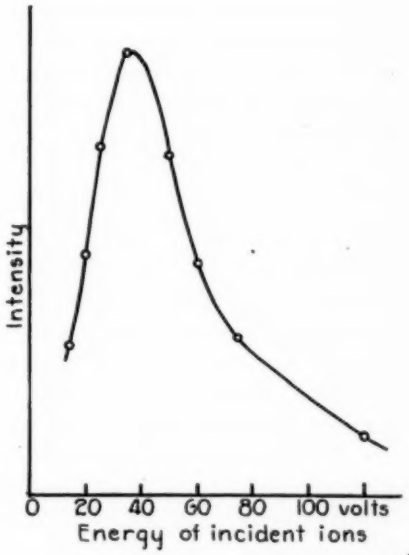

Fig. 10. Angle of incidence 67° Angle of reflection 66°.

By means of an ionization-gauge attached to the tube it was found that the pressure of residual vapour (presumably from the two greased joints) was about 10^{-4} mm, which means about 10^{12} molecules per cc. The number of molecules striking unit area per second is $nv/3$, where v is their temperature velocity; this comes to about 10^{16} per second. So that if it were one molecule out of every hundred hitting the surface that was adsorbed, a unimolecular layer would be formed in a few minutes.

Critical energy for intense scattering. Returning to the scattering from a heated target, we have seen from the curves in Fig. 6 that the intensity varies greatly with velocity of the incident beam. Fig. 10 shows the type of curve obtained by varying the energy of the incident ions for given angles of incidence and reflection. Very similar curves, showing a sharp maximum at about 40 volts were obtained for caesium and lithium. Almost identical curves were obtained with each apparatus. In those taken with the first each

point represents the area of a positive ray peak; in the second it represents a direct reading from the electrometer, the integration over velocities having been made by the apparatus. The position of the maximum is nearly independent of the angle of incidence or reflection.

Read obtained a curve for lithium with a maximum intensity at about 48 volts, but as his measurements were confined to the meridian plane, it was not clear whether the scattering was greater in all directions at 48 volts, or whether the ions were more concentrated on the meridian at this voltage. The scattering at higher and lower voltages might have been not less intense, but more diffuse. But we have found that at different voltages the scattering on either side of the meridian is equally diffuse.

The question immediately arises as to what becomes of the ions which are not scattered. They may (1) pick up an electron as they collide with the surface and be reflected neutral. (2) They may be adsorbed and reemitted later either neutral, or as an ion with very small energy. (3) They might accumulate on the surface, even at a red heat, their charge being neutralized by an influx of electrons into the target.

It is well known that platinum at an intense red heat emits alkali ions. In fact it was found that when the negative end of the target was connected to the upper slit of the positive ray box, (thereby making the target slightly positive with regard to the slit owing to the potential drop of the heating current) a copious positive ion current could be obtained at an intense red heat. In the final measurements the other end of the target was accordingly connected to the slit, and there was therefore a retarding field of a volt or less which would keep very slow ions out of the positive ray box. If therefore the non-scattered ions were adsorbed and reemitted with small thermal velocities, they would not have been collected, whether charged or neutral. This argument, however, does not seem to apply to Read's case.

Discussion

According to the wave mechanics a particle of mass m and velocity v is associated with a wave of wave-length h/mv. For the ions used in these experiments the wave-lengths are found to be of the order of 0.01 Angstrom. They correspond to gamma-rays, and it is difficult to predict what effects would be expected.

If we try to account for the results by multiple collisions between the ions and the atoms at the surface of the target, difficulties are encountered. At first sight, however, the phenomena appear to be qualitatively what would be expected from collisions between free particles. Thus it has been shown: (a) the least deviated ions retain the most energy, (b) the intensity is concentrated in a forward direction, the number of particles which are deflected through large angles being small, (c) the ions scattered from light atoms (adsorbed layer) give up a greater fraction of their energy than those scattered from heavy atoms (heated platinum).

On the other hand, when we consider it in detail we do not find agreement. Let V be the initial and v the final velocity of an ion of mass M, and let m

be the mass of a free atom with which it collides. Then if the ion is deflected through an angle ϕ, the velocity after a single collision is

$$v = V\{M\cos\phi \pm (m^2 - M^2\sin^2\phi)^{1/2}\}/(M+m)$$

We find that a platinum atom is so much heavier than potassium or lithium, that an ion can lose very little energy except in the case of the large deviations which are very improbable. Yet if the large losses of energy are the result of collisions with many atoms, why is the beam of ions scattered at a given angle so homogeneous? The difficulties are equally serious in the case of the layer adsorbed on a cold target, since this presumably consists mainly of carbon and oxygen atoms, which are so light that they can give the potassium ion only very small deflections. Thus $(m^2 - M^2\sin^2\phi)$ becomes negative when ϕ is greater than 18°; and the most probable deflection must be less than this, since the condition for maximum deflection is rare.

Finally there is the critical energy for intense scattering, the same for caesium, potassium, and lithium. The velocity and momentum of caesium and lithium ions having the same energy differ by a factor of 4.3, since they depend on the square roots of the masses. It has been pointed out that to interpret this maximum one needs evidence as to what becomes of the ions which are not scattered. Work is being continued in the hope of eliminating grease vapour from the tube, and of using a crystalline target.

In conclusion I wish to express my thanks to Professor K. T. Compton for extending to me the privilege of working in the Palmer Laboratory and for his interest in this work; to Professor H. D. Smyth for helpful discussion; and to the International Education Board, to whose grant of a fellowship my visit to America was due.

PALMER PHYSICAL LABORATORY,
PRINCETON UNIVERSITY.
May 31, 1928.

THE ELEMENT OF TIME IN THE PHOTOELECTRIC EFFECT

By Ernest O. Lawrence and J. W. Beams

Abstract

Time of appearance and cessation of the photoelectric effect from a potassium hydride surface.—A method has been devised which has made possible the study of the time variation of the photoelectric emission from a metal surface illuminated by light flashes of 10^{-8} sec. duration. The experimental arrangement has also yielded information on the speed of operation of the Kerr cell electro-optical shutter described in earlier work and has made possible for the first time the observation of the steepness of wave fronts traveling along wires resulting from spark discharges. Photoelectric emission begins in less than 3×10^{-9} sec. after the beginning of the illumination of a potassium hydride surface. The light shutter closes less abruptly than it opens and the experimental observations indicate that the sum of the time required for the shutter to close plus the time during which the photoelectric emission persists after cessation of irradiation is less than 10^{-8} sec. A wave traveling along a wire resulting from the sudden change of potential of one end by a spark discharge is so steep that the time necessary for about half the wave-front to pass a point 6 meters along the wire is 4.5×10^{-9} sec. Theoretical considerations bearing on these results are discussed.

Introduction

THE classical observations by Wien[1] and Dempster[2] of the decay of luminosity in a canal-ray beam have shown that the excitation of atoms and emission of light by atoms are not simultaneous events. Absorption and emission of light and the photoelectric effect are complementary atomic processes, and it is therefore of especial interest to inquire as to the course of events wherein electrons are ejected from atoms by radiation. How soon are electrons emitted from a metal surface after it is irradiated by light and in what manner does the electron emission persist after cessation of the illumination? The experiments described below have given an answer to this fundamental query.

Method

In order to study the element of time in the photoelectric effect it was necessary to devise a method capable not only of irradiating a metal surface for known intervals of time of about 10^{-8} sec but also capable of detecting at what instants relative to the time of irradiation electrons are ejected, again with precision greater than 10^{-8} sec.

In earlier work we[3] have described a method for producing short flashes of light. Two similar Kerr cells K_1 and K_2 (Fig. 1) were placed between crossed Nicol prisms N_1 and N_2 with the normals to their plate surfaces at right angles to each other. Thus, when the electric fields between the plates

[1] W. Wien, Ann. d. Physik **73**, 483 (1924).
[2] A. J. Dempster, Astrophys. J. **57**, 193 (1923).
[3] Lawrence and Beams, Proc. Natl. Acad. Sci. **13**, 207 (1927).

of both cells were of the same magnitude the cells compensated each other and light emerging from the second cell was plane polarized and unable to pass through the crossed Nicol N_2. Only when the electric field in one cell was greater than in the other was there double refraction causing light to pass through N_2. The Kerr cell plates were attached to a spark gap SG so that at a time after the beginning of the spark discharge equal to the length of wire connecting the cells to SG divided by the velocity of light the cells began their discharge. By using wire paths of different lengths to K_1 and K_2 the cells could be made to begin to discharge at times differing by as short intervals as desired. Thus, during these short time intervals light passing through K_1 and K_2 was doubly refracted and passed through N_2.

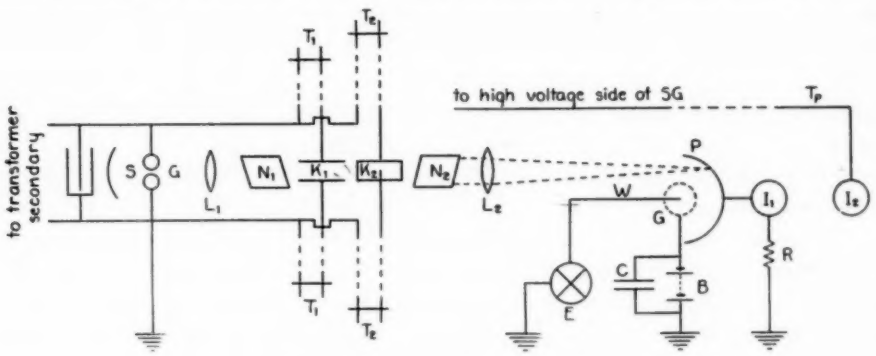

Fig. 1. Arrangement of apparatus.

Short light-flashes produced in this manner illuminated a potassium hydride surface P of a three-electrode photoelectric cell (Fig. 1). A brass ball I_1 (2 cm diam.) was attached to the electrode of P on the outside of the photoelectric cell and another brass ball I_2, which was attached to a wire T_p of variable length connected to the high voltage electrode of the spark gap, was placed at a distance from I_1 of usually from 10 to 15 cm. An india-ink resistance R of about 10^{10} ohms attached to the plate system maintained P at earth potential excepting when a change of the potential of I_2 quickly induced a change in potential of I_1. A grid G surrounding a collecting electrode W was maintained at a definite negative potential by a bias battery B of several hundred volts. A condenser C of one microfarad capacity maintained the potential of G constant even though the potential of P changed by several hundred volts in very short time intervals. The collecting electrode W was attached to a Dolezalek electrometer E. The various components of the system were carefully screened electrically.

Now the potential of I_2 alternated from about $-10{,}000$ volts to $+10{,}000$ volts with a frequency of sixty cycles inducing an alternating potential on I_1 and P. The resistance R was so high as not greatly to affect this rise and fall of potential. Because of the jumping of the spark the potential of I_2 did not alternate sinusoidally and P changed in a manner diagrammatically indicated by

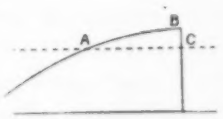

Fig. 2.

Fig. 2. The voltage rose to a maximum negative value every other half-cycle sinusoidally and then dropped suddenly to zero because of the breakdown of the spark gap resistance. The bias battery B maintained the grid G at a negative potential indicated by the dotted line so that only during a portion ABC of the negative half-cycle was the plate negative with respect to the grid—and during this time only electrons ejected from P passed over through the grid to the collecting electrode W. The drop in voltage BC of the plate was very sudden, occurring at a time after the spark discharge equal to the electrical path connecting the plate to the spark gap inductively through I_1 and I_2 divided by the velocity of light. Thus, the arrangement was such that the electric field drawing electrons from P to G could be reversed very quickly at various times subsequent to the beginning of the spark discharge by varying the length of wire T_p connecting I_2 to SG.

The flashes of light produced by the electro-optical shutter began and ended at definite times relative to the beginning of the spark. The time variation of emission of electrons by the flashes was therefore studied by observing the variation of electron current received by W with change of the time of reversal of the electric field between P and G. Clearly, if the wire paths T_p were so short that the field reversed before the light flash illuminated the surface no photo-electrons would reach W. Determining what length of wire was necessary to obtain an appreciable photoelectric current to the electrometer was therefore a measure of the instant at which the electrons first were emitted from the plate P. By further increasing the length of T_p in small steps the relative number of photoelectrons emitted during the course of the light flash and subsequent thereto was studied.

Apparatus

Electro-optical shutter. The Kerr cell plates of K_1 and K_2 were 8 cms long, 1 cm wide and were separated 0.5 cm, both pairs being in a single Pyrex tube containing carbon bisulphide. Thin microscope cover glasses sealed on the ends of the tube by water glass provided strain free windows, ordinary so-called strain-free optical glass being quite unsuitable for the purpose. A zinc spark gap was the source of light.

Photoelectric cell. The three electrodes of the photoelectric cell were of nickel, a semi-cylindrical plate P being mounted coaxially with a grid G which completely enclosed the collecting electrode W. The grid was a nickel cylinder of 6 mm in diameter and the distance between the plate and grid was 7 mm. The collecting electrode not only was screened by the grid but also was shielded by a copper guard-ring insealed both inside and outside. The cell was evacuated and carefully baked out prior to the formation of the potassium hydride surface on P—with the result that after sealing off the cell a very good vacuum was maintained. Because of the high vacuum and the existence of solid potassium metal in the tube, all metal parts became equally photoelectrically active in the course of a few days—even the hydride surface did not retain its characteristic photoelectric properties. Thus only during the first few days was the photoelectric sensitivity of P large in com-

parison to that of G—an essential condition for satisfactory performance, for obviously stray light scattered on the grid caused spurious emission of electrons.

Experimental Observations

Fig. 3 is a plot of the photoelectric currents to the collector W (ordinates) corresponding to various times of reversal of the electric field between P and G after the beginning of the spark discharge (abscissas). It is seen that as the time of cut-off of the photoelectric emission is delayed the current gradually increases to a point A where there is a more rapid rise of current with further delay of cut-off until a point B is reached where the photoelectric current no longer increases. Measuring the length of wire connecting the Kerr cells to the spark gap and noting the light path distance from the Kerr cells to the photoelectric cell it was estimated that the light flash began irradiating the plate P and reached maximum intensity at times indicated by the dotted lines A' and B'. It is seen that the marked change of slope of the experimental curve coincides approximately with the beginning of the light flash. It is evident, therefore, that the increased slope is due to photoelectrons ejected by the flash of light and, indeed, the coincidence of the beginning of the light flash with the change of slope leads to the conclusion that photoelectric emission begins directly a metal surface is irradiated. It is important to emphasize that in this experiment the measured times of beginning of the light flash and the beginning of the photo-electron emission were 13×10^{-8} sec. and 12.5×10^{-8} sec. respectively and therefore were equal to within 4 percent.

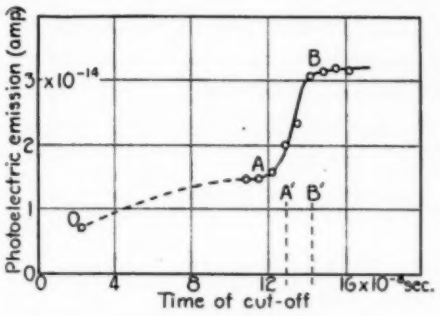

Fig. 3. Photoelectric currents to the collector for various times of cut-off after beginning of spark.

For some time the cause of the quite appreciable emission of electrons prior to the beginning of the light flash, represented by the portion of the curve from O to A, was a mystery. It was finally discovered that the spurious current was actually due to light passing through the shutter before the main flash started. It was found that although the shutter completely extinguished the light when the wire paths to the cells were equal, they failed to charge up to the same voltage when the leads T_1 and T_2 were of different lengths.

To eliminate this troublesome circumstance the wire paths were shortened a great deal thereby causing a flash to be produced during a much earlier stage of the spark. With this arrangement the data of Fig. 4 were obtained. Again the ordinates represent the photoelectric emission corresponding to various times of cut-off after the beginning of the spark. With a bias potential of 315 volts the inductor I_2 was so placed relative to I_1 that the induced potential on P was just sufficient to enable photo-electrons to pass

from P to G when I_2 was near its maximum negative potential. The bias was then reduced to 290 volts so that the photo-electrons were drawn from P to G by a potential difference of approximately 25 volts for a short time before the reversal of the electric field. Under these conditions the data of curve A were obtained. Next the bias voltage was further reduced to 266 volts so that the potential difference accelerating electrons from P to G was 49 volts, yielding the data of curve B. Curve C resulted from changing the bias to 243 volts. The time of beginning of the light flash is represented by the dotted line X, being the wire path T_1 plus the light path from the Kerr cells to the photoelectric cell divided by the velocity of light. Likewise the flash attained maximum intensity at a time subsequent to the beginning of the spark equal to the wire path T_2 plus the light path from the cells to

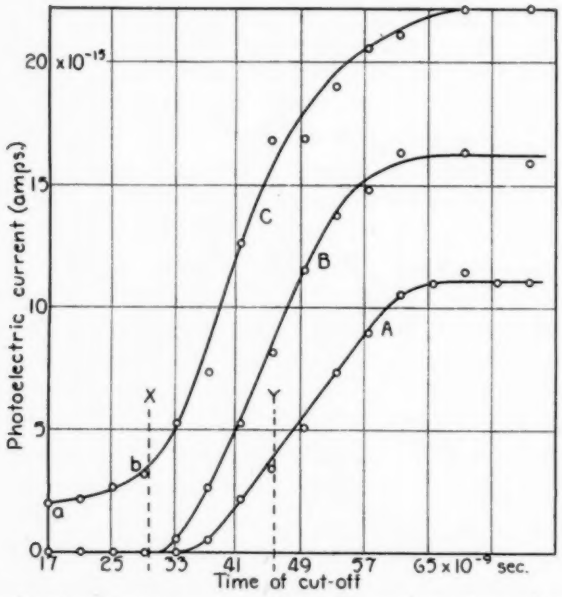

Fig. 4. Photoelectric currents to the collector for various times of cut-off after the beginning of the spark.

the photoelectric cell divided by the velocity of light, also recorded in Fig. 5 by the dotted line Y. A paper in process of publication[4] makes clear that there is no appreciable lag in the Kerr effect but that quite appreciable intervals of time required to discharge the Kerr cells affect the operation of the shutter in such a way that it does not cut off the light sharply at the instant that the second of the Kerr cells begins discharging. Assuming there exists no persistence of the electron emission after the surface is illuminated, the data indicate that the shutter continued to allow light to pass through for about 10^{-8} sec after the second Kerr cell began discharging. This estimate of the rate of decay of the double refraction in the Kerr cells is somewhat larger than the value arrived at in the recent independent investigation cited above. However, the uncertainty in the functioning of the shutter

makes it impossible to conclude with great precision that the photoelectric emission stops as abruptly with the illumination as it commences. It can be stated with confidence only that the sum of the time required for the double refraction in the Kerr cells to decay to a small value and the time that the photo-electron emission persists after the illumination is cut off is less than 10^{-8} sec.

Of even greater importance is the interpretation of the observations of the beginning of the electron emission. It is seen that the apparent beginning of the electron emission is not the same for the three sets of data embodied in curves *A*, *B*, and *C*. Because of the finite time required for the electrons to pass from *P* to *G* a correction to the apparent time of cut-off of the electron current is necessary. The magnitude of this correction is of course readily computed from the dimensions of *P* and *G* and the potential difference between *P* and *G* drawing the electrons to *G*. Including this correction the following times of beginning of the photo-electron emission are obtained from the data of Fig. 5.

Curve	Accelerating potential between *P* and *G*	Apparent time of beginning of photoelectric emission prior to time of beginning of light flash.
A	25 volts	0.8×10^{-9} sec.
B	49	2.6×10^{-9} sec.
C	72	4.5×10^{-9} sec.

The data indicate that with a large bias voltage and consequent small potential change of I_2 necessary to cut off the photoelectric current it appears that the electron emission began very nearly at the same instant the illumination commenced. Curves *B* and *C* indicate that for greater differences between the bias voltage and induced voltage the electron emission apparently began before the illumination. This is to be explained by the finite rate of fall of potential of *P* resulting from the discharge wave from the spark gap reaching the inductor I_2. Rogowski, Flegler and Tamm[4] have carried through some experiments which indicate that such traveling wave-fronts along wires are steeper than they were able to measure (10^{-8} sec). The present experiments are really the first definite observations of the steepness of such wave-fronts. The shift of the apparent time of beginning of the electron emission by 4.5×10^{-9} sec when the bias voltage was decreased from 315 volts to 243 volts shows that the traveling wave from the spark lowered the potential of *P* by 72 volts in about 4.5×10^{-9} sec. Because of the small capacities involved it therefore is to be concluded that the potential of I_2, as well as other points along the wire T_p changed 45 percent of the total amount within 4.5×10^{-9} sec. after the arrival of the front of the discharge wave from the spark.

Curve *C* differs from curves *A* and *B* in that instead of the electron current rising from zero a small electron emission was evident when the

[4] A very interesting study of traveling wave fronts by Rogowski, Flegler and Tamm (Archiv. f. Elektrot. **18**, 479 (1927)) is reviewed in a paper in process of publication in the Journal of the Franklin Institute.

photoelectric cell was presumably "cutting off" well before the beginning of the light flash (see portion *ab* of the curve). This was due to the greatest source of trouble in the experiments—oscillations. The photoelectric cell was the seat of troublesome high frequency oscillations. The difficulty was met, as curves *A* and *B* indicate, by using a high bias voltage so that the oscillations of the potential of *P* after the arrival of the discharge wave were not great enough again to give rise to a potential difference accelerating electrons to *G*. In the instance of curve *C* where the voltage, because of the low bias, had to drop 72 volts before the field between *P* and *G* reversed, the potential of *P* oscillated back again to an intermediate value during the light flash, and as a result electrons were drawn to *G* as the portion of the curve *ab* indicates. The photoelectric cell was not the only seat of troublesome oscillations and very elaborate precautions were necessary in the way of screening. Because of the very small photoelectric emission and the very sudden changes in potential of various parts of the circuit, spurious effects were always in evidence in the early stages of the experimental work and it seemed an impossible task to arrive at trustworthy results. However, all sources of trouble were ultimately eliminated and the present results are believed to be entirely reliable.

A general survey of the possible sources of systematic error in the present work leads to the conclusion that the observed highly precise coincidence of the beginning of the light flash and the beginning of the electron emission —within 0.8×10^{-9} sec. in the case of curve *A*—is probably fortuitous, the experiments being unable to detect with certainty a difference less than 3×10^{-9} sec. However, within these limits the photoelectric effect is instantaneous.

Discussion

The old quantum theory of the photoelectric effect was based essentially on the Einstein photoelectric equation yielding, with the aid of thermodynamics, general statistical laws which govern such atomic processes. Just as the old theory was not able to predict the time rate of decay of radiation from a group of excited atoms, it did not concern itself with the time required for absorption of light and emission of an electron. Similar remarks apply to a wave mechanics theory of the photoelectric effect worked out by Wentzel.[5] Wentzel has obtained a solution of the Schroedinger wave equation for the case of an atom perturbed by the electromagnetic field of an infinite plane wave train. For such a steady periodic perturbation of the atom a solution for ψ is obtained which is interpreted as an emission of an electron. However, the case of a limited wave train is not treated and, indeed, there is no way of telling how soon the atom gets into the steady perturbed state corresponding to this ψ solution after it is irradiated by light of a definite frequency. The Bohr theory regards the absorption of light as a process distinct from emission wherein an electron is raised to an outer orbit in the

[5] Wentzel, Zeits. f. Physik 40, 574 (1926).

atom, the emission of light occurring when the electron returns to its normal position. The photoelectric effect on this view is a particular case of light absorption in which the electron is removed completely from the atom. Recent experiments by d'E. Atkinson[6] have indicated that the excitation of an atom takes place in less than 10^{-10} sec. It is therefore to be expected on the Bohr idea that photo-electrons are ejected within a similar small interval of time after illumination—as the present experiments indicate.

The exponential decay of the radiation from a group of excited atoms observed by Wien and Dempster may be interpreted in two ways. Either individual atoms give off their radiation in this manner or they emit the radiation in very short intervals of time and that what was observed was the decay-curve of those atoms that were in the initial state for the radiation in question. Recent experiments by Traubenberg and Gebauer[7] have shown that a group of excited atoms moving with high velocity through an inhomogeneous electric field at each point of their path give off radiation having Stark effects corresponding to the electric field there. These observations clearly suggest that the latter of the above alternative hypotheses is correct—that atoms emit quanta of radiant energy practically instantly at quite appreciable times subsequent to excitation. Now if the photoelectric effect is regarded as a process of light absorption and subsequent emission by the atom of the absorbed energy in the form of an electron instead of a light quantum it is therefore natural to expect that photoelectric emission would persist after illumination of a metal surface. Because of the uncertainty of the rapidity with which the electro-optical shutter cut off the light in the present experiments it is impossible to determine with great precision whether or not such a persistence of the photoelectric effect exists. It can only be said that such an effect becomes inappreciable within 10^{-8} sec. after cessation of the illumination.

Slack[8] using a method devised by Webb has studied the duration of radiation produced by 10.2 volt electron impacts in hydrogen. The interpretation of his results rests on the assumption of the non-existence of a lag in the photoelectric effect. The present research has shown that this assumption is valid.

SLOANE LABORATORY,
YALE UNIVERSITY,
June 10, 1928.

[6] d'E. Atkinson, Roy. Soc. Proc. **A116**, 81 (1927).
[7] Traubenberg and Gebauer, Zeits. f. Physik. **44**, 11–12, 768 (1927).
[8] Slack, Phys. Rev. **28**, 1 (1926).

THE DISTRIBUTION OF THE HEAT EMISSION IN THE MAGNETIC HYSTERESIS CYCLE*

By F. Woodbridge Constant

Abstract

Warburg has shown that for a complete magnetic hysteresis cycle an amount of energy equal to the area of the *I-vs-H* loop is dissipated and appears as heat. But for a part of a cycle theory only states that energy $=\int_H^{H+\Delta H} HdI$ is supplied to the iron. Part of this energy appears as heat, while the rest is stored as magnetic potential energy and is released in another part of the cycle. The distribution of the heat emissions for successive steps along the hysteresis cycle was obtained experimentally from the rises in temperature produced in the iron or steel. The corresponding values of $\int HdI$ were obtained from the hysteresis loop. The difference between these quantities gave the potential energy throughout the cycle. The potential energy was greatest for $H=H_{max}$, zero for $H=0$. The heat emission was zero from $H=H_{max}$ to $H=0$, increased up to a little beyond $H=-H_c$, (H_c = the coercive force), and then decreased to $H=-H_{max}$. A cooling was never observed. The results are discussed in connection with a recent theory of atomic behavior in ferromagnetic metals.

I. Introduction

THE subject of magnetic hysteresis owes its complete development to Ewing,[1] who obtained the well-known "hysteresis loops," curves showing the cyclic relation between the magnetic force, H, and the magnetization, I. Ewing gave the name "hysteresis," meaning "to lag behind," since he found that I always fell behind H in the cycle.

It had earlier been shown by Warburg,[2] and later independently by Ewing,[3] that when a ferromagnetic material is taken through a continuous cycle of values of the magnetizing force, H, energy is dissipated through hysteresis. Warburg found this energy, in ergs per unit volume, to be equal to the area of the *I-vs-H* hysteresis loop, that is, $\oint HdI$, and this law is known by his name. This is for a whole cycle, at the end of which the material is in the same state as at the beginning, hence this energy must appear as heat, and cause a rise in the temperature of the material. Attempts have been made to check Warburg's Law from this rise in temperature, and Adelsberger[4] has recently done so to within 2 per cent.

If the magnetic force is increased from H to $H+\Delta H$, the energy supplied per unit volume is given by

$$w=\frac{1}{4\pi}\int_H^{H+\Delta H} HdH+\int_H^{H+\Delta H} HdI \qquad (1)$$

* Part of a dissertation presented for the degree of Doctor of Philosophy at Yale University

[1] J. A. Ewing, "Magnetic Induction in Iron and Other Metals," (1900).

[2] E. Warburg, Ann. d. Physik (4) **13**, 141–164 (1881).

[3] J. A. Ewing, Proc. Roy. Soc. **34**, 39–45 (1883).

[4] U. Adelsberger, Ann. d. Physik (4) **83**, 184–213 (1927).

where the first term represents the energy increment in vacuo, and is reversible, while the second represents the energy increment due to the presence of the iron or steel, part of which may be dissipated. Hence $\int HdI$ measures the energy supplied to the metal in any part of a hysteresis cycle. Now for this case theory does not give the heat emission, because it is not known how much of this energy is stored as magnetic potential energy. To obtain this potential energy theoretically involves a knowledge of the mechanism of magnetism, still far from completely explained. The purpose of the present work was to measure the heat emission, Δq, due to hysteresis in successive small steps of a cycle. Having obtained this and the corresponding energy supplied, the magnetic energy could be determined from

$$\Delta U = \int_{H}^{H+\Delta H} HdI - \Delta q \qquad (2)$$

where U is this potential energy. A knowledge of this function should throw important light on the fundamental mechanism of magnetism.

II. The Experimental Procedure

Experimentally the problem had two parts, (1) obtaining the hysteresis loops characteristic of the steel used, and (2) determining the temperature rise of the steel due to hysteresis as each step was taken along a loop.

The specimen was in the form of a ring, and the magnetic measurements were made by the ballistic method, with an over-damped d'Arsonval galvanometer.

For a whole cycle the heat emission $Q = \oint HdI$. In the case of soft iron, where $\oint HdI$ is about 10^4 ergs, the rise in temperature produced is only about 3×10^{-4} degrees C. But $\oint HdI$ increases with the hardness, and reaches 10^6 ergs in the case of the "K. S. Magnet Steel" reported by Honda and Saito.[5] Through the courtesy of the Bell Telephone Laboratories, cast rings of this steel were obtained. The analysis supplied was as follows: 33.44% Co, 6.51% W, 1.81% Cr, 0.74% C, 0.12% Mn, 0.01% Si, 0.007% P, traces of Ni and S, and 0% Mo, V and Cu. The rings as cast were 1.5″ (3.81 cm) in outer diameter with a cross-section $\frac{1}{4}$″ (0.635 cm) square. Tested by the ballistic method the steel gave hysteresis loops whose areas are given in Table I.

Table I. *Areas of the loops for the magnet steel.*

H_{max}	$\oint HdI$
560 gauss	510,000 ergs
1000 "	750,000 "
1190 "	840,000 "

Density of steel = 7.8 gm/cm³, Specific heat = 0.12 cal/gm.

[5] L. Honda and S. Saito, Phys. Rev. (2) **16**, 495–500 (1920).

The maximum magnetic force which could be applied was limited by the number of turns of wire which could be wound through the center of a ring before it was completely filled, and by the current which could be sent through this winding without overheating. Black enameled copper wire (B. and S. No. 18) was used, wound uniformly in seven separate layers. Each layer was connected through a reversing switch in series with the next. A special type of reversing switch was designed to avoid breaking the current. This was effected by making the switch short-circuit its section of the coil before reversing it. A constant current was supplied from high-capacity storage batteries, H being varied from $+H_{max}$ to $-H_{max}$ in seven steps by reversing successively each of the switches, while an eighth switch permitted a complete reversal of H in one step. As the number of turns varied for the different layers practically any desired initial value of H or increment ΔH could be produced by proper handling of the switches.

The space available for winding was slightly increased by grinding the inner circumference of the rings until the difference between the inner and outer radii was only 0.118″ (0.300 cm). This also insured a sufficiently small variation in H (which is $\propto 1/r$), from inner to outer circumference. This variation was less than that occurring for any single step of the hysteresis loop.

A careful search was made for other possible sources of heat than magnetic hysteresis. Precautions were first taken against eddy or Foucault currents. These were reduced both by laminating the ring, and by introducing a choke-coil of large self-inductance into the primary circuit to delay the rate of change of the induction through the steel. The lamination of the rings was difficult on account of the extreme hardness of the steel. Each ring was finally sliced in two by a rapidly rotating Alundum saw, a rubber disc containing carborundum imbedded in it. After slitting several rings they were ground down to a thickness of 0.07 cm, and in order that the steel should have sufficient heat capacity four such rings were insulated with an enamel baked on at 100°C, and placed together to form a single laminated ring. This lamination was found sufficient to eliminate eddy current heating, as the introduction of a choke coil, sufficient further to reduce this heating to 0.1% of its value without the choke coil, produced no alteration in the heating actually observed for any step of a cycle. The magneto-caloric effect of Weiss and Piccard[6] is a reversible thermal effect accompanying magnetization for such large values of H that the *I-vs-H* curve has become closed; in the region of smaller values of H where the branches of the hysteresis loop are separate this effect is included in the hysteresis heat.

The changes of temperature of the steel were recorded by copper-constantan thermocouples. Four thermocouples were used in series, four alternate junctions being soldered to the four laminae of the ring, and the other set of four junctions being sandwiched between two mica rings of the

[6] P. Weiss and A. Piccard, Comptes Rendus **166**, 352–354 (1918); Archives des Sciences (4) **45**, 329-335 (1918).

same size, placed next to the steel but separated from it slightly by little cubes of cork. Both steel and mica rings were included in the primary winding. The thermocouples were in series with a very sensitive low resistance Leeds and Northrup galvanometer, suitable for measuring small changes of e.m.f. The sensitivity of the galvanometer was 33 mm per microvolt, and the thermoelectric power of one thermocouple was 4.2×10^{-5} volts/°C. This gave a total temperature sensitivity of 2×10^{-4}°C for the series, whereas the heat rise per cycle calculated from values of $\oint H\,dI$ in Table I was of the order of 2×10^{-2}°C.

For such a sensitive battery of thermocouples it was essential to maintain the junctions at very steady temperatures. For this reason the primary winding and reversing switches described above were employed in order that the magnetic force could be changed without altering the current through the winding. By keeping this current constant it gradually heated the winding and rings up to a steady state when the heat was conducted away at the same rate at which it was generated. That this was necessary is seen from the fact that the energy dissipated in hysteresis, even for a complete loop, is 0.01 percent of that supplied per second by the magnetizing current.

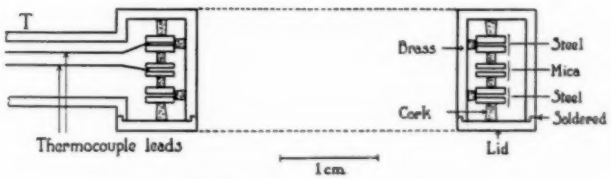

Fig. 1. The vacuum box.

This arrangement did not maintain the temperature of the thermocouples steady enough to prevent drift of the galvanometer. Another difficulty was that the thermocouples recorded only a few per cent of the predicted heating because the heat emitted in the steel was conducted away before the thermocouples and galvanometer (period 8 sec.), could record it. It was therefore necessary to insulate the rings. Experiment and theory showed that the best material insulators, such as silk, wool, or asbestos, were not sufficiently non-conducting, and that layers sufficiently thick to insulate had thermal capacities of the same order as that of the rings themselves. A vacuum box was therefore designed to hold the rings, Fig. 1. The box was of brass, with a lid which was soldered on after the rings and thermocouples had been introduced. The rings were kept 1 or 2 mm from the walls by a few cubes of cork. Two copper wires led in to the thermocouples from the galvanometer through a wax stopper and tube T. The whole box was evacuated through the tube T by means of an oil pump with liquid air trap, all joints being made vacuum tight with hard wax. The vacuum attainable was limited by the vapor pressure of this wax, but was sufficient to eliminate the convection and the heat capacity of the air, and greatly reduced the conduction. It

should be noted that the mica rings with the junctions between them were placed between two pairs of steel rings to give as symmetrical an arrangement as possible. With both sets of junctions vacuum insulated and inside the same brass enclosure very steady conditions were now obtained. The only loss of heat was along the thermocouple wires between alternate junctions, and this was reduced by using fine wire (B. & S. No. 40) for thermocouples.

The primary winding was wound outside the box. In order to obtain the large values of H_{max} desired the whole coil was placed in a water bath. A current of 30 amperes was then possible, and kept the water boiling quietly inside the winding. This insured a steady temperature of the box. As about 300 turns could be wound on, values of H up to 1200 gauss were obtained.

III. Results and Discussion

The ballistic galvanometer was calibrated by producing a known change of flux through the circuit in series with it, and gave: 1 mm deflection $=422.7$ maxwells.

Hysteresis curves for the magnet steel were obtained for $H_{max}=560$, 1000, and 1190 gauss, these same cycles being used for the measurements of the heat emission. The steel was also demagnetized by reversals and the initial magnetization curve found.

In the measurements of the heat emission a half cycle was covered in seven steps by reversing the switches in turn. Each reading was taken from six to ten times. A typical set of readings for the 1000-gauss cycle is given in Table II.

Table II. *Typical set of readings for the 1000 gauss cycle.*

H in gauss	1000 to 600	600 to 360	360 to 180	180 to −150	−150 to −420	−420 to −610	−610 to −1000
	0 mm	0 mm	0 mm	1.0 mm	5.0 mm	1.0 mm	1.0 mm
	0	0	0	1.0	4.5	3.0	1.0
	0	0	0	0	4.5	3.0	0.5
	0	0	0	1.0	4.0	4.0	1.0
	0	0	0	0.5	5.0	3.0	1.0
	0	0	0	0.5	3.0	4.5	2.0
	0	0	0	0	5.0	3.0	0.5
	0	0	0	1.5	5.0	2.5	1.0
	0	0	0	1.0	5.0	3.0	1.0
	0	0	0	0.5	4.0	3.0	1.0

The average values of each set of readings were taken, those obtained for the initial magnetization curve and for the 1000-gauss cycle being shown in Fig. 2.

The energy input, $\int H\,dI$, was measured from the graphs for each step. Assuming Warburg's Law, the area of the loop was equated to the total heat emitted in going around it, and each value of $\int H\,dI$ changed to corresponding galvanometer deflections in mm. Thus for the 1000-gauss cycle,

Total area of loop $=747{,}000$ ergs
Total heat emitted $=18.4$ mm deflection
40,500 ergs $=1$ mm deflection

Fig. 3 gives $\int H\,dI$ starting from demagnetization and going to $H=1000$, and then around half a cycle to $H=-1000$. This measures the total energy supplied to the steel at each point. The other curve shows the total heat emitted in the same process. The difference between these two curves is the energy stored potentially in the steel at each point, and this is represented in Fig. 4. Similar curves were obtained for the 560- and 1190-gauss cycles.

It is first evident that the energy supplied, $\int H\,dI$, and the energy appearing as heat are not in general equal for a step along a hysteresis cycle. As the heat emission lags behind, energy must be stored in the steel in some

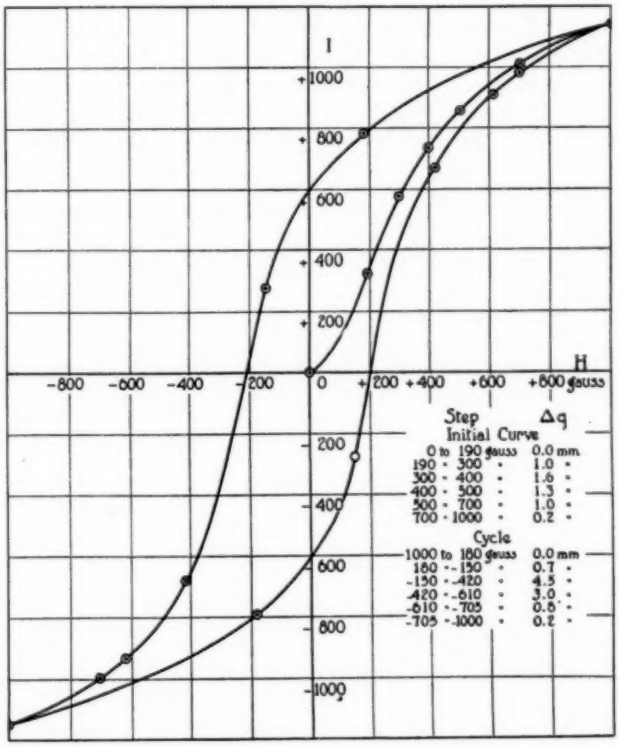

Fig. 2. The heat emission for the 1000-gauss cycle.

way. This agrees with the molecular theories of magnetism, an increase in magnetization setting up stresses and strains between the little magnets. A removal of the magnetic force relieves these strains and the energy is released. This agrees with the fact that the energy was always found to be greatest for $H=H_{max}$ and zero for $H=0$.

If magnetism is regarded as an atomic phenomenon, as the work of Stern and Gerlach[7] and others indicates, its explanation should be intimately connected with atomic theories. McKeehan[8] has presented a theory based

[7] O. Stern and W. Gerlach, Zeits. f. Physik, **9**, 349–352 (1922).

[8] L. W. McKeehan, Phys. Rev. (2) **26**, 274–279 (1925).

on the quantum hypothesis. Whether one uses the Bohr theory or the more recent theories of Heisenberg and Schroedinger the essential idea is that of discrete quantum states. In the case of a paramagnetic atom the resultant magnetic moment can take certain limited orientations with respect to the field at the atom considered, changes in the magnetization of a body as a whole resulting from various atoms suddenly undergoing a change from one orientation to another. Such discontinuous changes should be accompanied by a change in energy. Where the magnetization is changing most rapidly the heat emission might therefore be expected to be greatest. Such seems

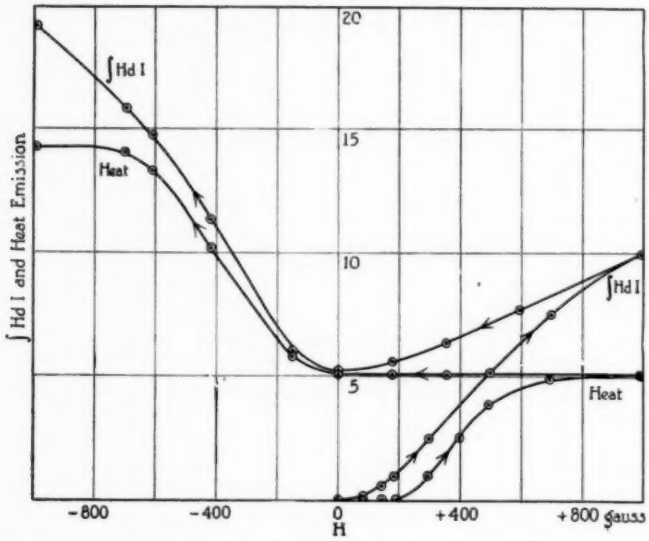

Fig. 3. The heat emission and $\int HdI$ for the initial curve and a half cycle.

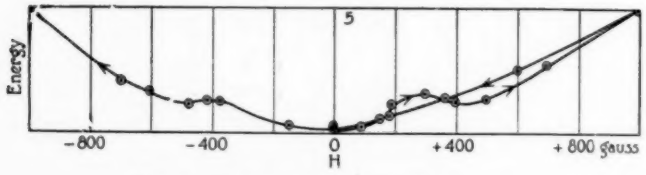

Fig. 4. The magnetic potential energy.

to be a possible explanation of the maximum slopes of heat-emission curves and minima in the energy curves around $H=400$, corresponding to the steepest part of the hysteresis loop and just beyond.

In no cases was a cooling of the steel observed, although from $H=H_{max}$ to $H=0$ energy is taken from the steel, i.e., $\int H\,dI$ is negative. Adelsberger[4] reports such a cooling, but in the present work the sensitivity and the number of steps per loop were probably not great enough to detect the small amounts of cooling which he found. In any event it appears that the energy taken from the steel is entirely supplied, or at least nearly so, from the amount

stored potentially in going from $H=0$ to $H=H_{max}$, and it is significant that this amount is just sufficient for the purpose. This probably means that the atomic magnetic axes have, at $H=0$ on the hysteresis loop, returned in most cases to parallelism with their initial directions. The residual magnetization shows, however, that the directions agreeing more closely with the magnetic force just previously applied are, in general, preferred.

From $H=0$ to $H=-H_c$ (H_c=the coercive force), a small amount of heat appears, while from the steepest part to a little beyond the rate of emission of energy is greater than the rate of supply, $\int H\,dI$, and the potential energy is temporarily reduced, producing the hump and dip in the energy curve, Fig. 4. There is a similar minimum for the energy curve of the initial branch, and it occurs at a similar point, beginning where the slope of the *I-vs-H* curve is greatest. Only half of a complete cycle is shown, the other half being symmetrical and giving a minimum which would come almost on top of that of the initial branch. Finally, for large negative values of H the heat emission decreases and the potential energy increases to a maximum for $H=-H_{max}$.

In conclusion I should like to express my sincere gratitude to Professor McKeehan for suggesting the problem, and for his generous help and criticism. Acknowledgment is also made of the financial assistance given by the Loomis Fellowship, established by Francis E. Loomis and Henry B. Loomis.

SLOANE PHYSICS LABORATORY
YALE UNIVERSITY
May, 1928

A GENERALIZED GIBBS BOLTZMANN EQUATION

By F. Russell Bichowsky

Abstract

A generalized form of the Gibbs Boltzmann canonical equation $1=\int\phi(\epsilon/kT)\,e^{-(\alpha+\epsilon)/kT}d\omega$ is derived by reversing the line of proof used by Gibbs in showing the correspondence of statistical formulas with thermodynamics. The proof involves only the assumption of the first two laws of thermodynamics, the idea that thermodynamic quantities are the physical average of complicated molecular processes, and the assumption that energy, entropy and temperature give a sufficient description of the system considered. The equation allows a treatment of statistics of the most generalized type of systems.

GIBBS[1] originally presented the equation for canonical distribution of a statistical system without proof. Proofs of this equation by Boltzmann and others depend on the assumption of a special type of system; namely, one in which the Maxwell distribution law holds, and are not of general validity. The present argument is free from special assumption limiting the type of system but it leads not to the canonical equation, but to a more general equation of which the canonical equation is a special case.

We start with the general thermodynamic equation for equilibrium

$$dE=TdS-Xdx-Ydy-\cdots \tag{1}$$

Here E is the total energy of the system considered, T its temperature, S its entropy, X, Y, $\cdots$ the generalized forces acting on the system from without; dx, dy, $\cdots$ are generalized displacements by which work is done on the system.

We now define $A=E-TS$, A so defined is the Helmholtz "free energy." Then by a simple transformation

$$dA=(A-E)dT/T-Xdx-Ydy-\cdots. \tag{2}$$

We have so far made use only of thermodynamic quantities; to make the transition from thermodynamics to statistical mechanics we note that the energy at equilibrium of any system to which these thermodynamic equations apply, as necessarily measured over a region of space large in comparison with the particles of which the system is composed, and over intervals of time long in comparison with the intervals between collisions, is not the

[1] Gibbs, Elementary Principles in Statistical Mechanics, New Haven, 1902.

instantaneous value of the energy ϵ of a given particle in the system multiplied by the number of particles n, but is equal to $n\bar{\epsilon}$ where $\bar{\epsilon}$ is the average value of the energy of the particles, the average being taken over a large enough region of phase (time, space and momentum) so that dE is measurably uniform. Similarly the other quantities in our thermodynamic equations are to be taken as the physical averages of corresponding molecular properties. We may thus define $\bar{\alpha}=A/n$; $\overline{X}=X/n$; $\overline{Y}=Y/n$; $\cdots$; $\bar{\theta}=1/u=kT/n$, the constant k being added for dimensional reasons. We might define $\bar{x}$ similarly, but this is needless as dx the displacement may always be taken large as compared with molecular distances. Equation (3) then becomes

$$\bar{\alpha}\delta\bar{u}/\bar{u}-\delta\bar{\alpha}=\bar{\epsilon}\delta\bar{u}/\bar{u}+\overline{X}dx+\overline{Y}dy+\cdots \tag{3}$$

But certain of these averages are not independent. The thermodynamic equations given define A and T as linear functions of the remaining variables. We therefore can omit the sign of average over u and α as the choice of average values for ϵ, x, y, $\cdots$ will automatically insure that we take the proper average of the other quantities.

The unweighted average of any function which varies over the range ω is given by the equation

$$n\bar{f}=\sum^{\omega} f_r n_r \tag{4}$$

or if the weighted average is required is

$$n\bar{f}=\sum^{\omega} B_r f_r n_r \tag{5}$$

In these equations f_r is the value of f at the point ω_r in the range. B_r is the weight to be attached (a number), n_r is the number of particles of the system with the same value f_r of the function f. Substituting this definition of an unweighted average in equation (4), multiplying both sides by $e^{-\alpha u}$, and substituting the equation for potential energy $\delta\epsilon/\delta x=-X$, $d\epsilon/dy=-Y\cdots$ we obtain

$$e^{-\alpha u}(-ud\alpha+\alpha du)=d\alpha\ e^{-\alpha u}\sum^{\omega} f(a\epsilon u)+u\ \delta x e^{-\alpha u}\sum^{\omega} f(a\epsilon u)\delta\epsilon/\delta x+\cdots$$

But the term on the left is a total differential $d(e^{-\alpha u})$. Therefore the term on the right must be a total differential and if put in the form

$$\sum(V\Delta v+W\Delta w)=O\ ;\ \text{then}\ \Delta V/\Delta W=\Delta W/\Delta v,$$

an equation which is justified if as Δv etc. approach zero $\Delta v/\Delta w\doteq\partial v/\partial w$. This will be true at least for all cases where the correspondence principle holds.

We first note that as far as the summation is concerned the term $e^{-\alpha u}$ is a constant and may be included in the summation. We may then substitute $g=e^{-\alpha u}f\ (\alpha\epsilon u)$.

After putting $V=\Sigma^{\omega}\epsilon g$, $W=\Sigma^{\omega}ug\partial\epsilon/\partial x$, $v=u$, $w=x$ our equation has the desired form. We thus obtain $g=\psi(\epsilon u)$ where ψ is any function and as our solution for $f(\alpha\epsilon u)$

$$1=\sum^{\omega}\phi(\epsilon/\theta)e^{-(\alpha+\epsilon)/\theta} \text{ or in the limit } 1=\int\phi(\epsilon/\theta)e^{-(\alpha+\epsilon)/\theta}d\omega$$

This is the desired generalized form of the canonical equation, the Gibbs, Boltzmann equation having the form in the limit $1=\int e^{-(\alpha+\epsilon/\theta}\,d\omega$. From the generalized form may be derived corresponding equations for partition of energy and other statistical results allowing a quite general treatment of all statistical problems of equilibrium.

There seems no very obvious method of determining further the form of the function $\phi(\epsilon/\theta)$. The third law[2] of thermodynamics that the entropy approaches zero as T becomes zero, requires at $T=0$, if $\delta\phi/\delta\omega_r$ is an analytical function for all r's that the value of $\phi(\epsilon/\theta)=1$ at $T=0$. But this is a limiting value and only true for systems in which energy and temperature are separate functions of the coordinates.

It would be of greatest importance to determine what extended form of entropy principle would fix this function at any temperature and state, but this may not be possible.

The significance of the function $\phi(\epsilon/\theta)$ from the point of view of statistics may be best seen if we carry out the proof just given using weighted instead of unweighted averages. Our final result becomes $1=\Sigma B\phi(\epsilon/\theta)$ or since B is a number and ϵ/θ is a number, the two indeterminate functions may be combined which gives formally the same result as before. That is to say, the function ϕ is a function which involves the weighing factors if any. Now from ordinary statistical proofs of the canonical equation we know that of the special cases worked out, if the weight assigned is 1 this function does not appear. It is therefore perhaps reasonable to identify this function with the *a priori* probability of statistical theory. This being the case a complete proof of the canonical equation is possible whenever the *a priori* weight can be fixed. This is usually done by some application of the Liouville method. This requires the existance of integration factors in the equation of motion of the type which occur in the Hamiltonian equations. But there may be no such factors. In other words systems may exist obeying all the laws of thermodynamics but for which the exact statistical laws cannot be worked by present methods. In these cases the use of our generalized canonical equation is the only method available.

The author wishes to express his indebtedness to Professors K. F. Herzfeld and F. D. Murnaghan of John Hopkins University.

NAVAL RESEARCH LABORATORY,
March 20, 1928.

[2] The so-called third law is really not a law of thermodynamics but a limiting equation of state like the law of perfect gases.

THE DIELECTRIC CONSTANT AND THE ELECTRIC MOMENT OF CO, COS, CS_2, AND H_2S

By C. T. Zahn and J. B. Miles, Jr.

Abstract

By the heterodyne null method used in previous investigations measurements of the temperature variation of the dielectric constant were made on a further series of gases. The results are very well interpreted by the Debye equation $(\epsilon-1)vT=AT+B$. The values for A are 0.000670 (CO), 0.002798 (CS_2), 0.001970 (COS), and 0.001223 (H_2S); and for B, 0.0078 (CO), 0.089 (CS_2), 0.352 (COS), and 0.722 (H_2S). These values of B give for the electric moment in c.g.s. e.s. units $\times 10^{18}$: 0.10 (CO), 0.326 (CS_2), 0.650 (COS), and 0.931 (H_2S). A comparison of all measurements made on the same apparatus with those of other observers is made, and a discussion of the notable discrepancies in this field is given. As a result of this investigation it seems likely that CS_2 and COS have a rectilinear structure like that of CO_2.

IN recent years a number of investigators have made experimental determinations of the variation of the dielectric constant of gases with temperature. A number of these observers have used the heterodyne method of beats between two high frequency electron-tube oscillators. With this method the accuracy of reproducibility is considerably greater than the accuracy of absolute values on account of the difficulty of calibrating the fixed capacities of the high frequency circuits. Therefore one would expect the various observers to differ only by a calibration factor characteristic for each observer (except in the case of v. Braunmühl to be mentioned later). The most notable disagreements are those in the experimental values of the electric moment of carbon dioxide and of carbon monoxide. The values of the electric moment of these molecules are of considerable importance as regards their type of molecular structure. In this connection one of the objects of this investigation was to determine the electric moment of CO, that of CO_2 having been previously found to be zero within the limits of experimental error by the same apparatus[1] used in this investigation. It was also thought of interest to measure the dielectric constant of the related compounds COS and CS_2. Another object of this investigation was to compare the data of various observers and to ascertain whether the discrepancies might be explained on the basis of calibration errors. For this purpose and also for its own sake the value of the electric moment of H_2S was determined. This value together with that of HCl[2] previously determined serves as a basis of comparison with the values recently determined by v. Braunmühl.[3]

The apparatus used in this work is the same as that described in a previous communication[2] on the dielectric constant of air, H_2, O_2, N_2, HCl, HBr, and

[1] C. T. Zahn, Phys. Rev. **27**, 455 (1926).
[2] C. T. Zahn, Phys. Rev. **24**, 400 (1924).
[3] v. Braunmühl, Phys. Zeits. **28**, 141 (1927).

HI. This apparatus has also been used to measure the dielectric constant of C_2H_2, C_2H_4, C_2H_6, and of $\alpha-C_4H_8$;[4] of H_2O at low pressures[5]; and of CO_2, NH_3, and SO_2.[1]

Experimental Results

As before the electric moment is calculated from Debye's equation:

$$(\epsilon-1)vT=AT+B$$

where ϵ is the dielectric constant, v is the specific volume referred to the ideal volume under S. P. T. conditions, T is the absolute temperature, and A and B are constants. The electric moment μ is given by

$$\mu^2=1.198\times10^{-36}B$$

where B is determined by the ordinate intercept of the graph of the Debye function $(\epsilon-1)vT$ plotted against T.

It should be noted here that the modifications in Debye's equation, which Pauli's[6] and Pauling's[7] applications of the Sommerfeld-Wilson quantum conditions introduced, are no longer required in the new matrix or wave mechanics. In fact Van Vleck[8] has shown that in general the new quantum mechanics leads to the same equation as that of the classical theory of Debye.

Table I. *Experimental data.*

T°K	p (cm Hg)	$(\epsilon-1)\times10^6$	$(\epsilon-1)v\times10^6$	$(\epsilon-1)vT$
		Hydrogen sulfide		
196.7	28.76	2604	4928	0.969
301.0	75.81	3308	3627	1.092
436.6	76.20	1821	2898	1.256
541.9	76.19	1298	2563	1.388
		Carbon monoxide		
89.8	50.69	1557	756	.0678
202.8	50.77	636	706	.1431
295.7	50.66	434	703	.2078
390.9	50.80	320	686	.2680
		Carbon bisulfide		
302.2	29.45	1096	3113	.940
395.4	29.20	805	3025	1.196
490.0	30.00	656	2978	1.458
		Carbon oxysulfide		
201.9	18.20	1216	3748	.7565
273.6	38.34	1647	3263	.8925
294.4	36.19	1398	3159	.9295
364.5	77.55	2255	2942	1.074

[4] C. P. Smyth and C. T. Zahn, Jour. Amer. Chem. Soc. **47**, 2501 (1925).
[5] C. T. Zahn, Phys. Rev. **27**, 329 (1926).
[6] W. Pauli, Jr., Zeits. f. Physik **6**, 319 (1921).
[7] L. Pauling, Phys. Rev. **29**, 145 (1927).
[8] Van Vleck, Phys. Rev. **29**, 727 (1927).

The experimental results are recorded in Table I. The actual observed value of $(\epsilon-1)$ was made between the pressure p (recorded in the second column) and a pressure of about 2 cm Hg rather than vacuum, since complete evacuation insulates the condenser plates thermally and thereby prevents temperature control. Since this lower pressure is relatively small no appreciable error is introduced by assuming that $(\epsilon-1)$ is proportional to the pressure and correcting the observed value accordingly to correspond to the full pressure p. This corrected value of $(\epsilon-1)$ for the pressure p is given in the third column. The value of v is gotten by correcting the ideal value $T/273p$ by the use of the van der Waals' constants obtained from Landolt-Börnstein. The values of $(\epsilon-1)v$ given in the fourth column are really values of $(\epsilon-1)$ referred to the ideal number of molecules per cc under

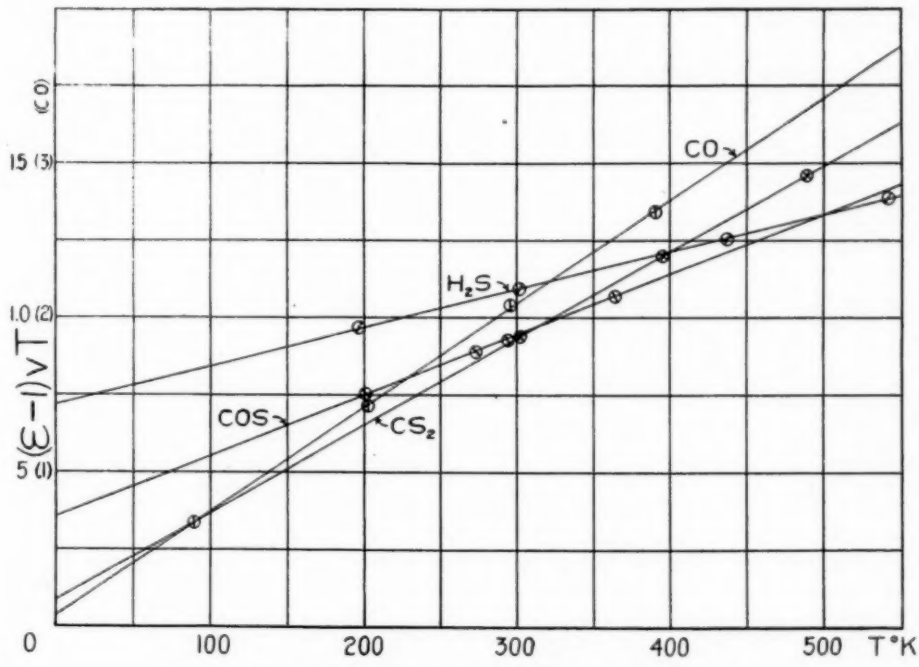

Fig. 1. The Debye function $(\epsilon-1)vT$ as a function of T.

S.P.T. conditions; that is, referred to constant density. For a molecule of zero electric moment these values of $(\epsilon-1)v$ should not vary with the temperature; but for a polar molecule they should increase more and more rapidly with decreasing temperature.

In Fig. 1 is plotted the Debye function $(\epsilon-1)vT$ against the temperature T for the purpose of determining the intercept B and then the electric moment μ. In Table II are given the values of A, B, and μ determined from the Debye lines of Fig. 1.

The H_2S was generated by dropping sulfuric acid onto sodium sulfide; it was then passed through concentrated sulfuric acid and through a P_2O_5

CO was produced by heating sodium formate with concentrated sulfuric acid and freed of CO_2 by passing it through potassium hydroxide. It was dried by passing it through a P_2O_5 tube, and further purified by passing it through a liquid air trap.
tube to absorb water vapor, and later fractionally distilled with the aid of liquid air.

TABLE II. *Debye constants.*

Gas	$A \times 10^6$	B	$\mu \times 10^{18}$ (c.g.s. e.s.u.)
H_2S	1223	0.722	0.93_1
CO	670	0.007_8	0.10
CS_2	2798	0.089	0.32_6
COS	1970	0.352	0.65_0

COS was made by dropping H_2SO_4 (5 volumes acid to 4 volumes H_2O) onto potassium thiocyanate. Then it was passed through potassium hydroxide solution to absorb CO_2, and through a charcoal tube to absorb other impurities, and then through calcium chloride, and finally it was distilled and stored over P_2O_5.

In order to obtain pure gaseous CS_2 first liquid CS_2 was purified by shaking it with mercury and mercuric sulfate until the unpleasant odor disappeared. Then it was evaporated into an evacuated vessel and stored over P_2O_5 until used. Each time either of the gases was used it was redistilled or, in the case of CO, passed through a liquid air trap. Whenever it was possible the gas was frozen and any non-condensible gases present were pumped off.

In the case of CS_2 some difficulty was encountered on account of the solubility of CS_2 in the small amount of grease collected around the stopcocks. The grease itself has no appreciable vapor pressure but there is a possibility that chemical action might occur. Since the results were very accurately reproducible for different specimens of the gas and with varying pressure conditions it is believed that no error was introduced by the presence of the grease. It is proposed, however, in connection with other experiments on vapors to make in the near future measurements on CS_2 at higher pressures and temperatures with an arrangement of apparatus which will obviate the above mentioned difficulty.

COMPARISONS WITH OTHER DATA

(a) *v. Braunmühl's data.* As was previously stated, v. Braunmühl[3] has published values for the electric moment of HCl and H_2S. His values differ widely from the values obtained with the apparatus used here. This difference, as will be seen, cannot be explained on the basis of a calibration error. v. Braunmühl has made no attempt to make an absolute calibration of his apparatus but has standardized the apparatus by taking the value of the dielectric constant of air under S.P.T. conditions from Landolt-Börnstein, 1.000547. This value should be compared with the value 1.000572[2] previously

published. If the errors are purely calibration errors one would expect all $(\epsilon-1)$ values to bear the constant ratio $547/572=0.956$; that is v. Braunmühl's values of $(\epsilon-1)$ should be consistently 4.4 percent less than ours, and his values of μ should be 2.2 percent less than ours. Actually his μ values are *greater* than ours in these two cases. The inconsistencies in the ratios

TABLE III.

Gas	v. Braunmühl	Zahn Zahn and Miles	Ratio $(\epsilon-1)^{1/2}$ or μ
$(\epsilon-1)$ Air	0.000547	0.000572	0.978
$(\mu\times10^{18})$ HCl	1.118	1.034	1.081
$(\mu\times10^{18})$ H_2S	1.101	.931	1.183

of Table III show that there are present errors other than calibration errors. H. A. Stuart[9] has pointed out a possible source of error in v. Braunmühl's work; namely, that he always compared the dielectric constant to be measured with that of oxygen at given pressures and at the same temperature as that of the other gas, assuming that the dielectric constant per molecule of oxygen is independent of temperature. According to Stuart recent accurate measurements seem to indicate that there is a definite small variation of the dielectric constant of oxygen with temperature, independent of the density variation. v. Braunmühl's data could no doubt be corrected on the basis of accurate measurements of oxygen at the various temperatures and pressures he used.

(b) *Watson's data.* Within the last year H. E. Watson[10] has made measurements with apparatus almost identical to ours on NH_3, PH_3, and AsH_3, and air and CO_2 for the purpose of comparison. Table IV gives a

TABLE IV.

Gas	Watson	Zahn	Ratio $(\epsilon-1)^{1/2}$ or μ
$(\epsilon-1)$ Air S. P. T.	0.000601	0.000572	1.025
$\mu\times10^{18}$ NH_3	1.48_5	1.44	1.031

comparison of his work with ours. For the two gases considered in this table the differences can be explained fairly satisfactorily by differences in calibration, since Watson's $(\epsilon-1)^{1/2}$ values are about 2.5 to 3 percent higher than ours in both cases.

(c) *Jona's data.* A similar comparison is given in Table V for Jona's[11] data. Since Jona found an anomalous behavior of the dielectric constant near the liquefaction point of these gases and since he also found a moment for CO_2 which almost certainly has none,[9] it is not surprising that the ratio is not constant.

(d) *Stuart's data.* One of the best arguments for at least the consistency of our experiments is shown by Stuart in Table 2 of the above mentioned

[9] H. A. Stuart, Zeits. f. Physik **47**, 457 (1928).
[10] H. E. Watson, Proc. Roy. Soc. **A117**, 43 (1927).
[11] M. Jona, Phys. Zeits. **20**, 14 (1919).

TABLE V.

Gas	Jona	Zahn	Ratio $(\epsilon-1)^{1/2}$ or μ
$(\epsilon-1)$ Air S.P.T.	0.000590	0.000572	1.016
$\mu\times10^{18}$ NH_3	1.53	1.44	1.063
$\mu\times10^{18}$ SO_2	1.76	1.61	1.093

article.[9] Our ratio of the $(\epsilon-1)$ values of CO_2 and air is consistent with that of Stuart and also with that of all the other four observers mentioned excepting Fritts, within the limits of experimental error. Also this very accurate work of Stuart has confirmed the results previously obtained on our apparatus for the electric moment of CO_2; namely, that its moment is zero within the limits of experimental error. A particularly convincing confirmation of this is the excellent agreement of our value of $(\epsilon-1)$ with the value of (n^2-1) recently determined by Fuchs.[12] (In this sense the Maxwellian law should hold only for nonpolar gases.)

(e) *Absolute values.* While the determination of the lead capacities in the high frequency circuits introduces a possible uncertainty in the calibration of our fixed capacities, still there is certain evidence in favor of the absolute values of our apparatus. This has been pointed out by Ebert and Keesom[13] as follows. Our value of ϵ for oxygen, 1.000518, gives for the molecular polarization, $M(\epsilon-1)/\rho(\epsilon+2)$, the value 0.1209. This value is practically coincident; first, with the value 0.1212, which Werner and Keesom[14] have obtained for the greater part of the existence region of liquid oxygen; and also with the value of the molecular *refractivity*, 0.1211, calculated[14] from the data of Levering and Dewar. These measurements of the molecular polarization in the liquid state should be relatively very accurate since the density of the liquid, and hence the measured effect, is about one thousand times as great as that of the gas. The authors claim an accuracy of about 2 per mil. The data of Ebert and Keesom on liquid nitrogen are not used for comparison since they are based on rough preliminary measurements and are not very consistent.

On the other hand one might object to the comparison of the molecular polarization of oxygen in the liquid state with that in the gaseous state. However, this procedure is very probably justified by the fact[13] that the molecular refractivity, 4.395, from data of Gerold,[15] of liquid *nitrogen*, is practically identical to that of gaseous *nitrogen*, 4.396.

ELECTRIC MOMENT OF CO_2 AND CO

Table VI gives a resumé of experimental values of the electric moment of CO_2 and CO determined by Debye's method of temperature variation of dielectric constant. It is interesting to note here that in the case of CO all the values of electric moment given by the various observers agree, well

[12] O. Fuchs, Zeits. f. Physik **46**, 519 (1928).

[13] L. Ebert and W. H. Keesom, Proc. Roy. Acad. Amsterdam **29**, 1888 (1926). See footnote p. 1192.

[14] W. Werner and W. H. Keesom, Proc. Roy. Acad. Amsterdam **29**, 306 (1926).

[15] E. Gerold, Ann. d. Physique (4) **65**, 93 (1921).

within the limits of experimental error; whereas in the case of CO_2 there is

TABLE VI. *Electric moment of CO_2 and CO.*

Observer	$\mu\times10^{18}$ (c.g.s.e.s. units) CO_2	CO	Observer	$\mu\times10^{18}$ (c.g.e.s. units) CO_2	CO
Jona (1919)[11]	0.303		v. Braunmühl (1927)[3]	0.145	0.124
Weight (1921)[16]	0.142	0.118	Forró (1928)[17]	0.208	0.118
Zahn (1926)[1]			Stuart (1928)[9]	0.00	
Zahn and Miles (1928)	<0.06	0.10			

a great divergence between the extreme values given: from zero to 0.303 $\times10^{-18}$. It is very difficult to understand why different observers should have such perfect agreement in the case of CO and still such a wide divergence in the case of CO_2. A possible explanation is suggested by the data given in Watson's[10] article on page 58, Table II. He gives two values of $(\epsilon-1)$ for CO_2 at two different frequencies, 1820 and 1070 kilocycles per second, which differ by about one-half percent. This observed variation with frequency is probably within the limits of experimental error, still one is tempted to suggest that it may be a real variation in the case of CO_2 and that possibly such an effect for CO is negligible. Since the various observations recorded in Table VI are made at probably widely differing frequencies the latter suggestion is not necessarily inconsistent with the facts. Any theory which would explain such a frequency variation would probably involve the temperature and would therefore require a modification of the Debye equation and at the same time explain the discrepancies in the *apparent* value of the electric moment obtained from Debye's equation. Of course, some of these discrepancies may be due to experimental errors such as have been suggested in the case of v. Braunmühl's method; or, indeed, they may all be due to experimental errors.

ELECTRIC MOMENT AND MOLECULAR STRUCTURE

H. A. Stuart[9] has recently discussed the question of the molecular structure of CO_2, and has shown that the existing data can in each case be interpreted in favor of a rectilinear, rather than a triangular arrangement of the three nuclei like that of the water molecule. The rectilinear molecule would certainly have a smaller electric moment than the triangular molecule since in the former the induction effects of the two oxygen molecules are opposite and either wholly or partially neutralize each other depending upon the equilibrium conditions of the molecule. For the case of the rectilinear molecule one cannot necessarily assert on the ground of symmetry that the electric moment must be zero.[18] This fallacy becomes evident if one considers the theoretical paper of Heisenberg[19] on the influence of the deformability of ions on the optical and chemical properties of molecules. He has here shown with a plausible model that molecules of the type M_1^+, M_0^{--}, M_1^+

[16] H. Weight, Phys. Zeits. **22**, 643 (1921).
[17] Magdalena Forró, Zeits. f. Physik **47**, 430 (1928).
[18] cf. J. W. Williams, Phys. Zeits. **29**, 177 (1928).
[19] W. Heisenberg, Zeits. f. Physik, **26**, 196 (1924).

will be built symmetrically around M_0 only if the polarizability of M_0 is below a certain limit which depends on the nature of the binding between M_0 and M_1. If the polarizability exceeds this limit the stable configuration is unsymmetrical. The electric moment resulting from such a dissymmetry would probably be much less than that of the same molecule arranged in a triangle. When the angle of the triangle is not too large the induction effects are almost additive; whereas when the angle is a straight angle, and hence the molecule is rectilinear, the dissymmetry is a differential effect. Heisenberg's theory applies to polar bindings but it is not inconceivable, in fact it seems probable, that such a type of equilibrium might exist in the case of non-polar bindings also.

Referring to Table II it is seen that CS_2 has an electric moment of 0.33×10^{-18} units. In view of the above considerations it is seen that the existence of a moment for CS_2 is not necessarily inconsistent with the absence of a moment in CO_2. Furthermore, it may be only a matter of degree; that is CO_2 may have a very small unmeasurable moment. Also CS_2 is probably a rectilinear molecule. A rough estimate of the moment of CS on the basis of that of COS and of CO would be about 0.75×10^{-18}. A large moment seems consistent with the fact that CS is a solid at ordinary temperatures. Then if CS_2 were a triangular molecule one would expect a moment of at least 0.75×10^{-18}, unless the angle of the triangle were very large and different from 180°, which hardly seems probable. Therefore the actual observed moment of 0.33×10^{-18} might easily be due to the differential dissymmetry associated with peculiar stability conditions introduced by the polarizability of the atoms.

The value of the electric moment of CS_2 here obtained seems to be at variance with the conclusions reached by Williams[18] who finds that CS_2 behaves in the liquid state as a dipole-free solvent. This latter observation may be made consistent with the existence of a moment in the following manner. First of all Williams states that it is very difficult to detect a small electric moment by his method and that the question must finally be decided by taking recourse to investigations on the gaseous molecules. Since the effect of the moment is proportional to its square, the effect for CS_2 is, for example, about one-tenth that for HCl, or about one-sixtieth that for acetone. Furthermore it is quite possible that a large amount of associated molecules of zero electric moment may be formed in the liquid state and thereby reduce the apparent moment to a negligibly small value.

The existence of a moment for CO is quite to be expected owing to the difference between C and O atoms. Finally in the case of COS it seems probable that the molecule is also rectilinear as in the cases of CO_2 and CS_2.

In conclusion the authors wish to express their thanks to Mr. J. F. Koehler for assistance in the construction of apparatus and in making the measurements here recorded.

PALMER PHYSICAL LABORATORY
PRINCETON UNIVERSITY
June 11, 1928.

THE ELECTRICAL RESISTANCE OF ALLOYS UNDER PRESSURE

By C. W. Ufford

Abstract

The average pressure coefficients to 12000 kg/cm² of electrical resistance for three series of alloys: lithium-tin, bismuth-tin, and calcium-lead, and for one calcium-magnesium alloy of 10 A% magnesium are given in tabular form. The variation with concentration of the pressure coefficient, the temperature coefficient, and the relative change of the temperature coefficient with pressure for these three series is comparable with the variation of the structure of the alloys as given by the equilibrium diagram. The conductivity and the pressure coefficient of a dilute solid solution of bismuth in tin are the same as those of pure tin under pressure. As hydrostatic pressure and impurities have the same effect on the pressure coefficient, electric conduction probably depends on geometrical properties of the conductor.

IN a forthcoming number of the Proceedings of the American Academy, data are given for the effect of hydrostatic pressure from atmospheric to 12000 kg/cm² upon the electrical resistance at two different temperatures of three series of alloys: lithium-tin, bismuth-tin, and calcium-lead, and of one alloy of calcium and magnesium containing 10A percent magnesium. Each series contains one metal with a positive and one with a negative pressure coefficient of electrical resistance, so that a large variation of the pressure coefficient as a function of the composition of the alloys is obtained. The pressure coefficients found by Bridgman[1] are used here for the end points, at the concentrations zero and one hundred percent.

The composition of the alloys was determined by weighing the two metals before they were melted in a vacuum in an electric furnace. The alloys were extruded into wires of about 0.05 inch in diameter in a cylindrical die made from Bessemer steel. The alloys rich in lithium and calcium were so brittle that they had to be heated to about eight-ninths of their melting temperature before extrusion was possible.

The change of resistance of the alloys, placed in the pressure apparatus, was measured on a potentiometer as described by Bridgman.[1] The pressure coefficients are estimated to have a probable error of less than 0.5 percent. The compositions of the bismuth-tin alloys have a probable error of ± 0.02 percent. The compositions of the alloys rich in lithium and calcium have a probable error as great as ± 6A percent.

The average pressure coefficients of electrical resistance from 0 to 12000 kg/cm², $(1/R_0)$ $(\Delta R/\Delta P)$, are given in Table I. If the pressure coefficients are plotted against the concentrations as abscissae, curves are obtained whose course may be correlated with the equilibrium diagrams of the alloys. The curves for the lithium-tin and the calcium-lead alloys, both of which form chemical compounds, are similar, the maxima and minima occurring approximately at the composition of the chemical compounds or

[1] P. W. Bridgman, (a) Proc. Am. Acad. **52**, 573 (1917); (b) Proc. Am. Acad. **56**, 61 (1921).

TABLE I. *Pressure coefficients of electrical resistance*

Composition	Average coefficient 0–12000 kg/cm²		Composition	Average coefficient 0–12000 kg/cm²	
Lithium-Tin Series			Calcium-Lead Series		
A% Sn	30°C	75°C	A% Pb	30°C	75°C
0	$.0_5772$	$.0_5772$	0	$.0_41236$	$.0_41172$
9.0	$.0_59047$	$.0_59374$	9.5	$.0_41434$	$.0_41502$
10.0	$.0_58634$	$.0_59046$	17.5	$.0_41382$	$.0_41516$
30.11	$-.0_41062$	$-.0_41063$	18.8	$.0_41422$	$.0_41374$
40.0	$-.0_56595$	$-.0_56864$	29.6	$-.0_53931$	$-.0_54127$
71.4	$-.0_58419$	$-.0_58381$	55.7	$-.0_54524$	$-.0_54894$
95.1	$-.0_58886$	$-.0_59017$	63.8	$-.0_57478$	$-.0_57424$
100.0	$-.0_59295$	$-.0_59434$	74.8	$-.0_41065$	$-.0_59997$
			90.0	$-.0_41131$	$-.0_41144$
			100.00	$-.0_41224$	$-.0_41243$
Bismuth-Tin Series					
A% Sn	30°C	0°C	A% Sn	30°C	0°C
0	$.0_42129$	$.0_4223$	23.32	$-.0_59729$	
Kahlbaum	$.0_42498$	$.0_4269$	30.20	$-.0_59451$	
.13	$.0_42331$	$.0_42220$	39.87	$-.0_59216$	$-.0_59126$
.53	$.0_57205$	$-.0_6910$	50.39	$-.0_58998$	$-.0_58856$
.89	$-.0_54178$	$-.0_58998$	68.51	$-.0_58185$	$-.0_57946$
5.02	$-.0_41034$	$-.0_41166$	90.00	$-.0_57621$	$-.0_57403$
10.01	$-.0_41503$	$-.0_41135$	97.99	$-.0_58131$	$-.0_58008$
			100.00	$-.0_59295$	$-.0_59204$
Calcium-Magnesium Series					
A% Mg	0°C		30°C		
10.0	$.0_41636$		$.0_41496$ average coefficient 0–6000 kg/cm²		

at the eutectic points, while the curves are straight in the regions of mechanical mixture between these compounds, where the law of mixtures would be expected to apply. In the bismuth-tin series, the positive pressure coefficient of bismuth becomes rapidly negative as tin is added in solid solution, indicating that the positive coefficient of bismuth depends on the crystal structure of the metal.

The curves of relative change of resistance with pressure plotted against pressure for all the alloys of the lithium-tin and the calcium-lead series exhibit what may be called the normal type of curvature; i.e., they are all convex toward the pressure axis whether the pressure coefficient is positive or negative. The alloys of the bismuth-tin series have the normal curvature except in the region of solid solutions of tin in bismuth, where the curves are concave toward the pressure axis. This is the first time, so far as is known, that curvatures of this abnormal type have been observed.

The bends in the curves representing the average temperature coefficients of resistance as functions of the concentrations in the lithium-tin and the calcium-lead series may be correlated with the concentrations at which eutectic points and chemical compounds occur, just as in the case of the pressure coefficients. Bends in the corresponding curve for the bismuth-tin series occur at the limits of solubility, the curve being nearly straight in the

region of mechanical mixtures, from 20 to 80A percent tin. The temperature coefficient of resistance becomes negative for solid solutions of tin in bismuth.

The bismuth-tin alloys obey Matthiessen's rule[2] in the region of mechanical mixtures, where the temperature coefficients of the alloys are less than those of the pure metals by approximately a constant amount. This rule does not hold for the lithium-tin or the calcium-lead series, nor would this be expected, because of the chemical compounds formed.

The change of pressure coefficient of resistance with temperature, which is the same as the change of the temperature coefficient with pressure, was small in all three series. The relative change of the pressure coefficient with temperature has maxima and minima at approximately the concentrations corresponding to chemical compounds in the lithium-tin and the calcium-lead series, and a peak in the region of solid solution of tin in bismuth in the bismuth-tin series.

Comparison of the initial and the final instantaneous pressure coefficients at 0 and at 12000 kg/cm² for the bismuth-tin series shows that tin becomes less soluble in bismuth, but bismuth more soluble in tin, as the pressure increases.

The physical properties of dilute electrolytes are often similar to those of the pure solvent which is subjected to pressure. A connection between effects due to solution and effects due to pressure can likewise be observed in the conductivity of a solid solution of bismuth in tin. 3.6A percent bismuth increases the volume of the tin lattice 1.7 percent, whereas a pressure of 9200 kg/cm² decreases the volume 1.7 percent. 3.6A percent bismuth decreases the electrical conductivity of tin 7.6 percent, while a pressure of 9200 kg/cm² increases the conductivity 7.8 percent. The average pressure coefficient of resistance of tin is reduced 17.2 percent by putting 3.6A percent bismuth into the lattice, and 19.7 percent by exerting a pressure of 9200 kg/cm². The corresponding changes in pure bismuth due to the addition of 1A percent tin do not exhibit the same regularity because of the sudden change in the properties of bismuth produced by slight impurities. If the specific volumes of very dilute solid solutions of tin in bismuth had been known, the agreement noted above might have been found in this latter case also.

The pressure coefficient-concentration curves show further that putting a foreign metal into a pure one increases the pressure coefficient of resistance of the pure metal algebraically. Similar results have been found for all the other alloys whose pressure coefficients have been measured. In all metals, hydrostatic pressure increases the pressure coefficient of resistance of the metal. These facts indicate that the electrical conductivity of a metal depends on the arrangement of its atoms in space or on the geometrical configuration of the crystal lattice, varying in the same way for all metals as the configuration is varied.

I take pleasure in thanking Professor Bridgman for his interest and assistance in carrying out this research.

THE JEFFERSON PHYSICAL LABORATORY
CAMBRIDGE, MASSACHUSETTS
June 25, 1928.

[2] A. Matthiessen, Pogg. Anallen **122**, 47 (1864).

EFFECT OF MAGNETIC FIELDS UPON THERMAL CONDUCTIVITY OF IRON, COPPER, GOLD, SILVER AND ZINC

By Hugh M. Brown

Abstract

A "bar method" was used to measure *thermal conductivity* and *electrical resistivity* for iron, copper, gold, silver and zinc in and out of a longitudinal field of 10,000 gauss, and transverse fields of 8,000 and 4,000 gauss. Copper-constantan thermo-couples "spot" welded to the bars were used to measure the temperatures. For iron, the 10,000 gauss longitudinal field caused a 1.14 percent decrease in heat conductivity and the transverse field of 4,000 gauss caused a 0.4 percent decrease. Electrical resistivity was increased 0.2 percent by the 10,000 gauss field. For copper, the thermal conductivity was decreased 0.23 percent by the 10,000 gauss field. In all the other cases the fields were shown to produce no effects large enough to detect, although the method would readily show any change as great as 0.04 percent. Zinc was used in the ordinary cast form, and in the slowly grown crystal bars. The values of electrical and thermal conductivity were higher in the crystal bar, but the magnetic fields produced no change in either bar. Thus, contrary to theories of Livens and others, these metals failed to show an increase in thermal conductivity in strong fields.

Introduction

THE effect of magnetic fields upon the thermal conductivity of metals has been investigated most fully for the ferro-magnetic elements iron and nickel. Considerable work has been done with bismuth and tellurium. The thermal conductivity of these metals seems to be decreased by magnetic fields. Livens[1] however, starting with the free electron theory arrives theoretically at the conclusion that all metals should show an increase in thermal conductivity in a magnetic field. He believes that in the ferromagnetic metals, the internal field may reverse the sign of the effect, as may also be the case for bismuth and tellurium. In this research, the effect of the magnetic field upon thermal conductivity is measured for iron, copper, gold, silver and zinc.

Experimental Methods and Apparatus

A "bar method" is used to measure the thermal conductivity. The magnitude of the thermal conductivity is given in terms of the temperatures at two points on the bar. Any slight changes in these temperatures due to the magnetic field may therefore be interpreted as a change of thermal conductivity.

O'Day[2] shows that when a current flows through a bar, cooled at the ends and radiating to a boundary at the same temperature, the equation of heat conduction takes the form:

[1] Livens, Phil. Mag. **30**, 526 (1915).
[2] O'Day, Phys. Rev. **23**, 245 (1924).

$$A\frac{d}{dx}\left(K\frac{d\theta}{dx}\right)-Is\frac{d\theta}{dx}+\left(\frac{I^2R_0\alpha}{J}-h\right)\theta=-\frac{I^2R_0}{J}$$

where θ is the temperature in degrees centigrade at any point on the bar relative to the temperature of the ends; A the cross section of the bar; $K=K_0(1-\beta\theta)$ the heat conductivity of the metal; $R=R_0(1+\alpha\theta)$ the resistance of the bar; I the current; s the coefficient of the Thomson effect; J the mechanical equivalent of heat in joules per calorie; h the radiation per cm of the bar. In this equation the change in thermal and electrical conductivity with temperature, its loss of heat by radiation, and the Thomson effect are taken into account. When the temperature distribution for the steady state is parabolic in the length of the bar, the value of the thermal conductivity is

$$K_0=R_0L^2I^2/2JA\theta_m$$

where K_0 is the heat conductivity of the metal at the temperature of the ends of the bar; R_0 the resistance of the bar at end temperature; L one-half the length of the bar; I the current giving the parabolic distribution of temperature and θ_m the temperature of the middle of the bar, referred to the ends as zero.

To obtain the value of the current to produce parabolic distribution, O'Day used the relation $\theta_m\equiv\frac{1}{2}Lp_0$ where p_0 is the temperature gradient at the end of the bar as measured by means of two thermocouples, one at the end of the bar, and one near the end. If the bar is long, the gradient may be obtained accurately in this manner, but if the bar is short, the temperature gradient is not even approximately linear, even for a short distance from the ends of the bar. To place bars longitudinally in a strong magnetic field necessarily limits the length of the bar and we have therefore in the present investigation had recourse to the following method of obtaining the value of the current necessary to produce parabolic temperature distribution.

One couple is placed at the end, one half-way to the middle, and one at the middle of the bar. When the temperature distribution is parabolic, the ratio of the temperature at the middle point to that at the second point is a constant for any form of parabolic distribution having zero temperature at the end points. The ideal value of this constant is computed. Then, as in O'Day's work, various currents are tried, and the one giving the correct ratio is used. For this current we have correct distribution, and the formula for heat conductivity is applicable.

To measure the Thomson effect O'Day used couples at 0.42 L from each end. These can also well be used to obtain the value of the current for parabolic temperature distribution. The couples near the ends can then be dispensed with, leaving five couples instead of seven, to accomplish all measurements.

The method of attaching the couples to the bar is of importance. In this work, two methods are used. First, for the metals of low melting point the bars are cast in a special iron mold, which holds the five thermocouple wires so that the ends barely enter the metal. When the casting cools, the

wires are held tightly. Copper and constantan wires No. 36 B. S. gauge are used and the wires of each couple enter the metal 0.8 mm on diametrically opposite sides of the bar. The bars being approximately 3 mm in diameter, the cross section is altered very little. It is seen then, that the couple circuit is closed by the bar itself, which is therefore the intermediate metal, but it is believed that no inconsistency is introduced by this feature. When direct current is used to heat the bar, there may be a slight IR drop between the two sides of the couple, but the true temperature is given by the average of the readings obtained with the current, first in one and then in the reverse direction.

A second method is used for metals of higher melting point. The couple wires of copper and constantan are "spot" welded on opposite sides of the bar. The bar is first marked with fine knife lines on opposite sides and exactly even in the longitudinal direction. The bars are then welded on the fine knife lines. In this manner, the cross section of the bar is scarcely altered, and the couple will give the temperature exactly at the surface of the bar. This method is used on the metals here discussed and seems to be an excellent method of attaching couples where insulation of the couple is not required.

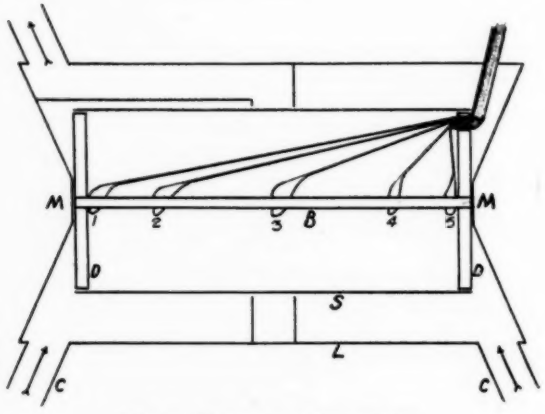

Fig. 1. Diagram of apparatus.

It is assumed in the derivation of Eq. (1) that the ends of the bar are at some definite temperature, which is the same as that of the region to which the bar radiates heat. To realize this condition the ends of the bar B (Fig. 1) are fitted into copper disks D, 5 cm in diameter and 3 mm thick. The bar fits rather tightly in each disk. The hole in the disk, and the end of the bar are tinned with solder, and then the disk is "sweated" onto the bar. This method gives a very good electrical and thermal contact between the bar and the disks. Around each disk a wide rubber band is stretched, and cemented with shellac. Over the whole is slipped a brass sheath S, forming an air-tight chamber around the bar. The length of the bar is 10 cm between the extreme couples which are 0.5 mm inside the end disks. The couple leads are carried through the end plates by a small rubber tube. The bar is heated by current from connections to the end plates. Heat radiates through

the air space from the bar to the walls of the chamber. The temperature of the whole sample chamber is kept constant by rapidly circulating ice water around it inside a second chamber L. The stream of ice water is taken from the bottom of a large box containing crushed ice and water, and directed through two connections CC to the ends of the sample chamber. A distributing valve is arranged to regulate the flow to each end in proper proportion to keep the two ends at the same temperature when heat is generated in the bar by the heating current. The water returns from each end of the bar along the brass sheath to an annular channel which leads entirely around the chamber, and is carried back to the top of the ice box, again to trickle down through the ice. By this means, the temperatures of the ends are held constant and equal, within a variation of 0.0025°C.

The other junctions of the couples are immersed in mercury in capillary tubes placed in a Dewar flask filled with shaved ice. A set of double-pole switches is arranged to connect any couple to a pair of bus wires leading to the galvanometer and a White double potentiometer (four-dial 10,000 microvolt range). The double potentiometer enables one to measure the temperature of any two different couples almost simultaneously. The galvanometer is of the D'Arsonval type, sufficiently sensitive to give 5 mm deflection per micro volt on a scale three meters distant. Whole microvolts are read on the potentiometer dials, always leaving less than one microvolt to be read on the scale.

To furnish the magnetic field, a magnet and auxilliary coil to obtain a field of 10,000 gauss across a 10.7 cm gap is used. The magnet gives almost 5,000 gauss in the middle of the gap, and of course the field is much stronger at the pole tips. The pole tips fit into the conical cups MM (Fig. 1). The ends of the water jacket are of thin copper, so that the tips of the poles come very close to the ends of the bar. A thin layer of asbestos is placed between the copper ends and the poles for thermal insulation. The field in the middle of the gap is strengthened by means of a 90 turn oil-cooled solenoid around the gap which carries a current of 800 amperes furnished by a motor-generator set. The field produced by both the magnet and the solenoid is 10,000 gauss in the middle of the gap, and slightly more near the pole tips. This field may be maintained continuously, thus allowing ample time for all measurements. The transverse field is obtained with the magnet alone, using wedge shaped tips and a 5 cm gap. The maximum field strength is then 8,000 gauss.

Measurements

A set of data consists of measurements on the following: half-length of the bar, L; cross section of the bar, A; resistance per centimeter of the bar, R; thermal e.m.f. of the couples; current, I, necessary to secure parabolic temperature distribution; temperature θ_m at middle of the bar with respect to the ends. Then as was shown above, the thermal conductivity of the sample can be computed in terms of these values from Eq. (1). The measurement of length is made by means of the vernier scale used to space the couples. The length of the bar is considered to be the distance between the

end couples. This distance is made 10 centimeters on all the bars investigated. The half-length L is then 5 centimeters. The cross section is measured in two ways: (a) the diameter is measured with micrometer calipers at many places on the bar, and the cross section computed; (b) a length of bar usually greater than that mounted, is weighed and the cross section computed, using best tabular values of the density for the pure metal. The average cross section given by the two methods is the one used in the computation. In the case of zinc, the density was determined experimentally. The resistance of the bar is determined by measuring the potential drop between copper sides of the different couples when a known current flows in the bar. The current is measured almost simultaneously with the same potentiometer by the drop over a standard 0.0001 ohm resistance. Error of spacing the couples along the bar are averaged out by taking the potential drop over all possible combinations. The average error of spacing was not usually more than 0.1 percent.

The thermal e.m.f. of the couples is measured by circulating water of various temperatures around the sample chamber, while the Dewar flask is filled with shaved ice. The constant for the welded couples never varies more than one microvolt in 1000 among different couples, even on bars of different metals. Concerning the absolute value of the constant, the junctions in the Dewar flask are assumed to be at zero degrees centigrade, and the temperature of the water bath is measured with a Haak thermometer graduated in tenths of degrees from 0 to 50°C.

A second bar is grown in a single crystal inside a glass tube. The metal is slowly cooled from the lower end upward at the rate of 2 cm per hour. Such bars, when broken, break at any point with the planes of the ends parallel. In the case of zinc, the bar grown in this manner has an elliptical cross section even though coolel in a round tube. The method is believed to have been first used by Professor A. F. Joffé, and at his suggestion the single crystal is used in this work. The cleavage plane of the bar used is inclined approximately 70° to the axis of the crystal.

Except for iron, alternating current is used for heating the bar. In the case of iron, the skin effect made it necessary to use direct current.

The values in the absence of a magnetic field of the specific electrical resistance ρ and heat conductivity K for all the metals investigated are presented in Table I.

TABLE I. *Values of specific resistance ρ and thermal conductivity K in the absence of a magnetic field.*

Metal	A cm²	L cm	I amp	θ_m °C	R (ohm/cm) $\times 10^6$	ρ (ohm/cm) $\times 10^6$	K_0 (cals/cm² °C)
Iron	.0794	5	35	38.92	151.3	11.99	0.179
Copper	.0510	5	60	6.523	30.84	1.575	0.994
Silver	.0783	5	100	6.751	19.06	1.492	1.08
Gold	.0779	5	75	8.471	28.50	2.219	0.726
Zinc	.0861	5	70	39.55	65.26	5.622	0.281
Zinc*	.0807	5	50	20.00	67.83	5.474	0.303

* Single crystal bar.

Though the purpose in this research is not to measure ρ and K_0 with exceptional accuracy, it is believed that the values on the resistivity ρ are accurate to at least 0.5 percent, and those on thermal conductivity K_0 to 1.0 percent. It is noted that the values of electrical and thermal conductivity for the single crystal of zinc are higher than for the ordinary bar. Griffiths[3] has recently shown that the heat conductivity of single crystal aluminum is the same as for cast aluminum. However, this does not indicate that zinc would act the same way, for zinc crystals are of a different system from those of aluminum.

The changes in ρ and K_0 due to the magnetic fields are given in the Table II. In each case the ratio of the value in the field to that with no field is given:

TABLE II. *Changes in ρ and K produced by the application of a magnetic field.*

Metal	Longitudinal Field 10,000 gauss‡		Transverse Fields 8,000 gauss		4,000 gauss	
	ρ'/ρ	K'/K	ρ'/ρ	K'/K	ρ'/ρ	K'/K
Iron†	1.0020	0.9886	1.0000	1.000	1.0000	0.996
Copper	1.0004	0.9977	1.0000	1.000	1.0000	1.000
Silver	1.0000	1.000	1.0000	1.000	1.0000	1.000
Gold	1.0000	1.000	1.0000	1.000	1.0000	1.000
Zinc	1.0000	1.000	1.0000	1.000	—	—
Zinc*	1.0000	1.000	1.0000	1.000	—	—

* Single crystal bar.
† The 10,000 gauss field gives 36,000 lines of induction measured by means of a fluxometer and a coil of very fine wire wrapped tightly around the bar.
‡ An 8,000 gauss longitudinal field produces a 0.21 per cent decrease in K_0 for copper.

DISCUSSION OF RESULTS

The precision and consistency of observations on the effect of the field are sufficient readily to detect a change in ρ as small as 0.02 percent, and in K_0 as small as 0.04 percent. Of the four non-magnetic metals, copper, silver, gold and zinc, only copper shows an appreciable change in heat conductivity. This change, a decrease of 0.23 percent in the longitudinal field, was verified with several different values of heating current, and with two field strengths. Loosening the magnetic poles does not affect the results, thus precluding any possibility of the change being caused by heat from the magnet, which becomes only slightly warm. For that matter, changing the temperature of the water bath does not appreciably change the results. Thus, if seems that the results for copper are contrary to Livens' theory, as has been the case for magnetic metals. Gold, silver, and zinc show no change in either electrical or thermal conductivity as much as 0.04 percent. It may be remarked that Little[4] has recently found arsenic to show no change in thermal or electrical conductivity with a magnetic field.

It is interesting that the 4,000 gauss transverse field changes the heat conductivity of iron 0.4 percent, while the 8,000 gauss field produces no

[3] Griffiths Roy. Soc. Proc. A **115**, 236 (1926).
[4] Little, Phys. Rev. **28**, 418 (1926).

change as great as 0.04 percent. Grunmach and Weidert[5] report that they found the resistance of iron first to increase with field strength and then to decrease having no change at 10,000 gauss. It appears possible that this behavior is paralleled in the case of heat conductivity.

The writer wishes to express appreciation of the kindly interest and helpful advice in this research of Professor E. E. Hall, who suggested the problem. He wishes also to thank Dr. Marcus O'Day for valuable assistance in beginning the work.

UNIVERSITY OF CALIFORNIA,
DEPARTMENT OF PHYSICS,
July 20, 1927.*

[5] Grunmach and Weidert, Phys. Zeits. **7**, 729 (1906).

* Received December 17, 1927 Ed.

HIGH FREQUENCY SOUND RADIATION FROM A DIAPHRAGM

By R. B. Lindsay

Abstract

Calculation of the intensity of the high frequency sound radiation from a circular oscillator.—By a hydrodynamical-acoustical method a calculation is made of the intensity of the high frequency sound radiation from a circular piston-like oscillator at a distance from the oscillator greater than $2a$, where a is the radius. It is shown that there is no parallel "beam" of sound of cross-sectional area equal to the area of the oscillator, but that nevertheless most of the sound energy is contained in a cone of solid angle $\pi(0.45\lambda/a)^2$ ster-radians where λ is the wave-length of the radiation. Solution of the problem for points at *great* relative distance from the source then yields a result analogous to that obtained for the Fraunhofer diffraction of light through a circular aperture. The corresponding formula is $\pi(0.61\lambda/a)^2$. Comparison is made between the two methods and they are shown to be essentially the same, the difference in the formulae being due to difference in interpretation solely.

Introduction

THE increasing use of high frequency sound radiation for subaqueous signalling has rendered important the calculation of the intensity of such radiation at a distance from the source, usually a piezo-electric quartz oscillator. Crandall[1] has given an approximate treatment, and in the French engineering literature[2] there is reference to the fact that the high frequency radiation from a piston-like source is confined to a beam of solid angle $\pi(0.61\lambda)^2/a^2$, where λ is the wave-length of radiation and a is the effective radius of the circular source, and $\lambda < a$. This would mean that the lateral spreading of the sound is confined to a plane angle 2 arc $\tan(0.61\lambda/a)$. The calculation of these latter quantities is presumably based on the analogous optical problem of the Fraunhofer diffraction of light by a circular aperture in an infinite screen. The present writer believes that it is worth while to give a more complete treatment of the problem from the standpoint of hydrodynamics and sound.

Calculation of Intensity of Sound Radiation from a Circular Oscillator

We shall assume that the source or oscillator can be considered as replaced by an equivalent circular piston of radius a, of such a character that the normal maximum displacement velocity at *each* point of the piston surface is the *same* and equal to $\xi_0 e^{i\omega t}$ where ξ_0 is thus constant and ω is $2\pi\nu$, where ν is the frequency of the vibration. The problem is to calculate the intensity due to this source at a point in a plane parallel to the piston surface and

[1] Crandall, Theory of Vibrating Systems and Sound, 1926, p. 137, ff.

[2] See, for example, F. Collin, Le Génie Civil, Vol. 86, 1925, pp. 38–40.

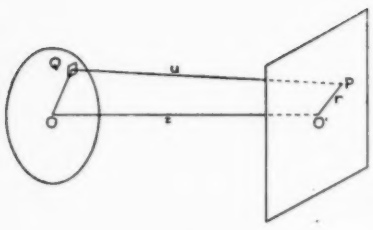

Fig. 1.

distant z from O, the center of the piston. Let such a point be P (see Fig. 1) and let its coordinates with respect to O' as origin be x_0, y_0, and its distance from O' then is $r=(x_0^2+y_0^2)^{1/2}$. The first step is to find the velocity potential at P. Lord Rayleigh[3] proved the general theorem that if a bounded surface radiates sound into the region on one side of it the velocity potential at a distant point P is given by

$$\phi_P=-(1/2\pi)\iint(\partial\phi/\partial n)(e^{-iku}/u)dS \tag{1}$$

wherein $\partial\phi/\partial n$ is the normal component of the displacement velocity at the surface, u is the distance from the surface element dS to the point P and the integration is taken over the whole radiating surface. In the present case if we take the surface element at point Q with coordinates x, y, z referred to O' the integral becomes

$$\phi_P=-\frac{\dot{\xi}_0e^{i\omega t}}{2\pi}\int_{-a}^{+a}\int_{-(a^2-x^2)^{1/2}}^{+(a^2-x^2)^{1/2}}\frac{e^{-iku}}{u}dx\,dy \tag{2}$$

Now from the figure, we have

$$u=[z^2+(x-x_0)^2+(y-y_0)^2]^{1/2} \tag{3}$$

Transforming from rectangular to polar coordinates $x-x_0=\rho\cos\theta$; $y-y_0=\rho\sin\theta$ yields

$$\phi_P=-\frac{\dot{\xi}_0e^{i\omega t}}{2\pi}\int_{\theta_1}^{\theta_2}\int_{\rho_1(\theta)}^{\rho_2(\theta)}\frac{e^{-ki(\rho^2+z^2)^{1/2}}}{(\rho^2+z^2)^{1/2}}\rho d\rho d\theta \tag{4}$$

where the limits for ρ and θ will depend on the relative magnitudes of r and a. For $r<a$ and $r>a$ they are such that the resulting integration becomes extremely complicated. We shall therefore confine ourselves to the case where $r=a$. We then have $\rho_1(\theta)=0$, $\rho_2(\theta)=2a\cos\theta$; while $\theta_1=-\pi/2$ and $\theta_2=+\pi/2$. Transforming back to u and θ, we finally have for the velocity potential

$$\phi_P=-\frac{\dot{\xi}_0e^{i\omega t}}{\pi}\int_0^{\pi/2}\int_z^{(z^2+4a^2\cos^2\theta)^{1/2}}e^{-iku}du d\theta \tag{5}$$

Let us make the assumption that $z>2a$. Then to a first approximation the evaluation of (5) depends on the calculation of the integrals

$$\int_0^{\pi/2}\cos k[z+(2a^2/z)\cos^2\theta]d\theta \text{ and } \int_0^{\pi/2}\sin k[z+(2a^2/z)\cos^2\theta]d\theta \tag{6}$$

[3] Rayleigh, Theory of Sound, Vol. II, §278, §302.

which in turn depend on the calculation of

$$\int_0^{\pi/2} \left.\begin{matrix}\cos\\ \sin\end{matrix}\right\} \left(\frac{2a^2k}{z}\cos^2\theta\right) d\theta$$

Making use of the identity $\cos^2\theta = \frac{1}{2}(1+\cos 2\theta)$, we have

$$\int_0^{\pi/2} \left.\begin{matrix}\cos\\ \sin\end{matrix}\right\} \left[\frac{a^2k}{z} + \frac{a^2k}{z}\cos 2\theta\right] d\theta$$

$$= \left.\begin{matrix}\cos\\ \sin\end{matrix}\right\} \frac{a^2k}{z} \cdot \int_0^{\pi/2} \cos\left(\frac{a^2k}{z}\cos 2\theta\right) d\theta \left.\begin{matrix}-\sin\\ +\cos\end{matrix}\right\} \frac{a^2k}{z} \cdot \int_0^{\pi/2} \sin\left(\frac{a^2k}{z}\cos 2\theta\right) d\theta \quad (7)$$

The substitution $\psi = \pi/2 - 2\theta$ yields

$$\frac{1}{2} \left.\begin{matrix}\cos\\ \sin\end{matrix}\right\} \frac{a^2k}{z} \cdot \int_{-\pi/2}^{+\pi/2} \cos\left(\frac{a^2k}{z}\sin\psi\right) d\psi - \frac{1}{2} \left.\begin{matrix}\sin\\ \cos\end{matrix}\right\} \frac{a^2k}{z} \cdot \int_{-\pi/2}^{+\pi/2} \sin\left(\frac{a^2k}{z}\sin\psi\right) d\psi$$

of which the second term is zero since the sine is an odd function, while the first is simply

$$\frac{\pi}{2} \left.\begin{matrix}\cos\\ \sin\end{matrix}\right\} \frac{a^2k}{z} \cdot J_0\left(\frac{a^2k}{z}\right) \quad (7a)$$

where J_0 denotes the Bessel's function of zero order.

Now for the *excess pressure* at P, we have from acoustical theory[4]

$$p = -\rho_0\dot{\phi}_P = \frac{i\omega\rho_0\dot{\xi}_0 e^{i\omega t}}{2\pi} \iint \frac{e^{-iku}}{u} du d\theta \quad (8)$$

where ρ_0 is the density of the medium (in this case water). Using the value given in (7) and (7a) we have for the *real* part of p

$$p_{\text{Real}} = -\tfrac{1}{2}\rho_0 c\dot{\xi}_0 \{ \cos\omega t \cdot [J_0(a^2k/z)\cos k(z+a^2/z) - \cos kz] + \sin\omega t \cdot [J_0(a^2k/z)\sin k(z+a^2/z) - \sin kz]\} \quad (9)$$

In nearly all acoustical problems the most useful expression for the intensity, that is the rate of flow of sound energy per sec. per unit area, is[5]

$$I = \overline{p^2_{\text{Real}}}/\rho_0 c \quad (10)$$

where c is the velocity of sound in the medium under consideration and the bar indicates the time average. Introducing (9) there results for the intensity of the radiation at the point P where $r = a$

$$I_P = (\rho_0 c\dot{\xi}_0^2/8)[1 - 2J_0(a^2k/z)\cos(a^2k/z) + (J_0(a^2k/z))^2] \quad (11)$$

Inspection of (11) shows at once that the only value of a^2k/z for which $I = 0$, is itself equal to zero, corresponding to an infinite z. This means that there

[4] See, for example, Crandall, loc. cit., p. 115.
[5] See, for example, Crandall, loc. cit., p. 92.

is no parallel beam of sound of cross sectional area equal to the area of the oscillator. Nevertheless *most* of the sound is confined to a relatively narrow conical region extending outward with its apex at the oscillator. We can see this as follows. The velocity potential at the point O' on the axis (i.e. for $r=0$) may be obtained by carrying out the integration indicated in equation (5) using as u limits z and $(z^2+a^2)^{1/2}$ and as θ limits 0 and 2π. The result is

$$\phi_{0'}=(2/ik)\xi_0 e^{i\omega t}\left[e^{-ik(z^2+a^2)^{1/2}}-e^{-ikz}\right] \tag{12}$$

whence using the same reasoning as above we arrive at the expression for the intensity at O'

$$I_{0'}=2\rho_0 c\xi_0^2 \sin^2(ka^2/4z) \tag{13}$$

We now seek the value of ka^2/z such that

$$I_r/I_{0'}=1/10 \tag{13}$$

and find by the use of tables that this is true for $ka^2/z=2.82$ to two decimal places. Hence in the diagram (Fig. 2) we have

$$\delta=2 \text{ arc tan } (a/z)=2 \text{ arc tan } (0.45\lambda/a) \tag{15}$$

recalling that $k=\omega/c=2\pi/\lambda$ where λ is the wave-length of the sound. This gives the lateral "spread" of the outgoing radiation. The corresponding solid angle at O is thus $\pi(0.45\lambda)^2/a^2$ steradians. It is clear that for practical purposes most of the radiation is confined to this cone, which has a somewhat smaller vertical solid angle than that given by the expression $\pi(0.61\lambda^2/a^2$.

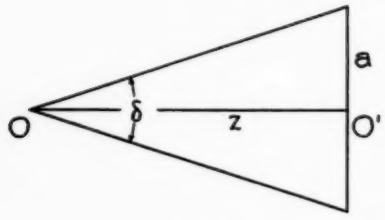

Fig. 2.

As an illustration, consider an oscillator with $a=10$ cm emitting waves of frequency 50,000 cycles, apparently the practical upper limit for signalling purposes because of the increase of the viscosity damping with frequency. This corresponds to a wave-length of 2.92 cm. We then have $\delta=15°$ approximately. According to the formula of the introduction we get $\delta=20°$ nearly. The difference, of course, is due to difference in interpretation of the problem. It may be worth while to carry through the calculation leading to that formula to see wherein the difference lies.

Returning to Eq. (3), we can write it if z is large and if $r>a$ so that x^2+y^2 can be neglected compared with $x_0^2+y_0^2$ and the product terms,

$$u=z\left(1+\frac{x_0^2+y_0^2-2x_0x-2y_0y}{2z^2}\right) \tag{16}$$

The velocity potential then becomes (see (2))

$$\phi_P=-\frac{\xi_0 e^{i\omega t}}{2\pi z}e^{-ik(z+r^2/2z)}\int_{-a}^{+a}\int_{-(a^2-x^2)^{1/2}}^{+(a^2-x^2)^{1/2}} e^{ik(x_0x+y_0y)/z}dxdy \tag{17}$$

involving evaluation of the integrals

$$\int_{-a}^{+a}\int_{-(a^2-x^2)^{1/2}}^{+(a^2-x^2)^{1/2}} \left.\begin{matrix}\cos\\ \sin\end{matrix}\right\} \frac{k}{z}(x_0x+y_0y)dydx \tag{18}$$

Let $kx_0/z=l$ and $ky_0/z=m$. Now introducing the rotation of axes

$$x=\frac{lx'}{(l^2+m^2)^{1/2}}-\frac{my'}{(l^2+m^2)^{1/2}}\,; \quad y=\frac{mx'}{(l^2+m^2)^{1/2}}+\frac{ly'}{(l^2+m^2)^{1/2}}$$

we have for an arbitrary function F

$$\int_{-a}^{+a}\int_{-(a^2-x^2)^{1/2}}^{+(a^2-x^2)^{1/2}} F(lx+my)dydx=\int_{-a}^{+a}\int_{-(a^2-x'^2)^{1/2}}^{(a^2-x'^2)^{1/2}} F(l^2+m^2)^{1/2}x')dy'dx'$$

If F is an odd function the result is zero. If F is an even function, we have or the integral

$$2\int_{-a}^{+a} F((l^2+m^2)^{1/2}x')(a^2-x'^2)^{1/2}dx'$$

Now letting $x=a\cos\psi$, we have[6]

$$\int_{-a}^{+a}(a^2-x^2)^{1/2}\cos\left((l^2+m^2)^{1/2}x\right)dx$$
$$=a^2\int_0^{\pi}\sin^2\psi\cos\left(kar\cos\psi/z\right)d\psi \quad =\pi a^2\frac{J_1(kar/z)}{kar/z} \tag{19}$$

Making use of (19) in the evaluation of (17) and computing I_P as before we find

$$I_p=\frac{\rho_0 c\xi_0^2k^2a^4}{2z^2}\left[\frac{J_1(kar/z)}{kar/z}\right]^2 \tag{20}$$

Now $I_P=0$ for that value of r for which $J_1(kar/z)=0$. According to Stokes the first root of $J_1(x)=0$ is $x=1.22\pi$. To this corresponds, then $r/z=0.61\lambda/a$, whence the statement made in the introduction follows. The larger factor 0.61 results then from the fact that the intensity is made to go to zero for the value of r sought. This then corresponds to the radius of the inner bright spot produced on a distant screen by the diffraction of light through a circular aperture. Here as before, however, by far the most of the sound is concentrated in a cone the base of which at distance z is a circle of radius r' such that $I_{r'}/I_{r=0}=1/10$. Indeed if we calculate r' from (20) to satisfy this condition we obtain

$$r'/z=0.435\lambda/a \text{ or } \delta=2 \text{ arc tan } 0.435\lambda/a \tag{21}$$

in good agreement with the value in (15) obtained by our somewhat simpler previous method.

SLOANE LABORATORY,
YALE UNIVERSITY,
May 11, 1928.

[6] See, for example, Weber, Partiellen Dif. Gleichungen der Math. Phys., Vol. 1, §68 or Gray, Mathews, and MacRobert, Bessell Functions, 1922, p. 46.

INTERNAL FRICTION IN METALS

By R. H. Canfield

Abstract

A tubular specimen of the metal is made the elastic control of a heavy pendulum bar. The system can be set into forced vibrations, either bending or twisting the specimen, by a measured periodic magnetic force-couple. The resonance amplitude and frequency, with the moment of the impressed force-couple, yield the ratio of the energy dissipated in one cycle to the energy of the vibration. The tubular form of the specimen enables the relation between dissipation and stress-amplitude to be studied in detail, at least for torsion. For normal (unfatigued) metal, the internal friction appears to be entirely associated with shear. This is not borne out in certain specimens of fatigued or overstrained metal; but these exceptions are easily accounted for. If the energy dissipated per cc. per cycle of stress-amplitude is represented by F, the relation of friction to stress-amplitude is given by the formula $F=8\phi W(1-f_0/f)$ where W is the total strain energy, ϕ is the coefficient of internal friction, and f_0 is a "threshold" stress-level which is zero initially, but takes on larger values as the vibration history becomes longer. If $f_0=0$, this formula is the same as that proposed by Kimball, viz. $F=\xi f^2$. The coefficient ϕ here introduced is independent of systems of units and to a certain extent independent of the vibration history. If f is less than f_0 the dissipation is negligible; if f is greater than another much higher level f_1, F increases faster than any power of f. Repeated cycles of high amplitudes cause all the constants gradually to change; f_0 decreases again, ϕ increases many fold, the upper limit itself may change. These progressive changes are probably associated with the progress of fatigue.

Introduction

PREVIOUS workers, using various methods, have found values of the internal friction (often considered to be viscosity) which are not in marked agreement, even as to order of magnitude. Kimball and Lovell[1] have done much to clarify the situation by showing: (1) that the dissipative forces are independent of the strain-velocity, hence not to be described as due to viscosity; (2) that at least for certain stress-ranges the work dissipated is proportional to the square of the stress-amplitude.

The method used by previous workers has most often been to determine the rate of decay of elastic vibrations of one type or another, though Kimball's very important results were obtained by an accurate measurement of the energy lost in rotating a bent rod. In nearly every case the experiments have been open to two objections: (1) the small size of the specimens, which exaggerates errors dependent on surface conditions, and (2) the use of solid specimens in which different portions of the metal pass through very different stress-cycles. Results will be presented in this paper which show that the behavior of the metal depends on the stress-amplitude even for very small

[1] Kimball and Lovell, Phys. Rev. 30, 6 (1927).

values of the latter, and that the process of fatigue produces changes which can only be studied in a homogeneously strained specimen.

Apparatus

Fig. 1 is a schematic view of the apparatus used. The specimen S (shown enlarged in the upper right hand corner) is of hollow section, about one cm inside diameter and 1.2 cm outside. At the ends it is much enlarged and threaded to screw into the pendulum bar above and the heavy base-bar below. Both these bars have longitudinal slots, and are provided with bolts by which the specimen is rigidly clamped in place. No evidence of slipping could be detected. The base-bar is in turn bolted to a concrete pier weighing about 200 kilos.

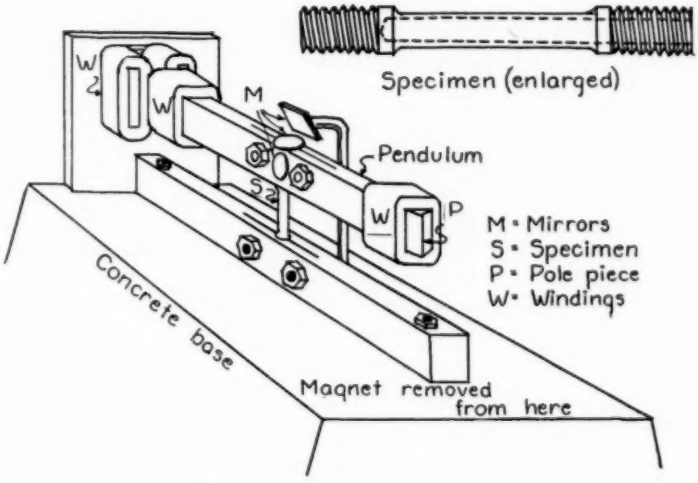

Fig. 1. Diagram of apparatus

The pendulum bar, 40 cm long, and weighing about 8 kilos, is made of cast iron. It carries coils W at its ends, as well as wedge-shaped pole-pieces P, which may be rotated so that their edges are horizontal. At the ends of the base-bar are standards supporting U-shaped electromagnets. These are so arranged that a pole piece of the pendulum is between the two poles of each magnet. One of these has been omitted in the figure, to permit a better view of the pendulum. These latter magnets are likewise capable of rotation so that their edges are horizontal.

It is plain that if both these magnets are maintained at a constant strength, while an alternating current is passed through the pendulum windings, a periodic impulse-couple will be exerted on the pendulum. This couple will produce torsion of the specimen if the arrangements are as shown; but if the fixed magnets and pole pieces are turned to a horizontal position the couple will produce bending.

Vibrations set up in the pendulum are measured by means of concave mirrors, M, which reflect the image of a straight lamp filament on a scale. For torsion the mirror is placed on the side of the pendulum; for bending

it is placed horizontally on top and used in conjunction with a plane mirror tilted at an angle of 45°. The scale distance is 122 cm, and the amplitude of the band of light ranges up to 10 cm, and may be measured to 0.1 mm.

The remainder of the apparatus consists of a motor driven commutator for producing the required alternating current, together with resistances and meters for controlling and measuring the frequency and intensity of the alternating current and the intensity of the direct current in the fixed magnets.

The motor (1/6 hp) is connected through springs to a long shaft which carries three commutators. One of these, very accurately made, with carbon brushes and protective condensers, is used to reverse the pendulum current. A 120 volt d.c. laboratory circuit supplies all the power used. The second commutator is the means of measuring the frequency of the system. Through it a large condenser is alternately charged from a battery and discharged through a milliammeter, the steady readings of which are found to be proportional to the frequency throughout the range covered (15 to 30 per sec.) with a precision of perhaps 0.2 per cent. The third commutator is provided with a pair of diametrically opposite brushes attached to a frame which can be rotated about the axis of the shaft, the angular position being determined by an index and protractor to 0.5°. This last arrangement is used for two purposes: (1) to study the form of the wave of magnetization in the pendulum, and (2) to measure the lag in phase between the vibrations and the impressed couple.

To study the curve of magnetization, a few turns of wire were passed round the pole pieces of one of the fixed magnets. The alternating current induced in these by the changing magnetism of the pendulum was conducted through the third commutator to a galvanometer. The movable pair of brushes was placed at various angles, and the corresponding galvanometer readings recorded. These readings can be shown to be proportional to the total magnetic flux through the coil at that part of the wave of magnetization corresponding to the brush setting. In this way the curve shown in Fig. 2 was obtained. It is seen to be practically a square topped wave. In fact, since the experiments were made at resonance frequency, where the lag between vibration and impulse-wave is 90°, most of the work is done by the couple when it has its most nearly constant value.

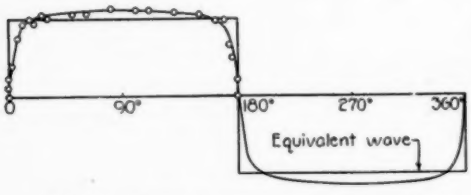

F ig. 2. Form of wave of magnetization.

Finally it may be worth mentioning that the speed of the motor is controlled by supplying its armature, separately from the field, with current drawn from a potentiometer carrying two amperes. From this it passes through a carbon compression rheostat with a spring under the screw. This device permits the extremely precise speed control demanded in the experiment.

Constants and Corrections

The moment of inertia of the pendulum for torsion is of fundamental importance. It was determined by two independent methods, involving nothing novel, and the result is considered correct to 0.2 percent.

In the case of the bending vibrations the center of oscillation is at a point about half way down the specimen. This point was exactly located by calculations from elastic theory. From the location of this point it was then easy to deduce the moment of inertia for bending vibrations.

The most difficult to determine, and perhaps the most doubtful, constants of the apparatus are those which determine the strength of the couple exerted when known currents pass through the windings. The method used was to measure photographically the amplitude of the static deflections produced by known couples, also measured photographically. These couples were then multiplied by a constant less than unity determined from the form of the magnetization curve described above. The results were a series of curves giving factors by which the product $I_f I_m$ of the currents in the fixed and moving magnets is to be multiplied to obtain the torque exerted. This factor varied from about 1.3×10^6 to 2×10^6 dyne-cm per ampere squared.

Finally to ascertain the dissipative forces within the specimen, we must eliminate those outside it. It was established that there was negligible vibration, hence negligible dissipation, either in the base-bar or the pendulum itself, or at the clamped surfaces. About 80 percent of the whole amplitude is due to strain in the straight tubular part of the specimen and for various reasons it is safe to assume that a like portion of the total dissipation takes place in this section.

There remain two ways other than internal friction by which energy may be absorbed: the air, either by friction or by radiation of sound; and eddy currents set up in the solid cores of the magnets. The correction for air was established by attaching to the pendulum a light duplicate pendulum some distance above the original, and observing how this increased the total dissipation of energy. The correction for eddy currents was arrived at by comparing the rates of decay of free vibrations when the magnets were excited and unexcited. The result was two correction-formulas which affect the final results only by a small percentage.

These corrections are perhaps negligible compared to other uncertainties in the experiment, but were in all cases duly allowed for.

Theory

The theory of forced vibrations of the type to be considered here is better developed from energy equations than from a differential equation. We picture the pendulum vibrating at a steady amplitude while acted upon by a periodic force-couple of magnitude $\pm L$, the $\pm$ sign indicating that the couple is suddenly reversed twice during each period. This assumption corresponds to the square-topped wave of magnetization found to exist in the apparatus as used. Let the frequency be n and let the pendulum make harmonic vibrations according to the equation: $\theta = a \sin(2\pi nt - \alpha)$, where

θ = angular displacement, a is the amplitude, t the time, and α the lag in phase between impressed couple and vibration. Then the work done by the external couple in one complete vibration is given by

$$\text{Work} = 4La \sin \alpha \tag{1}$$

Evidently the work done on the specimen is a maximum when $\alpha = \pi/2$.

Let the energy dissipated by internal friction during each vibration be F, where F is a function of the amplitude only and increases with the amplitude. We then have

$$4La\sin \alpha = F(a) \tag{2}$$

If F is a function of degree higher than unity, a will have its maximum value for a given L when $\alpha = \pi/2$, i.e., when the external work is a maximum. Finally, where A is the amplitude at resonance,

$$4LA = F(A) \tag{3}$$

Let us now revert to the specimen itself. Assuming for simplicity's sake the existence of only one type of stress, e.g., shear, the elastic strain-energy w per unit volume is given by $w = f^2/2E$, where f is the stress amplitude and E the appropriate elastic modulus. The total elastic energy W of the specimen will be

$$W = \int\int\int f^2 dv/2E \tag{4}$$

where the integration extends throughout the volume of the specimen. This is the same as the potential energy of the pendulum at maximum displacement, which is the same as its kinetic energy at mid-swing. Hence

$$W = 2\pi^2 I n^2 a^2 \tag{5}$$

where I is the moment of inertia of the pendulum.

In order to deal in detail with the function F which represents the energy dissipated per cycle, I propose to introduce as a hypothesis a law of internal friction with which the experiments turn out to be in agreement. Let us assume first that the type of stress is either simple shear or simple tension, so that the strain-energy can be discussed in terms of one variable stress. In Fig. 3 let OX be the axis of strains and OY the axis of stresses, and let OA be the curve of stress *vs.* strain for this material, so that in the absence of internal friction a cycle of stress would be $OAOA'O$. Assume that the actual history of a stress cycle is the parallelogram $B'BCC'B$, during which the work done per unit volume is equal to the area of the parallelogram. Further let the rule for determining the half-height AB be as follows

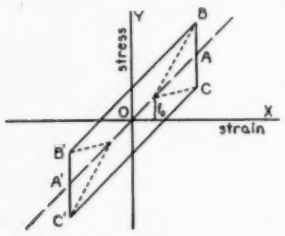

Fig. 3. Hypothetical stress-cycle.

$$AB = \phi(f - f_0) \tag{6}$$

where ϕ is the coefficient of internal friction, defined by this equation, and f_0 is a limiting stress, below which the friction stress AB is negligible or follows a different law. It is now plain that the energy per unit volume dissipated during one cycle will be $4\phi(f^2-f_0f)/E$, and for the entire specimen

$$F=\int\int\int 4\phi(f^2-f_0f)dv/E \tag{7}$$

In the case of a hollow tubular specimen under torsion all parts of the metal are subjected to nearly the same stresses, so that the volume integrals of Eqs. (4) and (7) may be expressed as simple products, and we have

$$F=8\phi W(1-f_0/f) \text{ or } F=8\phi W(1-A_0/A) \tag{8}$$

where A_0 is the amplitude corresponding to the stress f_0. Substituting in Eq. (8) the values of F given by Eq. (3), and of W given by Eq. (5), we finally obtain

$$L=4\pi^2In^2\phi(A-A_0) \tag{9}$$

Thus, according to our assumption, a curve where L is plotted against A should be a straight line intersecting the A-axis at a point A_0.

The situation is more complicated if, as is the case in bending, all parts of the specimen are not subjected to the same stress-cycles. Here the curve L *vs.* A will not be a straight line; but it will intersect the A-axis at A_0, and its slope will approximate the value given by Eq. (9) for large amplitudes.

If we still further limit ourselves to cases where $f_0=0$, which is often true for specimens without fatigue history, our cancellations are performed under the sign of integration and Eq. (9) becomes

$$L=4\pi^2In^2A\phi \tag{10}$$

which will then be true either for torsion or bending.

It only remains to note that the special restriction $f_0=0$ renders our present law of internal friction identical with that used by Kimball and Lovell and others; i.e., the energy dissipated per cycle is proportional to the stress-amplitude squared. In fact, the energy dissipated per cycle is put by Kimball equal to ξf^2 where ξ is Kimball's constant of internal friction, from which it is evident that

$$\xi=4\phi/E \tag{11}$$

The points in favor of ϕ as a coefficient of internal friction are (1) that it is dimensionless, and hence independent of systems of units; (2) that its definition is closely analogous to that of the ordinary friction coefficient, and (3) that its use in conjunction with Eqs. (7) and (9) does appear to represent the facts as developed in the ensuing experimental results.

The form of the tuning curve for a vibration performed under the above conditions may be obtained by calculating the work done during two suc-

cessive quarter swings, and eliminating sin α from the resulting equations. It turns out to be

$$a = L/2\pi^2 I\left[n_r^2(1+2\phi) - n^2\right] \tag{12}$$

where a is the amplitude corresponding to frequency n, n_r is resonance frequency, and the brackets indicate that the positive value of the quantity within them is to be used.

There is a simple relation between ϕ and the logarithmic decrement δ. If we define δ by the equation $A = A_0 e^{-nt\delta}$, where A is the amplitude of free vibration after nt complete vibrations which started at amplitude A_0, it turns out that if $f_0 = 0$,

$$\delta = 4\phi \tag{13}$$

Experiments and Results

Hollow specimens of the following metals were used: Armco iron (a nearly pure metal); Navy brass, cold drawn; phosphor bronze, annealed. In addition there were solid specimens of mild steel, copper, aluminum, Monel metal, Tobin bronze, and machine steel. The hollow specimens, except the Armco iron, had a fatigue history prior to these experiments; the solid specimens, except the mild steel, were new. The procedure was to measure the specimen, insert it in the apparatus, and then, starting with the smallest possible current in the windings, adjust the frequency of the exciting impulse until resonance was obtained. The amplitude of the resonance peak A was noted,

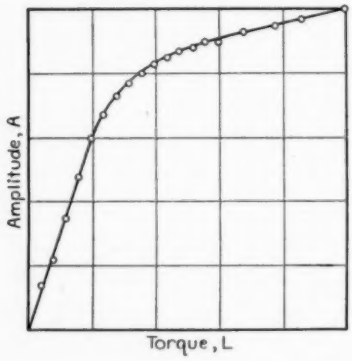

Fig. 4. Solid specimen of mild steel (torsion).

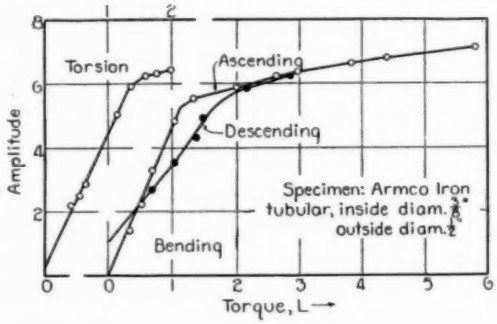

Fig. 5. Torsion and bending curves for armco iron.

along with the frequency n, and the exciting couple L. Then L was increased and the process was repeated. As soon as it was plain that the upper limit of simple friction had been passed, the pendulum, magnets and mirror were adjusted for the other mode of vibration, and the process repeated.

An analysis of numerous curves representing the relation between torque and amplitude showed in all cases the features demanded by the theoretical deductions given above. A certain range of amplitudes (sometimes rather

short) was always found where the simple law of friction held true, as evidenced by the curve's being linear. Nearly always, at least in the initial observations, the threshold stress f_0 was zero indicating that the dissipated energy was proportional to the square of the stress-amplitude. Fig. 4 illus-

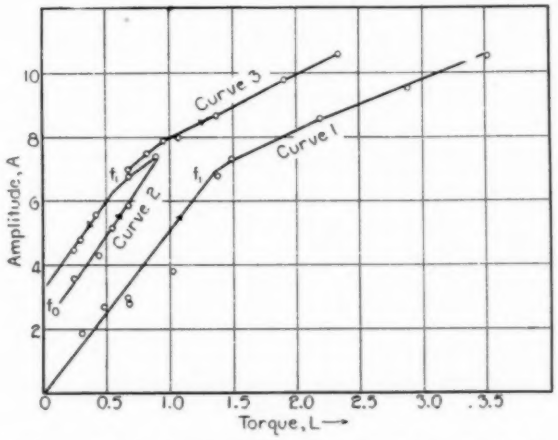

Fig. 6. Effect of repeated vibration on brass (torsion).

trates such a result. In this case the specimen was solid and the upper limit f_1 of the simple friction range is not as clearly defined as in Fig. 5, which represents results both for torsion and bending of a hollow specimen.

The reversals of high stress-range for the right-hand curve of Fig. 5 apparently resulted in a change of properties as indicated by the "descending"

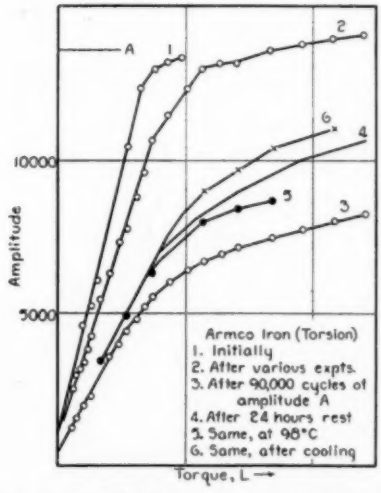

Fig. 7. Armco Iron (Torsion): 1. Initially; 2. after various expts.; 3. after 90/000 cycles of amplitude "A"; 4. after 24 hours rest; 5. same, at 98°C; 6. same, after cooling.

portion of this curve. Here there has been an increase of ϕ, indicated by the flatter slope; and the threshold stress f_0 has made its appearance. The limit f_1 is unchanged.

Fig. 6 shows the results of torsion experiments on a hollow brass specimen. Here the increase of f_0 with fatigue is very plain, but ϕ remains nearly constant, as does f_1.

Fig. 7 shows the results of a whole series of torsion experiments on Armco iron, made some days after the preceding ones. It will be seen that the fatigue treatment after curve 2 was taken has decreased f_1 to a marked degree, has increased ϕ, and has decreased f_0.

The only experiment involving the effect of temperature is shown by curve 5 of Fig. 7. A temperature of 98° has not changed ϕ or f_1, but has decidedly increased the dissipation above f_1. The same temperature has a very marked effect on the elastic constants, and a like change in ϕ would easily have been observed.

The threshold stress f_0 seems on the whole to be a feature of overstrained or fatigued metals. It was observed initially only in three specimens, steel, Tobin bronze, and Monel. The first two of these were known to have been cold-rolled. That it may disappear in some cases after a period of rest is indicated by the curves for specimens used in 1925, e.g., Fig. 4.

The upper limit f_1 of the straight line relation is in some cases about equal to the elastic limit, in others far below it. Values of this constant are tabulated in the last column of Table 1. It is recorded as a shear stress, and it is noteworthy that it has practically the same value whether derived from the twisting or the bending curve.

TABLE I

No.	Material	Friction coefficients		$\frac{\phi_B}{\phi_S}$	$\frac{E}{3N}$	Limiting shear (Kg. per cm²)	
		ϕ_S (Torsion)	ϕ_B (Bending)			Torsion	Bending
1	Aluminum	0.0075	0.0065	0.86	0.81	169	162
2	Navy Brass*	.0060	.0048	.79	.82	623	667
3	Copper††	.0076	.0063	.83	.82	76	41
4	Armco Iron	.0065	.0051	.78	.86	810	890
4a	Armco Iron*	.0084	.0087	1.04	.81	—	—
5	Monel	.0063	.0053	.84	.82	114	137
6	Cold-rolled Steel†	.0030	.0051	1.70	.75	—	—
6a	Cold-rolled steel*	.0059	.0062	1.05	.75	693	745
7	Tobin Bronze†	.0060	.0068	1.13	.82	142	109
8	Phosphor Bronze†	.0018	—	—	—	570	—
8a	Phosphor Bronze*	.0083	.0027	.32	.82	194	218
9	Mild Steel*	.0140	—	—	—	1180	—

* Fatigue history in laboratory
† Cold-worked material
†† Annealed material

RELATION OF INTERNAL FRICTION TO SHEARING STRAIN

One object of the study was to determine what relation could be found between the coefficients of friction for torsion and bending. The experimental results are given in Table I. It will be noted that for the first five specimens the ratio ϕ_B/ϕ_S is approximately equal to the fraction $E/3N$, where E is Young's modulus and N is the rigidity modulus, the ratio being determined

experimentally. The energy of any state of strain may be represented as the sum of two parts, i.e., shear energy and dilatation energy. In torsion the energy is 100 percent shear; in bending the fraction of the total energy due to shear is $E/3N$. Thus, it is plain that if ϕ_B/ϕ_S is equal to $E/3N$, it is only the shear energy which is dissipated by internal friction.

The remaining five observations do not, at a first glance, confirm the conclusion that the friction is associated with shear only, but reasons which readily account for this discrepancy are close at hand. It will be seen from a later paragraph that continued vibration at high amplitudes (i.e., fatigue) increases ϕ. There is evidence to show that bending fatigue increases bending friction without affecting twisting friction, and vice versa. Recalling that the planes of maximum shear for bending are at an angle of 45° with those for twisting, we perceive that all these facts arrange themselves coherently if we view the friction as localized in certain planes of certain crystal grains, and as being altered by repetitions of the gliding along those planes. As an example, the phosphor-bronze specimen had received a great amount of twisting fatigue prior to these experiments, but no bending fatigue. Entry 8 in Table 1 gives the value of ϕ_S for this metal at the commencement of work in 1927. It had already a fatigue history dating back to 1925. Before the observations under entry 8a were made, it received an added, severe amount of twisting fatigue, resulting in the increase of ϕ_S from 0.0018 to 0.0083; but at this latter time ϕ_B was only 0.0027. Other observations, which space does not permit including, bear out the same conclusions.

TABLE II. *Values of ϕ calculated by Eq. (11) from values presented by Kimball and Lovell.*

Material	Coefficients of Internal Friction		Experimenter
	ϕ_S	ϕ_B	
Aluminum		0.0008	K
Brass		.0012	K
Swedish iron		.0020	K
Phosphor-bronze		.0008	K
Monel metal		.0004	K
Cold-rolled steel		.0012	K
Steel	0.00060	.00048	V
Brass	.00017	.00008	V
Aluminum	.00021	.00150	V

K—Kimball & Lovell; V—Voigt

Table II presents a series of values of ϕ calculated by Eq. (11) from values presented by Kimball and Lovell[1] representing their own results as well as those of other experimenters. The values are on the whole lower than those obtained by the writer. The discrepancy can be accounted for if we assume that the specimens used by the other workers had a fairly large threshold stress f_0, since the calculations of Table II presuppose that this is zero. It is also certain that some of the specimens of the present paper, due to prior fatigue history, possessed unusually large coefficients. It is also true that some experimenters have worked at *very* low stress ranges, precisely those which are beyond the reach of study by the present method.

SUMMARY

1. It is found that for a certain range of stresses the energy dissipated per unit volume per stress-cycle is proportional to $f(f-f_0)$ where f is the stress-amplitude and f_0 is a threshold stress below which the friction is zero or of a very small order.

2. The threshold f_0 is a function of the mechanical history, being probably zero in unstrained material, increased by cold-working or fatigue, decreased again by severe fatigue.

3. The upper limit f_1 of the friction range is affected to a much less extent by physical history, but severe fatigue makes it lower. Above f_1 the energy dissipated increases faster than below it, and is no longer a quadratic function of the amplitude.

4. The dissipation of energy by internal friction in metals without history of overstrain or fatigue seems only to accompany shearing stress. Pure dilatation is frictionless.

5. Severe fatigue increases the coefficient of internal friction. This change when due to torsion proceeds to some extent independently of the same effect caused by bending (which involves a shear stress on planes of different orientation than does torsion), and vice versa.

In concluding I wish to thank Professor A. G. Christie for the services of his shop and mechanician, and both him and Professor J. S. Ames for kindly interest in the work.

THE JOHNS HOPKINS UNIVERSITY,
April 18, 1928.

BOOK REVIEWS

The Physics of Crystals. ABRAM F. JOFFÉ. Edited by Leonard B. Loeb. Pp. xi+198, 61 figs. McGraw-Hill Book Company, New York, 1928. Price $3.00.

Students of the solid state have long been tantalized by rumors of revolutionary scientific (as well as political) experiments in Russia. The scattered and sometimes almost inaccessible papers containing the results of these experiments did no more than whet our appetites for more. To the University of California belongs the credit for arranging a course of lectures in English by the guiding genius in these studies, and to the editor and publisher of the volume in hand for presenting the substance of these lectures to a wider public. No one interested in the mechanical or electrical behavior of matter in the solid state can afford to overlook the facts here presented.

Dr. Joffé is an experimentalist whose acuity and ingenuity have overcome many obstacles. He is, like Tyndall, a staunch believer in the simplicity of nature, and allows no apparent complexity of behavior to undermine this belief. He and those he leads have again and again proven that it is possible always to untangle the relations between phenomena by the most straight-forward methods if the experimental conditions are rigorously controlled.

The most interesting lectures of the series are, to this reviewer, those dealing with the plastic deformation of crystals and with their electrical conductivity. Particularly in the first of these subjects a great deal of half-baked argument would never have been offered to the scientific public if the results of these studies had been circulated more promptly.

Those who have heard Dr. Joffé speak in English know that the editor must have contributed much to the smoothness of the text. There has been some sacrifice of accuracy and more of picturesqueness and force, and in a few places the meaning has escaped (*e.g.* near the bottom of p. 38, *cf.* the better description on p. 45) or absurdities appear (*e.g.* "Both definitions differ . . . ." on p. 69). The reviewer does not like the expression "especially true" (p. 105), nor the symbol $1/\Omega$ (pp. 81, 82) for ohm^{-1} cm^{-1}. "Rhombedodecahedral" (p. 35) is customarily reduced to dodecahedral because the regular dodecahedron is crystallographically impossible. The transliteration of Russian names is, as usual, irritating. We now have Shucarev to add to Schükarew, Schukarev, Sčukareff, and Sčukarev, and other names also appear in unfamiliar forms.

L. W. MCKEEHAN

Die physikalischen Grundlagen der elektrischen Festigkeitslehre. N. SEMENOFF and ALEXANDER WALTHER. Pp. vii+168, 116 figs. Julius Springer, Berlin, 1928. Price RM. 16.50.

This monograph deals principally with experiments on the electrical break-down of dielectrics carried on by the authors and others in the electrotechnical laboratories in Leningrad under the general direction of Dr. Abram Joffé. The scale of these experiments and the general point of view of the experimenters are, however, those of physics rather than of engineering. For example, we find here a complete account of the penetration of electrostatic fields through the meshes of wire grids and screens, and a good description of the use of thermionic sounding electrodes (according to these authors independently devised by Semenoff in Russia and by Langmuir in this country). Furthermore, we find a clear and non-partisan discussion of the high-vacuum discharges described by Lilienfeld, Millikan (consistently misspelled in the text but not in the references), Rother, and del Rosario.

The minute detail into which the authors enter when they describe the results of varying material, shape and dimensions of specimen, surrounding medium, temperature, and voltage-time relations in tests of electric break-down make this part of the book—about two-thirds of the whole—difficult except to the specialist in high-tension insulation. The lack of an index will be felt most at this point.

The text is nearly free from errors but reference to figures or equations is incorrect in four places, and two of the figures themselves (46 and 47) are defective. One suspects that a photomicrograph (fig. 48) is upside down and wonders what the magnification was. For i_0 on p. 75,

l. 33 read i_N, and for *niedrigen* on p. 133, l. 16 read *hohen*. The symbol n means two different things in the same analysis on pp. 37–38.

It will surprise physicists to read on p. 43 that the energy of electrons within a metal is equal to that of the molecules and obeys the Maxwellian distribution-law. Crystallographers will object that a_0 in fig. 104 and later in the text is not the lattice constant but only half of it. (The numerical value for a_0 is correct.) Like all books put forth by this publisher the paper, typography and binding are excellent. L. W. McKeehan

Handbuch der Anorganischen Chemie. R. Abegg, Fr. Auerbach and I. Koppel. Volume Four, Section Three, Part One. **The Rare Gases.** Eugen Rabinowitsch. Pp. xii+522 50 figs. and 232 tables. Verlag von S. Hirzel, Leipzig 1928. Price bound 48 R.M.

A new volume of Abegg always affords great pleasure to the inorganic chemist. This new volume is no exception; the book is excellent in content as well as appearance. It is not only readable and interesting but is a valuable addition to the literature in this field.

Unlike the other volumes of Abegg, almost all the material has been compiled by one author, hence, this volume has a uniform style throughout and partakes more of the nature of an enlarged textbook than a handbook.

Because the book is primarily for the chemist, the discussion of the physical properties is very complete, including much explanatory and theoretical material. The physical properties are not taken up in the usual form and sequence but according to the mechanics of their origin.

There are four main divisions. Part One treats of the occurrence, preparation, detection and application of the gases. Part Two discusses nuclear phenomena, such as isotopy, structure of the nucleus, etc. Part Three discusses atomic properties, including chemical properties, position in the Periodic Table, dielectric and magnetic properties, etc. This part deals largely with spectra from the view point of the quantum theory. Part Four takes up the molecular properties, phenomena dependent upon masses of the gases, such as diffusion, effusion, density, adsorption, solubility and hydrate formation. The book closes with a systematic register of the literature up to the first half of the year 1927; the author states that this bibliography is almost "lückenlose.". Lillian Cohen

Müller-Pouillets Lehrbuch der Physik. 11. Auflage. Fünfter Band, Zweite Hälfte: **Physik des Kosmos.** Unter Mitwirkung von P. ten Bruggencate, R. Emden, K. Graff, J. Hellerich, J. Hopmann, H. Kienle, E. von der Pahlen, C. Wirtz, herausgegeben von A. Kopff. Pp. xii+595, figs. 139. Friedrich Vieweg and Sohn, Braunschweig, 1928. Bound, 39.50 RM; Unbound, 36 RM.

It has been said that the most interesting results of modern physics are best exemplified in the sky. The present work by a number of authors is one volume of an elaborate work on general physics, and gives an excellent general survey of astrophysics written from the point of view of the physicist. Technical details for the professional astronomer are largely omitted. The advantages and disadvantages of joint authorship are apparent, the treatment and emphasis being uneven in places, but this is no particular defect. The work is not a popular treatise, but it may be read to advantage by any one with a modest equipment in mathematics and physics, and of course possessing some familiarity with scientific German. The work may be recommended to the professional astronomer, to the advanced student, and especially to the trained worker in allied fields who desires to know something of the present state of astronomical science. The book is well printed and the illustrations are good. Joel Stebbins